Second Series *April, 1928* *Vol. 31, No. 4*

THE

PHYSICAL REVIEW

THE REFLECTION OF X-RAYS BY PLANE SURFACES

By H. E. Stauss

Abstract

The reflection of the $K\alpha_1$ radiation of molybdenum by plane surfaces of glass and quartz and by sputtered films of nickel, platinum, and silver has been investigated. It was found that the critical angle of reflection of nickel was smaller for transparent films than for opaque ones. The critical angles for both nickel and platinum were lower than the values calculated from the electron theory. The experimental value for the critical angle of silver agreed with the theoretical within the limits of error of the experiment. Doan has found experimental values of the critical angle for films of a number of metals that agree with those predicted by the theory, and Edwards has obtained similar results using solid reflectors. If it is to be granted that the theory does hold true in the case of nickel and platinum, too, it is necessary to assume that the densities of sputtered films of nickel and platinum are less than those of the metals. Further it must be assumed that in the case of nickel the density varies with the thickness of the film, being smaller for the thinner films.

The observed critical angle for quartz was smaller than the theoretical value, as though the surface density was less than the average density. Both glass and quartz surfaces showed a weak residual reflection beyond the critical angles, of a type that was not present in the sputtered films. The phenomenon may be caused by irregular densities over the surface due possibly to the polishing or to the heterogeneous composition of the two substances.

The Experimental Method

THE experiments described in this paper were performed for the purpose of studying the reflection of x-rays by plane surfaces. The general principles underlying the investigation are well presented in other papers,[1,2,3] and need not be discussed here. The experimental method used by the author was, in brief, to split a beam of homogeneous x-rays with the mirror itself, causing part to be reflected and allowing part to pass by undeviated, and to determine the angle of reflection by measuring the separation of the two resulting beams on a photographic film. Fig. 1, which is not drawn to scale, shows the arrangement of the apparatus. The x-rays from the target A are reflected by the calcite crystal B, and are split by the mirror D. No slits were used except to prevent undesirable radiation from getting into the room. A narrow beam was secured by taking the radiation from the target of a water-cooled tube at a glancing angle of 14°; the crystal was relied upon to

[1] R. L. Doan, Phil. Mag. **4**, 100 (1927).
[2] H. W. Edwards, Phys. Rev. **30**, 91 (1927).
[3] H. E. Stauss, Nature **114**, 88 (1924).

limit the beam of monochromatic radiation that was used to a small angular width. The edge of the mirror farther from the x-ray tube was over the center of rotation of the spectrometer and did not move appreciably during the rotation of the mirror. The edges of the beams used in the measurements were those determined by this farther edge of the mirror, and were as well defined as if they had been limited by a slit. The distance from crystal to mirror edge was 30 cm. The $K\alpha_1$ radiation of molybdenum, of 0.7076A wave-length, was used throughout the work.

The experimental procedure involved turning the mirror through successively increased angles and making ten minute exposures in each position. The pictures were taken at a distance of 98.1 cm from the mirror edge until the reflected beam was invisible; then the distance was shortened to about 11 cm. In the new position of the film the reflected line became visible again, and the procedure for the longer distance was continued. The angles of reflection could be determined directly from measurements of the films

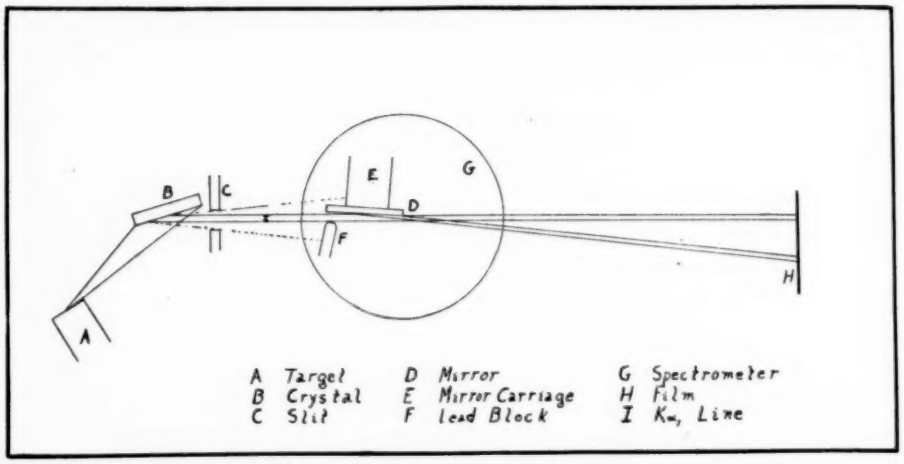

Fig. 1. Experimental arrangement.

at the greater distance until the reflected line became too weak to be measured accurately.

For these larger angles and for those with the film at the shorter distance the angular displacements of the reflector from a standard position, as measured by a sensitive optical system, were used to determine the angles of reflection. The sensitiveness of the system depended upon the use of monochromatic light and of a low-power microscope to read the deflections of the image. The source was a filament of a tungsten red-lamp, such as is used in dark-rooms. The real image of the filament was observed directly by the microscope at a distance of 181.0 cms from the mirror. A collodion color filter was placed over the objective of the microscope. It, together with the red glass of the lamp, permitted only a very narrow band of the spectrum in the extreme red to reach the microscope. An extremely sharp image was formed, whose edge could be read absolutely to 0.02 mm. Small angular displacements of the mirror could be read with a probable error of less than 0.2″.

The relative intensity of the reflected to the primary beam was found by comparing the relative blackening of the two visually. As both lines always appeared on the same films, this method consisted merely of a simple comparison of the densities of two lines produced under the same conditions. The relative values of the densities at the two different distances were obtained by taking pictures for one angle in both positions in each series and the results were checked by calculations based on the geometry of the apparatus. More accurate values of the relative intensities were not necessary since the final angle of reflection is the important datum. The results were plotted and are shown in Fig. 2. It should be noted that all the angles in the graphs are measured relative to a standard position with the optical system—the standard position for each trial being one of the angles at which the reflected line was strong.

In this method the error made in measuring any angle of reflection is the error made in determining the standard position added to the error made

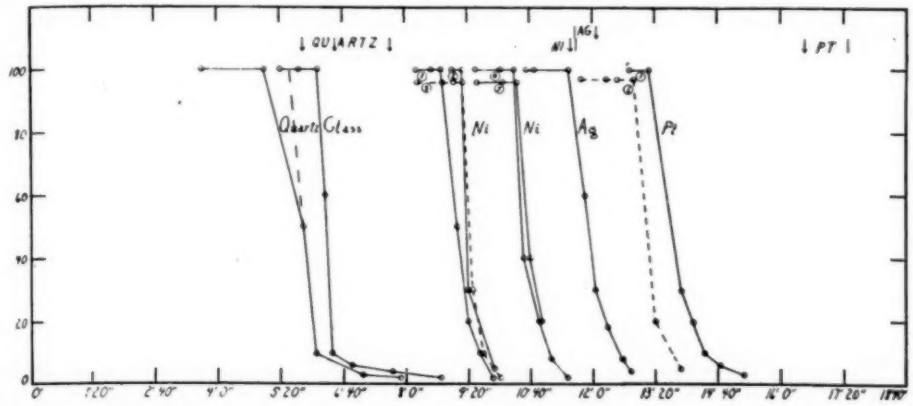

Fig. 2. The relative intensity of the reflected to the primary line plotted against angle of reflection.

in reading the displacements from it. The second error is negligible compared to the first and may be neglected. The error made in measuring the reference angle is half the angular width of the beam, if the effect of the penumbra of the lines on the measurements is neglected. The angular spread of the primary beam in this experiment, 43″, was determined by measuring its width at two different positions. Actually, however, a penumbra occurs on each edge of the lines within which the intensity varies from zero on the outside to the full intensity of the beam. Fig. 3 illustrates the effect, where both a_1b_1 and a_2b_2 are penumbrae. It also illustrates the error in the determination of the angle of reflection, if the effect of the penumbra is neglected; a_1b_2 is the distance that would be measured, while b_1b_2 is the desired distance. As all readings must be made from somewhere within this penumbra, an error is introduced into the result which is indeterminable. If all readings are assumed to have been made in the region of zero to half intensity, as seems likely to be the case, the error made in determining an angle lies between

one-quarter and three-quarters of the width of the beam, or between 11″ and 33″. The actual error is probably somewhat larger, however, because the effect of the penumbra upon the determination of the spread of the beam has been neglected. The measured values of the angles will always be greater than the true values.

The critical angle of reflection that is desired is the final angle of reflection, which was apparently increased in this method by the curvature of the mirror, but the error was only 4″ and could be corrected for. An examination of the curves shows that the drop in relative intensity of reflection between the value of 100 and 20 (the limit of visibility at the greater distance)

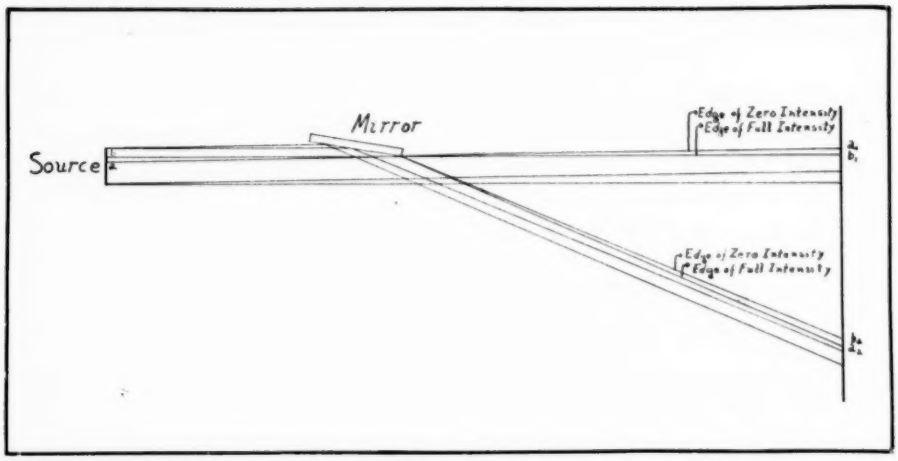

Fig. 3. A diagram illustrating the effect of the penumbra upon the measurements. For convenience in drawing, the crystal has been used as the "source" of the radiation (see Fig. 1). The beam that comes from it, if this is one of the characteristic radiations, has a definite angular width without the use of any slits. In the sketch this angular width is the angle subtended by ab, a_1b_1 or a_2b_2 at the mirror. The drawing differs from that in which the source emits radiation in all directions in that the limiting rays are defined by the "source" (or crystal) instead of by slits. For example, no rays outside the length of ab of the crystal can strike the mirror edge, because that would require a greater angular width of the beam than is found experimentally.

does cover approximately 50″ as would be expected, although the total drop including that at the shorter distance, occurs through an appreciably larger angle. If this additional reflection is due to very weak radiation with more than 43″ spread, it may be neglected and the critical angle assumed to be the limit of visibility at 98.1 cm, or a relative intensity of 20 for the two beams. The true value of this angle will then be 15″ to 37″ less than the measured angle. In view of the uncertainties of the corrections to be applied, all of the angles used in the graph are uncorrected.

Results

The substances investigated were glass, quartz, and films of silver, nickel, and platinum sputtered on the glass surface. In the case of nickel it was discovered that the critical angle depended upon the thickness of the film.

Curves 1 and 2, Fig. 3, represent the reflection from two transparent films sputtered in hydrogen, and curve 3 that from one sputtered in nitrogen Curves 4 and 5 represent the reflection from the same opaque film of nickel sputtered in hydrogen. The difference between the two sets of curves is about 80″, more than can be attributed to experimental error. The phenomenon can be explained easily if it is assumed that the thin films are less dense than the thick ones. This is in accord with the results of J. D. Hanawalt and L. R. Ingersoll[4] who found that nickel films sputtered in hydrogen are less dense than the metal itself. However, to explain the present case, it must be assumed that the low density is not due to the presence of hydrogen in the film, but to the thinness of the film or to the presence of any gas in it. If Lorentz's theoretical formula for the critical angle of reflection is true, the difference in density of the two types of films is about 23 percent of the more dense one.

If, further, the critical angles are compared with the theoretical values, it is found that they are much smaller than can be accounted for by experimental error in the case of both nickel and platinum. The theoretical critical values are shown in the upper part of the graph, the arrows indicating those obtained by neglecting the effect of the critical frequencies and the straight lines those found by assuming these to be the absorption frequencies and using Stoner's distribution of electrons. Curve 1 for platinum represents the reflection for an opaque film sputtered in hydrogen and curve 2 for one sputtered in nitrogen. If the discrepancy between experimental and theoretical values is to be explained as being due to density changes, both the nickel and platinum films, even those that are opaque, must have lower densities than the metals themselves. Considering Lorentz's formula as true again, the density of the platinum is only about 75 percent of that of the metal.

The following table shows the approximate densities of the films, if Lorentz's formula is assumed to hold.

Element	Nature of Film	Density of Element (gms/cc)	Density of Film (gms/cc)
Ni	Transparent	8.90	4.13
	Opaque	8.90	5.44
Pt	Opaque	21.37	14.1

The experimental value of the critical angle for the silver film falls between the two theoretical values. The accuracy is not great enough to allow a choice between them. The theoretical angle for quartz (the middle arrow) is also larger than the observed. This discrepancy may possibly be caused by a low surface density, or by the composition of the surface being different from that of the interior.

An anomalous behaviour was observed in the case of some of the reflectors when the critical angle had been reached. The reflected line, as observed at the shorter distance, continued to be present for glass and quartz for much greater angles of rotation than for the sputtered elements, although

[4] J. D. Hanawalt and L. R. Ingersoll, Nature **119**, 234 (1927).

the film of platinum sputtered in hydrogen (curve 2) shows somewhat the same effect. This can hardly be attributed to weak radiation which has a greater spread than 43′′ because not all the surfaces show the effect. Neither can it be attributed to lack of planeness in the surfaces since the sputtered films should have all the irregularities of the glass. The effect can be explained if it is assumed that the density over the surface varies and that the residual reflection comes from the more dense areas. A variable surface density is easily understood for glass and quartz, as these were polished The polishing. agent may have become imbedded in them, or the polishing may have altered their surfaces—for instance, to form minute silicon and even oxygen crystals. In the case of platinum any variation of density must be due to sputtering.

Another possible explanation of the phenomenon for glass and quartz is that on account of their composition, the x-rays were able to follow varying types of paths in their short course within the surface—paths ranging from those containing only one kind of atom to those containing only the other. In this way there would arise varying speeds within the reflector and varying indices of refraction, and hence varying critical angles of reflection. No calculations of the extreme types of paths can be made because nothing is known of the nature of the surface which matter presents to x-rays or of the depth of penetration into the surface. However, it is interesting to calculate the critical angles for quartz if the oxygen is assumed to be replaced by silicon (but assuming the number of atoms per cubic centimeter to remain unchanged), and if the silicon is replaced by oxygen. These angles serve as an approximation to the limits within which the variations of path might be expected to affect the critical angle; they are shown in the graph by the arrows to the right and to the left, respectively, of the center arrow. It is seen that the distance between them covers the total fall in intensity. Moreover the value for oxygen is nearest the observed value of the critical angle, as though the surface was covered by oxygen.

In conclusion it may be stated that results have been obtained for sputtered films of nickel and platinum and for quartz which do not agree with theory unless it is assumed that these surfaces have lower densities than the metals and materials themselves. The reflectors of heterogeneous composition, glass and quartz, showed a weak residual reflection beyond the critical angle that must be related in some way to the nature of their surfaces. These phenomena are now being investigated further, with the view of determining the relation between them and the densities of the reflecting surfaces.

This experiment was performed at the University of California. The author wishes to express his sincerest thanks to the members of the Physics Department, particularly to Professor Brackett, for their help and encouragement throughout its entire course.

BRACE LABORATORY OF PHYSICS,
UNIVERSITY OF NEBRASKA,
November, 1927.

SERIES SPECTRA OF POTASSIUM AND CALCIUM

By I. S. Bowen

Abstract

Several of the strongest extreme ultra-violet lines in the K_{III}, K_{IV}, Ca_{IV}, and Ca_{V} spectra are given their series designtion. In K_{II} several lines are identified in addition to those found by DeBruin. The absolute value of the terms of K_{II} are determined thus fixing the ionization potential at 31.7 volts. 137 lines are classified in Ca_{III} and the term values of the levels involved are calculated. These correspond to an ionization potential of 51.0 volts.

I. *Six-Electron Systems.* Hopfield and Dieke[1] have called attention to a triplet PP' group which they traced from S_I to K_{IV}. Since this group follows the irregular doublet law it can be definitely identified as the PP'

TABLE I

Triplet PP′ groups in six-electron systems.

Ion	Int.	λI.A. Vac.	ν	Δν	Series designation
S_I			72380.		aP_2-bP_1
			72174.		aP_1-bP_0
			72019.		aP_2-bP_2
			71985.		aP_1-bP_1
			71805.		aP_0-bP_1
			71625.		aP_1-bP_2
				21348.9	
Cl_{II}	4	1063.77	94005.3		aP_2-bP_1
	4	1067.95	93637.4		aP_1-bP_0
	5	1071.03	93367.9		aP_2-bP_2
	3	1071.77	93304.0		aP_1-bP_1
	4	1075.22	93003.9		aP_0-bP_1
	3	1079.07	92672.7		aP_1-bP_2
				20426.1	
A_{III}		871.11	114796.		aP_2-bP_1
		875.56	114213.		aP_1-bP_0
		878.78	113794.		aP_2-bP_2
		879.62	113685.		aP_1-bP_1
		883.22	113222.		aP_0-bP_1
		887.45	112682.		aP_1-bP_2
				20387.	
K_{IV}	4	737.15	135658.		aP_2-bP_1
	4	741.94	134782.		aP_1-bP_0
	4	745.26	134181.		aP_2-bP_2
	3	746.39	133978.		aP_1-bP_1
	4	750.00	133333.		aP_0-bP_1
	4	754.66	132510.		aP_1-bP_2
				20497.	
Ca_V	4	637.89	156766.		aP_2-bP_1
	3	643.10	155497.		aP_1-bP_0
	5	646.51	154678.		aP_2-bP_2
	3	647.82	154364.		aP_1-bP_1
	4	651.49	153495.		aP_0-bP_1
	3	656.71	152275.		aP_1-bP_2

[1] Hopfield and Dieke, Phys. Rev. **27**, 638 (1926).

group to be expected on the return of a $3s$ electron that had been excited to a $3p$ orbit. The wave-lengths and frequencies of these groups along with the corresponding group in Ca_V are given in Table I. The frequencies for S_I were given by Hopfield and Dieke[1] while those for A_{III} were determined by Dorgelo and Abbink.[2] The data for Cl_{II}, K_{IV} and Ca_V represent new determinations.

II. *Seven-Electron Systems.* Turner[3] has given the wave-lengths of six lines in the extreme ultra-violet spectrum of Cl_I. Four of these can be arranged in a doublet PP' group, the position and separations of which are approximately those to be expected for the combination between the $4k^2P$ term of the $s^2p^4 \cdot s$ configuration and the a^2P term of the s^2p^5 configuration. A corresponding PP' group is found in the table of the "blue" argon spectrum in the extreme ultra-violet given by Dorgelo and Abbink. In this case the

TABLE II

Doublet lines in seven-electron systems.

Ion	Int.	λI. A. Vac.	ν	$\Delta\nu$	Series designation
Cl_I	2	1335.8	74863.		aP_2-4kP_1
	5	1347.2	74225.	884.	aP_2-4kP_2
	3	1351.7	73979.	883.	aP_1-4kP_1
	5	1363.5	73342.		aP_1-4kP_2
A_{II}		718.05	139266.		aP_2-4kP_1
		723.35	138246.	1436.	aP_2-4kP_2
		725.53	137830.	1430.	aP_1-4kP_1
		730.91	136816.		aP_1-4kP_2
K_{III}	2	466.78	214234.		aP_2-4kP_1
	3	470.08	212730.	2163.	aP_2-4kP_2
	2	471.54	212071.	2168.	aP_1-4kP_1
	2	474.92	210562.		aP_1-4kP_2
Ca_{IV}	2	335.36	298189.	3134.	aP_2-4kP_2
	2	338.92	295055.		aP_1-4kP_2
A_{II}		919.79	108720.	1431.	aP_2-bS
		932.06	107289.	21157.	aP_1-bS
K_{III}	5	765.65	130608.	2162.	aP_2-bS
	4	778.54	128446.	20875.	aP_1-bS
Ca_{IV}	6	665.96	152448.	3127.	aP_2-bS
	5	669.70	149321.		aP_1-bS

identification is confirmed by the fact that the separation of the a^2P term is within 8 frequency units of the value predicted by Meissner[4] from the difference in the limits of the series of lines in A_I that are based on these

[2] Dorgelo and Abbink, Zeits. f. Physik **41**, 753 (1927).
[3] Turner, Phys. Rev. **27**, 397 (1926).
[4] Meissner, Zeits. f. Physik **39**, 172 (1926); **40**, 839 (1927).

two terms in the A_{II} ion. Assuming the identification of these two groups it is possible to predict the position and separations of the corresponding lines in K_{III} and Ca_{IV}. In K_{III} a strong PP' group is observed as predicted and in Ca_{IV} part of the group is found, the remainder being obscured by other strong lines.

Another group of lines that should be emitted by a seven-electron system is the combination of the a^2P term of the s^2p^5 configuration with the b^2S term of the sp^6 configuration. These pairs, having the same separation as that found in the PP' groups and following the irregular doublet law, have been traced from A_{II} to Ca_{IV}. These lines are among the strongest lines in the spectrum as would be expected from the fact that they are the resonance lines of these ions. The lines identified in these seven-electron systems are collected in Table II.

III. *Eight-Electron Systems.* Meissner[4] has made a very complete analysis of the A_I spectrum and DeBruin[5] has classified a large number of lines of the spark spectrum of potassium as due to jumps between various terms of K_{II}. More recently DeBruin[6] has been able to correlate about one-half of these terms with the corresponding terms of argon, as analyzed by the Meissner. On plates recently taken at this laboratory it has been possible to identify several very strong extreme ultra-violet lines as transitions between DeBruin's terms and the single ground term of the s^2p^6 configuration. These lines are given in Table III.

TABLE III

Series lines in K_{II}

Int.	λI. A. Vac.	ν	Series designation
5	600.75	166459.	$3p-4s_2$
5	607.90	164501.	$3p-3d_5$
4	612.61	163236.	$3p-4s_4$
2	615.40	162496.	$3p-4s_5$?

The series of s_2 and s_3 levels (Meissner's notation) in K_{II} are based on the a^2P_1 term of K_{III} while the s_4 and s_5 terms are based on the a^2P_2 term. Consequently for the higher members of these series the s_2, s_3 levels are separated from the corresponding s_4, s_5 levels by a frequency difference approximately equal to $a^2P_2-a^2P_1$. The identification, in Section II, of certain lines in the K_{III} spectrum fixes the separation in this a^2P term and therefore makes possible the approximate prediction of the separation between the $5s_2$, $5s_3$ terms and the $5s_4$, $5s_5$ terms. When this is done it is evident from the agreement in this separation as well as in the inner quantum numbers and position that DeBruin's Y_2, Y_3, Y_4 and Y_5 terms should be identified with these $5s_5$, $5s_4$, $5s_3$ and $5s_2$ terms respectively. Since DeBruin has already identified the $4s$ terms this fixes two successive members of a series from which the absolute term values can be calculated by the use of the Rydberg formula.

[5] DeBruin, Proc. R. S. Amsterdam, **29**, 713 (1926).

[6] DeBruin, Dissertation, Amsterdam, 1927.

Table IV gives the classification of 137 lines in the Ca_{III} spectrum. The wave-lengths above 2250A are taken from Anderson[7] while the remainder represent new determinations. The notation used in the present article follows that of Meissner for the s and p terms except that the preceding numeral is changed, in conformity with recent usage, to agree with the total quantum number of the excited electron. The correlation of the terms in

TABLE IV
Series lines in Ca_{III}

Int.	λI. A. Vac.	ν	Series designation	Int.	λI. A. Vac.	ν	Series designation
5	403.734	247688.	$3p-4s_2$	0*	1905.98	52466.4	$3D_3-4p_9$
5	409.948	243933.	$3p-4s_4$	2	1907.46	52425.7	$4p_7-5s_3$
2	490.56	203851.	$3p-3D_1$	4	1910.17	52351.4	$3D_7-4p_6$
2d	1270.54	78706.7	$3D_1-4p_2$	3*	1935.79	51658.5	$4p_6-5s_2$
2	1278.38	78224.0	$3D_1-4p_5$	4	1939.72	51553.8	$3D_6-4p_8$
2	1281.50	78033.6	$3D_1-4p_3$	6	1943.12	51463.6	$4p_{10}-4D_2$
3	1297.96	77044.0	$3D_2-4p_3$	5	1948.31	51326.5	$3D_8-4p_6$
1	1310.58	76302.1	$3D_2-4p_4$	3	1952.16	51225.3	$3D_7-4p_7$
2	1317.60	75895.6	$3D_1-4p_6$	4	1953.06	51201.74	$p_3-5s_4, 3D_6-4p_9$
3	1334.94	74909.7	$3D_2-4p_6$	2	1958.18	51067.8	$4p_9-4D_4$
1	1355.37	73780.6	$3D_2-4p_7$	5	1964.70	50898.4	$4p_9-5s_5$
1	1359.81	73539.7	$3D_1-4p_8$	5	1968.03	50812.2	$4p_{10}-4D_1$
2	1385.39	72181.8	$3D_2-4p_9$	1	1972.01	50709.7	$4p_8-4D_4$
3	1459.87	68499.2	$3D_3-4p_3$	3	1978.63	50540.0	$4p_8-5s_5$
4	1463.41	68333.5	$3D_1-4p_{10}$	2	1989.61	50261.1	$4p_4-5s_2$
2	1480.55	67542.5	$3D_4-4p_3$	4	2000.44	49989.0	$3D_7-4p_8$
4	1484.92	67343.7	$3D_2-4p_{10}$	4	2001.61	49959.8	$4p_7-5s_4$
2	1496.92	66803.8	$3D_4-4p_4$	3	2003.74	49906.7	$4p_4-5s_3$
3	1506.94	66359.6	$3D_3-4p_6$	1	2010.55	49737.6	$3D_9-4p_2$
0	1528.89	65406.9	$3D_4-4p_6$	3	2014.75	49633.9	$3D_7-4p_9$
4	1555.48	64288.8	$3D_4-4p_7$	4d	2019.42	49519.2	$4p_3-5s_2$
6	1562.50	64000.0	$3D_3-4p_8$	3	2021.48	49468.7	$4p_7-4D_4$
5	1571.31	63641.2	$3D_3-4p_9$	2	2027.34	49325.7	$4p_8-5s_2$
0*	1584.82	63098.6	$4p_{10}-4D_5$	2	2028.38	49300.4	$4p_7-5s_5$
4	1586.19	63044.1	$3D_4-4p_8$	1	2030.67	49244.8	$3D_9-4p_5$
1	1595.24	62686.5	$3D_4-4p_9$	4	2034.12	49161.3	$4p_9-4D_3$
1	1688.81	59213.3	$4p_{10}-5s_2$	3	2039.01	49043.4	$3D_9-4p_3$
1	1698.95	58859.9	$4p_{10}-5s_3$	4	2042.27	48965.1	$3D_8-4p_8$
1	1716.23	58267.2	$4p_9-4D_5$	4	2047.31	48844.6	$4p_8-5s_4$
1*	1726.88	57907.9	$4p_8-4D_5$	3	2047.80	48832.9	$4p_2-5s_3$
3	1738.56	57518.9	$3D_5-4p_5$	3	2049.02	48803.8	$4p_8-4D_3$
3	1744.61	57319.4	$3D_5-4p_3$	3	2057.30	48607.4	$3D_8-4p_9$
3	1762.14	56749.2	$3D_6-4p_2$	3*	2062.83	48477.1	$4p_3-5s_3$
3	1773.29	56392.4	$4p_{10}-5s_4$	2	2068.30	48348.9	$4p_6-4D_4$
0	1777.93	56245.2	$3D_6-4p_5$	2	2070.21	48304.3	$3D_9-4p_4$
4	1783.92	56056.3	$3D_6-4p_3$	2	2075.55	48180.0	$4p_6-5s_5$
4	1794.31	55731.7	$4p_{10}-5s_5$	5	2099.23	47636.5	$3D_8-4p_{10}$
4	1800.24	55548.1	$4p_6-4D_5$	6	2129.88	46951.0	$4p_4-4D_4$
5	1807.91	55312.5	$3D_6-4p_4$	3*	2132.17	46900.6	$3D_9-4p_6$
5	1812.17	55182.5	$3D_8-4p_6, 3D_7-4p_2$	6	2141.07	46705.6	$4p_3-5s_4$
1	1828.43	54691.7	$3D_7-4p_5$	1	2144.47	46631.6	$4p_9-4D_2$
2	1849.51	54068.4	$3D_5-4p_7$	6	2153.15	46443.6	$4p_6-4D_3$
6*	1854.72	53916.5	$3D_6-4p_6$	2	2161.07	46273.4	$4p_8-4D_2$
3	1860.50	53749.0	$3D_7-4p_4$	4	2164.18	46206.9	$4p_3-4D_4$
6	1870.28	53467.9	$3D_8-4p_3$	5	2172.27	46034.8	$4p_2-5s_5$
5	1872.39	53407.7	$4p_3-4D_5$	3	2183.98	45788.0	$3D_9-4p_7$
1*	1892.92	52828.4	$3D_5-4p_8$	2	2191.95	45621.5	$4p_8-4D_1$
3	1894.17	52793.6	$3D_6-4p_7$	3	2205.08	45349.8	$4p_2-5s_4$
0	1896.94	52716.5	$4p_2-4D_5$	2	2219.91	45046.9	$4p_4-4D_3$

* May be blend with impurity or high order line.

[7] Anderson, Astrophys. J. 59, 76 (1924).

TABLE IV continued

Inf.	λI. A. Vac.	ν	Series designation	Int.	λI. A. Air	ν	Series designation
1	2220.56	45033.7	$4p_7-4D_2$	6	2704.87	36959.4	$4s_3-4p_2$
2	2245.01	44543.2	$3D_9-4p_8$	4	2771.27	36073.9	$4s_5-4p_7$
	I. A. Air			6	2791.63	35810.8	$4s_4-4p_6$
2	2252.65	44378.4	$4p_7-4D_1$	7	2813.88	35527.6	$4s_3-4p_4$
0	2256.33	44306.0	$4p_3-4D_3$	7	2866.57	34874.7	$4s_2-4p_2$
2	2276.54	43912.8	$4p_6-4D_2$	7	2869.95	34833.6	$4s_5-4p_8$
0	2310.87	43260.5	$4p_6-4D_1$	7	2881.80	34690.4	$4s_4-4p_7$
1	2351.40	42514.8	$4p_4-4D_2$	9	2899.78	34475.3	$4s_5-4p_9$
3	2393.20	41772.3	$4p_3-4D_2$	2	2907.90	34379.0	$4s_2-4p_5$
1	2431.08	41121.5	$4p_3-4D_1$	8	2924.33	34185.9	$4s_2-4p_3$
1	2442.54	40928.6	$4p_5-4D_1$	7	2988.61	33450.6	$4s_4-4p_8$
1	2472.52	40432.3	$4p_2-4D_1$	6	2989.30	33442.9	$4s_2-4p_4$
5	2497.67	40025.3	$4s_5-4p_2$	6	3028.66	33008.3	$4s_3-4p_7$
6	2541.49	39335.2	$4s_5-4p_3$	8	3119.66	32045.5	$4s_2-4p_6$
3	2587.09	38642.0	$4s_4-4p_2$	4	3233.02	30921.9	$4s_2-4p_7$
2	2590.34	38593.5	$4s_5-4p_4$	5	3367.81	29684.4	$4s_2-4p_8$
6	2620.82	38144.6	$4s_4-4p_5$	8	3372.68	29641.5	$4s_5-4p_{10}$
6	2634.17	37951.4	$4s_4-4p_3$	7	3537.75	28258.5	$4s_4-4p_{10}$
3	2686.73	37208.9	$4s_4-4p_4$	6	3761.62	26576.8	$4s_3-4p_{10}$
8	2687.78	37194.4	$4s_3-4p_5$	5	4081.74	24492.5	$4s_2-4p_{10}$

calcium arising from an excited *d* electron with the corresponding terms in argon is, in many cases, doubtful and therefore all of these terms are labeled with a *D* with subscripts numbered in the order of their term values.

The terms that have been identified in Ca_{III} are listed in the first column of Table V. The inner quantum number of the term, *J*, is given in the second column and the value of the term in the third column. In the fifth column the corresponding terms of K_{II} are listed using DeBruin's notation. The

TABLE V

Term values in eight-electron systems.

		Ca_{III}			K_{II}		A I
Term	*J*	Term value	Δν	DeBruin's Notation	Term value	Δν	Meissner's Notation
$4s_5$	2	170583.5		X_2	94130.0		$1s_5$
			1383.5			730.0	
$4s_4$	1	169200.0		X_3	93400.0		$1s_4$
			1681.4			1912.5	
$4s_3$	0	167518.6		X_7	91487.5		$1s_3$
			2085.0			1312.0	
$4s_2$	1	165433.6		X_8	90175.5		$1s_2$
$5s_5$	2	85210.0		Y_2	44061.5		$2s_5$
			663.4			417.4	
$5s_4$	1	84546.6		Y_3	43644.1		$2s_4$
			2462.3			1734.1	
$5s_3$	0	82084.3		Y_4	41910.0		$2s_3$
			355.9			291.8	
$5s_2$	1	81728.4		Y_8	41618.2		$2s_2$
$3p$	0	413127.			256637.		$1p_0$
$4p_{10}$	1	140941.6		P_1	73428.6		$2p_{10}$
			4833.4			3180.1	

TABLE V (*continued*)

Ca_{III}					K_{II}		A_I
Term	J	Term value	$\Delta\nu$	DeBruin's Notation	Term value	$\Delta\nu$	Meissner's Notation
$4p_9$	3	136108.2		P_2	70248.5		$2p_9$
			358.7			297.1	
$4p_8$	2	135749.5		P_3	69951.4		$2p_8$
			1239.2			845.5	
$4p_7$	1	134510.3		P_4	69105.9		$2p_7$
			1121.5			623.3	
$4p_6$	2	133388.8		P_5	68482.6		$2p_6$
			1398.1			1089.3	
$4p_4$	1	131990.7		P_6	67393.3		$2p_4$
			742.5			418.0	
$4p_3$	2	131248.2		P_7	66975.3		$2p_3$
			193.2			110.3	
$4p_5$	0	131055.0		P_8	66865.0		$2p_5$
			496.4			362.8	
$4p_2$	1	130558.6		P_9	66502.2		$2p_2$
						4641.3	
				P_{10}	61860.9		$2p_1$
				X_4	93200.7		$3d_6$
						1059.8	
$3D_1$	1	209281.9		X_5	92140.9		$3d_5$
			990.3			436.2	
$3D_2$	2	208291.6		X_6	91704.7		$3d_3$
			8542.9			5903.1	
$3D_3$	3	199748.7		X_9	85801.6		$3d_4$
			954.0			691.4	
$3D_4$	2	198794.7		X_{10}	85110.2		$3d_1''$
			10220.1				
$3D_5$	1	188574.6					$3d_2$
			1270.8				
$3D_6$	1–2	187303.8					$3s_1''''$
			1564.6				
$3D_7$	2	185739.2					$3s_1''$
			1023.8				
$3D_8$	3	184715.4					$3s_1'''$
			4419.8				
$3D_9$	1	180295.6					$3s_1'$
$4D_1$	1	90128.1		Y_6	41232.1		$4d_5$
			651.7			450.9	
$4D_2$	2	89476.4		Y_7	40781.2		$4d_3$
			2531.4			1210.5	
				Y_8	39570.7		
						660.1	
$4D_3$	3	86945.0		Y_9	38910.6		$4d_4$
			1904.5			1469.8	
$4D_4$	2	85040.5		Y_{10}	37440.8		$4d_1''$
			7199.4			3921.9	
$4D_5$	3?	77841.1					$4s_1'''$
				Y_{11}	33512.9		

sixth column gives the absolute value of these K_{II} terms as fixed by the method mentioned above. In the last column the corresponding levels of A_I are listed in Meissner's notation.

These term values fix the ionization potential of K_{II} as 31.7 volts and of Ca_{III} as 51.0 volts.

NORMAN BRIDGE LABORATORY OF PHYSICS,
CALIFORNIA INSTITUTE OF TECHNOLOGY, PASADENA.
January 20, 1928.

THE SHAPE AND INTENSITIES OF INFRA-RED ABSORPTION LINES

By David M. Dennison

Abstract

An expression for the shape of an infra-red absorption line is developed on the basis that the principal factor in the broadening of a line is the limitation of the length of wave train a molecule may absorb due to its perturbation by thermal collisions. The shape of the line is accordingly found by expanding the finite wave train with a Fourier integral and then integrating over the distribution of lengths of wave train given by the kinetic theory of gases. The absorption coefficient as found in this way may be expressed to a high approximation by means of two damping curves involving the number of molecules per unit volume, the temperature, and σ the effective diameter.

To apply this result to the analysis of observed infra-red spectra allowance must be made for the low spectrometer resolution due largely to the wide slits employed. Two expressions are developed, holding for all but very weak lines, which relate the area under the absorption line *Abs.* the minimum value of the transmission $T_{\min}$ and the true intensity α with the slit width a, the cell length l, and the molecular constants.

$$\text{Abs} = [5.412\alpha n\sigma^2 l]^{1/2}/[\pi hm]^{1/4}$$

$$\text{Abs} = -2.42a \log_{10} T\text{min}$$

It is shown that these formulae are capable of interpreting the absorption lines of the infra-red spectrum of HCl observed by R. F. Paton and yield a value of 10.8×10^{-8} cm for σ. The meaning of σ, the distance to which two molecules may approach without altering each others phases, as well as the range of validity of the assumptions is discussed and a correction to the absorption area formula for faint lines is deduced. In connection with a consideration of the absorption measurements of HCl by Kemble and Bourgin, a computation is made of the effective moving charge of the molecule giving the value $\epsilon = (.199)\ 4.77\times10^{-10}$ E.S.U.

Introduction

THE many observations which have been made of the infra-red absorption spectra of gases show clearly that the absorption lines are not confined to a single frequency but possess a definite shape and a finite width. A number of factors may be enumerated which combine to determine the form of the line: (a) Doppler effect; (b) an effect corresponding to the damping of a classical oscillator; (c) a resonance effect between neighboring molecules; (d) an effect due to the limitation of the length of the wave trains which may be absorbed by the molecules. The relative importance of these effects will depend largely upon the frequency being absorbed and upon the physical state of the gas. A simple calculation[1] shows that in the infra-red region,

[1] An estimate of the order of magnitude of effect (b) may be made by the following computation. A classical oscillator of frequency ν, mass m and effective charge ϵ, has a lifetime τ due to damping, where $\tau = 3c^3m/8\pi^2\epsilon^2\nu^2$. The width of the corresponding absorption line $\Delta\nu$ is given by $\Delta\nu = 1/\tau$. Setting in the appropriate values of the constants for the HCl

for normal temperatures and pressures, effects (a) and (b) are completely negligible in their influence upon the shape of the absorption lines although they may play an important role in determining the form of the high frequency x-ray lines. Holtsmark,[2] L. Mensing,[3] and others have met with considerable success in explaining the breadth of lines in the visible region of the spectrum on the basis of (c), the resonance effect between neighboring systems. This effect, while it may have some influence in determining the shape of the infra-red lines, appears to be of a smaller order of magnitude than (d) and we shall confine our attention in this paper to showing that this latter effect is capable of furnishing a satisfactory description of the infra-red absorption lines.

We may arrive at an expression for the form of an absorption line caused by a limitation of the wave train due to the thermal collisions with the following consideration which must hold as well in the new wave mechanics as in the classical mechanics. If the time during which a collision takes place between molecules is very short compared with the time t between collisions, the problem is identical with that of an undisturbed molecule upon which falls for a time t a radiation field ρ. If the radiation field ρ is uniform in frequency and if the molecule has a proper frequency ν_0, the intensity with which it will absorb the frequency ν is proportional to the square of the Fourier density integral

$$I_{\nu,t}=\left[\int_0^{t/2}\cos(2\pi\nu x)\cos(2\pi\nu_0 x)dx\right]^2=\frac{1}{4}\left[\frac{\sin(\nu_0-\nu)\pi t}{2\pi(\nu_0-\nu)}+\frac{\sin(\nu_0+\nu)\pi t}{2\pi(\nu_0+\nu)}\right]^2.$$

Since the breadth of the line is in general very small compared with the frequency, we may neglect the second member and write,

$$I_{\nu,t}=\frac{\sin^2(\nu_0-\nu)\pi t}{16\pi^2(\nu_0-\nu)^2}.$$

The width of the absorption line as given by this expression is of the order $1/t$ and for purposes of estimation, we may take t to be $\bar{l}$, the mean time between collisions. The kinetic theory of gases furnishes a relation between $\bar{l}$, n the number of molecules per unit volume, $\bar{c}$ the mean value of the velocity of each molecule, and σ the effective diameter of the molecule.

$$\bar{l}=1/(2)^{1/2}\pi\sigma^2 n\bar{c}$$

The conception of a collision between two molecules which we must employ, is an encounter such that the phase of the molecules is sensibly altered

molecule and letting $\epsilon=\alpha(4.77)\times10^{-10}$ we find $\Delta\nu=\alpha^2(1.1)\times10^{9}$. Remembering that α is less than unity (about 1/5 for HCl) it will be seen that the broadening due to damping is far smaller than attributable to effect (d), in fact by a factor of about 10^8.

[2] J. Holtsmark, Physik. Zeits. **25**, 73 (1924).

[3] L. Mensing, Zeits. f. Phys. **34**, 611 (1925).

leading to a limitation in the length of the wave train being absorbed.[4] The effective molecular diameter σ is the distance to which two molecules may approach without changing each others phases. It will presumably be of the order of magnitude generally found for molecular diameters and we may estimate it to have the value 5×10^{-8} cm. Setting this in we obtain $\bar{t}=2\times10^{-10}$ sec. The width of the line is then of the order $\Delta\nu=5\times10^{9}$ waves per sec. and corresponds in the HCl spectrum to about one hundredth the distance between consecutive lines. While this is from five to ten times smaller than the apparent width as observed by Imes[5] and others, we shall show that it is capable of explaining the experimental curves when the low spectrometer resolution is taken into account.

1. The Equations Governing the Absorption

As a rough approximation we might, as in the introduction, let t be the average time between collisions. A more exact expression may, however, be obtained by putting in the proportion of molecules whose time between collisions lies between t and $t+dt$ and finally integrating over all values of t. The following expressions are well known from the kinetic theory of gases.

The proportion of molecules of velocity c having a path length lying between l and $l+dl$ is $e^{-l/\lambda_c}\,dl/\lambda_c$ where λ_c, the mean path length is given by,

$$\lambda_c = hmc^2/\pi^{1/2}n\sigma^2\psi(ch^{1/2}m^{1/2})$$

with

$$\psi(x)=xe^{-x^2}+(2x^2+1)\int_0^x e^{-y^2}dy$$

Here n is the number of molecules per unit volume, m the mass of each molecule and $h=1/2kT$.

The proportion of molecules of velocity c having a time between collisions lying between t and $t+dt$ is evidently $e^{-ct/\lambda_c}\,cdt/\lambda_c$ and the proportion of all molecules having a time between collisions lying between t and $t+dt$ is,

$$N_t=4h^{3/2}m^{3/2}\pi^{-1/2}\int_{c=0}^{\infty} e^{-hmc^2-ct/\lambda_c}(c^3/\lambda_c)dtdc$$

Let the total intensity with which light of frequency ν is absorbed by molecules of proper frequency ν_0 be proportional to P_ν where P_ν is the extinction coefficient of the gas, expressed as a function of the frequency.

$$P_\nu=\int_0^\infty I_{\nu t}N_t dt=\kappa\int_0^\infty\int_0^\infty e^{-hmc^2-ct/\lambda_c}\frac{c^3\sin^2(\nu_0-\nu)\pi t}{\lambda_c(\nu_0-\nu)^2}dcdt$$

[4] Clearly the whole calculation is founded upon the approximation usually employed in the kinetic theory of gases, namely that the molecules are impenetrable spheres of diameter σ, and may be expected to hold only in the region where the time between collisions is very much longer than the time of a collision.

[5] E. Imes. Astrophys. Jour. **50**, 251 (1919).

The integration with respect to the time may be performed immediately giving,

$$P_\nu = 2\pi^2\kappa \int_0^\infty \frac{e^{-hmc^2}c^2dc}{(c^2/\lambda^2)+4\pi^2(\nu_0-\nu)^2}$$

By making the substitution $x^2=hmc^2$ we obtain,

$$P_\nu = \kappa' \int_0^\infty \frac{e^{-x^2}x^2dx}{(n^2\sigma^4\psi^2/4\pi hmx^2)+(\nu_0-\nu)^2} \tag{1}$$

It is customary to designate the integral of the absorption coefficient P_ν over all frequencies as α the total intensity of absorption.[6]

$$\alpha = \int_0^\infty P_\nu d\nu = \kappa' \int_0^\infty \int_0^\infty \frac{e^{-x^2}x^2dxd\nu}{(n^2\sigma^4\psi^2/4\pi hmx^2)+(\nu-\nu_0)^2}$$

$$= 2\pi(\pi hm)^{1/2}(\kappa'/n\sigma^2)\int_0^\infty e^{-x^2}(x^3/\psi(x))dx.$$

This last integral has already been evaluated by numerical quadrature.[7] Solving for k' we find,

$$\kappa' = (2n\sigma^2\alpha/0.650\pi^{3/2}h^{1/2}m^{1/2})$$

Eq. (1) cannot be evaluated except by means of numerical quadrature. A large number of points found in this way shows, however, that the function,

$$y = \int_0^\infty \frac{x^2e^{-x^2}dx}{(\psi^2/x^2)+z^2}$$

may be represented with an accuracy greater than one per cent by means of the two equations:

$$y = (0.411/6.67+z^2) \text{ from } z=0 \text{ to } z \leqq 3$$

and

$$y = (0.440/7.60+z^2) \text{ from } z \leqq 3 \text{ to } z=\infty$$

Consequently the absorption coefficient P_ν may be represented by

$$P_\nu = (1.244\alpha n\sigma^2/\pi^{3/2}h^{1/2}m^{1/2})\frac{1}{(6.67n^2\sigma^4/4\pi hm)+(\nu-\nu_0)^2} \tag{1}'$$

from $\nu-\nu_0=0$ to $\nu-\nu_0 \leqq (3n\sigma^2/2\pi^{1/2}h^{1/2}m^{1/2})$ and

[6] To integrate this function with respect to the frequency ν, we replace $\nu-\nu_0$ by y and integrate between the limits $+\infty$ and $-\infty$. This procedure involves a certain approximation since while the upper limit of y is $+\infty$, its lower limit is really $-\nu_0$, but no appreciable error will be introduced since the integrand has become vanishingly small in this region. These remarks will also apply to some of the integrations which follow.

[7] Tait, Edin. Trans. **33,** 74 (1886).

$$P_\nu = (1.353\alpha n\sigma^2/\pi^{3/2}h^{1/2}m^{1/2})\frac{1}{(7.60n^2\sigma^4/4\pi hm)+(\nu-\nu_0)^2} \qquad (1)''$$

from $\nu-\nu_0 \cong (3n\sigma^2/2\pi^{1/2}h^{1/2}m^{1/2})$ to $\nu-\nu_0=\infty$. A certain test of the accuracy with which P_ν is represented by these relations may be found by integrating them over all frequencies when it is found that,

$$\int_0^\infty P_\nu d\nu = (1.000)\alpha$$

The absorption coefficient P_ν may be taken as representing the true shape of the spectral line where the transmission curve of such a line as determined by a spectrometer of infinitely high resolving power would be,

$$T_\nu = e^{-P_\nu l} \qquad (2)$$

where l is of course the length of the absorption chamber.

The experimental measurements of the infra-red lines which have been made up to the present, however, have been made with instruments of low resolving power, where indeed the region of irresolution has been considerably greater than the true width of the line as given by Eq. (2). It is evident that the observed transmission curve will be intimately connected with the degree of resolution, that is, it will be governed by the broadness of the spectrometer slits as well as by the number of lines of the grating used.

Essentially the infra-red spectrometer (for example, that used by Imes) has the form shown in Fig. 1, where the light after passing through the

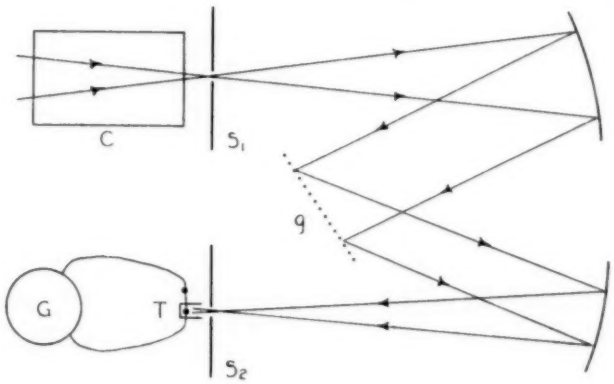

Fig. 1

absorption cell C is defined by a slit s_1, of width a. After being diffracted by the grating g, it passes through a further slit s_2 of width b and falls upon the thermopile T. We may now define the resolution of the spectrometer by saying that the intensity with which the thermopile receives a frequency ν is ρ_{ν_i} where ν_i is the computed frequency falling on the thermopile, (i.e. that frequency which the thermopile would receive if the spectrometer had an infinitely high degree of resolution). The percentage transmission recorded by the instrument at the frequency ν_i is now

$$T_{\nu_i}=\frac{\int_0^\infty \rho_{\nu_i} e^{-P\sigma l} d\nu}{\int_0^\infty \rho_{\nu_i} d\nu} \tag{3}$$

The form of ρ_{ν_i} is dependent upon the resolution of the grating and upon the widths of the slits s_1 and s_2. Assuming the intensity of the source of radiation to be independent of the frequency, that is, that the background is uniform over the region of the line, we may consider two separate cases.

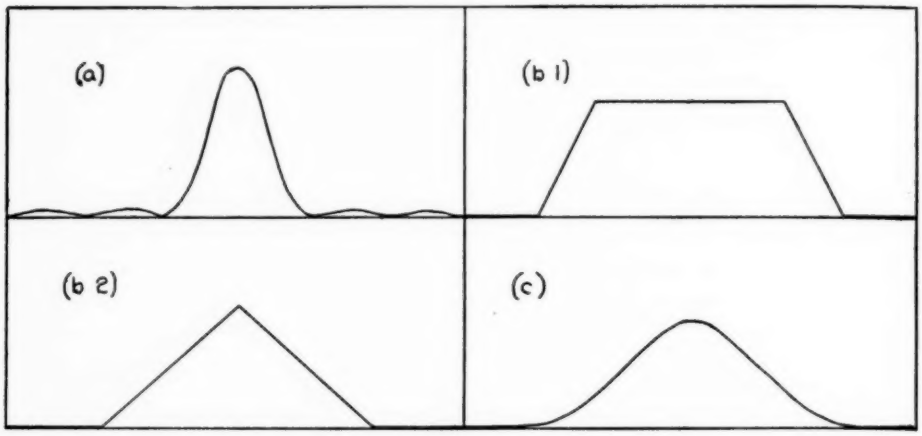

Fig. 2

(a) Let the slits be both infinitely narrow, in which case ρ_{ν_i} is determined by the number of lines of the grating used, m, and the order of the spectrum, n. From optical theory we have the following expression for ρ_{ν_i} which is reproduced in Fig. 2(a).

$$\rho_{\nu_i}=\frac{\sin^2\{(\nu_i-\nu)\pi mn/\nu_i\}}{(\nu_i-\nu)^2}$$

The degree of resolution of the grating has been defined as the distance from the central maximum to the first minimum.

$$\delta\nu=\nu_i/mn$$

(b) The second case which we may consider is that where the grating has perfect resolution, $m=\infty$ but where the slits have a finite width. In general, we might suppose them to be unequal with $a>b$. It may then be shown that ρ_{ν_i} is constant from

$$\nu=\nu_i-a/2+b/2 \text{ to } \nu=\nu_i+a/2-b/2$$

from which points it decreases linearly to zero at $\nu_i+(a+b)/2$ and $\nu_i-(a+b)/2$ respectively, as pictured in Fig. 2 (b1). When the two spectro-

meter slits are made equal, $a=b$, the distribution ρ_{ν_i} assumes the triangular form shown in Fig. 2 (b2).

It appears that in most of the work done in the infra-red region, the degree of resolution of the grating is higher than that afforded by the width of the slits. Imes, for example, gives the figures

$$\delta\nu = 0.39\times 10^{10} \text{ waves per sec.}$$

whereas he states that at the center of the HCl band

$$a=b=7.3\times 10^{10} \text{ waves per sec.}$$

It seems very probable, therefore that ρ_{ν_i} has a form similar to Fig. 2 (b2) but rather softened by the irresolution of the grating as shown in Fig. 2 (c). Such a curve appears to be very similar to a Gauss error curve and various estimates show that the Gauss curve may be used for ρ_{ν_i} without introducing any considerable errors. In this case we let

$$\rho_{\nu_i} = e^{-(\nu_i-\nu)^2(2.77)/a^2} \tag{4}$$

where the constant 2.77 is introduced in order that the half-value of ρ_{ν_i} may coincide with the corresponding point of the curve b (2). Setting this value into Eq. (3) we have

$$T_{\nu_i} = (2.77/\pi a^2)^{1/2} \int_0^\infty e^{-P_\nu l - 2.77(\nu_i-\nu)^2/a^2} d\nu \tag{5}$$

This expression, with the aid of Eqs. (1)′ and (1)″ defining P_ν, determines the shape and intensity of the observed absorption lines and may be evaluated by numerical quadrature. A particular value of the transmission, namely its minimum value, can be expressed as an explicite function of the constants by introducing an approximation for P_ν. For lines where the maximum absorption is not too small, an examination of the magnitude of the constants shows that (1)′ and (1)″ may be replaced by

$$P_\nu = \frac{1.353\alpha n\sigma^2}{\pi(\pi hm)^{1/2}(\nu-\nu_0)^2} \tag{1}'''$$

The validity of this approximation rests on the fact that for small values of $\nu-\nu_0$ where (1)‴ is sensibly different from (1)′ and (1)″, the integrand of (5) has already become vanishingly small. In the last section of this paper the errors of the approximation (1)‴ will be discussed. Using the above substitution the observed transmission at the point ν_i will be

$$T_{\nu_i} = (2.77/\pi a^2)^{1/2} \int_0^\infty exp.\left[-\frac{1.353\alpha n\sigma^2 l}{\pi(\pi mh)^{1/2}(\nu-\nu_0)^2} - \frac{2.77(\nu-\nu_i)^2}{a^2}\right] d\nu \tag{5}'$$

This equation determines the shape of the line and may be integrated at the center of the line where $\nu_i=\nu_0$. The minimum value of the transmission is accordingly,

$$T_{min} = exp.\left[-2(1.194\alpha n\sigma^2 l)^{1/2}/a(\pi hm)^{1/4}\right] \tag{6}$$

or taking the logarithm of $T_{\min}$ to the base 10 we find,

$$(\log_{10} T_{min})^2 = 0.520\alpha n\sigma^2 l/a^2(hm)^{1/2} \qquad (6)'$$

An expression for the total area under the absorption curve, Abs, may be obtained which will be found to be independent of the form of ρ_{ν_i}.

$$Abs = \int_0^\infty (1-T_{\nu_i})d\nu_i = \int_0^\infty \left\{1 - \int_0^\infty \rho_{\nu_i} e^{-P\nu l} d\nu \Big/ \int_0^\infty \rho_{\nu_i} d\nu\right\} d\nu_i$$

In general the distribution of frequencies reaching the thermopile will be symmetrical about ν_i and will depend only upon the absolute magnitude of $\nu - \nu_i$. In that case we may integrate the second member on the right hand side of the equation with respect to ν_i and obtain,

$$Abs = \int_0^\infty d\nu_i - \int_0^\infty e^{-P\nu l} d\nu$$

The variable ν_i may now be changed to ν without altering the value of the expression. The final integration may be readily performed if we use the approximate expression $(1)'''$ for P_ν.

$$Abs = (5.412\alpha n\sigma^2 l)^{1/2}/(\pi hm)^{1/4} \qquad (7)$$

By combining Eqs. $(6)'$ and (7) we may obtain a relation between the area under the absorption curve, the maximum value of the absorption and the slit width a.

$$Abs/\left|\log_{10} T_{min}\right| = 2.42a \qquad (8)$$

Eq. (6) has been found by introducing into (3) a simplified expression for P_ν and for ρ_{ν_i}, the Gaussian error curve. An idea of the sensativeness of (3) to the form of ρ_{ν_i} may be gained by assuming that the grating employed has infinitely good resolution and that the slits s_1 and s_2 have the same width, a. That is, we may use instead of the error curve, the triangular intensity distribution shown in Fig. 2 (b2). We then have

$$T_{\nu_i} = \int_{\nu_i - a}^{\nu_i} (a - \nu_i + \nu) e^{-P\nu l} d\nu \Big/ \int_{\nu_i - a}^{\nu_i} (a - \nu_i + \nu) d\nu$$

In the particular case of the center of the line, where $\nu_i = \nu_0$ and where we use the approximate expression $(1)'''$ for P_ν we find,

$$T_{min} = (2/a^2) \int_0^a (a - x) e^{-p^2/x^2} dx \qquad (9)$$

where $x = \nu - \nu_0$, and $p^2 = 1.353\alpha n\sigma^2 l/\pi(\pi hm)^{1/2}$. This definite integral may be expanded in a series which is rapidly convergent for values of $p/a \leqq 1$.

$$T_{min}=e^{-p^2/a^2}-3.545(p/a)\left\{1-(2/\pi^{1/2})\int_0^{p/a}e^{-x^2}dx\right\}$$
$$+(p^2/a^2(\log(a^2/p^2)-0.5772)+p^4/a^4-p^6/2\cdot 2!a^6$$
$$+p^8/3\cdot 3!a^8-\cdots \qquad (9)'$$

A comparison of (6) and (9)′ shows that the two are in almost perfect agreement for values of $T_{\min}$ between 1. and 0.5 (i.e., between zero and fifty percent absorption), at $T_{\min}=0.3$ the divergence is about 1 percent at 0.1 about 5 percent and even below this the divergence is not very great.

The substantial agreement between Eqs. (6) and (9)′ over the majority of their ranges shows that in interpreting most of the observed infra-red absorption lines, we may employ either the Gaussian or the triangular distribution for ρ_{ν_i} without introducing serious errors.

2. The Analysis of Experimental Absorption Curves

We propose to apply the equations developed in the preceding section to an analysis of the infra-red spectrum of HCl.[8] Although a great many observations of these lines have been made, the majority are unsuited to our purpose since they were made with the intention of determining the positions of the lines with great accuracy rather than their intensities.

A set of measurements which appears to be very satisfactory as regards the determination of intensity was taken by Dr. R. F. Paton[9] and I am greatly indebted to him for the use of his original data and curves. Paton observed the infra-red spectrum of HCl for three different temperatures of the gas, 20°C, 100°C, and 250°C, using the same spectrometer arrangement that Imes had used but with somewhat shorter absorption cells. The curves taken at the lower temperatures present a series of regular lines between which the absorption falls to a low value if not completely to zero. The third curve taken at 250°C shows several obvious irregularities in the absorption intensities presumably due to the greater experimental difficulties involved and we shall accordingly confine our attention to the lower temperature curves.

Many sources of error tend to make an accurate determination of the form of the absorption lines very difficult and a study of Paton's data reveals that the areas of absorption deduced from his curves may be in error by amounts of the order of 10 percent. The very faint lines at either end of the band have not been included in the present analysis since both the observational error is greatest for them and also the approximation of Eq. (1)‴ for P_r will hold least well.

The observed spectrum of HCl at 20°C, plotted as a function of the relative absorption and θ the angle of the grating was planimetered and the

[8] A certain error will no doubt exist since the HCl lines are not single as demanded by our theory but each is accompnaied by a weaker satellite due to the isotope effect of the Cl. The effect of two lines close together is, in first approximation at least, merely additive as the consistency and freedom from systematic error of our results show.

[9] R. F. Paton, Phys. Rev. **15**, 541 (1920).

areas under each line in the square unit of relative absorption times grating angle appear in the second column of Table I. The third column contains $T_{\min}$, the value of the relative transmission at the center of the line and the fourth column shows the absorption area divided by the absolute value of the logarithm of $T_{\min}$ to the base 10. The values in column four appear to be

TABLE I

Calculations based on Paton's absorption curves for HCl at 20°C. Tube length = 4 cm; temperature = 20°C; atmospheric pressure.

Line No.	Abs×10²	$T_{\min}$	Abs×10² / $-\log_{10} T_{\min}$	Abs	$K\alpha$	Abs / $(K\alpha)^{1/2}$
−8	3.28	0.49	11.1	2.36	0.236	4.85
−7	5.43	.32	11.0	4.01	.460	5.92
−6	7.58	.20	10.8	5.71	.786	6.45
−5	8.65	.16	10.9	6.65	1.184	6.10
−4	10.32	.115	11.0	8.11	1.560	6.49
−3	9.51	.10	9.51	7.71	1.722	5.87
−2	8.71	.14	10.2	7.10	1.524	5.75
−1	6.56	.20	9.3	5.43	.920	5.66
+1	7.80	.165	10.0	6.71	.975	6.80
+2	10.11	.10	10.1	8.83	1.720	6.73
+3	9.14	.10	9.1	8.12	2.055	5.66
+4	8.34	.10	8.3	7.51	1.96	5.37
+5	7.42	.13	8.4	6.78	1.59	5.37
+6	7.26	.205	10.6	6.71	1.114	6.35
+7	5.49	.30	10.5	5.14	.688	6.20
+8	3.55	.45	10.3	3.37	.365	5.59

nearly constant in agreement with Eq. (8) and the non-systematic variations which do occur may without doubt be ascribed to the experimental errors. By setting the average value, 10.1, into Eq. (8) we obtain the slit width a in terms of the grating angle θ, or from the grating equation in terms of frequency.

$$\delta\theta = 2.50' \; ; \qquad \delta\nu = 10.5\times 10^{10}$$

Paton does not explicitly give the slit width that he used but the above values are of the correct order of magnitude. It appears at first a little strange that our computed value for $\delta\nu$ is somewhat larger than Imes' slit width of 7.3×10^{10}, whereas a general inspection of Imes' and Paton's curves indicates that the latter must have used the same if not narrower slits. The explanation for this probably lies in the fact that the real distribution of intensity ρ_{ν_i} entering the thermopile may be somewhat larger than the ρ_{ν_i} computed from the slit widths due to inaccuracies in the focus or in the optical system.

The fifth column of Table I contains the area under each band line in the units of relative absorption times waves per cm. This may readily be found from the grating equation, the frequency being taken sensibly constant over the region of each line.

$$\lambda = K \sin\theta \; ; \; \delta\nu = \left[K^2\nu^4 - \nu^2\right]^{1/2}\delta\theta$$

where $K = 6.7682\mu$ according to Paton's data.

The sixth column of Table I contains numbers proportional to the theoretical intensities of the fundamental vibration rotation band lines of HCl at a temperature of 20°C as computed by a method to be described in the next paragraph. From Eq. (7) the total area of absorption is seen to be proportional to the square root of α, the true intensity of the line. Accordingly the value of $Abs/(k\alpha)^{1/2}$ has been tabulated (column seven) and appears to be constant within the limits of error. Here, as in the fourth column of the table, it is very satisfactory that the divergences from constancy are of the accidental sort and are not systematic.

The theoretical intensities will be given by the following relation[10]

$$\alpha_j{}^i = 2\pi^3 N_i \nu_j{}^i g_j (\epsilon a_i{}^j)^2 / 3hcg_i$$

where the intensity $\alpha_j{}^i$ is the integral of the absorption coefficient over the region of the line corresponding to a transition from the ith to the jth quantum state. N_i is the number of molecules in the ith state, $\nu_j{}^i$ the frequency of the transition and g_j and g_i are the weights of the jth and ith states respectively. $\epsilon a_i{}^j$ is the amplitude of the electric moment of a transition from the jth to the ith states which before the advent of the new mechanics had to be taken as some undetermined mean of the classical amplitudes in these two states.

Oppenheimer[11] has derived, on the basis of the matrix mechanics, the amplitudes of the lines in the fundamental band of an anharmonic vibrator rotator and gives, (under a somewhat different notation)

$$\left(a^{\,1\ \ m-1}_{\,0\ \ m}\right)^2 = \frac{h}{2\pi^2\mu\nu_0}\left(\frac{m}{2m-1}\right)\left(1+4\gamma m\left(1+\frac{5}{8}\gamma m-\frac{3}{8}\gamma\right)\right)$$

$$\left(a^{\,1\ \ m}_{\,0\ \ m-1}\right)^2 = \frac{h}{2\pi^2\mu\nu_0}\left(\frac{m}{2m+1}\right)\left(1-4\gamma m\left(1-\frac{5}{8}\gamma m-\frac{3}{8}\gamma\right)\right)$$

where $\qquad m=1,\ 2,\ 3,\ \cdots;\quad$ and $\quad \gamma = h/4\pi^2 I\nu_0$

I is the moment of inertia of the unexcited molecule and ν_0 the normal frequency of vibration.

These quantities may be substituted into equation (10) giving for example the intensities of the lines in the negative branch.

$$\alpha^{0m}_{1m-1} = \frac{\pi\epsilon^2 nme^{-Wm/kT}F}{3c\mu\sum_0^\infty (2m+1)e^{-Wm/kT}}$$

where

$$F = \frac{\nu^{0m}_{1m-1}}{\nu_0}\left(1+4\gamma m\left(1+\frac{5}{8}\gamma m-\frac{3}{8}\gamma\right)\right)$$

$$g_m = 2m+1$$

[10] See for example D. M. Dennison, Phil. Mag. 1, 195 (1926).
[11] J. R. Oppenheimer, Proc. Camb. Phil. Soc. 23, 327 (1926).

and

$$N_m = \frac{n(2m+1)e^{-W_m/kT}}{\sum(2m+1)e^{-W_m/kT}}$$

In the sixth column of Table I we have tabulated the values of $K\alpha$,[12]

$$K\alpha = me^{-W_m/kT}F \tag{11}$$

using the work of Colby, Meyer, and Bronk[13] to determine the energy and the frequencies entering F. The constant K has then the value,

$$K = 3c\mu \sum_0^\infty (2m+1)e^{-W_m/kT}/\pi\epsilon^2 n \tag{12}$$

Kemble and Bourgin[14] have arrived at values for the true absorption α by observing the lines with a series of different absorption cells of varying length. They plotted the integral of the apparent absorption coefficient over the line against the cell length and extrapolated to zero cell length. This procedure may be justified by remembering that if the cell length is short and the absorption small, the apparent absorption coefficient $\log T_{\nu_i}/l$ may be replaced by $(1-T_{\nu_i})/l$. Its integral over the line we have shown to be

$$(1/l)\int_0^\infty (1-T_{\nu_i})d\nu_i = (1/l)\int_0^\infty (1-e^{-P_\nu l})d\nu$$

If l is very small $e^{-P_\nu l}$ may be developed and only the first two terms retained giving,

$$(1/l)\int_0^\infty P_\nu l d\nu = \alpha$$

by definition.[15]

In Table II we have given in the second column our values of $K\alpha$ and in the third column, the experimental values of α as observed by Kemble and Bourgin. The last column, the quotient of the two preceding columns is seen to be very nearly constant with an average value of, $K = 4.00\times10^{-12}$.[16]

[12] A corresponding expression $K\alpha = F'me^{-W_{(m-1)}/kT}$ gives the intensities of the lines of the positive branch.

[13] Colby, Meyer, and Bronk, Astrophys. Journ. **57**, 7 (1923).

[14] E. C. Kemble and D. G. Bourgin, Nature **117**, 789 (1926).

[15] In Eq. (7) we have shown $\int_0^\infty (1-T_{\nu i})d\nu_i$ to be proportional to the square root of α instead of to α as here. This is of course due to the fact that Eq. (7) is based on an approximate expression for $P_\nu l$ which does not hold when the maximum value of $P_\nu l$ is small.

[16] In a recent paper (Phil. Mag. **1**, 195, 1926) the author attempted to compute the effective charge ϵ through the absolute absorption of the near infra-red bands. His estimates of the absorption were considerably too small due to the influence of the large slit widths used by the experimenters. The value of ϵ may now be more accurately computed by means of Eq. (12) using $K = 4.00\times10^{-12}$. This yields $\epsilon = (0.199)\times4.77\times10^{-10}$ E.S.U., which may be compared with the effective charge ϵ' obtained by dividing the permanent electric moment

TABLE II

Line No.	$K\alpha$	$\alpha\times10^{-10}$	$K\times10^{12}$
−6	0.786	22.55	3.49
−5	1.184	29.62	3.99
−4	1.560	37.62	4.15
−3	1.722	41.25	4.17
−2	1.524	37.48	4.06
−1	.920	23.78	3.87
+1	.975	24.50	3.98
+2	1.720	41.8	4.11
+3	2.055	49.0	4.20
+4	1.96	47.0	4.17
+5	1.59	37.9	4.20
+6	1.114	26.6	4.19
+7	.688	16.32	4.21
+8	.365	9.06	4.03
+9	.182	4.60	3.96
+10	.0768	2.35	3.27

We are now in a position to compute σ, the effective diameter of the HCl molecule. The average value of the seventh column of Table I is 5.95, whence, in waves per second,

$$Abs/\alpha^{1/2}=11.9\times10^{-6}\times3\times10^{10}$$

Introducing this value into Eq. (7) we find

$$\sigma=10.6\times10^{-8}\text{cm}$$

The value for σ just obtained is essentially larger than the distance between the nuclei which from band spectra data has been found for HCl to be 1.26×10^{-8} cm.[17] This result is by no means inconsistent with our theory since the diameter σ entering our equations is that minimum distance to which a molecule may approach another molecule without altering its phase, that is, without interrupting its wave train. It is very probable that for a highly dipol molecule such as HCl, σ will be considerably greater than the nuclear separation. Before discussing this question further, we shall proceed to examine Paton's second curve.

This curve, taken at the temperature of 105°C, contains somewhat more lines than the 20°C curve, and is represented by the data in Table III. The fourth column seems again to be sensibly constant and has the average value 8.7, yielding the following values for the slit width expressed in degrees or in waves per second.

$$\delta\theta=2.16'\ ;\ \delta\nu=9.1\times10^{10}$$

by the distance between the nuclei. Using C. T. Zahn's (Phy. Rev. **24,** 400 (1924)) measurements of the electric moment, we find $\epsilon'=1.03\times10^{-18}/1.265\times10^{-8}=(0.171)\times4.77\times10^{-10}$. While these two values ϵ and ϵ' are of the same order of magnitude, there is no reason to suppose that they should be exactly equal since they are a measure of quite different properties of the molecule for which the "effectiveness" of the true distribution of charge need not be the same.

[17] The molecular diameter as determined from viscosity measurements is of course also much larger than the nuclear separation and has a value of about 5×10^{-8} cm.

Patons' data do not show any evidence of the spectrometer or slit adjustment being changed between the taking of the 20° and the 105° curve although the difference between 2.50′ and 2.16′ seems a little too great to be wholly attributable to the experimental error in the curves.

The fifth column of Table III contains the area under the absorption curve measured in relative absorption times waves per cm and the sixth column has a set of values proportional to the theoretical intensities as defined

TABLE III

Tube length = 6 cm; temperature = 105°C; atmospheric pressure.

Line No.	Abs×10²	T_{min}	$\frac{\text{Abs}\times 10^2}{-\log_{10} T_{min}}$	Abs	$K\alpha$	$\frac{\text{Abs}}{(K\alpha)^{1/2}}$
−10	2.10	.59	9.2	1.45	.140	5.61
−9	3.12	.44	8.8	2.20	.278	5.92
−8	4.35	.35	9.5	3.15	.505	6.13
−7	5.48	.25	9.1	4.06	.827	6.03
−6	6.08	.14	7.1	4.59	1.233	5.47
−5	8.23	.14	9.6	6.34	1.634	6.44
−4	8.50	.11	8.9	6.69	1.930	6.11
−3	8.71	.12	9.5	6.99	1.961	6.21
−2	7.80	.135	9.0	6.36	1.624	6.11
−1	6.30	.175	8.3	5.23	.937	6.51
+1	5.21	.19	7.2	4.48	.975	5.28
+2	7.80	.12	8.5	6.83	1.753	5.89
+3	8.45	.10	8.5	7.50	2.190	5.70
+4	8.77	.11	9.2	7.90	2.230	5.87
+5	8.28	.135	9.5	7.55	1.965	5.90
+6	5.97	.20	8.6	5.53	1.538	4.81
+7	5.16	.25	8.5	4.83	1.080	4.97
+8	2.96	.42	7.9	2.81	.655	3.66
+9	1.88	.56	7.5	1.80	.389	3.02
+10	1.77	.66	9.8	1.72	.203	3.93

by Eq. (11). In computing the molecular diameter from the average value 5.48 of the seventh column we must remember that K, the proportionality factor, is a function of the temperature. In fact from equation (12),

$$\frac{K_1}{K_2}=\frac{n_2\sum_0^\infty(2m+1)e^{-Wm/kT_1}}{n_1\sum_0^\infty(2m+1)e^{-Wm/kT_2}}$$

from which we obtain the value,

$$K_{378}=(1.65)K_{293}=6.62\times10^{-12}$$

The absorption area divided by the theoretical intensity is then given by

$$Abs/\alpha^{1/2}=14.1\times10^{-6}\times3\times10^{10}\text{ waves/sec.}$$

The molecular diameter may be computed as before through the use of Eq. (7); we obtain

$$\sigma = 11.0 \times 10^{-8} \text{ cm}$$

in good agreement with the value previously determined from the 20°C curve.

3. Discussion

The very satisfactory manner in which the equations of §1 have interpreted the experimental curves of Paton leaves little doubt but that they are of the correct general form. The agreement of itself however does not guarantee the correctness of the meanings we have given to the constants of the formulae. From the fact that the molecular diameter of HCl as computed from the observed absorption, is of the expected order of magnitude we may conclude that the limitation of wave trains due to collisions is at least one of the principal factors in broadening the absorption lines. On the other hand the interaction of elastic spheres upon which conception the equations of §1 are based would appear to be somewhat inadequate to describe the state of the gas except in the limiting case where the mean free path λ is very long compared with σ. A simple computation shows that this is hardly true in the experiments of Paton, for $\lambda/\sigma = 1/2^{1/2}\pi n\sigma^3$, whence, substituting the value of σ and n, the number of molecules per unit volume, we find, $\lambda/\sigma \leqq 9$. A series of observations of the absorption with the gas at reduced pressure would indicate with what accuracy our value of σ represents the effective distance to which two molecules may approach without perturbing each others wave trains.

Leaving the question of the interpretation of the constants and returning to the assumption that our formulae give the correct form of the absorption we notice that Eqs. (6)′ and (7) should be of very general use since they allow us to compare the relative intensities of a set of lines. A correction term may be applied to Eq. (7) for analyzing absorption curves whose maximum absorption is small. Eq. (7) is based on the approximate expression (1)‴ for P_ν and has the form,

$$Abs = \int_{-\infty}^{+\infty} (1 - e^{-a^2/x^2}) dx = 2a\pi^{1/2}$$

where $a^2 = 1.353\alpha n\sigma^2 l/\pi(\pi hm)^{1/2}$.

For absorption lines whose maximum value of P_ν l is not large we must represent P_ν by Eq. (1)″ in which case we obtain the following approximate expression for the absorption area.[18]

[18] An exact calculation would of course involve both Eqs. (1)′ and (1)″ but the error introduced by using Eq. (1)″ alone will certainly not be appreciable in the first order correction terms and probably not even in the second.

$$Abs = \int_{-\infty}^{+\infty} (1 - e^{-a^2/(b^2+x^2)})\,dx \tag{13}$$

$$= 2a(\pi)^{1/2}\left(1 - \frac{b^2}{4a^2} - \frac{3}{32}\frac{b^4}{a^4} - \cdots\right) + \left(\frac{11}{8}\frac{b^3}{a^2} + \cdots\right)e^{-a^2/b^2}$$

where

$$b^2 = 7.60n^2\sigma^4/4\pi hm$$

Substituting the values of the constants we find that the corrections to the data of Table I are within the experimental error, for example, the correction to the strong lines such as +3, is about 0.3% whereas the largest correction (to the weakest line, −8) is only 2.7%. No doubt errors of this same order of magnitude are incurred by using the approximation (1)''' to obtain Eq. (6)', the relative transmission at the center of the line.

No attempt has been made in the present paper to compare the observed shapes of the absorption lines with the shape determined by Eq. (5) since the experimental observations now available do not appear to be sufficiently accurate to make such a comparison fruitful. A few points have, however, been computed by numerical quadrature for a particular line and these agree with the observed points to within the experimental error.

DEPARTMENT OF PHYSICS,
UNIVERSITY OF MICHIGAN,
November 26, 1927.

Note added in proof. February 28, 1928. Unfortunately no discussion has been included in the above paper of a very interesting article by D. G. Bourgin (Phys. Rev. V. **29**, p. 794, (1927)) which gives a detailed exposition of the experimental work underlying the Bourgin and Kemble letter to Nature (l.c.). These new data appear to be completely in accord with the theoretical formulae we have developed. In Table I, Bourgin gives the variation of the absorption area with tube length which may be compared with our Eq. (13). Selecting two representative lines +1 and +4, we construct the following table where the second and fourth columns contain Bourgin's values converted into the units of relative absorption times waves per cm and the third and fifth columns the corresponding computed values letting $\sigma = 10.8 \times 10^{-8}$ cm. The agreement is satisfactory.

Tube length	+1 Abs	Comp.	+4 Abs	Comp.
2.97	4.81	5.27	6.28	7.17
.996	3.13	2.97	4.35	4.08
.54	2.34	2.14	3.38	2.63
.248	1.42	1.38	2.15	1.96
.169	1.08	1.06	1.64	1.57
.0988	.725	.737	1.16	1.11

In Fig. 6A, Bourgin shows the change in maximum absorption coefficient for the line $+3$ with tube length. His curve appears to fall very close to the values predicted by our Eq. (6) if the spectrometer slit width is taken as $a = 14 \times 10^{10}$ waves/sec. Bourgin does not explicitly give the slit width in frequency units but from his Fig. 3 it appears to be of this order of magnitude.

Using the experimental intensities of the lines $+1$ and -1 together with the simple formula for the Einstein coefficients, Bourgin computes the effective moving charge to be $\epsilon = (.173) \times 4.77 \times 10^{-10}$. We believe our value of $\epsilon = (.199) \times 4.77 \times 10^{-10}$ to be somewhat more accurate since it is based on the mean of the experimental intensities of all the lines from -6 to $+10$, and since the theoretical formulae of Oppenheimer which we use take into account the perturbations between the anharmonic vibration and the rotation.

CERTAIN MULTIPLETS IN THE SPECTRA OF Cb III AND Cb IV*

By R. C. Gibbs and H. E. White

Abstract

Relative positions of certain multiplets in two and three electron systems of the second long period with wave-lengths for Zr III, Cb IV and Cb III.—Applying the irregular doublet law to the data already known for the triad of multiplets ^3DF, $^3DD'$, and ^3DP, (ds-dp) in the two electron systems of Sr I and Yt II, the corresponding multiplets for Zr III and Cb IV have been identified. Similarly the triad of multiplets $^4F'D'$, $^4F'F$, and $^4F'G'$(d^2s-d^2p) in the three electron systems of Yt I and Zr II has been extended to Cb III and the stronger lines of the $^4F'G'$ multiplet of Mo IV. In passing successively from element to element in both of these iso-electronic systems the shift in the frequency of the radiated lines for each of these multiplets is approximately constant.

IT HAS been shown, for certain sequences of iso-electronic systems in the first long period of the periodic table, that when an electron in a $4p$ orbit jumps to a $4s$ orbit in the presence of 0, 1, 2, or 3, etc., $3d$ electrons the resulting radiated frequencies follow very closely the irregular doublet law.[1]

In the second long period one should expect similar relations to hold for the transition of an electron from a $5p$ orbit to a $5s$ orbit, in the presence of $4d$ electrons. This we have found for a certain triad of multiplets in the two-electron systems Sr I, Yt II, Zr III, and Cb IV, and the three-electron systems Yt I, Zr II, and Cb III.

For the two-electron systems the transition $4d5p$ to $4d5s$ gives rise to the triad of triplets, $^3D_{1,2,3}-^3P_{0,1,2}$, $^3D_{1,2,3}-^3D'_{1,2,3}$, and $^3D_{1,2,3}-^3F_{2,3,4}$ which were already known for Sr I and Yt II. A linear extrapolation of the strongest radiated frequencies in these two elements (the irregular doublet law) was sufficient to determine the corresponding triplets in first Zr III, and then Cb IV. The triplets of Zr III were first identified by C. C. Kiess, the relative term values being kindly sent to the authors before publication. The wave-lengths and intensities of these multiplets, given in Table I, are from our own measurements. The term values, taken with respect to the limit toward which these terms converge, are only extrapolations based upon known relations with term values of other elements.

Two of the corresponding multiplets of Cb IV are given in Table II, the third one lying just outside the region of air transmission.

In the three-electron systems the transition $4d^25p$ to $4d^25s$ gives rise chiefly to the triad of quartets $^4F'_{2,3,4,5}-^4G'_{3,4,5,6}$, $^4F'_{2,3,4,5}-^4F_{2,3,4,5}$, and

* The assistance of a grant to the first author from the Heckscher Research Foundation of Cornell University which enabled us to obtain the results described in this report is gratefully acknowledged.

[1] R. C. Gibbs and H. E. White, Phys. Rev. **29**, 426, 655 (1927).

TABLE I

*Zirconium III triplets**

$(ds-dp)$ λ(air)

Term values	$^3D_3$ 183123.0	(730.4)	$^3D_2$ 183853.4	(404.3)	$^3D_1$ 184257.7
	40		10		2
	2448.90		2405.82		2382.64
$^3P_2$ 142300.6	40822.4		41553.4		41957.4
659.0			20		15
			2444.60		2420.67
$^3P_1$ 142959.4			40894.0		41298.4
248.3					10
					2406.19
$^3P_0$ 142711.0					41546.7
	50		40		
	2643.79		2593.69		
$^3D_3'$ 145309.8	37813.2		38543.6		
911.1	12		40		30
	2709.06		2656.48		2628.25
$^3D_2'$ 146220.8	36902.2		37632.5		38036.8
821.7			14		30
			2715.79		2686.29
$^3D_1'$ 147042.5			36810.9		37215.0
	100				
	2620.57				
$^3F_4$ 144974.8	38148.2†				
1606.3	40		40		
	2735.78		2682.17		
$^3F_3$ 146581.1	36541.9		37272.2		
519.6	3		10		30
	2775.24		2720.08		2690.50
$^3F_2$ 147100.7	36022.3		36752.6		37156.7

* Identified by C. C. Kiess. Wave-lengths and term values by authors. (See text)
† Kiess selected $\nu = 37522.6$ for this line. (Indicated by a dotted line in Fig. 1.)

$^4F'_{2,3,4,5} - {}^4D'_{1,2,3,4}$. Again making a linear extrapolation of frequencies from these quartets already known for Yt I and Zr II, all three multiplets for Cb III, Table III, have been determined as well as several of the stronger lines of the $^4F'G'$ multiplet for Mo IV.

The diagrams of Figs. 1 and 2 are drawn to show not only the linear progression of frequency with atomic number but also the relative intensities of the lines and the increase of the term separations in going from one element to the next. The exactness of this linearity of frequency with atomic number is more definitely shown by the differences appearing in the first, third, and fifth columns of Table IV. This linear relation, which constitutes the *irregular doublet law*, is to be expected whenever the transition of electrons involves a change in the azimuthal quantum number but no change in the total quantum number.

TABLE II

Columbium IV triplets
$(ds-dp)$ λ(air)

Term values	$^3D_3$ 290773.7 (1180.7)	$^3D_2$ 291954.4 (565.5)	$^3D_1$ 292519.9
	10	10	
	2084.06	2033.98	
$^3D_2'$ 242805.8	47967.9	49148.8	
1388.4	2	7	10
	2146.18	2093.12	2068.63
$^3D_3'$ 244194.2	46579.6	47760.3	48325.6
1397.9		5	7
		2156.24	2130.26
$^3D_1'$ 245592.1		46362.3	46927.8
	20		
	2032.49		
$^3F_4$ 241588.9	49184.8		
2609.2	10	10	
	2146.37	2093.29	
$^3F_3$ 244198.1	46575.6	47756.4	
661.4	3	5	3
	2177.29	2122.70	2097.51
$^3F_2$ 244859.5	45914.2	47094.9	47660.4

Using the interval rule Kiess selected for the transition $^3D_3-{}^3F_4$, in Zr III, the line at $\nu=37522.6$. This line gives for the intervals between the $^3F_{2,3,4}$ levels the ratio 981:520, the theoretical value being 4:3. Although the use

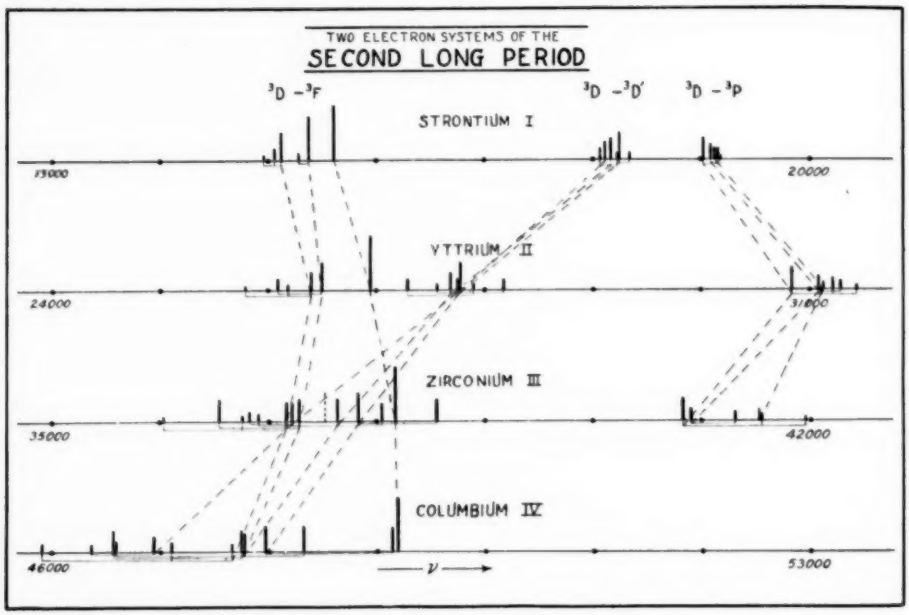

Fig. 1.

TABLE III

Columbium III quartets.
$(d^2s - d^2p)$ λ (air)

Term values	$^4F_5'$ 194142.9	(909.8)	$^4F_4'$ 195052.7	(728.4)	$^4F_3'$ 195781.1	(515.3)	$^4F_2'$ 196296.4
	100						
	2457.04						
$^4G_6'$ 153455.9	40687.0						
1605.2	30		80				
	2557.97		2499.77				
$^4G_5'$ 155061.1	39081.8		39991.6				
1449.4	2		25		70		
	2656.50		2593.78		2545.67		
$^4G_4'$ 156510.5	37632.4		38542.2		39270.6		
1319.7			2		15		60
			2685.75		2634.20		2598.91
$^4G_3'$ 157830.2			37222.5		37950.9		38466.2
	70		20				
	2413.96		2362.04				
$^4F_5$ 152729.8	41413.1		42323.0				
919.1	20		60		20		
	2468.75		2414.50		2372.75		
F_4 153648.9	40494.0		41403.8		42132.3		
773.6			40		50?		25
			2460.47		2417.13		2387.48
$^4F_3$ 154422.4			40630.3		41358.7		41872.4
595.6							60
					?		2421.93
$^4F_2$ 155019.6					40761.5		41276.8
	40		20		2		
	2313.39		2265.68		2228.89		
$^4D_4'$ 150929.6	43213.3		44123.1		44851.4		
307.3			25		15		2
			2281.56		2244.28		2218.61
$^4D_3'$ 151236.6			43816.1		44543.8		45059.1
606.4					25		10
					2275.26		2248.87
$^4D_2'$ 151843.7					43937.4		44452.8
490.1							20
							2273.95
$^4D_1'$ 152333.7							43962.7

of the stronger line at $\nu = 38148.2$ gives a still greater interval ratio it appears to fit into the frequency diagram of Fig. 1 much better than the dotted line at $\nu = 37522.6$.

Starting with the data for the stripped atoms of Sr, Yt, and Zr,[2] Table IV, it is seen that the screening effect due to the addition of first one and then a second $4d$ electron is to shift the spectral lines toward the longer wave-

[2] R. C. Gibbs and H. E. White, Proc. Nat. Acad. Sci., **12**, 551 (1926).

lengths by very nearly the same frequency interval, $\Delta\nu$ second and fourth columns, and at the same time to increase the multiplicity.

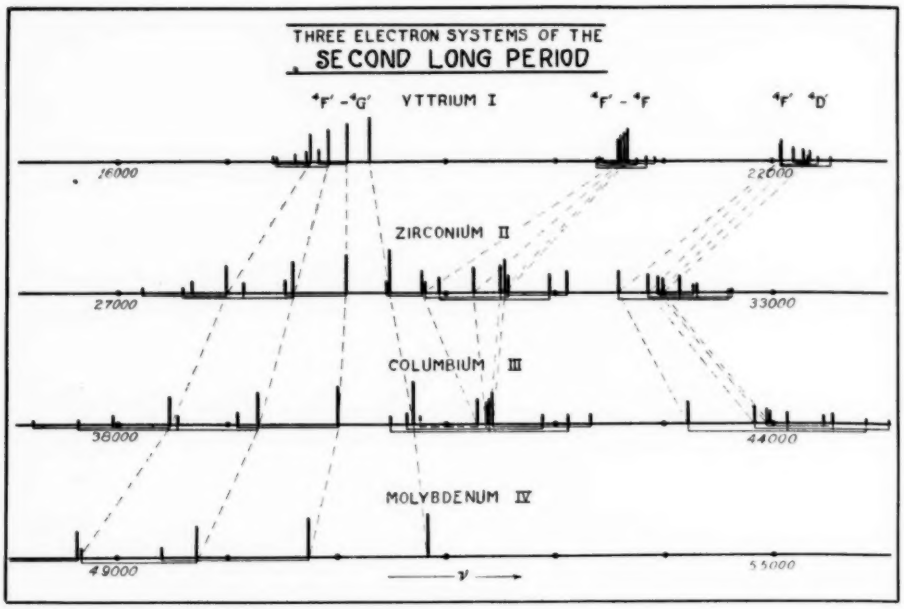

Fig. 2.

Since the known term values for Rb I, Sr I, and Sr II are nearly the same as those for the corresponding terms for K I, Ca I, and Ca II, we may reasonably expect the term values of Yt I, II, Zr II, III, Cb III, IV, and Mo

TABLE IV

Screening due to successive addition of "4d" electrons.

ν	$\Delta\nu$	ν	$\Delta\nu$	ν
$^2S_1-{}^2P_2$ $s-p$	*Screening*	$^3D_3-{}^3F_4$ $ds-dp$	*Screening*	$^4F_5'-{}^4G_6'$ d^2s-d^2p
Sr II		Sr I		
24516.7	8912.4	**15604.3**		
10971.3		11340.1		
Yt III		Yt II		Yt I
35488.0	8543.6	**26944.4**	8656.1	**18288.3**
10713.5		11203.8		11184.8
Zr IV		Zr III		Zr II
46201.5	8053.3	**38148.2**†	8675.1	**29473.1**
		11036.6		11213.9
		Cb IV		Cb III
—	—	**49184.8**	8497.8	**40687.0**

TABLE V

Values of $(\nu/R)^{1/2}$. *Two electron systems.*

Terms	Sr I	Diff.	Yt II	Diff.	Zr III	Diff.	Cb IV
$^3P_2$	0.4592	0.3361	0.7953	0.3434	1.1387		
$^3D_3'$	.4668	.3459	.8127	.3380	1.1507	0.3368	1.4875
$^3F_4$	.4919	.3254	.8173	.3320	1.1493	.3344	1.4837
$^3D_3$	.6198	.3360	.9558	.3360	1.2918	.3360	1.6278

Values of $(\nu/R)^{1/2}$. *Three electron systems.*

Terms	Yt I	Diff.	Zr II	Diff.	Cb III	Diff.	Mo IV
$^4D_4'$	0.4801	0.3562	0.8363	0.3364	1.1727		
$^4F_5$	.4935	.3485	.8420	.3377	1.1797		
$^4G_6'$	.5149	.3328	.8477	.3348	1.1825	0.3358	1.5183
$^4F_4'$	.6571	.3365	.9936	.3365	1.3301	.3365	1.6666

IV to be nearly the same as those for Sc I, II, Ti II, III, V III, IV, and Cr IV respectively. The method used in computing the $(\nu/R)^{1/2}$ values given

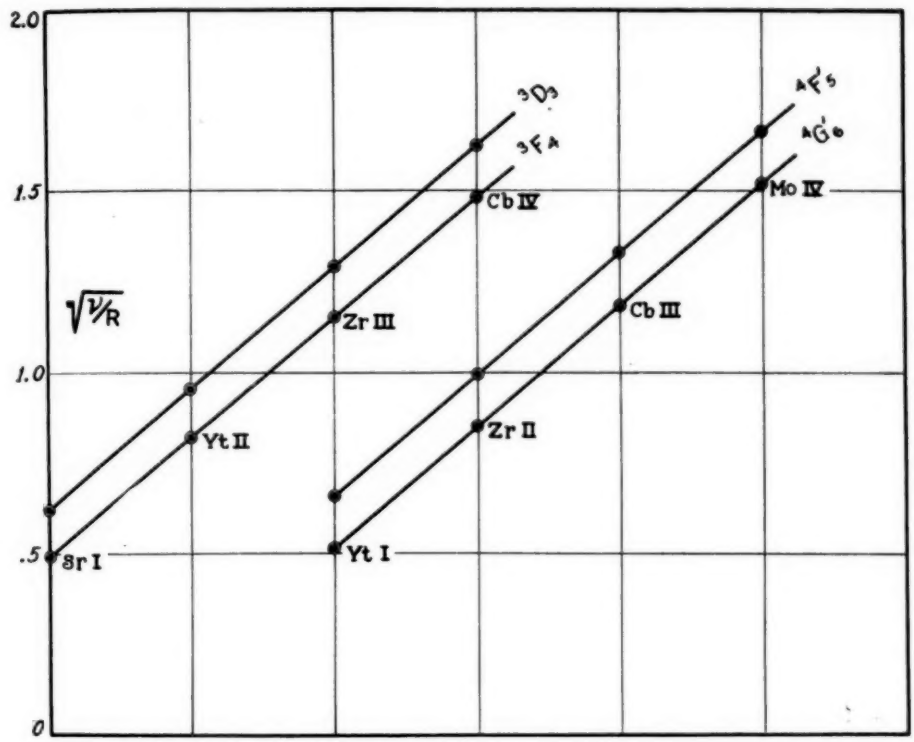

MOSELEY DIAGRAM

Fig. 3.

in Table V and Fig. 3 is the same as was used for some of the corresponding elements in the first long period.[3]

Taking the value of $(\nu/R)^{1/2}$ for the $^3D_3$ level of Sr I, which is known, and being guided by the slope of the $5p$ and $5s$ lines on the Moseley Diagram for the one-electron systems for these elements, values of $(\nu/R)^{1/2}$ are assumed for the $^3D_3$ level of Yt II and Zr III, from which the term values of the $^3D_3$ levels are computed. The corresponding term values for the $^3F_4$ levels are then obtained by the subtraction of the radiated frequencies in these elements. The values of $(\nu/R)^{1/2}$ can now be determined for the $^3F_4$ levels and the $\Delta(\nu/R)^{1/2}$ for the two terms thus obtained for each element should be almost the same as the corresponding difference for the same terms in Sr I. If such is not the case slightly different values of $(\nu/R)^{1/2}$ for the $^3D_3$ levels are taken and the process is repeated until suitable values of $\Delta(\nu/R)^{1/2}$ are obtained. The $^3P_2$ and $^3D_3'$ terms are then determined directly from the observed radiated frequencies. The same method was followed in determining the $(\nu/R)^{1/2}$ values shown in Table V for the three electron systems.

CORNELL UNIVERSITY,
December 24, 1927.

[3] R. C. Gibbs and H. E. White, Proc. Nat. Acad. Sci. **13**, 525 (1927).

INTENSITIES IN THE HYDROGEN SPECTRAL SERIES

By Francis G. Slack

Abstract

The absolute intensities of the components of the most important lines of the first six series in the spectrum of the hydrogen atom as computed on the basis of the wave mechanics are tabulated. The components are summed to give the total line intensities per atom in the initial state. The probability coefficients for the components and lines are also tabulated. The results of comparison between experiment and theory are briefly discussed and an experiment for giving values more directly comparable with the calculated values is suggested.

IN view of the current interest in intensity measurements it seems worth while to present the following tables of intensities computed for the components of the more important lines of the first several series in the spectrum of the hydrogen atom. Schrödinger,[1] Epstein,[2] Sommerfeld and Unsöld,[3] Eckart,[4] and others have computed the relative intensities of certain lines or components of lines and Y. Sugiura[5] has recently published a tabulation which the following tables duplicate and expand.

The absolute intensities given in this paper were computed from the expression given by Born and Jordan[6] for the energy radiated per second as the result of the change in state of an excited atom:

$$\text{Intensity} = (4e^2/3c^3)\ (2\pi)^4\ (\nu_{nn'})^4\ (q^{nn'})^2\ \text{ergs/sec.} \qquad (1)$$

where e, c, and ν have their ordinary meanings and $(q^{nn'})$ is the matrix element depending on the space coordinates and characteristic quantum numbers of the atom in the states n and n' and is proportional to the energy radiated in a transfer from state n to n'. The n and n' here refer to the elementary quantum states characterized by three quantum numbers. Since the derivation of the expressions for the matrix element from the wave mechanics has been carried through by the above mentioned authors it is not repeated here. The expressions are taken directly from Sommerfeld and Unsöld[3] as developed by Wentzel[7] in polar coordinates. For the quantum change $n \rightarrow n'$; $l \rightarrow l' = l-1$ where n is the total quantum number and $(l+1)$ is the azimuthal quantum number:

$$(J^{nn',ll'}) = 2^6 l a_0^2 (\phi^{nn',ll'})^2/(\psi^{n,l})(\psi^{n',l'})$$

[1] E. Schrödinger, Ann. d. Physik, **80,** 437 (1926).
[2] P. S. Epstein, Phys. Rev., **28,** 695 (1926).
[3] A. Sommerfeld und A. Unsöld, Zeits. f. Physik, **38,** 237 (1926).
[4] Carl Eckart, Phys. Rev., **28,** 927 (1926).
[5] Y. Sugiura, Journal de Physique et le Radium, March (1927).
[6] M. Born und P. Jordan, Zeits. f. Physik, **34,** 858 (1925).
[7] G. Wentzel, Naturwiss., **14,** 621 (1926).

where:

$$(\phi^{nn',ll'}) = \left(\frac{nn'}{n+n'}\right)^4 \sum_{s=l}^{n-1} \sum_{s'=l'}^{n'-1} \left(\frac{-2n'}{n+n'}\right)^s \left(\frac{-2n}{n+n'}\right)^{s'} \binom{n+l}{n-s-1} \binom{n'+l'}{n'-s'-1} \frac{(s+s'+3)!}{(s-l)!\,(s'-l')!}.$$

$$(\psi^{n,l}) = n^3 \sum_{s=l}^{n-1} \sum_{s'=l}^{n-1} (-1)^{s+s'} \binom{n+l}{n-s-1} \binom{n+l}{n-s'-1} \frac{(s+s'+2)!}{(s-l)!\;(s'-l)!}$$

$a_0 = h^2/4\pi^2 me^2 =$ radius of first Bohr orbit.

The expression $(J^{nn',ll'})$ as here defined gives the sum of the intensities of the individual sub-states due to the magnetic splitting up without regard to the number of sub-states or their statistical weights. In order to obtain intensities for one electron per sub-state we must divide the above values by their statistical weights as defined by Sugiura,[4] that is $g_k = (2l+1)$. This will average over the degenerate states in our expression and we may write: $(q^{nn'})^2 = (J^{nn',ll'})/(2l+1)$ and substituting these values in Eq. (1) we obtain the intensities of the components as tabulated in column 3 of the Tables. Also in order to sum up the components to obtain the total line intensity per atom of total quantum number n we must multiply each of the component intensities by $(2l+1)/n^2$ before adding. (Since there are n^2 sub-states.) In this manner the values in column 5 were obtained. The probability values in columns 4 and 6 were obtained by dividing the energy radiated per second in the components and in the total lines respectively by $h\nu$, the energy of a single transfer, thus giving the number of transfers per second or the probability coefficient. It is also possible, as done by Sugiura, to obtain the total probability of line emission from any state by summing in a similar manner over all components beginning in this state.

The first column in the Tables gives the quantum change giving rise to the emission. $n_a = l+1$ is the azimuthal quantum number, n_r the radial quantum number, so that $n = n_a + n_r$. The second column gives the statistical weight of the component. The third and fourth columns give the intensities and probabilities of the components respectively and the fifth and sixth columns the line intensity and probability. The last column gives the value of ν for the line. The tables are arranged by series for convenience but since the intensities are absolute values comparison between tables is permissible. (See Table I)

The author has attempted to use the values in the above tables to compute the number of atoms in the various excited states as a function of the time elapsed after certain equilibrium conditions were reached. The object was to compute the constant of the well known "Abklingungs Kurven" of W. Wien[8] on the assumption that the atoms enter the observation chamber

[8] W. Wien, Ann d. Physik, **73**, 483 (1924). Note: The futility of using the decay constants of the single lines is shown by Sugiura.

TABLE I

Theoretical intensities in the hydrogen spectrum.

Quantum change $n_a n_r$ $n_a' n_r'$	Stat. wt. $(2l+1)$	Component intensity ergs/sec.	Component probability	Line intensity ergs/sec.	Line prob.	Wave no. ν
			1st Series—Lyman			
20 – 10	3	10.2×10^{-3}	63.2×10^{7}	7.65×10^{-3}	47.4×10^{7}	82270
21 – 10	3	3.24	16.9	1.08	5.64	97630
22 – 10	3	1.38	6.83	.260	1.28	103120
23 – 10	3	.710	3.44	.085	.412	105310
24 – 10	3	.435	2.08	.036	.173	106410
25 – 10	3	.295	1.40	.018	.086	107510
26 – 10	3	.220	1.04	.011	.049	108050
			2nd Series—Balmer			
30 – 20	5	19.35×10^{-5}	6.47×10^{7}			
21 – 11	3	6.78	2.26	13.23×10^{-5}	4.42×10^{7}	15240
12 – 20	1	1.89	.632			
31 – 20	5	8.36	2.07			
22 – 11	3	3.95	.975	3.42	.845	20570
13 – 20	1	1.04	.258			
32 – 20	5	4.27	.946			
23 – 11	3	2.25	.497	1.15	.254	23040
14 – 20	1	.575	.127			
33 – 20	5	2.55	.543			
24 – 11	3	1.43	.298	.488	.102	24380
15 – 20	1	.357	.075			
34 – 20	5	1.60	.324			
25 – 11	3	.944	.191	.226	.046	25180
16 – 20	1	.228	.046			
35 – 20	5	1.04	.207			
26 – 11	3	.660	.131	.115	.023	25710
17 – 20	1	.157	.031			
36 – 20	5	.685	.134			
27 – 11	3	.446	.087	.060	.012	26070
18 – 20	1	.107	.021			
			3rd Series—Paschen			
40 – 30	7	1.45×10^{-5}	1.38×10^{7}			
31 – 21	5	.753	.720			
22 – 12	3	.323	.309	$.946\times10^{-6}$	$.904\times10^{7}$	5333
22 – 30	3	.037	.035			
13 – 21	1	.188	.180			
41 – 30	7	.697	.455			
32 – 21	5	.522	.341			
23 – 12	3	.252	.165	.338	.221	7800
23 – 30	3	.023	.015			
14 – 21	1	.139	.091			
42 – 30	7	.387	.216			
33 – 21	5	.346	.193			
24 – 12	3	.172	.096	.142	.079	9142
24 – 30	3	.014	.008			
15 – 21	1	.091	.051			
43 – 30	7	.240	.123			
34 – 21	5	.225	.115			
25 – 12	3	.118	.060	.066	.034	9950
25 – 30	3	.0090	.0046			
16 – 21	1	.061	.031			

TABLE I (*continued*)

Quantum change $n_a n_r$ $n_a' n_r'$	Stat. wt. $(2l+1)$	Component intensity ergs/sec.	Component probability	Line intensity ergs/sec.	Line prob.	Wave no. ν
44−30	7	$.157\times10^{-6}$	$.076\times10^{7}$			
35−21	5	.157	.076			
26−12	3	.084	.041	$.034\times10^{-6}$	$.017\times10^{7}$	10475
26−30	3	.0062	.0030			
17−21	1	.043	.021			
45−30	7	.116	.054			
36−21	5	.128	.060			
27−12	3	.062	.029	.020	.0095	10835
27−30	3	.0045	.0021			
18−21	1	.033	.016			
			4th Series—Brackett			
50−40	9	20.8×10^{-7}	43.0×10^{5}			
41−31	7	12.6	26.1			
32−22	5	7.26	15.0			
32−40	5	.246	.507	13.2×10^{-7}	27.3×10^{5}	2468
23−13	3	3.60	7.43			
23−31	3	.0092	.019			
14−22	1	6.09	12.54			
51−40	9	9.94	13.3			
42−31	7	9.85	13.2			
33−22	5	6.58	8.81			
33−40	5	.094	.126	5.75×10^{-7}	7.68×10^{5}	3807
24−13	3	3.88	5.19			
24−31	3	.0075	.010			
15−22	1	3.11	4.16			
52−40	9	7.94	8.75			
43−31	7	8.65	9.55			
34−22	5	4.28	4.73			
34−40	5	.057	.063	3.33×10^{-7}	3.67×10^{5}	4618
25−13	3	2.38	2.63			
25−31	3	.0041	.0045			
16−22	1	1.98	2.19			
			5th Series			
60−50	11	4.20×10^{-7}	16.0×10^{5}			
51−41	9	2.63	10.0			
42−32	7	1.97	7.50			
42−50	7	.045	.17			
33−23	5	1.14	4.32	2.60×10^{-7}	9.88×10^{5}	1338
33−41	5					
24−14	3	.617	2.35			
24−32	3					
15−23	1	1.97	7.50			
61−50	11	2.40	5.69			
52−41	9	2.46	5.82			
43−32	7	1.97	4.66			
43−50	7	.0093	.022			
34−23	5	1.27	3.01	1.48×10^{-7}	3.52×10^{5}	2150
34−41	5					
25−14	3	1.01	2.40			
25−32	3					
16−23	1	1.10	2.60			

TABLE I (*continued*)

Quantum change $n_a n_r$ $n_a' n_r'$	Stat. wt. $(2l+1)$	Component intensity ergs/sec.	Component probability	Line intensity ergs/sec.	Line prob.	Wave no. ν
			6th Series			
70−60	13	1.13×10^{-7}	7.10×10^{5}			
61−51	11	.635	4.00			
52−42	9	.617	3.89			
52−60	9	.0113	.071			
43−33	7	.421	2.65			
43−51	7			0.665×10^{-7}	4.18×10^{5}	809.6
34−24	5	.235	1.48			
34−42	5					
25−15	3	.051	.32			
25−33	3					
16−24	1	1.04	6.53			

in more or less highly excited states and further excitation being impossible cascade down to the final normal states according to the probabilities given above. Thus Wien's curves would give simply the relative number of atoms in the initial states as a function of the time which as computed is a complicated expression depending on the probabilities of all transfers between still higher states and on the probability of leaving the state in question to all lower states. It was found that quantitative calculations on various assumptions of initial distribution among the states etc. did not check well. However from simple calculations it is seen that the ratio of the number of atoms entering the states $n=3$, $n=4$, $n=5$, giving rise to the first three Balmer lines, to the number of atoms leaving these states is very closely the same for the three states. Thus on the above assumption one would expect the same "decay constant" for the three lines as found by Wien and as denied by other theoretical considerations.[9] The theory that a large part of the intensity observed in the "decay curves" comes from "new excitation," that is atoms dropping into states capable of radiating the lines under observation from higher states, is substantiated by recent experiments of Hertel[10] and Rupp[11] where the intensity of the polarized light in the canal stream is shown to decay much more rapidly than the total intensity. The polarization is due to impacts within the discharge tube and canal and apparently disappears as soon as the atom has emitted a quantum of radiation though the atom need not necessarily return immediately to the ground state.

It is interesting to remark on the comparison of the computed relative intensities of the lines with experimental results. (For the relative component intensities the calculated and experimental values have been shown to agree reasonably well. For the fine structure as split up in the Stark

[9] G. Mie, Ann. d. Physik, **66**, 237 (1921); J. Palacios, Ann. d. Physik, **79**, 55 (1926); R. d'E. Atkinson, Proc. Roy. Soc. **A116**, 81 (1927).

[10] K. L. Hertel, Phys. Rev., **29**, 848 (1927).

[11] E. Rupp, Ann. d. Physik, **84**, 94 (1927).

Effect by Schrödinger[1] and by Epstein,[12] for the normal components by Eckart[4] and by Sommerfeld and Unsöld.[3]) Ornstein[13] in a recent paper has made a comparison of the line intensities as computed by Schrödinger[1] with the experimental values obtained by Bongers.[14] The values quoted from Schrödinger however are computed on the basis that there are an equal number of atoms in the various initial states ready to emit the Balmer lines while actually only 9/16 of the atoms in the 4 quantum state and 9/25 of those in the 5 state etc. can emit the Balmer lines. Also there is no reason to believe that under the experimental conditions there were an equal number of atoms in each excited state. Thus the experimental results are really not comparable with the values calculated for one atom in each state. Results of Crew and Hulburt[15] and other observers show that the observed intensities depend on the mode of excitation and other conditions which may determine the number of atoms in each excited state. Only if this were the same for all states would the observed results be comparable with the calculated values above.

The author suggests the following method of obtaining a direct comparison between the calculations and experiment. If the relative intensities of the lines of two series, whose initial states overlap, are obtained simultaneously it would be possible by assuming the calculated intensities to hold for one series to compute the relative numbers of atoms in the various states and using these values to compute the relative intensities per atom for the second series for comparison with their calculated values.

DEPARTMENT OF PHYSICS,
COLUMBIA UNIVERSITY,
December 20, 1927.

[12] P. S. Epstein, Phys. Rev., **28,** 695 (1926). Note: Certain of the intensities as calculated by Epstein are in error due to irregularities in integrating over the angular coordinate. (Counting twice instead of once the component $m=0$.)

[13] L. S. Ornstein, Phys. Zeits., **28,** 688 (1927).

[14] J. A. Bongers, Utrecht Dissertation (1927).

[15] W. H. Crew and E. O. Hulburt, Phys. Rev., **29,** 843 (1927).

THE ZEEMAN EFFECT AND STARK EFFECT OF HYDROGEN IN WAVE MECHANICS; THE FORCE EQUATION AND THE VIRIAL THEOREM IN WAVE MECHANICS

By Arthur Edward Ruark

Abstract

The Zeeman levels of hydrogenic atoms are determined by a new and simple method, neglecting terms in H^2. The frequency of the Larmor precession is $L=L_0\,(1+E/mc^2)$. L_0 is the frequency of precession obtained by Newtonian mechanics and E the energy of the atom. This agrees with a formula of Pauli obtained by ordinary relativity mechanics. The formulae for the first order Stark effect and for the Paschen-Back effect can be obtained by similar methods.

An extension of Ehrenfest's law of motion for a particle is proved. It is applicable to any conservative system. From it, a theorem of wave mechanics analogous to the virial theorem is obtained.

1. The Zeeman Effect and Stark Effect of Hydrogen in Wave Mechanics

THE Zeeman effect of hydrogen has been treated in terms of the new mechanics by several authors, neglecting the modifications due to the relativistic change of mass of the electron. Heisenberg and Jordan[1] studied the Zeeman effect by means of matrices. Epstein[2] treated the problem by obtaining the energy of a system composed of the atom and the apparatus which produces the field. This procedure is advantageous, for it is capable of showing the nature of the interaction between the atom and the magnetic field. For example, it is well known that when a quantum jump occurs there may be an exchange of angular momentum between the atom and the field producing mechanisms, as well as a contribution of angular momentum to the radiation field. This indicates that we might expect a difference between the energy of a quantum and the decrease of energy of the emitting atom, because of a possible interchange of energy between the atom and the magnet. The calculation of Epstein shows that the correct result is the same as that obtained by neglecting the reaction of the atom on the field,—that is, by treating the field strength H as quite independent of the behavior of the emitting atom. Brillouin[3] has treated the problem in wave mechanics, without the modifications due to relativity.

The method is to set up the wave equation, and transform it to coordinates rotating about the lines of magnetic force with the frequency $L_0=eH/4\pi mc$ of the Larmor precession. (The charge of the electron is taken to be $-e$, where $e=4.77\ 10^{-10}$ electrostatic units.) In these coordinates the

[1] Heisenberg and Jordan, Zeits. f. Physik **37**, 263 (1926).
[2] Epstein, Proc. Nat. Acad. Sci. **12**, 634, (1926).
[3] Brillouin, J. de Physique **8**, 74, (1927).

wave distribution is identical with that of the field free atom and the solution contains the factor

$$\exp\left[i(m\zeta-2\pi\nu_0 t)\right], \tag{1}$$

m being the equatorial quantum number, $h\nu_0$ the energy of the atom, and ζ the equatorial angle, as measured in the rotating coordinates. The equatorial angle ϕ in the resting coordinates is given by

$$\phi=\zeta+2\pi L_0 t.$$

Substituting this in (1) we obtain

$$\exp\left[im\phi-2\pi i(\nu_0+mL_0)t\right] \tag{2}$$

Thus the energy in the resting coordinates is

$$E_0+mL_0h=E_0+\frac{meHh}{4\pi mc} \tag{3}$$

It is possible to solve the problem in relativistic wave mechanics in a somewhat similar fashion, but there is a complication which would make it necessary to resort to perturbation methods. In ordinary relativity mechanics, the variation of mass of the electron causes small but rapid variations of the speed of the Larmor precession. In relativistic wave mechanics, a corresponding effect appears. It is found that there is no privileged coordinate system in which the wave system appears like that of the field free atom. The velocity of precession which will make the layer of the ψ distribution between radii r and $r+dr$ appear like the corresponding layer of the undisturbed atom is found to be a function of r. We are confronted with a problem analogous to that of motions within a nebula, instead of that of a rigid rotating body. To avoid these complications, we adopt a much shorter method, based on the virial theorem for a system of particles.

In either relativistic or Newtonian mechanics, the theorem may be stated as follows:

For a system of particles in periodic motion or in a steady state,

$$\overline{\sum mv^2}=-\overline{\sum(xX+yY+zZ)}.$$

m is the actual mass, (not the rest mass) of a typical particle of the system, x, y, z, its coordinates, and X, Y, Z, the components of force acting on it. $\sum$ indicates a summation over all the particles and the bars denote time averages. It is shown in many texts[4] that if the potential energy V_0 of an

[4] See appendix of any edition of Sommerfeld's "Atombau." The following is a useful extension of this theorem:

If the potential energy is the sum of several functions, $V_1+V_2+\cdots$, homogeneous in the coordinates, and of degrees n_1, n_2, $\cdots$, respectively, then

$$\overline{\sum mv^2}=n_1\bar{V}_1+n_2\bar{V}_2+\cdots$$ (next page)

atom or molecule is a homogeneous function of the coordinates, of the nth degree, then the virial theorem reduces to

$$\overline{\sum mv^2} = \overline{nV_0} \tag{5}$$

For the particles of an atom, subjected to Coulomb forces, $n=-1$, and in non-relativistic mechanics, (5) yields the relations,

$$-\overline{T_0} = \overline{V_0}/2 = E_0, \tag{6}$$

where E_0 is the total energy. If a uniform constant magnetic field H is applied, then each electron experiences an additional force $-(e/c)[v\mathbf{H}]$. The average value of the potential energy is unchanged, and if $\overline{T}$ is the time average of the kinetic energy, then (4) yields the result

$$T = -\frac{\overline{V_0}}{2} + \frac{e}{2mc}\overline{Hp_H} \tag{7}$$

where p_H is the component of angular momentum parallel to the field. It must be noted that p_H is not the same as the variable conjugate to ϕ, which we call p_ϕ. In the presence of an electromagnetic field having the vector potential A_x, A_y, A_z, the variables conjugate to x, y, and z, are given by the relations

$$p_x = mv_x - eA_x/C.$$

For a magnetic field parallel to the Z-axis

$$A_x = -\tfrac{1}{2}yH, \quad A_y = \tfrac{1}{2}xH, \quad A_z = 0.$$

A brief computation shows that

$$p_\phi = p_H - eH(x^2+y^2)/2c = p_H - 2\pi L_0 m(x^2+y^2), \tag{8}$$

which tells us that p_ϕ is the angular momentum in the *rotating* coordinates.

In equation (7) p_H can be replaced by p_ϕ if we are interested only in terms containing the first power of H. Since ϕ is an ignorable coordinate, p_ϕ is constant. Adding to (7) the equation

$$\overline{V} = 2E_0,$$

and neglecting the term in H^2, we get

$$T+V = E = E_0 + (eH/2mc)p_\phi \tag{9}$$

In ordinary mechanics, we write for p_ϕ its quantized value $mh/2\pi$, and obtain the change of energy $\Delta E \equiv E - E_0$:

$$\Delta E = L_0 m h, \quad m = 0, \pm 1, \pm 2, \cdots. \tag{10}$$

This follows at once from Euler's theorem for homogeneous functions if we substitute

$$-(\partial V_1/\partial x) - (\partial V_2/\partial x) - \cdots$$

for X in (4), and similar expressions for Y and Z.

To solve the same problem in wave mechanics, we start with (9) in the form

$$p_\phi - \Delta E/2\pi L_0 = 0. \tag{9a}$$

This is really a Hamilton-Jacobi equation to determine p_ϕ. By going through the usual variation principle procedure, using the complete wave equation, we can show that it is legitimate to substitute the operator $h\partial/2\pi i\partial\phi$ for p_ϕ, to obtain a simplified wave equation from (9a). Applying the operator thus formed to the wave amplitude function, ψ, we have

$$\frac{h}{2\pi i}\frac{\partial\psi}{\partial\phi} - \frac{\psi\Delta E}{2\pi L_0} = 0. \tag{11}$$

The solution is $\psi = Fe^{im\phi}$, where F represents the part of ψ depending on coordinates other than ϕ, and $mh = \Delta E/L_0$. In order to make this solution have the same period as the corresponding classical motion of the electron, it is necessary that m be an integer, so we arrive at the formula (10) for the change of energy in the presence of the field.

In relativistic wave mechanics the value of ΔE is obtained by a similar device. Pauli[5] solved the corresponding problem in ordinary mechanics, including the effect of the variation of mass with velocity. His result is this:

$$\Delta E = L_0\left(1+\frac{E_0}{mc^2}\right)2\pi p_\phi \tag{12}$$

The evaluation of E proceeds just as before, in both ordinary and wave mechanics, the final formula being

$$\Delta E = L_0\left(1+\frac{E_0}{mc^2}\right)mh, m = 0, \pm 1, \pm 2, \tag{13}$$

The methods used in this section are extensions of those introduced by the author in a previous paper[6] and are capable of other applications. For example, the first order Stark effect and the Zeeman levels of atoms exposed to a very strong magnetic field are easily obtained. Each case must first be examined by the aid of the general wave equation, however, to be sure that the simplified procedure is legitimate.

2. The Force Equation and the Virial Theorem in Wave Mechanics

Ehrenfest[7] has derived an equation which can be considered as a generalization of Newton's law of motion, by considering the motion of the center of gravity of the wave group accompanying a particle. His proof is given for a particle with only one degree of freedom, but can easily be extended to a conservative system containing any number of particles, as follows:

[5] Pauli, Zeits. f. Physik **31**, 373 (1925). Handbuch der Physik, volume 23, page 154.
[6] Ruark, J.O.S.A. and R.S.I. **16**, 40, (1928).
[7] Ehrenfest, Zeits. f. Physik, **45**, 455 (1927).

Let the ith particle in the system have mass m_i, and Cartesian coordinates x_i, y_i, z_i. Define new coordinates by the relations

$$X_i = m_i^{1/2} \cdot x_i, \quad Y_i = m_i^{1/2} \cdot y_i, \quad Z_i = m_i^{1/2} \cdot z_i.$$

Then the element of volume in the coordinate space used by Schrödinger is

$$d\tau = dX_1 dY_1 dZ_1 dX_2 \cdots$$

The wave equation is

$$\Delta\Psi - \frac{8\pi^2}{h^2} V\Psi - \frac{4\pi i}{h} \frac{\partial \Psi}{\partial t} = 0. \tag{14}$$

Also

$$\Delta\Psi^* - \frac{8\pi^2}{h^2} V\Psi^* + \frac{4\pi i}{h} \frac{\partial \Psi^*}{\partial t} = 0. \tag{15}$$

if Ψ^* is the complex conjugate of Ψ.

We shall need the auxiliary relation

$$\Psi\Delta\Psi^* - \Psi^*\Delta\Psi + \frac{4\pi i}{h}\left(\frac{\partial \Psi^*}{\partial t}\Psi + \frac{\partial \Psi}{\partial t}\Psi^*\right) = 0. \tag{16}$$

Let us *define* the X-coordinate of the nth particle by the equation

$$\xi_n = \frac{\int X_n \Psi\Psi^* d\tau}{\int \Psi\Psi^* d\tau} = \int X_n \Psi\Psi^* d\tau \tag{17}$$

(The denominator is unity because Ψ is normalized.)

Differentiating ξ_n with respect to t, we obtain

$$\dot{\xi}_n = \frac{h}{2\pi i} \int \Psi \frac{\partial \Psi^*}{\partial X_n} d\tau, \tag{18}$$

after using (16) and integrating by parts.

In evaluating the integral, we use the fact that Ψ and its derivatives vanish at the boundaries of the coordinate space in problems of the type dealt with here. Equation (18) defines the momentum of the center of gravity of the wave group, in the coordinate space. Differentiating (18),

$$\ddot{\xi}_n = \frac{h}{2\pi i} \int \left(\frac{\partial \Psi}{\partial t} \frac{\partial \Psi^*}{\partial X_n} + \Psi \frac{\partial^2 \Psi^*}{\partial X_n \partial t}\right) d\tau \tag{19}$$

We replace $\partial\Psi/\partial t$ and $\partial^2\Psi^*/\partial X_n \partial t$ by their values obtained from the wave equation and $\ddot{\xi}_n$ reduces to

$$\int \Psi\Psi^* \left(-\frac{\partial V}{\partial X_n}\right) d\tau - \frac{h^2}{8\pi^2 m} \int \left(\Delta\Psi \cdot \frac{\partial \Psi^*}{\partial X_n} - \Psi \frac{\partial \Delta\Psi^*}{\partial X_n}\right) d\tau$$

Integrating the last term by parts, and applying Green's theorem to the second integral, we find that it vanishes. Then, if we write $\xi_n = m_n^{1/2}\,\bar{x}_n$, we have

$$m_n^{1/2}\ddot{\bar{x}}_n = \int \Psi\Psi^*(-\partial V/\partial(m_n^{1/2}\cdot x_n))d\tau$$

or

$$m_n\ddot{\bar{x}}_n = \int \Psi\Psi^*(-\partial V/\partial x_n)d\tau \tag{20}$$

This is the generalized law of motion, which reduces to Newton's if appreciable values of Ψ are confined to a narrow range in the immediate neighborhood of $\bar{x}_n$; for then the right-hand member reduces to $-(\partial V/\partial \bar{x}_n)\int \Psi\Psi^* d\tau$, or $(-\partial V/\partial \bar{x}_n)$ since Ψ is so normalized that the last integral is unity.

Schrödinger showed that the group velocity of a nearly-monochromatic "Wellenpaket" is such that the point of coinciding phase obeys the laws of classical mechanics. The content of his theorem is different from that of equation (20), although the two are related. Equation (20) holds true whenever (14) is valid, provided Ψ is properly normalized. In many ways it is to be considered more fundamental than Schrödinger's theorem.

Let us apply (20) to obtain a theorem analogous to the virial theorem of ordinary mechanics. Dropping the use of bars to denote centroids and noting that $d(mx\dot{x})/dt = m\dot{x}^2 + mx\ddot{x}$, we have for each particle

$$\overline{m\dot{x}^2} = -\overline{mx\ddot{x}} + \overline{d(mx\dot{x})/dt} \tag{21}$$

where now the bars denote time averages. Summing equations of this type over all the coordinates and applying the usual restriction that the system is either periodic or in a condition of kinetic equilibrium, we obtain the generalized virial theorem, on substituting the values of x, $\dot{x}$, and $\ddot{x}$.

I wish to thank Professor J. H. Van Vleck and Professor J. J. Weigle for very helpful discussions of this paper.

MELLON INSTITUTE OF INDUSTRIAL RESEARCH,
UNIVERSITY OF PITTSBURGH, AND
GULF PRODUCTION COMPANIES.
December 4, 1927.

EXTENSION OF THE VIOLET CN BAND SYSTEM TO INCLUDE THE CN TAIL BANDS[1]

By Francis A. Jenkins

Abstract

Measurements of fine-structure lines of tail bands.—Wave-numbers of band lines accurate to about 0.02 cm^{-1} are given for 13 of the CN tail bands as excited by the reaction of acetylene with active nitrogen. The table also includes estimated intensities of the lines. Each band has a doublet P and a doublet R branch like the stronger violet CN bands, but the doublet separations vary markedly, being undetectable in the majority of the bands. Large perturbations, which affect several lines of each branch, are also found.

Assignment of tail bands to the violet CN system.—The combination principle is applied to determine the relative vibrational quantum numbers for the tail bands. The constants B' and B'' are then evaluated for each band, and by plotting these against vibration quantum number, n, it is found that they represent a continuation of the constants of the ordinary violet CN bands to the higher values of n. The tail bands are thus merely the high-n members of the ordinary CN sequences, and those measured are shown to be the (11,9), (12,10), (13,11), (9,8), (10,9), (11,10), (12,11), (10,10), (11,11), (12,12), (13,13), (14,14) and (15,15) bands of the violet system. With this assignment, the tail bands give $B''=1.894-0.0181n''$ as compared to $1.891-0.0173n''$ obtained by Kratzer from the low-n bands of the system. The band-origins are calculated, and the vibrational term differences obtained therefrom satisfy the combination principle exactly. The linear extrapolation of ω'' checks the above assignment of vibrational quantum numbers. Both B' and ω' show a non-linear variation with n. There is evidence for perturbations in the vibrational terms.

New features of band-spectrum structure.—According to the above results, the violet CN system includes some bands shaded to the violet and others shaded to the red (the tail bands), with an intermediate type in which the lines have practically equal spacing on a frequency scale. Also the band-origins of a given sequence, with increasing n, pass through a maximum of frequency, the result being that a sequence may form a "head" composed of bands. One of the rotational perturbations is investigated, and the deviations of the terms from their expected values in this case give a typical "resonance" curve, resembling that found by Schrödinger in the Al II *line* spectrum. A diagram of the vibrational intensity distribution in the violet CN system is discussed. Certain anomalous bands of longer wave-length are found which do not fit into the system.

Relation to theory of $^2S \rightarrow {}^2S$ bands.—In agreement with Mulliken's predictions, the first line of the R branch is found to be double, that of the P branch not being resolved. The intensity difference for the doublet components for low m is observed, and the estimated relative intensities are in satisfactory quantitative agreement with the theory.

Introduction

THE carbon arc spectrum of cyanogen, or more exactly of the CN molecule,[2] shows three series of faint heads, of which two lie between the

[1] A preliminary account of this investigation was given in a paper before the American Physical Society at the Chicago meeting, November, 1927.

[2] The evidence that the red and violet band systems originally attributed to CN are really due to this compound seems now to be practically conclusive. Cf. R. T. Birge, Phys. Rev. **23**, 294 (1924) (Abstract) and R. S. Mulliken, Nature **114**, 858 (1924).

strong sequences λλ4216, 3883 and 3590 of the violet system, and one on the short-wave side of the 3590 sequence. They have become known as the "tail" bands, a name derived from the early theory of their origin proposed by Thiele.[3] It will not be profitable to discuss this theory in detail, nor the attempts which have been made to justify it, since later work has shown it to be unfounded.[4] Thiele, from a supposed analogy to series in line spectra, was led to regard each of the faint heads as the result of a drawing together of the series of structure lines from one of the stronger bands, which at this point was supposed to approach a series limit, as in line spectra. When higher dispersion was used, particularly in the work of Uhler and Patterson,[4] this structure for the "tails" was not confirmed. They are over-run by lines from the strong CN sequences, however, and it was difficult to obtain unambiguous results.

In seeking an alternative interpretation of the tail bands in terms of modern band spectrum theory, we are met with the difficulty that they are shaded in the opposite direction from the ordinary CN bands, *i.e.*, to the red. This would indicate that they represent a different band system, though at first sight so closely related to the ordinary CN bands. The difference in the direction of shading is not an important one, however, and as will be shown presently the tail bands are merely further members of the violet CN system having large vibrational quantum numbers.

The excitation of the CN spectrum by active nitrogen has furnished at the same time the most definite disproof of Thiele's theory and the basis for the newer correct interpretation. A study of the reproduction given by Rayleigh and Fowler,[5] showing a comparison of low-dispersion spectrograms of the CN bands from active nitrogen and from the arc, gives sufficient evidence for discarding the theory of "tails." In the active nitrogen spectrum there is in every case a wide gap between a strong band head and the tail supposed to correspond to it. Moreover, the tail bands are relatively stronger than in the arc. They are not confused by overlapping series from the stronger sequences, since the latter are considerably shortened by the absence of lines of large rotational quantum number in a low-temperature source.

The above considerations led the writer to attempt high-dispersion photographs of the spectrum from active nitrogen, with a view to determining whether the tail bands represent the higher members of the ordinary CN sequences. This possibility was originally suggested by Mulliken, and is discussed in a recent article by Jevons.[6] Jevons' work consisted chiefly of measuring the lines of the λ3590 sequence, which has a remarkable appearance in the active nitrogen spectrum (see Fig. 1, *A*). He also measured some of the lines of the tail bands on the long-wave side of λ3883, but the bands

[3] T. N. Thiele, Astrophys. Jour. **6**, 65 (1897).

[4] See, for example, H. S. Uhler and R. A. Patterson, Astrophys. Jour. **42**, 434 (1915) and R. T. Birge, Phys. Rev. **11**, 136 (1918).

[5] R. Strutt and A. Fowler, Proc. Roy. Soc. **86A**, 112 (1912). Plate 6, Fig. 6A.

[6] W. Jevons, Proc. Roy. Soc. **112A**, 407 (1926).

were apparently too faint to permit a consistent quantum analysis. With the much greater intensity and resolving power on the plates used in the present work, such an analysis has been possible, and has led to very definite conclusions.

Experimental[7]

The source was a continuous-flow active nitrogen tube similar to that used in previous work with this mode of excitation.[8] Acetylene was allowed to leak slowly into the nitrogen afterglow, the rate being adjusted to obtain the best intensity of the purplish-blue luminescence of the CN spectrum. Taking the light end-on through a quartz window, the spectrum was photographed in the second order of the 21-foot Rowland concave grating at Harvard University. The stable mounting of this grating, and the very effective method of temperature control, have been adequately described elsewhere.[9] The exposure time was from 5 to 13 hours and the theoretical resolving power (with the slit-width used) was practically attained. The iron spectrum from a source complying with the specifications of the new international arc was photographed twice on each set of plates, once before and once after the band exposure.

Thirteen of the tail bands were obtained with sufficient intensity for measurement. Three of these lie on the short-wave side of the 3590 sequence, and were designated A1, A2, and A3, in the order of increasing wave-length. Four others, B1 to B4, extend toward the red from the 3590 sequence; the first of these appears on Fig. 1, *A*. The B1 band was the first one not badly confused with the many crowded lines of this sequence. The remaining 6 tail bands, C1 to C6, cover the whole region between the 3883 and 4216 sequences, their intensity decreasing and the heads becoming stronger relative to the rest of the band as they approach the latter sequence (see Fig. 1, *B* and *C*). The preliminary designations will be convenient in discussing the method of determining vibrational quantum numbers, as in Table II.

Measurements were made with a comparator, the screw of which had previously been found[8] to be free from appreciable errors. At least two settings were made on each line. The iron arc standards given by Meggers, Kiess and Burns[10] were used exclusively in computing wave-lengths. Table I gives the wave-numbers in vacuum of all lines measured, as well as intensity data and the wave-length in air of the null-line of each band. For all except the faintest lines, the mean error should not exceed 0.02 cm^{-1}. The designation by rotational quantum numbers, m, and the assignment of vibrational quantum numbers, will be discussed below.

[7] The experimental part of this work was completed while the writer was a National Research Fellow at Harvard University.

[8] F. A. Jenkins, H. A. Barton and R. S. Mulliken, Phys. Rev. **30**, 150 (1927). R. S. Mulliken, Phys. Rev. **26**, 1 (1925).

[9] E. C. Kemble, R. S. Mulliken and F. H. Crawford, Phys. Rev. **30**, 438 (1927).

[10] W. F. Meggers, C. C. Kiess and K. Burns, Bull. Bur. Stan. **19**, 263 (1924).

TABLE I

Wave-numbers and term-differences for CN tail bands. The symbols in italics have the following significance: m = rotational quantum numbers in the final state (they are ½ unit lower than those heretofore used, in accordance with the new quantum mechanics); $\Delta_2F'(m)$ = combination difference $R(m)-P(m)$; $\Delta_2F''(m)=R(m-1)-P(m+1)$; *p* = lines evidently displaced by perturbations; *h* = line forming the head of the band; *d* = diffuse lines probably representing unresolved doublets. Wherever there is a regular series of doublets, the components of each are bracketed. The numbers are estimated intensities referred to the strongest line of the band as 10 and the first lines as 1 (or 5 and ½ if the lines are double). The intensities are recorded throughout the band only for the (13, 13) band, which is without perturbations and consists of single lines. Relative intensities in the other bands are the same except where specifically given. This is done where the doublet components show as appreciable intensity difference, and in the regions of the perturbations. The letter *b* indicates a blend with a line from another band, which renders the intensity anomalous.

m	$R(m)$	$P(m)$	$\Delta_2F'(m)$	$\Delta_2F''(m)$
	A1 (11, 9) λ3437.843			
2	29,089.28			
3	092.17	29,068.93	23.24	24.32
4	094.93	064.96	29.97	31.12
5	097.61	061.05	36.56	38.06
6	100.06	056.87	43.19	44.96
7	102.55	052.65	49.90	51.91
8	104.75	048.15	56.60	58.89
9	106.84	043.66	63.18	65.76
10	108.82	038.99	69.83	72.70
11	110.60	034.14	76.46	79.61
12	112.27	029.21	83.06	86.49
13	113.84	024.11	89.73	93.35
14	115.29	018.92	96.37	100.34
15	116.37	013.50	102.87	107.27
16	117.48	008.02	109.46	113.98
17	118.39	002.39	116.00	120.94
18	119.13	28,996.54	122.59	127.77
19	119.74	990.62	129.12	134.61
20	120.43	984.52	135.91	141.44
21	120.76 *h*	978.30	142.46	148.50
22		971.93		155.35
23		965.41		
24		958.63		
25		951.92		
26		944.79		
27		937.67		
	A2 (12,10) λ3469.079			
1	28,824.21			
2	827.08			17.29
3	829.83	28,806.92	22.91	24.02
4	832.41	803.06	29.35	30.83
5	834.79	799.00	35.79	37.73
6	837.00	794.68	42.32	44.54
7	839.12	790.25	48.87	51.42
8	840.93	785.58	55.35	58.29
9	842.67 *d*	780.83	61.84	65.09
10	844.08 844.36	775.84	68.38	72.00
11	845.18 845.52	770.67 *d*	74.68	78.91
12	846.20 846.77	765.43 765.17	81.18	85.53
13	847.15 847.58	759.99 759.66	87.54	92.37
14	847.58 847.82	754.33 753.89	93.59	99.36
15	*p* 849.16 *2*	748.19 747.81		106.03
16	" 849.84 *6*	741.84 741.50		
	" 850.80 *7*	*p* 734.76 *5*		
	" 851.65 *6*	" 734.06 *4*		
	" 853.08 *7*	" 731.90 *5*		
	" 855.28 *3*	" 727.52 *6*		
	" 857.39 *2*	" 727.04 *4*		
	" 860.32 *1*	" 718.71 *3*		
		" 716.64 *3*		
		" 706.01 *9*		

m	$R(m)$	$P(m)$	$\Delta_2F'(m)$	$\Delta_2F''(m)$
	A3 (13, 11) λ3504.812			
2	28,533.03			
3	535.66	28,513.37	22.29	23.74
4	538.09	509.29	28.80	30.51
5	540.31	505.15	35.16	37.20
6	542.30	500.89	41.41	44.05
7	544.20	496.26	47.94	50.77
8	545.78	491.53	54.25	57.65
9	547.23	486.55	60.68	64.32
10	548.48	481.46	67.02	71.14
11	549.49	476.09	73.40	77.83
12	550.36	470.65	79.71	
	p 550.87 *7*	*p* 465.39 *5*		
	" 551.47 *h*	" 464.91 *5*		
	" 548.65 *4*	" 459.02 *3*		
	" 547.56 *4*	" 452.78 *4*		
	" 546.35 *4*			
	" 544.87 *3*			
	" 543.45 *2*			
	B1 (9, 8) λ3616.643			
0	27,645.51			
1	648.94	27,638.62	10.32	10.46
2	652.37	635.05	17.32	17.46
3	655.66	631.48	24.18	24.31
4	658.97	627.86	31.11	31.47
5	662.23	624.19	38.04	38.48
6	665.46	620.49	44.97	45.48
7	668.64	616.75	51.89	52.49
8	671.76	612.97	58.79	59.44
9	674.85	609.20	65.65	66.41
10	677.86	605.35	72.51	73.43
11	680.89	601.42	79.47	80.38
12	683.83	597.48	86.35	87.39
13	686.73	593.50	93.23	94.37
14	689.55	589.46	100.09	101.33
15	692.32	585.40	106.92	108.29
16	695.09	581.26	113.83	115.20
17	697.80	577.12	120.68	122.20
18	700.40	572.89	127.51	129.18
19	702.95	568.62	134.33	136.09
20	705.45	564.31	141.14	143.00
21	707.90	559.95	147.95	149.94
22	710.23	555.51	154.72	156.89
23	712.49	551.01	161.48	163.77
24		546.46		170.70
25		541.79		
26		537.01		
27		532.17		
28		521.43		
	B2 (10, 9) λ3638.382			
0	27,480.64 *d* 483.32 *1*			
1	484.01 *2*	27,473.62 *1*	10.04	10.67
2	486.54 *b* 487.41 *3*	470.20 *2* 469.75 *1*	17.00	17.34
3	489.54 *3* 490.61 *b*	466.67 *3* 465.98 *2*	23.75	24.36

TABLE I (*continued*)

m	$R(m)$	$P(m)$	$\Delta_2F'(m)$	$\Delta_2F''(m)$
4	27,492.64 *4* 493.74 *b*	27,463.11 *4* 462.12 *3*	30.58	31.15
5	495.74 *b* 496.80 *5*	459.43 *5* 458.41 *4*	37.35	38.09
6	498.65 *4* 499.75 *5*	455.63 *5* 454.58 *4*	44.10	45.07
7	501.60 *b* 502.64 *5*	451.78 *5* 450.63 *5*	50.92	51.93
8	504.40 *5* 505.46 *5*	447.85 *5* 446.70 *5*	57.66	58.89
9	507.14 508.20	443.78 442.68	64.44	65.81
10	509.88 510.85	439.65 438.60	71.24	72.71
11	512.53 513.47	435.47 434.46	78.04	79.60
12	515.14 515.97	431.25 430.27	84.79	86.54
13	517.55 518.48	426.93 425.99	91.55	93.46
14	519.94 520.78	422.56 421.62	98.27	100.34
15	522.26 523.10	418.10 417.25	105.01	107.20
16	524.52 525.23	413.58 412.74	111.71	114.11
17	526.87 527.49	408.98 408.17	118.60	120.93
18	528.87 529.57	404.34 403.55	125.28	127.98
19	530.81 531.48	399.57 398.82	131.95	134.81
20	532.66 533.34	394.80 394.02	138.59	141.60
21	534.44 535.18	389.88 389.21	145.27	148.46
22	536.29 536.93	384.91 384.17	152.07	155.30
23	537.85 538.54	379.85 379.18	158,68	162.21
24	539.36 540.04	374.72 374.09	165.30	168.98
25		369.50 368.92		

B3 (11,10) λ3665.261

1	27,282.01			
2	285.13	27,268.48	16.65	17.16
3	288.13	264.85	23.28	24.01
4	291.08	261.12	29.96	30.85
5	293.91	257.28	36.63	37.72
6	296.64	253.36	43.28	44.54
7	299.27	249.37	49.90	51.40
8	301.79	245.24	56.55	58.24
9	304.23	241.03	63.20	65.08
10	306.53	236.71	69.82	71.95
11	308.76	232.28	76.48	78.74
12	310.85	227.79	83.06	85.59
13	312.88	223.17	89.71	92.42
14	314.76	218.43	96.33	99.25
15	316.58	213.63	102.95	106.05
16	318.26	208.71	109.55	112.90

m	$R(m)$	$P(m)$	$\Delta_2F'(m)$	$\Delta_2F''(m)$
17	27,319.76	27,203.68	116.08	119.73
18	321.19	198.53	122.66	126.52
19	322.52	193.24	129.28	133.27
20	323.74	187.92	135.82	140.10
21	324.72	182.42	142.30	146.90
22	325.75	176.84	148.91	153.60
23	326.58	171.12	155.46	160.41
24	327.21	165.34	161.87	167.24
25	327.84	159.34	168.50	173.95
26	328.33	153.26	175.07	180.70
27	328.61 *h*	147.14	181.47	187.52
28		140.81		

B4 (12,11) λ3697.109

3	27,052.69	27,029.81	22.88	
4	055.54	026.06	29.48	30.53
5	057.98	022.16	35.82	37.52
6	060.43	018.02	42.41	43.96
7	062.71	014.02	48.69	50.82
8	065.08	009.61	55.47	57.48
9	066.94	005.23	61.71	64.47
10	068.81 *d*	000.61 *d*	68.20	71.03
11	070.45 *d*	26,995.89 *d*	74.56	77.68
12	072.65 073.12	991.44 990.82	81.75	
	p 074.29 *4*	*p* 986.87 *4*		
	" 074.88 *4*	" 985.74 *4*		
	" 078.60 *4*	" 980.49 *4*		
	" 082.49 *d*	" 979.31 *2*		
	" 099.04 *3*	" 974.81 *6*		
		" 969.28 *6*		
		" 963.29 *3*		
		" 946.67 *3*		
		" 936.64 *2*		

C1 (10,10) λ3894.090

0	25,675.85 *0* 676.43 *1*			
1	679.14 *b* 679.78 *2*	25,669.38 *1*	10.08	10.38
2	682.32 *2* 683.26 *4*	665.98 *2* 665.55 *1*	17.03	17.17
3	685.53 *3* 686.58 *4*	662.65 *3* 661.94 *1*	23.76	24.00
4	688.74 *3* 689.86 *4*	659.24 *4* 658.34 *2*	30.51	30.85
5	691.97 *5* 693.11 *5*	655.73 *4* 654.67 *3*	37.34	37.71
6	695.13 *4* 696.29 *3*	652.13 *5* 651.06 *4*	44.12	44.59
7	698.34 *5* 699.41 *5*	648.52 *5* 647.38 *4*	50.92	51.41
8	701.45 702.50	644.87 *5* 643.74 *5*	57.67	58.28
9	704.49 705.57	641.15 640.04	64.44	65.09
10	707.59 708.59	637.41 636.36	71.21	71.92
11	710.62 711.54	633.63 632.60	77.97	78.76
12	713.60 714.56	629.83 628.83	84.75	85.58
13	716.55 717.43	625.98 625.03	91.49	92.43
14	719.46 720.30	622.11 621.19	98.23	99.22

TABLE I (*continued*)

m	*R*(*m*)	*P*(*m*)	$\Delta_2F'(m)$	$\Delta_2F''(m)$
	25,722.46	25,618.20		
15			105.04	106.01
	723.17	617.35		
	725.16	614.31		
16			111.68	112.92
	725.95	613.44		
	727.94	610.31		
17			118.43	119.67
	728.71	609.47		
	730.63	606.28		
18			125.15	126.51
	731.43	605.49		
	733.35	602.14		
19			131.92	133.24
	734.12	601.48		
	735.99	598.16		
20			138.55	140.06
	736.69	597.43		
	738.58	594.04		
21			145.25	146.84
	739.26	593.31		
	740.97	589.84		
22			151.87	153.63
	741.77	589.16		
		585.62		
23				160.33
		584.96		
		581.36		
24				
		580.73		
		577.05		
25				
		576.47		
		572.70		
26				
		572.13		

C2 (11,11) λ3920.759

0	25,501.39			
1	504.69	25,494.70	9.99	10.19
2	507.87	491.20	16.67	17.00
3	511.02	487.69	23.33	23.78
4	514.09	484.09	30.00	30.51
5	517.12	480.51	36.61	37.29
6	520.08	476.80	43.28	44.07
7	522.96	473.05	49.91	50.83
8	525.79	469.25	56.54	57.58
9	528.57	465.38	63.19	64.31
10	531.27	461.48	69.79	71.10
11	533.95	457.47	76.48	77.83
		453.53 5		
12	*p* 536.57 *d*		83.13	*p* 84.32
		p 453.36 5		
	539.01 5	" 449.99 4		
13			89.69	" 92.41
	" 539.63 9	449.27 5		
		" (444.25) 1		
		?448.76 2		
	" 539.63 9	" (448.11) 2		
14			96.35	" 98.98
	541.40 4	445.06 5		
		" 443.26 3		
	" 542.81 3	440.83 5		
15			102.94	"104.36
	543.75 4	" 439.86 4		
	" 545.33 5	436.52 4		
16			109.52	"111.48
	546.01 5	" 435.79 4		
	" 547.57 4	432.11 4		
17			116.09	"118.29
	548.21 4	" 431.49 4		
	" 549.74 5	427.69 4		
18			122.67	"125.01
	550.37 6	" 427.08 4		
	" 551.81 4	" 423.21 4		
19			129.24	"131.72
	" 552.44 4	" 422.56 3		
	" 553.83 3	" 418.67 3		
20			135.85	"138.40
	" 554.54 7	" 417.99 3		
	" 555.72 3	" 414.09 3		
21			142.37	"145.08
	" 556.46 2	" 413.36 3		

m	*R*(*m*)	*P*(*m*)	$\Delta_2F'(m)$	$\Delta_2F''(m)$
	25,557.53 2	25,409.58 3		
22			148.89	"151.57
	558.45 2	408.63 3		
	" 559.33 5	*p* 405.17 3		
23			155.44	"157. 14
	" 560.59 1	" 403.87 2		
	" 558.91 3	" 401.25 2		
24	" 561.03 2			
	" 561.56 1	" 399.06 2		
	" 562.73 2	" 398.68 1		
	" 563.34 4	" 397.57 0		
	" 563.81 2	" 394.31 1		
	" 564.75 d	" 390.41 0		
	" 565.95 0	" 389.72 1		
	" 566.32 0	" 386.69 1		
	" 567.06 d	" 385.79 0		
	" 567.77 6	" 382.10 1		
	" 568.34 2	" 377.02 3		
	" 569.41 0	" 374.69 d		
	" 570.52 0	371.80 1		
	" 571.48 0	370.68 1		
		366.36 1		
		365.71 1		
		360.76 1		
		360.32 1		
		354.94 1		
		354.72 1		
		348.95 d		

C3 (12,12) λ3953.333

0	25,291.24			
1	294.38	25,284.63	9.75	10.07
	297.27 3	281.34 1		
2			16.29	16.75
	297.65 1	281.00 2		
	300.18 3	277.88 2		
3			22.82	23.46
	300.73 2	277.39 3		
	303.00 4	274.30 4		
4			29.31	30.20
	303.63 3	273.71 3		
	305.68 5	270.62 4		
5			35.81	36.92
	306.45 4	269.88 4		
	308.29 5	266.80 4		
6			42.35	43.56
	309.19 4	265.98 5		
	310.78 b	263.00 5		
7			48.80	50.29
	311.82 5	261.99 5		
	313.20	259.00		
8			55.32	56.98
	314.34	257.90		
	315.51	254.90		
9			61.80	63.68
	316.74	253.75		
	317.71	250.73		
10			68.30	70.34
	319.07	249.46		
	319.78	246.45		
11			74.70	77.06
	321.19	245.11		
	321.70	242.05		
12			81.14	83.71
	323.24	240.61		
	323.47	237.52		
13			87.48	90.41
	325.03	236.02		
	325.03	232.85		
14			93.72	97.16
	326.53	231.28		
		227.96		
15	*p* 326.25 10			103.74
	" 326.96 6	226.43		
16	" 328.64 0	222.78		
	" 330.50 1	221.30		
	" 332.42 5	*p* 216.08 5		
	" 332.81 6	" 215.90 5		
	" 333.25 4	" 215.34 5		
	" 335.17 d	" 212.26 1		
	" 336.14 0	" 209.92 4		
	" 337.19 3	" 209.07 4		
	" 338.07 3	" 205.52 1		
	" 339.06 3	" 202.79 4		

TABLE I (*continued*)

m	R(m)	P(m)	$\Delta_2F'(m)$	$\Delta_2F''(m)$
	25,339.51 5	25,202.52 4		
	p 340.22 3	p 202.05 3		
	" 340.95 1	" 195.21 3		
	" 341.60 0	" 194.47 3		
	" 342.20 0	" 193.49 1		
	" 342.61 6	" 191.31 1		
	" 343.02 4	" 190.03 0		
	" 343.35 9	" 189.24 3		
	" 343.59 h	186.96		
		183.26		
		179.60		
		177.39		
		176.00		
		174.18		
		172.85		
		171.44		
		166.38		
		165.39		
		160.00		
		159.30		
		153.62		
		153.04		
		147.21		
		146.71		
		140.53		
		140.25		
		133.87 d		
		127.12 d		
		120.28 d		
		113.36 d		

C4 (13,13) λ3791.110

0	25,051.95 1			
1	054.89 2	25,045.34 1	9.55	10.07
2	057.82 4	041.88 3	15.94	16.60
3	060.64 6	038.29 5	22.35	23.22
4	063.34 7	034.60 7	28.74	29.87
5	065.91 8	030.77 8	35.14	36.49
6	068.34 8	026.85 9	41.49	43.14
7	070.71 9	022.77 9	47.94	49.72
8	072.90 9	018.62 10	54.28	56.42
9	074.94 9	014.29 10	60.65	62.99
10	076.88 10	009.91 10	66.97	69.62
11	078.71 9	005.32 10	73.39	76.23
12	080.35 9	000.65 10	79.70	82.85
13	081.90 9	24,995.86 10	86.04	89.45
14	083.29 8	990.90 9	92.39	96.06
15	084.55 8	985.84 9	98.71	102.65
16	085.65 8	980.64 9	105.01	109.25
17	086.66 8	975.30 9	111.36	115.83
18	087.49 8	969.82 8	117.67	122.42
19	088.23 8	964.24 8	123.99	128.99
20	088.75 7	958.50 8	130.25	135.62
21	089.16	952.61 7	136.55	142.15
22	089.42 h	946.60 7	142.82	148.72
23	089.42	940.44 6	148.98	155.29
24		934.13 6		161.73
25		927.69 5		
26		921.10 4		
27		914.32 4		
28		907.42 3		
29		900.38 3		
30		893.14 2		
31		p 886.11 1		
		" 885.76 1		
32		" 878.13 2		

C5 (14,14) λ4034.557

0	24,781.96			
1	784.98	24,775.61	9.37	9.84
2	787.81	772.12	15.69	16.42
3	790.46	768.56	21.90	23.01
4	792.95	764.80	28.15	29.60
5	p 795.33 d	760.86	34.47	36.17
	" (795.33) d			
6	" 796.64 2	756.78	40.29	42.75
	" 797.51 2			
		p 752.73		
7	" 799.82 d		47.24	p 49.32
		" 752.44		
		" (749.64) 0		
8	801.50	" 748.24 1	53.75	55.90
		" 747.26 4		
	" 803.25 5			
9		" 743.95 d	59.30	62.42
	" 803.80 3			
10	804.77	739.08	65.69	p 68.96

m	R(m)	P(m)	$\Delta_2F'(m)$	$\Delta_2F''(m)$
		p 24,734.73 3		
11	24,806.12		71.83	75.47
		" 734.29 6		
12	807.45	729.30	78.15	82.03
13	808.40	724.09	84.31	88.65
14	809.23 d	718.80	90.43	95.12
15	809.84 d	713.28 d	96.56	101.59
	810.24			
16		707.64 d	102.77	108.09
	810.59			
	810.59	701.88		
17			109.05	114.65
	811.01 h	701.63		
		695.90		
18				121.21
		695.63		
19		689.79		
		689.40		
20		683.42		
		682.97		
21		676.88		
		676.41		
22		670.14		
		669.61		
23		663.19		
		662.54		
24		655.88		
		655.22		
		p 647.80 1		
		" 647.45 2		
		" 645.40 1		
		" 639.01 2		
		" 634.41 1		
		" 629.22 1		
		" 624.39 0		
		" 615.30 4		

C6 (15,15) λ4083.176

1	24,489.69			
2	492.55 d			16.17
3	495.11 d	24,473.52	21.59	22.85
	497.07 2			
4		469.70 d	27.61	29.33
	497.56 4			
	499.21 3	465.99 5		
5			33.68	35.69
	499.72 5	465.56 3		
	501.19 4	461.82 5		
6			39.83	42.21
	501.72 5	461.42 4		
	502.90 4	457.49 5		
7			45.94	48.69
	503.49 5	457.01 5		
	504.46	453.00		
8			52.03	55.11
	505.13	452.53		
	505.90	448.36		
9			58.13	61.63
	506.52	447.80		
	507.03	443.47		
10			64.20	68.10
	507.69	442.86		
	508.15	438.38		
11			70.29	74.53
	508.65	437.84		
	509.01	433.12		
12			76.46	81.03
	509.57	432.54		
	509.57	427.63		
13			82.43	87.51
	510.03	427.12		
	510.03	422.06		
14			88.65	93.84
	510.84 h	421.51		
	510.33	416.22		
15			94.62	100.47
	510.84	415.71		
		410.20		
16				106.80
		409.72		
17		404.00		
		403.56		
18		397.41		
		397.11		
19		390.96		
		390.58		
		384.17		
		383.80		

Term Analysis

Description of bands. The most striking feature of the structure of these bands is perhaps the occurrence of certain large "perturbations" in the line series such as those at λλ3964 and 3928 (Fig. 1, *D* and *G*). Instead of being merely a displacement of one line from its expected position, as is the case in most perturbations hitherto known,[11] these extend over a number of consecutive lines of the series. In some places the displacements become so large that the assignment of rotational quantum numbers to the lines becomes uncertain. Aside from these irregularities, we find each band composed of a *P* and an *R* branch with a single missing line, or null-line, exactly as in the ordinary violet CN bands. The lines of each branch are in some bands composed of doublets, the separation at first increasing rapidly from zero, or nearly zero, near the null-line. In others, the lines are single throughout the band. The magnitude and course of the doubling varies greatly from one band to another, without apparent regularity (see Fig. 2, below). Thus in Fig. 1, *D*, the C3 band is seen to consist of wide doublets which encounter a perturbation at λ3947 (in the *R* branch) and λ3964 (in the *P* branch), while the next band in the series, C4 (Fig. 1, *E*), shows no appreciable doubling. In another case, the C2 band, part of which is shown in Fig. 1, *G*, the lines which are at first single suddenly split into doublets on passing the perturbation at λ3928.

The phenomena of perturbations and abnormal doubling seem to be related and are probably due to certain conditions of "resonance" in the molecule. Although undoubtedly of interest, they do not help greatly in the arrangement and interpretation of the bands, which is the purpose of this paper. They will therefore only be referred to incidentally in the following discussion, which will be chiefly concerned with the regularities which the bands show, and the conclusions to be drawn from these. Thus only the lines falling in regular series will be considered in the term analysis, and where doubling occurs, the center of each doublet will be used in applying the combination principle. A more complete consideration of the perturbations and of the variations in rotational doubling will be given in a later paper.

Term formula. The structural features of these bands (doublet *P*, doublet *R* branches, one missing line) show at once that they belong to a class of bands due to a $^2S \rightarrow {}^2S$ electron transition in the molecule, of which the violet CN system is the best known example.[12] In bands of this type, the rotational energy terms for low quantum numbers may be represented by[12,15]

$$F(j_k) = Bj_k(j_k+1) \pm \delta j_k = B\left[(j_k+\tfrac{1}{2})^2 - \tfrac{1}{4}\right] \pm \delta j_k, \qquad (1)$$

using the quantum numbers of the new mechanics. Here j_k takes integral values, and the corresponding angular momentum, $j_k h/2\pi$, includes the slight contribution from the electron system. That is, $j_k = m + \epsilon_k$, where

[11] National Research Council Bulletin No. 57, "Molecular Spectra in Gases," p. 90.
[12] R. S. Mulliken, Phys. Rev. **30**, 138 (1927).

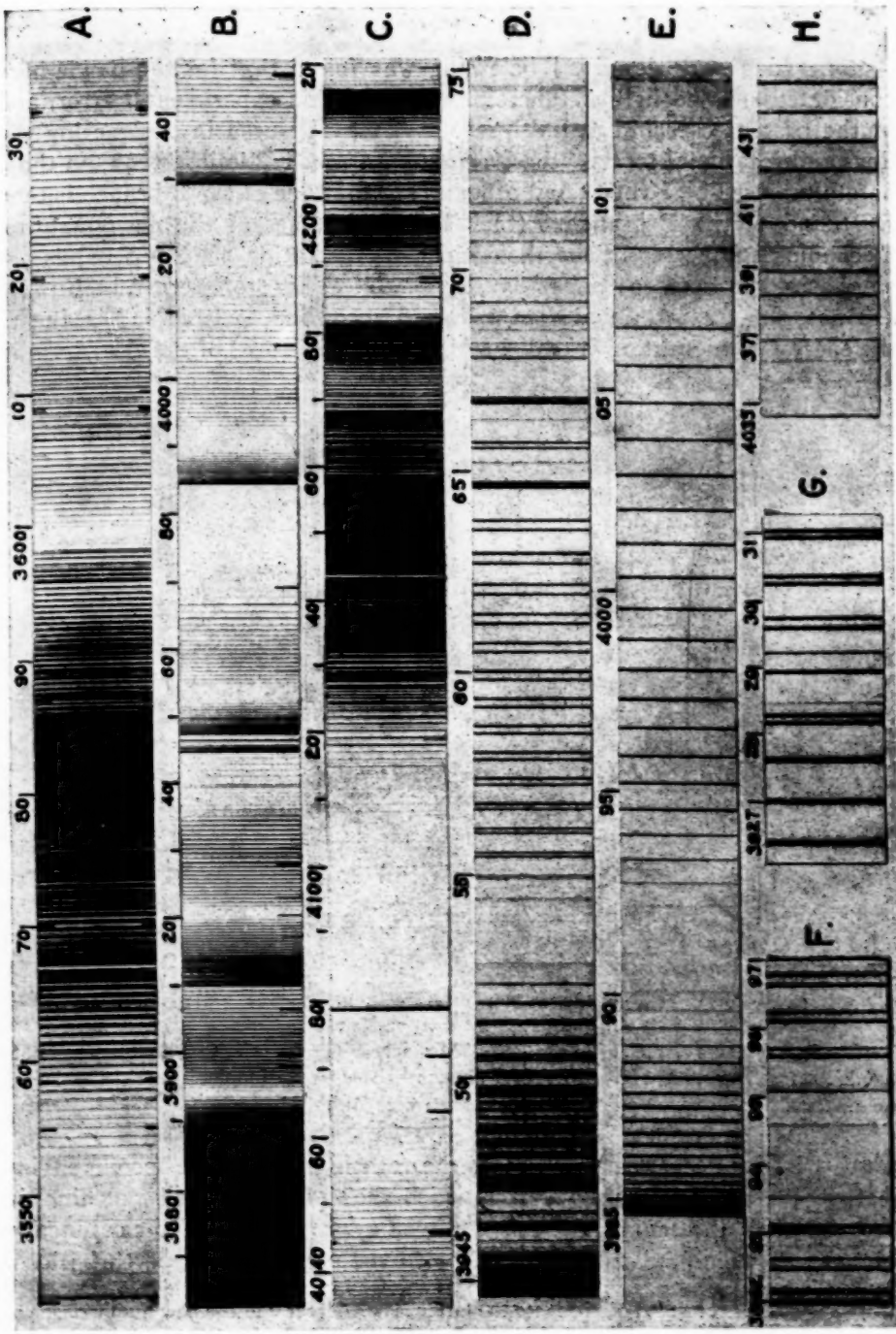

Fig. 1. CN spectrum from active nitrogen.

A. More intense portion of the sequence $n''-n' = -1$. The head at λ3542.27 is that of the A_4 band, (14,12), of the next sequence to the violet. The intensity minimum at the null-line of the B_1 band, (9,8), shows plainly at λ3617. A few doublets of the *R* branch of the B_2 band, (10,9), which does not form a head, are visible at the extreme right. Second order; iron arc comparison spectrum. *B.* and *C.* Tail bands C_1 to C_6, showing also the 4216 sequence of ordinary CN bands and the beginning of the 3883 sequence. First order; iron arc comparison spectrum. Cuts *D* to *H* are details from this set of tail bands with greater enlargement. *D.* C_3 band, (12,12), showing doubling and perturbations. Second order. *E.* C_4 band, (13,13). Second order. *F.* Region of the null-line of the C_1 band, (10,10). Note the unequal intensities of the doublet components. The long-wave component of $R(1)$, at λ3893.1, is strengthened by coincidence with a line of the (9,9) band. Second order. *G.* Beginning of the perturbation in the *P* branch of C_2, (11,11). Second order. Cf. Fif. 4 and text, p. 555. *H.* First few lines of the *P* branch of C_5, (14,14). The perturbations of $P(8)$, λ4039.6, and $P(11)$, λ4041.8, are evident. First order.

$\epsilon_k \ll m$. In a way described below, it was found that for the bands here considered ϵ_k is negligible. Therefore $j_k = m$ within experimental error, and in the present case integral values of m'' may be used in designating the lines and rotational terms,[13] these being uniformly 1/2 unit lower than those heretofore used by Kratzer and others. The first line of the R branch is then $R(0)$, and of the P branch, $P(1)$. The advantages of the new quantum mechanics numbering in the theoretical interpretation of $^2S \rightarrow {}^2S$ bands are emphasized in a recent paper by Mulliken.[12] The $\pm \delta j_k$ term[14] in Eq. (1) accounts for the rotational doubling, and according to Kemble[15] is due to the energy of orientation (parallel and anti-parallel to j_k) of the electron spin

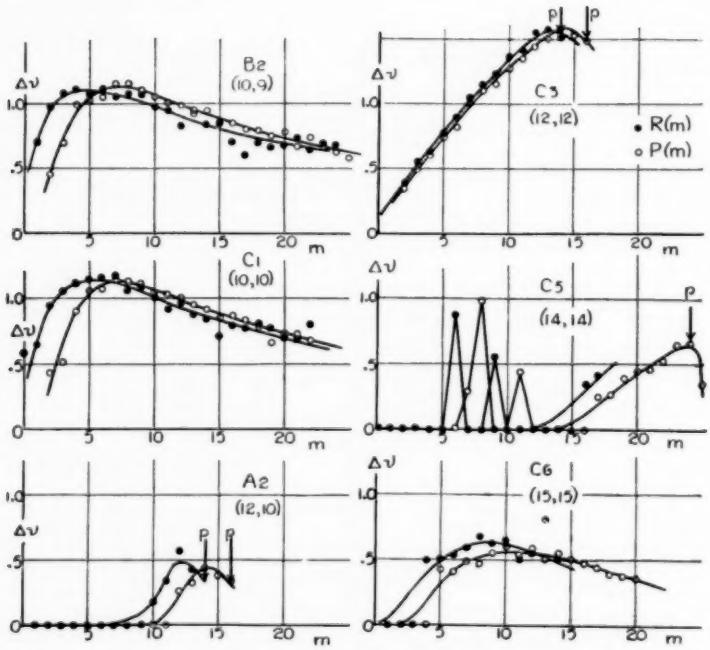

Fig. 2. Doublet separations in the P and R branches. Circles refer to P doublets and dots to R doublets. The vertical arrows marked p indicate the last true doublet before the beginning of a perturbation, in which doublets are no longer recognizable.

vector s in the net magnetic field of the rotating nuclei and accompanying electrons. As will be seen in Fig. 2, which shows the doublet separations in the tail bands, the separations are not even approximately a linear function of m, a fact which may be connected with the prevalence of perturbations.

[13] m is here used instead of j because the latter is half-integral in the new numbering, and has two values differing by unity for the components of each double level while these have the same value of m (and of j_k). It is only when it is necessary to distinguish between the components that j must be used.

[14] The exact form of this term in the new mechanics is uncertain but is immaterial for the present discussion.

[15] "Molecular Spectra in Gases," pp. 345–6.

Combination relations. For bands having only P and R branches, combinations between the lines of a band yield the following term differences:

$$\Delta_2F'(m)=R(m)-P(m)=F'(m+1)-F'(m-1)$$
$$=4B'(m'+\tfrac{1}{2})+8D'(m'+\tfrac{1}{2})^3+\cdots \quad (2)$$
$$\Delta_2F''(m)=R(m-1)-P(m+1)=F''(m+1)-F''(m-1)$$
$$=4B''(m''+\tfrac{1}{2})+8D''(m''+\tfrac{1}{2})^3+\cdots$$

The quantities Δ_2F' are characteristic of the initial state only, and are identical for bands of the same initial vibrational quantum number, while an analogous statement holds for Δ_2F'' in the final state. These combination differences are given in Table I. On comparing their values for the various bands, certain agreements are found, which require the relative assignment of vibrational quantum numbers represented in Table II.

Doubling and perturbations. The values of n' and n'' having been established, except for an additive constant c in each, it becomes of interest to see whether the doubling observed in certain bands is in the initial levels or in the final levels, or both, and also whether as is usual the perturbations are confined to the initial state. Fig. 2 is of interest in this connection. If the doubling is wholly in the initial state, the curve for the R branch should coincide with that for the P branch when the former is displaced two units to the right. This is very nearly true for all except the C3 band. In this case there is evidently a large doubling in the final state, but also a small initial-state doubling, since the R and P curves do not exactly coincide. The latter doubling is given by the curve for A2, since the final state of this band, $n''-c''=4$, has single levels. With the reasonable assumption that bands having strictly single lines have no appreciable doubling in either initial or final levels, the conclusion from such comparisons is that all final state levels are practically single except those of $n''-c''=5$, and that there is doubling in the initial state for $n'-c'=2$, 4, 6 and 7. The large perturbation in C2 is repeated in B4 and A3, while that in C3 is found in A2 and probably also in B4. Thus there is a perturbation in the final state $n''-c''=4$ beginning at $m''=12$, and in the initial state $n'-c'=4$ beginning at $m'=15$. Two small initial-state perturbations occur in the C5 band, affecting chiefly the rotational states $m'=7$ and 10 (cf. Fig. 2 and Fig. 1, H). The P branches of C4 and C5 also show irregularities beginning at $P(31)$ and $P(25)$ respectively. These cannot be definitely assigned to the initial or final state.

Assignment of the tail bands to the violet CN system. Since the tail bands are of the $^2S\rightarrow{}^2S$ type like the ordinary violet CN bands, and are found in the same spectral region, we are led to suppose that they are merely a further development of the well-known violet system. The fact that they are shaded to the red requires that $B'<B''$, while in the ordinary CN bands $B'>B''$. For the latter, Kratzer[16] gives: $B'=1.959-0.0221\,n'$, $B''=1.891-0.0173\,n''$,

[16] A. Kratzer, Ann. der Physik 71, 72 (1923).

TABLE II

Band constants and relative vibrational quantum numbers. As shown in the text, the probable values of the additive constants in the vibrational quantum numbers are $c'=8$, $c''=7$.

$n''-c''=1$	2	3	4	5	6	7	8	
$n'-c'$								
1 B1 $B'=1.7278$ $B''=1.7496$ $\nu_0=27,642.10$							Av.	$B'=1.7278$ $D'=-7.33\times10^{-6}$
2	B2 1.6968 1.7325 27,476.94	C1 1.6964 1.7137 25,672.69					$\omega'=1602.76$	1.6966 −7.41
3	A1 1.6630 1.7318 29,079.70	B3 1.6624 1.7141 27,275.45	C2 1.6631 1.6945 25,498.07				1542.42	1.6630 −7.50
4		A2 1.6292 1.7147 28,817.87	B4 1.6281 1.6941 27,040.49	C3 1.6281 1.6768 25,287.98			1483.58	1.6285 −7.59
5			A3 1.5969 1.6943 28,524.07		C4 1.5956 1.6591 25,048.63			1.5960 −7.67
6						C5 1.5629 1.6427 24,778.89		1.5629 −7.76
7	$\omega''1804.25$	1777.38	1752.51	1722.93			C6 1.5307 1.6226 24,483.85	1.5307 −7.85
Av. $B''=1.7496$ $D''=-6.60\times10^{-6}$	1.7323 −6.63	1.7138 −6.65	1.6945 −6.68	1.6768 −6.70	1.6591 −6.73	1.6427 −6.75	1.6226 −6.78	

so that if bands of sufficiently large n are present, B' for these may be less than B''. Preliminary values of these coefficients for the tail bands were calculated by taking 1/4 the mean of several values of $\Delta_2F/(m+\frac{1}{2})$, that is, neglecting the higher power terms in the last members of Eqs. (2). Plotting the resulting B' and B'' against vibrational quantum number, and comparing with the values for these quantities for low n from the ordinary CN bands, it was found that a very reasonable extrapolation was possible. The curves obtained were practically identical with those of Fig. 3B. Since B'' varies linearly and has the same slope as found by Kratzer for low n'', the assignment of n'' values for the tail bands is fairly certain. The additive constant c'' of Table II becomes 7. The strictly linear relation $B=B_0-\alpha n$ for the final state agrees with results on the NOβ bands,[8] where a long range of n'' is observed. For the initial states, c' cannot be determined with certainty

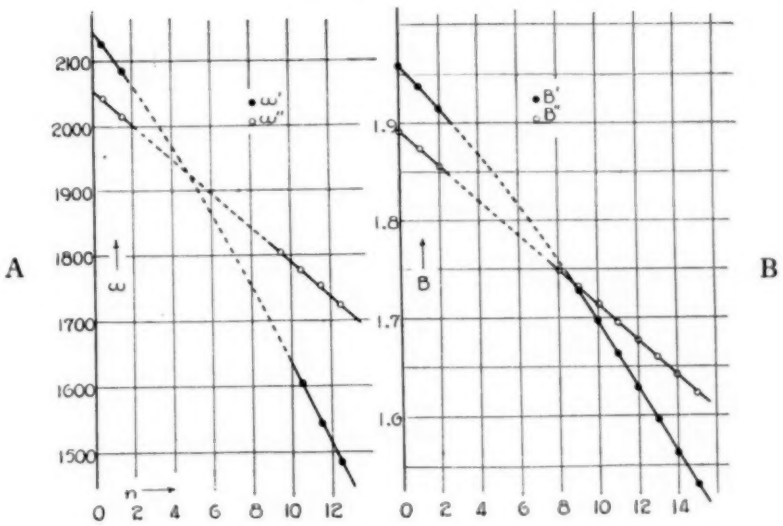

Fig. 3. Extrapolation of vibrational and rotational constants.

by this extrapolation, since the slope of the $B':n'$ curve is considerably greater for the tail bands than for low values of n', so that B' cannot decrease linearly throughout. However, a very rough calculation of the positions of the high n bands from Kratzer's vibrational term formulae (which amounts to an extrapolation of the *vibrational* constants) shows that with the numbering used $c'-c''$ can have only one reasonable value, namely 1. This means that the tail bands extending to the red from λ3883 (the C series) must represent the higher members of the sequence $n''-n'=0$ of the violet CN system. Hence $c'=8$, and the absolute vibrational quantum numbers of the tail bands as members of this system are found within the error of the linear extrapolation of B'', or about 1/6 unit. This assignment is followed in designating the bands in Table I, and also in Figs. 3A, and 5.

Evaluation of band constants. More precise values for the constants in the rotational energy function have been computed, using a method proposed

by Birge.[17] This involves first a theoretical calculation of the coefficient D_0, which is the D of Eqs. (2) for the state $n=0$, from approximately known values for B_0 and ω_0. The formula given by Pomeroy[18] may then be used to determine β in the relation $D=D_0+\beta n$. In this way the following equations were obtained: $D'=(-6.543-0.087n')10^{-6}$, $D''=(-6.403-0.025n'')10^{-6}$. The resulting values of this coefficient for the tail band will be found in Table II. Knowing its value for each vibrational state, it is possible to add a small corrective factor to the observed ΔF's for that state and obtain another set of quantities ΔF^* practically linear in m, which are given by the expression:

$$\Delta_2 F^*(m)=\Delta_2 F(m)-8D(m+\tfrac{1}{2})^3=(4B-8D)(m+\tfrac{1}{2}+\epsilon_k). \tag{3}$$

Thus a least squares solution of ΔF^* as a function of $m+\frac{1}{2}$ gives B and ϵ_k for the state considered. Preliminary computations for the initial and final states of the (12,11) band, a very regular band having single lines, showed the constant term, $4B\epsilon_k$, to be zero within the accuracy justified by the data. Assuming this to be the case for the other vibrational states, Eq. (3) becomes to a sufficient approximation: $\Delta_2 F^*(m)=4B(m+\frac{1}{2})$. This was the relation used in determining B' and B'' for each band by the method of least squares.[19] The results of this calculation are summarized in Table II, and the mean values are shown graphically in Fig. 3B. Using the data from the tail bands alone, we find: $B''=1.8944-0.0181n''$. This agrees well with Kratzer's equation for B'' in the ordinary CN bands, quoted above, and leaves little doubt that the present interpretation of the tail bands is correct, as well as the assignment of vibrational quantum numbers. At least a cubic is required to represent the variation of B' with n' at all satisfactorily.

Band origins and the vibrational terms. An independent value for the origin of a band can be calculated from each band line, provided the functions $F'(m)$ and $F''(m)$ are known, since one has for the origin

$$\nu_0=R(m)+F''(m)-F'(m+1)=P(m)+F''(m)-F'(m-1) \tag{4}$$

If in Eq. (1) the quantum number j_k (here equal to m) is given the values zero or -1, $F(m)$ becomes zero in each case. Hence for the nul-line, $R(-1)$ or $P(0)$, the quantity $F''-F'$ vanishes and the wave-number is identical with that of the origin. This is only true when the quantum numbers of the new mechanics are used, for in the previous numbering the wave-number of the null-line was $\nu_0+\frac{1}{4}(B'-B'')$. The origin of each of the tail bands has been calculated from the first few lines of the R and P branches, assuming $F(m)=B[(m+\frac{1}{2})^2-\frac{1}{4}]$ since for these lines the higher power terms are negligible. The resulting values of ν_0 are entered in Table II. They may now be used to investigate the vibrational terms. The mean nuclear vibration

[17] "Molecular Spectra in Gases," pp. 173–4. The procedure used is an adaptation of "method three."

[18] W. C. Pomeroy, Phys. Rev. **29**, 59 (1927).

[19] In this case we have the simple relation $4B=\Sigma[\Delta_2 F\times(m+\frac{1}{2})]/\Sigma(m+\frac{1}{2})^2$.

frequency, ω (expressed in cm^{-1}), for two adjacent vibrational states is given by the term-difference for these states.[20] Differences of this sort which can be directly evaluated by the combination principle are also given in Table II, and are plotted against n in Fig. 3A. It will be seen that ω'' is practically a linear function of n, as found by Birge and Sponer[21] for a large number of band systems. The linear extrapolation from low n values gives the best agreement when c'' of Table II is 7, an entirely satisfactory check on the conclusion reached from the extrapolation of B'', considered above. However, although the smooth curves of Fig. 3A show that the magnitude and variation of ω are consistent with the present idea of the true nature of the tail bands, a closer study of the variations of this quantity reveals some interesting irregularities. The best straight line through the four values of ω'' observed in the tail bands is given by $\omega_n'' = 2059.98 - 26.89n''$, which corresponds fairly well with Kratzer's equation from the ordinary CN bands: $\omega_n'' = 2055.64 - 27.50n''$. But, taking the deviations of the observed $\omega_{9.5}''$ to $\omega_{12.5}''$ from the first equation, we obtain -0.28, -0.26, $+1.76$ and -0.93 cm^{-1}, and hence a straight-line relation is not strictly accurate. That the probable error in the ν_0 values is less than 0.02 cm^{-1} is evidenced by the complete agreement in each case where the combination can be applied to vibrational terms ($\omega_{9.5}'' = 1804.25$, 1804.25; $\omega_{10.5}'' = 1777.38$, 1777.38—such agreement is partly accidental). Therefore the above deviations are real, and their lack of definite trend indicates that no simple function can be used to represent all the observed values of ω''. Only three values of ω'' can be found directly, but here also some anomaly is probably present, since they require a marked curvature in the opposite direction from that to be expected from Fig. 3A. These observations indicate the existence of certain perturbations of the vibrational terms,[22] but the number of ω values available is not sufficient to decide how many of the terms are thus displaced. On this account, the representation of the vibrational terms by accurate formulae, to calculate the null-line positions of all bands of the violet CN system, is unfortunately not possible.

Discussion of Results

New features of band-spectrum structure. The assignment of the tail bands to the violet CN system makes this the first known system having some bands shaded to the violet and others to the red. The transition from the former type to the latter in a given sequence takes place where $B' = B''$, or according to Fig. 3B near the (7,6), (9,9) and (10,11) bands in the sequences $n'' - n' = -1$, 0 and $+1$, respectively. The first bands of each sequence have the head on the low-frequency side of the origin, its distance from the latter increasing rapidly as the value of B' approaches that of B''. In this region

[20] "Molecular Spectra in Gases," p. 131.

[21] R. T. Birge and H. Sponer, Phys. Rev. **28**, 259 (1926).

[22] Such "vibrational perturbations" would not be without precedent. See R. T. Birge, Phys. Rev. **28**, 1157 (1926), where a displacement of one of the final levels of the CO Ångström bands is noted.

heads cease to be formed, due to the infinite number of rotational lines developed, and the bands are nearly symmetrical with almost equally spaced lines like the infra-red vibration-rotation bands. Shortly after B' becomes less than B'', the head reappears on the high-frequency side of the origin, becoming more pronounced as it approaches the intensity maximum of the R branch. The observed tail bands are all "shaded" to the red, although for those of lowest n, (9,8), (10,9) and (10,10), the quantity of $B'-B''$ is so small that no heads are formed at all in active nitrogen. The approximate symmetry of the (9,8) band, B1, may be seen in Fig. 1, A.

Another consequence of our interpretation of the tail bands is that the frequencies of the bands of a given sequence may pass through a maximum, eventually becoming smaller than that of its first band.[23] It is only beyond this point that the bands are readily observed, since here they are not confused with the stronger first members of the sequence. This explains how the high-n bands of a sequence can appear as tail bands on the *red* side of the head of its first band. The reversal of a sequence occurs where $\omega'=\omega''$, *i.e.*, near the (4,3), (5,5) and (6,7) bands of the -1, 0 and $+1$ sequences, interpolating the values on Fig. 3A. This figure emphasizes the general parallelism which is known to exist between B and ω, first pointed out by Birge[24] and Mecke.[25] It may be expressed by the qualitative rule that, if we define[26] the direction of degradation of a sequence as that of increasing n, bands are degraded in the same direction as the sequences they form. That the rule is not exact may be seen from the fact that the bands of the zero sequence, for instance, are shaded toward the violet ($B'>B''$) between $n=5$ and 9, whereas the sequence is here already proceeding toward the red ($\omega'<\omega''$).

The perturbations of rotational terms (and probably also of vibrational terms) are a very unusual feature of these bands, but were perhaps to be expected for bands of such large vibrational quantum numbers.[27] The two most extensive rotational perturbations occur in the states $n''=11$ and $n'=12$. Although the systematic study of these by means of the combination principle has not yet been completed, some interesting observations have been made on the first part of the perturbation in the (11,11) band, which is shown in Fig. 1, G. Fig. 4 gives the deviations of the lines of the P branch from the formula for band lines given by the coefficients B and D of Table II, for the evaluation of which only lines up to $m=11$ were used in this case. It will be seen that one series of lines passes through the first part of the perturbation, as far as $m=18$, with perfect regularity. The other components of the doublets, however, first resolved at $m=12$, draw rapidly away from the regu-

[23] That is, a sequence forms a "head" composed of bands analogous to the head formed by the lines of a band. Such a head of bands occurs in the CaF bands at λ5833. Cf. S. Datta, Proc. Roy. Soc. **99A,** 436 (1921). Plate 6 III.

[24] R. T. Birge, Phys. Rev. **25,** 240 (1925) (Abstract).

[25] R. Mecke, Zeits. f. Physik, **32,** 823 (1925).

[26] "Molecular Spectra in Gases," p. 77.

[27] The curves given by Uhler and Patterson (Ref. 4) show that the number of perturbations in the bands of the 3883 sequence increases rapidly with n.

lar components with increasing displacements toward the violet, and at the same time their intensity diminishes. But before these have disappeared another series appears on the long-wave side of the regular series, forming relatively wide doublets with the latter, and soon equalling it in intensity. The assignment of m values to the lines contains, of course, an element of arbitrariness when the deviations become so large, particularly in the case of the third, weakest component for $m = 13$ and 14 These last were included, however, because they lie on the smooth curves, and because of the intensity relations shown in the figure. It should also be mentioned that there is at least one weak line in this vicinity which is probably not accounted for on this arrangement. Since the initial levels of the (11, 11) band are entirely regular, and probably without appreciable doubling (see the (11, 10) band),

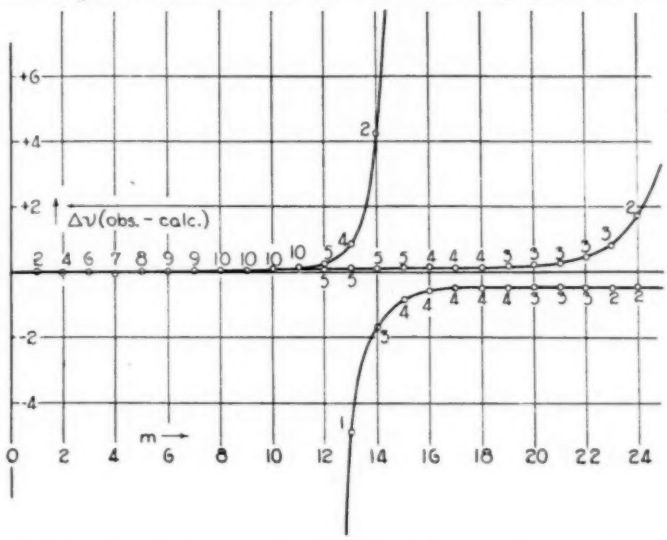

Fig. 4. Displacement of lines at a perturbation. The $\Delta\nu$ is the difference between the observed wave-numbers in the P branch of the (11,11) band and those given by $P(m) = \nu_0 + B' - 2B'M + (B' - B'' + 6D')M^2 - 4D'M^3 + (D' - D'')M^4$, where $M = m + \frac{1}{2}$ and the coefficients are those of Table II. The numbers given the estimated intensities of the lines. Most of these lines, except that of intensity 1, are visible on Plate I, *G*.

the curves of Fig. 3 also give the displacements of the rotational *terms* of the final state from the values to be expected by extrapolation of the terms from $m'' = 1$ to 11. The figure shows only one of the discontinuities which occur in this band; there is at least one other before regular series again become recognizable at about λ3940. Here a series of doublets with decreasing separation appears, showing no further irregularities. A similar structure occurs beyond the perturbations in the (12, 12) band (Plate I, *D*), where a series of such doublets may be seen in the P branch beginning at λ3970.

After Fig. 4 had been drawn, a remarkably similar case was found in the work of Schrödinger[28] on a perturbation which occurs in the $3^3D - n^3F$ series of the Al II line spectrum.[29] It appears as a discontinuity in the Rydberg

[28] E. Schrödinger, Ann. d. Physik. **77,** 43 (1925), Cf. Figs. 3 and 4.

[29] The writer is indebted to Dr. E. U. Condon for drawing his attention to this article.

corrections for the F terms, which at a certain value of n suddenly change from positive to negative. Schrödinger obtained curves very like those for the perturbed components in Fig. 4. The similarity even extending to a double occurrence of one total quantum number at the maximum of the perturbation. Since the form of the curves was suggestive of resonance, he proposed that the perturbation was due to the near coincidence of the frequencies of the perturbed *lines* in the fundamental series with the frequency of the resonance jump in the core. The latter frequency should be nearly that of $1^2S-2^2P_1$ in Al III, and this was indeed found to be the case. Just what frequencies are in resonance in the present instance is not yet obvious, but it seems significant that such an "anomalous dispersion" curve is obtained at a band-spectrum perturbation,[29a] since it indicates definitely that all such perturbations may be due to a more or less marked resonance within the molecule.

Relation to theory of $^2S\rightarrow{}^2S$ *bands.* Theoretical equations for the intensity distribution in the branches of a $^2S\rightarrow{}^2S$ band have recently been derived by Mulliken.[12] He finds that for the lowest values of m there should be an appreciable inequality in the intensities of the two components of the doublets forming the P and R branches. With increasing m the inequality should decrease rapidly, the components soon becoming practically equal in intensity. It is difficult to find experimental evidence for this effect, since usually the doublets are unresolved in the region where intensity differences should appear. Three of the tail bands show an exceptionally large doubling, the components being resolved down to $R(0)$ and $P(2)$ in the (10,9) and (10,10) bands (doubling in the initial state), and to $R(2)$ and $P(2)$ in the (12,12) band (doubling chiefly in the final state). In these cases the predicted intensity differences are observed, and, as far as can be decided by visual estimates, Mulliken's theoretical intensities[30] are quantitatively verified. Thus the components of the first line, which are resolved only in the case of $R(0)$ in the (10,9) and (10,10) bands, are approximately in the ratio 2:1. Also, allowing for occasional superpositions, the stronger component of one doublet equals the weaker component of the next higher m, and the intensity difference of the two components becomes imperceptible at about $m=9$ or 10 (see Fig. 1, D and F, also intensity data of Table I). This agrees with the theoretical requirement that the R_1 and R_2 components of the R branch doublets (and also P_1 and P_2), for which $j=j_k+\frac{1}{2}$ and $j_k-\frac{1}{2}$ respectively, should differ in intensity in approximately the ratio of their j values. The stronger components are therefore R_1 and P_1, and we find that the usual order of sub-levels,[12] $F_1>F_2$, holds for the states $n'=10$ and $n''=12$. According to Mulliken, the weaker components of the lines $R(0)$ and $P(1)$ are really the first lines of two weak Q branches, in each of which the intensity falls off sharply with increasing m. Further members of these Q branches will fall on top of the R and P lines unless there is a rather large doubling in

[29a] Curves undoubtedly of the same type were found by Birge in an investigation of the P branch of the (2, 2) band. See "Molecular Spectra in Gases" p. 90, Fig. 6.

[30] Fig. 1a of Ref. 12.

both initial and final states, which is not the case in any of the tail bands. However, it is important theoretically that the first line of a branch is observed as double in the only case where it would be expected to be resolved, that of the $R(0)$ line mentioned above. The fainter component of this line is to be designated $Q_{21}(0)$ in Mulliken's notation. It is also possible that the weakest member of the triplets into which the lines $R(6)$ and $P(8)$ of the (14,14) band are split by a perturbation (Fig. 1, *II*) may be a Q line, but

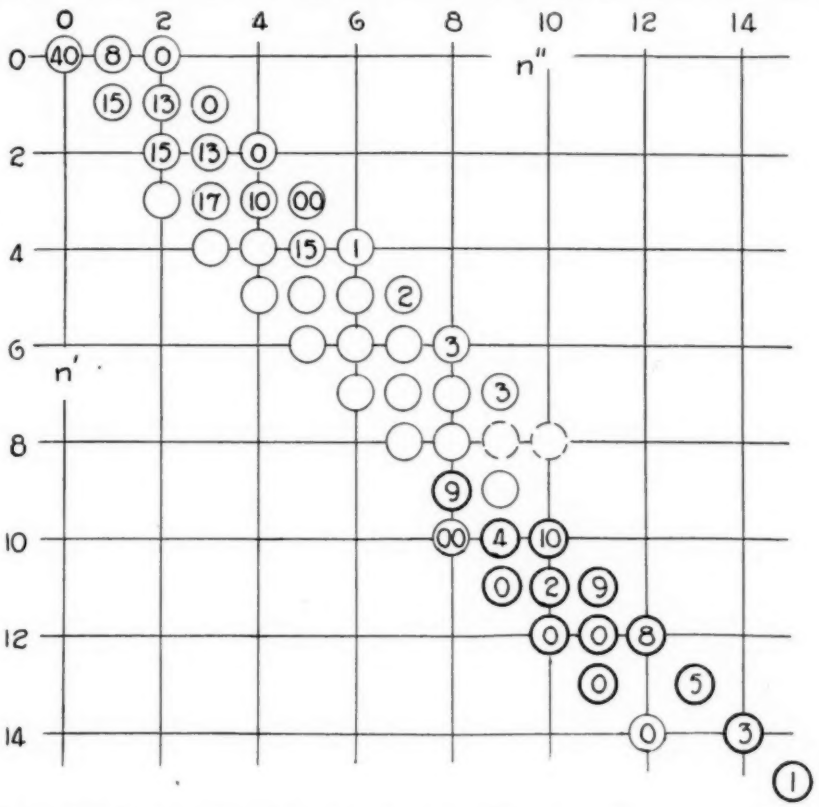

Fig. 5. Relative intensities of bands in the violet CN system. The heavy circles below at the right represent the tail bands measured. Circles without numbers represent bands which are probably present, but the intensities of which cannot be estimated, since they fall in the part of the sequence where there is much overlapping. Broken circles indicate that it is uncertain how far the corresponding sequences extend with appreciable intensity. The intensities of all of the tail bands, and of the (0, 0) and (0, 1) bands, were determined by comparing individual band lines. Others were estimated from the apparent intensity of the head, and are much less accurate. The mean of the intensity in the first and second orders is given.

the intensity relations are not right and, as was found above, anomalous lines occur near perturbations which cannot be thus interpreted.

Vibrational intensity distribution in the violet CN system. The relative intensities of the bands of the system as obtained from active nitrogen are given in Fig. 5. The excitation of bands of high vibrational quantum number is typical of a certain class of active nitrogen spectra in which the emitting

molecule is produced by a chemical reaction in the after-glow.[31] The distribution of molecules among the initial vibrational states is in this case far from a thermal one, and anomalous effects often occur; in Fig. 4 a preference for the even-numbered initial states $n'=0$, 2 and 4 will be noted. The maximum of intensity in a sequence occurs in general at much higher vibrational quantum numbers in active nitrogen than in the arc. This accounts for the unusual appearance of the -1 sequence in active nitrogen, since here the first one or two bands are completely absent, and the intensity maximum comes at or near the point of reversal of the sequence, where the bands are approximately symmetrical, *i.e.*, do not form heads. Unfortunately the intensity estimates cannot be carried through a whole sequence (except for the weak -2 sequence) owing to the overlapping of bands near the turning point, but the strength and dense spacing of the lines in this region show that there is no pronounced minimum here. Perhaps the most surprising feature brought out in Fig. 5 is the predominance of the 0 sequence of tail bands, for otherwise the usual rule holds that the larger the absolute magnitude of Δn, the higher the values of n' (or n'') for the most intense bands.

There is a series of faint doublets and other indications of band structure on the long-wave side of the 4216 head, which probably belong to the higher members of the $+1$ sequence. Also what is apparently a sequence of bands having its intensity maximum near the point of reversal (in appearance very similar to the 4606 ($+2$) sequence) was found further to the red than 4606, the heads occurring at λλ4715.06, 4698.11, 4684.74, 4680.17 and 4678.38. It was at first thought that these were bands of the $+3$ sequence, but calculations of the approximate positions to be expected for such bands show that this is impossible, the wave-numbers of the observed heads being a great deal too large. No correlation of these bands with the violet CN system has been obtained.

The writer is indebted to Professor R. S. Mulliken for calling his attention to the desirability of new data for the tail bands.

NEW YORK UNIVERSITY,
UNIVERSITY HEIGHTS, N. Y.,
January, 1928.

[31] R. S. Mulliken, Phys. Rev. **25**, 292 (1925); *ibid.* **26**, 333 (1926); W. Jevons, Ref. 6. In the CN spectrum, it is important that if CCl_4 is used instead of C_2H_2, the tail bands are relatively much weaker, but the red CN system is very intense. The differences may be due to the large amount of energy liberated in the decomposition of the latter substance.

ABSORPTION AND SCATTERING OF MERCURY VAPOR FOR THE LINE 2536

JULIUSZ ZBYSZKO ZIELINSKI

ABSTRACT

A beam from a mercury arc is passed through a vessel filled with mercury vapor of 16.2°C, and excites in it resonance radiation of wave-length 2536. The absorption coefficient and the scattering coefficient of this radiation have been measured. It was found: (a) the absorption coefficient is 1 cm^{-1} and is not changed measureably by the admission of air up to 4 mm pressure, although the resonance radiation is strongly quenched by the air; (b) in vacuum the scattering coefficient is equal to the absorption coefficient within the limits of the experimental error. This proves the assumption first made by Wood that in vacuum there is no true absorption, but that the whole loss of energy is due to scattering. For higher pressures, the scattering coefficient diminishes. The data found are in good agreement with previous direct measurements of Wood and Stuart.

IF THE light of the mercury emission line 2536 passes through mercury vapor, it is absorbed. The absorbed energy can either be transformed into heat (true absorption) or it can be re-emitted as resonance radiation, as was found by Wood.[1] The presence of other gases diminishes the amount of resonance radiation, as found by Wood,[2] Stuart[3] and others.

According to the classical theory, the total absorption of mercury vapor for the line 2536 should be the same in the case of mercury vapor alone as for mercury vapor in the presence of another gas. From measurements of Fuchtbauer, Joos and Dinckelacker[4] and Trumpy[5] it follows that the total absorption is changed by other gases of many atm. pressure. Their method of measuring the total absorption was based upon the fact that the line 2536, in the presence of a gas at high pressure, appeared so wide that several photometric determinations could be made across the line. The increase in the width of the absorption line by the admission of air to the exhausted tube containing the vapor was observed by R. W. Wood.[6]

In the present investigation, a method was employed which enabled measurements to be made of the total absorption in both cases, and, at the same time, of the true absorption, as distinguished from scattering (resonance radiation).

GENERAL DESCRIPTION OF THE METHOD

If a nearly parallel beam from a mercury arc passes through an evacuated quartz vessel filled with mercury vapor it excites resonance radiation which

[1] R. W. Wood, Phil. Mag. (6) **23**, 689 (1912); Phys. Zeits. **13**, 353 (1912).
[2] R. W. Wood and M. Kimura, Phil. Mag. (6) **32**, 329 (1916).
[3] H. A. Stuart, Zeits. f. Physik **32**, 262 (1925).
[4] C. Fuchtbauer, G. Joos and O. Dinkelacker, Ann. d. Physik **71**, 204 (1923).
[5] B. Trumpy, Zeits. f. Physik **40**, 594 (1926).
[6] R. W. Wood, Physical Optics, p. 488.

can be photographed. The decrease of this resonance radiation along the primary beam which is proportional to the decrease of the intensity of the radiation (capable of exciting resonance) in the primary beam itself, enables us to measure the total loss of energy (true absorption and scattering) along the primary beam in the mercury vapor. This method has been applied first by Wood,[2] then by Goos and Meyer[7] for the same purpose, but they did not make detailed measurements with different pressures of added gas. Hughes and Taylor have published new measurements on the subject by a different method in a paper which appeared after the completion of this investigation.[8]

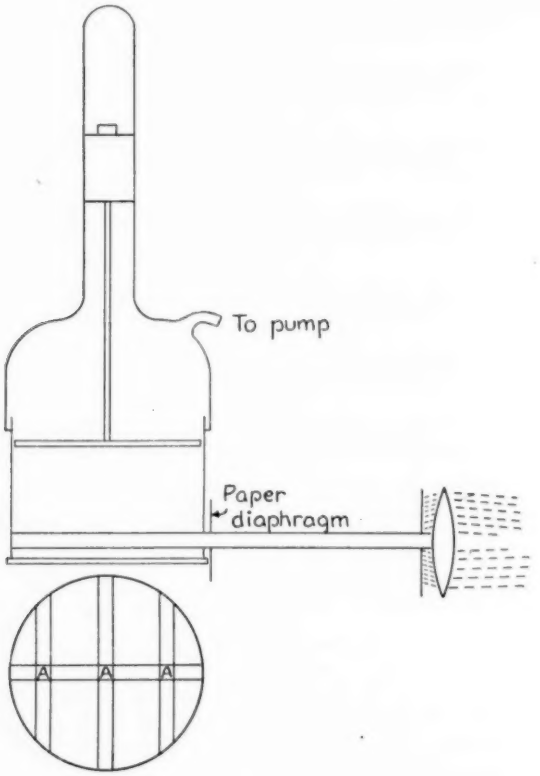

Fig. 1.

The resonance radiation from the primary beam in its outward passage excites the atoms in parts not illuminated directly by the primary beam, giving rise to secondary radiation, and by comparing the intensity of this with that of the resonance radiation from the primary beam we can calculate the absolute amount of scattering. To test this value the depth of the vessel in the direction perpendicular to the primary beam was varied by means of a movable disk covered with smoke to avoid reflection.

[7] F. Goos and H. Meyer, Zeits. f. Physik **35**, 803 (1926).
[8] A. Ll. Hughes and A. R. Thomas, Phys. Rev. **30**, 466 (1927).

Apparatus

The mercury resonance lamp was constructed from an open cylinder of fused quartz, to one end of which was sealed a glass tube. Within the vessel was a metallic disk attached at right angles to a glass rod which was connected to an iron cylinder, sliding in the glass tube. This could be moved to and fro by means of an electromagnet. The metallic disk was uniformly covered with turpentine smoke. On the outside of the plate which closed the vessel were fixed three narrow strips of a cellophane film, which were used as intensity marks. The transmission of the film strips for the line 2536 was tested by Professor Pfund and found to be 43 percent. The mercury resonance lamp was set up in a box which contained a thermo-regulator, the sensitivity of which was 0.2°C. The temperature inside the box was kept constant by means of a red incandescent lamp which was turned on or off by a telegraphic relay connected with the thermo-regulator. A camera, furnished with a quartz lens faced the resonance lamp, in a direction perpendicular to the exciting beam. The mercury arc, which excited the resonance lamp, was cooled with running water and air, and pressed against the front of the lamp by a magnetic field to avoid reversal. The light was focussed by a system of quartz lenses on the mercury resonance lamp, the lens nearest the resonance lamp having a diaphragm to make the beam nearly parallel. The illuminated side of the resonance lamp was covered with black paper perforated by a small rectangular opening, giving the primary beam a height of 4 mm and a depth of 2 mm. The resonance lamp was exhausted by a mercury vapor pump, and the pressure read by gauges, one reading between 10^{-3} and 10^{-4} mm, the other from 0.1 to 10 mm. Air was admitted to the system through a set of drying towers.

Method of Operating

After obtaining a vacuum of at least 10^{-2} mm and a constant temperature of 16.2°C, the arc was lighted, the beam made parallel to the front plate of the resonance lamp, and the diaphragm in front of the arc focussed by means of a barium platino-cyanide screen on the opening of the black paper covering the resonance lamp. The center of the opening was 6 mm behind the front plate. In spite of the fact that neither visible nor ultra-violet light hit the front plate, one could see with a rested eye a faint bluish light in the whole mercury resonance lamp which was more intense where the beam passed through. This light was probably scattered from the walls of the cylinder, but it was found to have no measurable effect on the photographic plate.

Next, four different series of exposures were taken. In the first, the mercury vapor alone was present. Next, three series were taken for different pressures of air in the resonance lamp, namely 0.4, 1.5, and 4 mm. For each pressure the disk inside the resonance lamp was placed in three different positions. In the first it was very near the primary beam but did not touch it, in the second and third it was pushed back. The position of the disk was known by reading the shadow of the iron cylinder upon a fixed scale. A fourth

exposure was taken with an absorption vessel before the arc. It consisted of a highly exhausted quartz bulb containing mercury vapor. The purpose of this was the following:

As the emission line from the mercury arc is much broader than the absorption line from the resonance lamp, the absorption coefficient would not be the same for the different parts of the emission line so that in the beam the center of the line would gradually be abstracted on its way through the vessel, and therefore the average absorption coefficient would be diminished. Besides, the outer parts of the line will excite less resonance radiation, so that for these outer parts the ratio between the secondary and the primary radiation would be smaller. If we now introduce the absorption vessel the center of the 2536 line in the exciting light is cut out, and the intensity observed is then due entirely to the outer parts of the line. If we subtract this intensity from the intensity observed without the absorption vessel, we get the effects due to the center of the exciting line alone.

The plates were developed in Eastman-Kodak developer at constant temperature, and with equal times of development.

Evaluation of the Plates

The photographic plates were measured on the recording densitometer at Princeton University.* On every curve was marked the zero for the densitometer and the fogging of the plate. To get the relation between densitometer readings and the corresponding intensities of the light, one should print intensity marks on each plate. Instead, the following simpler method was used. On all plates the photometer readings inside a cellophane absorption-strip were taken. For the same place the photometer reading was found which would be there without the absorption strip by extrapolating from both sides. Each plate should give nine sets of this kind (three strips each measured in the primary beam, and 4 and 8 mm above), but not always could all nine measurements be made. We then plot (Fig. 2) the photometer readings inside of an absorption strip against the corresponding extrapolated readings. It appears that the points from all plates fall very closely on the same curve which was drawn so as to best fit them. From this the relation between photometer readings and intensity was obtained in the following way:

We call arbitrarily the intensity belonging to the reading 4.5 of the densitometer 1000. The corresponding reading inside the strip would be 9 according to the curve. As the strip has a transmission of 43 percent, the corresponding intensity will be 430. We must now determine which photometric reading we would get inside the strip at a point where the extrapolated intensity would be 430 and, therefore, the extrapolated reading 9. We find on the curve the value 18.5, the corresponding intensity of which is $0.43 \times 430 = 184.9$. We proceed in the same manner and find that the photometric

* We wish to express our thanks to Professor K. T. Compton for his permission to use this instrument.

reading inside of a strip would be 33.5 if the extrapolated reading is 18.5. Therefore, the intensity corresponding to the photometric reading 33.5 is 0.43×184.9. In this way a curve giving the intensities for every photometric reading was found.

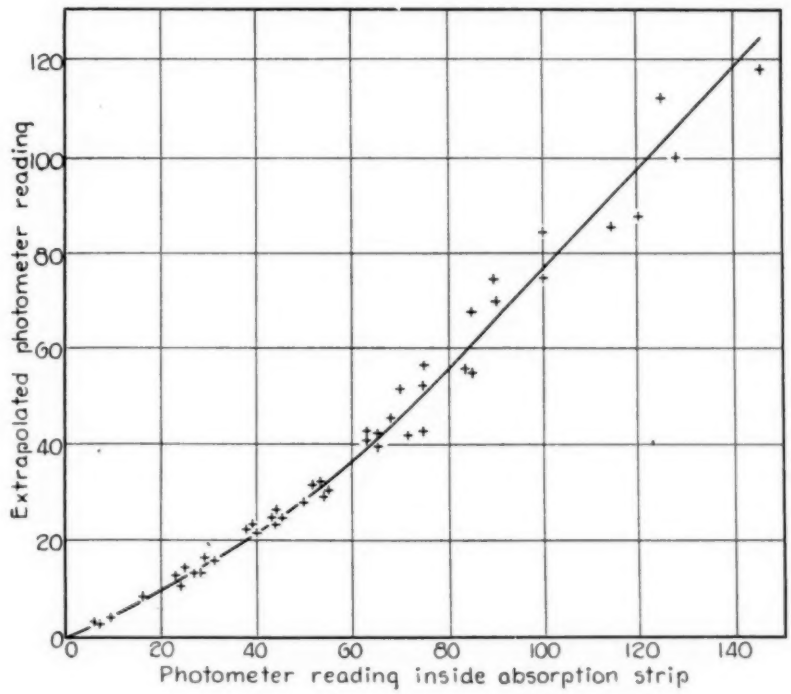

Fig. 2.

In the evaluation of the plates the photometric readings for a number of successive places were taken from the records of the densitometer. The curve gives corresponding intensities. The intensities corresponding to the fogging of the plates were subtracted from these values. The position of

TABLE I

Intensities of resonance radiation in primary beam and at various distances from it.
Mercury vapor at 16.2°C, no foreign gas.

Primary beam		Secondary radiation 4 mm height		Secondary radiation 8 mm height		Primary Beam after passing through absorption vessel	
D	*I*	*D*	*I*	*D*	*I*	*D*	*I*
8.75	1020	8.75	245	6.75	100		
12.75	425	15.75	85	8.75	91	3.75	101
19.75	177	19.75	55	14.75	48	8.75	83
28.75	72	28.75	22	19.75	29	15.75	71
32.75	54			28.75	9.5	21.75	46
				32.75	6.5	25.75	35

each spot was fixed by measuring the horizontal distance from the first absorption strip, the vertical distance from the middle of the primary beam.

Table I gives an example for vacuum with the disk close to the primary beam. D is the horizontal distance (in mm) from the place where the beam enters the vessel; I, the intensity after subtracting the fogging.

Total Absorption

We subtract now the intensities measured with the absorption vessel before the arc from the main values as described on page 562. The logarithms of the resulting intensities in the primary beam which are due to the center of the line alone, are plotted in Fig. 3 against the distance (disk close to the

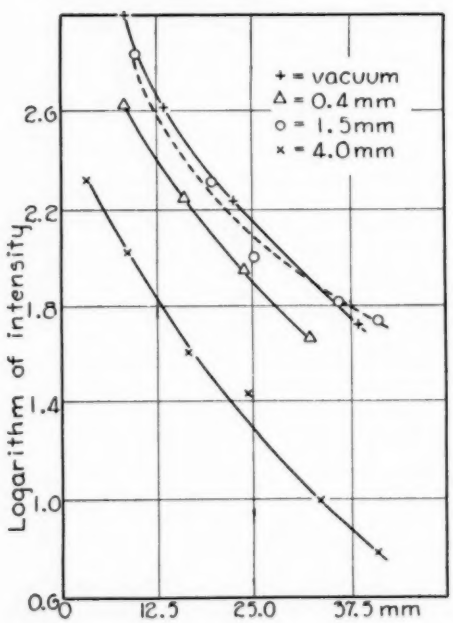

Fig. 3.

beam). The slope of these curves gives the absorption coefficient. As the figure shows the curves are parallel for all pressures in spite of the fact that the resonance radiation at 4 mm pressure of air is less than one-half of the radiation in vacuum. (Wood, Stuart.) The intensity of the primary beam for 1.5 mm pressure is in our experiment about the same as for vacuum (the curves coincide practically), while it should be about 60 percent. On the other hand, the radiation for 4 mm is ten times smaller than in vacuum while it should be only four times as small. This must be explained by changes in the mercury arc from one measurement to the other. These changes will not affect our results because we have to compare only intensities on the same plate to evaluate absorption and scattering.

The fact that the curves are parallel means that the absorption coefficients are not changed by 4 mm of air in agreement with the classical theory. It

should be mentioned that the pressure of 4 mm is far too small to alter the width of the line.

If the absorption were constant along the beam the curves would be straight lines. This is not true, but the deviation is not large, less than it would have been if the effects of the outer part of the line had not been subtracted.

If we define the absorption coefficient α by the equation

$$I = I_0 e^{-\alpha z}$$

where z is the distance along the beam we get the following average value over the distance from 0 to 18.5 mm:

TABLE II

Absorption coefficient of mercury vapor (pressure that of the saturated vapor at 16.2°C) in the presence of air at various pressures.

Air pressure:	0 mm	0.4 mm	1.5 mm	4 mm
Absorption coefficient:	1.09	0.95	1.09	0.90

giving as average $\alpha = 1$ cm^{-1}. This means a reduction of the intensity to half of its value over a distance of 7 mm in excellent agreement with the results of Wood and of Goos and Meyer who worked in vacuum (pure mercury vapor) and at slightly different temperatures.

If we plot the intensities of the primary beam after preliminary passage through the bulb of mercury vapor (the primary resonance now being due to the outer part of the exciting line 2536) we get for α 0.3 to 0.5. As expected, the value is smaller than the one for the center of the line.

SCATTERING COEFFICIENT

If a beam of light of intensity I passes through a volume element $dxdydz$ the amount of light scattered will be proportional to I, to the size of the element and to a coefficient β, the scattering coefficient, the scattered light being $\beta I dxdydz$.

The calculation of the absolute value of β from our measurements would demand an exact formula for the distribution of scattered light through the whole vessel for all values of β. Unfortunately the mathematical difficulties are too great, and therefore, an approximate calculation had to be made.

Assume that we have a parallel primary beam of light. We measure x upward, y in the direction away from the observer and z along the beam. The intensity would be

$$I = I_0 e^{-\alpha z}$$

We will assume that the resonance radiation is unpolarized (rather high pressure and stray magnetic fields). Then a volume element in the primary beam will emit an amount of scattered light equal to $\beta I dxdydz$. If we photograph a volume element emitting an amount of light $I' dxdydz$ with a camera, the axis of which is parallel to the y axis, the intensity on the photographic plate will be proportional to the amount of light emitted divided by $dxdz$, the cross section of the source normal to the line of vision,

and multiplied by a constant B which depends on the aperture of the camera. The intensity will therefore be $e^{-\alpha y}BI'dy$, dy being the depth of the source in the line of vision. In our case this will be $B\beta Idye^{-\alpha y}$, y being the distance from the source to the window.

Now the light emitted from this volume element will produce in another volume element $dXdYdZ$ a secondary radiation of the amount $\beta dXdYdZ$ $(1/4\pi r^2)e^{-\alpha r}\beta Idxdydz$. The intensity of this radiation on the photographic plate will be

$$Be^{-\alpha Y}\beta dY(1/4\pi r^2)e^{-\alpha r}\beta Idxdydz$$

because now the cross section is $dXdZ$, the radiation has to penetrate the further distance Y through the mercury vapor while the geometric condition which determines B is the same as in the primary beam. We get, therefore, for the ratio between the intensity at the place X above the primary beam compared with the intensity in the primary beam

$$(\beta\times 0.4/4\pi)\quad \int dY\cdot\int dze^{-\alpha(Y-y_0)}e^{-\alpha(z-z_0)}e^{-\alpha r}/r^2$$

Here we have assumed that the primary beam has so little depth and height that the integration over x, y can be replaced by a multiplication with its cross section 0.2×0.4 cm square. We measure x and y from the middle of the primary beam and make our calculation at a place $z_0=0.875$ cm (meaning the horizontal distance from the place where the beam enters the vessel). The calculation was made for the height $X=0.4$ and 0.8 cms for which the intensities were determined photometrically. We call the intensity of the primary beam I_1, the intensity for 0.4 cm I_2, for 0.8 I_3. The integration was performed graphically for different values of Y, and the result integrated graphically over Y. We find as contributions of the directly excited fluorescence radiation

Disk at front		Disk at back	
$X=0.8$	$0.0328\beta I_1$	$X=0.8$	$0.0445\beta I_1$
$X=0.4$		$X=0.4$	$0.15\ \beta I_1$

We next take into account the exciting effect of secondary radiation from other places. For this purpose we proceed in the following way: The layer in the height 0.8 is acted upon by the secondary radiation coming from the layer between the primary beam and the considered layer. This exciting layer has the same height of 0.4 cm as the primary beam, an average distance 0.4 cm from the considered layer 0.8, and a measured intensity of emitted light, namely, I_2. Closer consideration shows that it does not matter much that in this case the source of radiation is spread out into a layer instead of being a narrow beam. Therefore, the layer 2 acts on the layer 3 in the same way in which the primary beam acts on the layer 2. Finally, the layer three will excite the layer 2 in the same way in which the layer 2 excites the layer 3.

As last correction we take into account the excitation by the secondary radiation from the considered layer itself. For this purpose we divide the layer into a number of parallel beams, among which the intensity distribution has been calculated previously. Adding these the influence of the layer on itself turns out to be 0.4 I. We therefore get the following formula:

$$I_2(\text{calc.}) = \beta(0.15I_1 + 0.4I_2 + 0.15I_3)$$

for the layer at $X = 0.4$ independent of the position of the disk.

$$I_3(\text{calc.}) = \beta(0.0445I_1 + 0.15I_2 + 0.4I_3)$$

for the layer at $X = 0.8$ with the disk back or in the middle,

$$I_3(\text{calc.}) = \beta(0.0328I_1 + 0.15I_2 + 0.4I_3)$$

with the disk in front.

The results are shown in Table III.

TABLE III

Scattering coefficient for mercury vapor (pressure of saturated vapor at 16.2°C) for various pressures of air added.

Air pressure in mm.	Pos. of Disc.	$X=0.4$ β	$X=0.4$ β (ave.)	$X=0.8$ β	$X=0.8$ β (ave.)
0	Front	0.92		0.86	
	Middle	0.95	1.06	1.03	0.90
	Back	1.30		0.82	
0.4	Front	0.86		0.81	
	Middle	0.99	0.85	0.83	0.76
	Back	0.71		0.65	
1.5	Front	0.55		0.42	
	Middle	0.85	0.69	0.44	0.47
	Back	0.67		0.62	
4	Front	0.54			
	Middle	0.77	0.65		

If we compare the values of β average in the table with the data of Wood[2] and Stuart[3] for the quenching of the resonance radiation we find:

TABLE IV

Comparison of relative scattering coefficient with results of Wood and of Stuart.

Pressure	Layer 0.8 cm	Layer 0.4 cm	Wood	Stuart
0	1	1	1	1
0.4 mm	0.84	0.80	0.80	0.78
1.5 mm	0.52	0.65	0.60	0.43
4 mm		0.61	0.40	0.25

Except for the highest pressure the agreement is as good as can be expected. The absolute value of β in vacuum, 0.98 as average between the two layers is identical in the limits of the errors of observation with the absorption

coefficient α, confirming an opinion expressed by Wood as early as 1912 and since this time often repeated that in vacuum there exists no true absorption but that the whole loss of energy in the primary beam is due to scattering. This had been proved by Paschen[9] for the infrared radiation of excited helium, and made probable by him also for mercury.

I express my sincere thanks to Professor R. W. Wood for suggesting this problem and for his continuous encouragement and advice, and also to Professors Pfund and Herzfeld for their help.

PHYSICS DEPARTMENT,
THE JOHNS HOPKINS UNIVERSITY,
December 18, 1927.

[9] F. Paschen, Ann. d. Physik **45**, 625 (1914).

A QUANTITATIVE STUDY OF THE CHANGES PRODUCED IN THE ABSORPTION BANDS OF CERTAIN ORGANIC FLUORESCENT DYE SOLUTIONS BY ALTERATIONS OF CONCENTRATION AND TEMPERATURE

By William E. Speas

Abstract

The forms of the absorption bands have been obtained for solutions of rhodamin-B and eosin at different concentrations and temperatures; also for solutions of fluorescein, uranine, and resorcinol-benzein at various temperatures. It has been found that an increase in concentration produces the same general effect on the absorption bands as a lowering of the temperature of the solutions. In a concentrated aqueous solution of rhodamin-B there are two prominent bands in the visible which overlap. Change in concentration produces unsymmetrical modifications in the forms of the bands, one band growing at the expense of the other. Increase in the temperature of the concentrated solution produces the same effect on the bands as a reduction in concentration. Temperture changes produce only a slight effect on the absorption of a dilute solution. Increase in concentration of an alcoholic solution of rhodamin-B produces an increase in the absorption per molecule and a shift of the bands towards the red. Lowering the temperature of a dilute solution produces an effect similar to that due to an increase in concentration. Decrease in temperature of a concentrated solution produces an increase in absorption which is less than for a dilute solution, and produces no observable shift in the bands. Increase in concentration of an alkaline alcoholic solution of eosin produces a slight increase in absorption, and a shift of the bands towards the violet. Decrease in temperature produces a similar effect which is more marked for a dilute solution than for a concentrated solution. Increase in temperature in neutral alcoholic solutions of fluorescein and eosin causes a marked increase in the absorption, but no shift of the bands. The solutions become colorless at very low temperatures. Increase in temperature of an alcoholic solution of uranine produces an increase in the intensity of the band, and a shift of the band towards the red. Increase in temperature in alcoholic solutions of resorcinol-benzein causes a decrease in absorption with no appreciable shift of the bands.

A theory recently proposed by Merritt to account for the form of the absorption bands of the organic dye solutions on the long wave-length side has been tested with the data herein recorded and has been verified for dilute aqueous solutions of rhodamin but not for the other solutions.

SOLUTIONS of the organic dyes usually possess absorption bands that are sharply defined and relatively simple in form, while the fact that there are prominent bands in the visible spectrum makes it possible to measure the absorption by means of the spectrophotometer rather than by more complicated methods. Such solutions seem therefore specially suited for use in studying the absorption of liquids. The fact that the organic dyes often show fluorescence and anomalous dispersion adds to the significance of such a study.

The work described in the present paper deals chiefly with the influence of temperature upon the absorption of certain fluorescent dyes.

Experimental

Measurements of absorption were made of fluorescein, eosin, uranine, and resorcinol-benzein in alcoholic solution, and of rhodamin-B both in alcoholic and aqueous solutions. A few measurements were also made with solid films of rhodamin and of eosin.

With the exception of uranine, which was the ordinary commercial dye, from Heller and Merz, all of the materials used were of unusual purity. The rhodamin-B, prepared with special care, was furnished by the Du Pont Company. The fluorescein and eosin were prepared by A. J. Hemmer.[1] The resorcinol-benzein, prepared by C. Wang, has been studied for absorption at ordinary temperatures by Orndorff, Gibbs, and Shapiro.[2] In making the alcoholic solutions the best grade of absolute ethyl alcohol was used. The solutions were kept in a dark room in Pyrex glass.

In measuring the absorption of the solutions two similar cells were used, one containing the solution and the other the solvent alone, and the transmission of each was measured throughout the spectrum by a Lummer-Brodhun spectrophotometer. Slit width corrections for diffraction, as determined by Nichols and Merrit, were applied.[3] If T is the transmittance of the layer of the solution, i.e. the ratio of the two corrected slit widths, then the coefficient of absorption is given by

$$\beta = (1/cd) \log_{10} (1/T)$$

where d is the thickness of the layer of the solution and c the concentration in grams per liter. Since in each case the same solution was used for the whole absorption curve the use of Beer's Law, which is often violated, introduces no error. In most cases the cell-thickness was so chosen as to keep the slit-width at least as great as 0.1 mm, for slit-width corrections are uncertain for widths smaller than this.

The cells were made of two circular plates of Pyrex glass separated by a cylinder of Pyrex glass 2.5 cm in diameter, ground to the desired height. The thickness of the cells ranged from 0.008 cm to 4.00 cm and was uniform to within 0.01 mm. The thin cells were made by using glass cylinders of 3 mm height and fitting into them circular pieces of hard glass of uniform thickness so as to reduce the thickness of the liquid layer. The cells were placed in brass tubes with threaded ends, the heights of the brass cylinders being slightly less than the heights of the glass cylinders. The end plates could thus be forced tightly against the ends of the glass cylinders to prevent leakage. No cement was used. The cooling arrangement, which was designed by Professor Gibbs, consisted of a rectangular brass box 10 cm thick with a

[1] W. R. Orndorff and A. J. Hemmer, J. A. C. S. **49**, 1272 (1927).

[2] W. R. Orndorff, R. C. Gibbs, and C. V. Shapiro, J. A. C. S. **48**, 1327 (1926).

[3] E. L. Nicholas and E. Merritt, Studies in Luminescence, Carnegie Inst. Pub., No. 152, p. 168.

capacity of about two liters. Two cylindrical brass tubes, into which the cells fitted snugly, passed parallel to each other through the box (Fig. 1). The box was insulated by a heavy coating of felt. By means of a trolley arrangement each cell could be brought in turn in front of the slit of one of the collimators of the spectrophotometer.

For temperatures above room-temperature water was placed in the box and heated with an electric heating coil. For low temperatures the cooling mixture that proved to be the most satisfactory consisted of a mixture of equal parts of carbon tetrachloride and chloroform, which was cooled by carbon dioxide snow. This forms a slush at approximately $-75°C$. For lower temperatures petroleum ether was used, which was first cooled down by adding carbon dioxide snow and then cooled still more by bubbling liquid air through it.

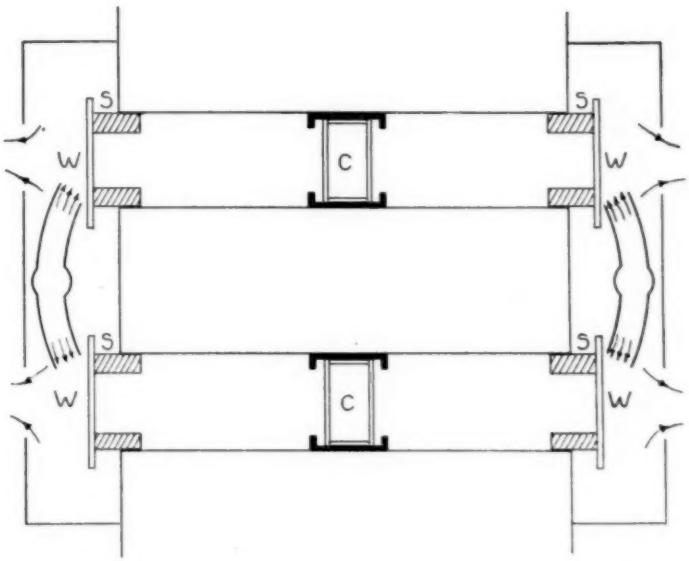

Fig. 1. Illustrating method of preventing moisture from accumulating on the cells.

Considerable difficulty was experienced in preventing moisture and frost from accumulating on the end plates of the cells. The method which proved successful is illustrated in Fig. 1. Cork stoppers, *S*, (shaded in the figure) which fitted into the cylindrical openings of the cooling box, were bored out with holes two centimeters in diameter. Glass plates were cemented on to the large ends of the corks with shellac. A heavy coating of shellac was placed on the corks to stop the pores. Two pasteboard-box covers were pierced with two holes each so spaced that when the covers were tied on against the box they were opposite the windows. Streams of dry air were directed against the windows *W* and it was found that when the air was flowing steadily no moisture collected either on the ends of the cells *C* or on the windows at a temperature as low as $-90°C$.

The low temperatures were measured with a calibrated pentane the r mometer.

The results are shown graphically in Figs. 2 to 6, the observed absorption coefficients being in each case plotted against wave-numbers (i.e. the number of waves per millimeter).

Discussion of Results

Rhodamin-B in aqueous solution. There is a marked difference in the absorption bands of dilute and concentrated solutions (Fig. 2, I). Intermediate forms can be obtained by using intermediate concentrations. If we start with a dilute solution and gradually increase the concentration the band

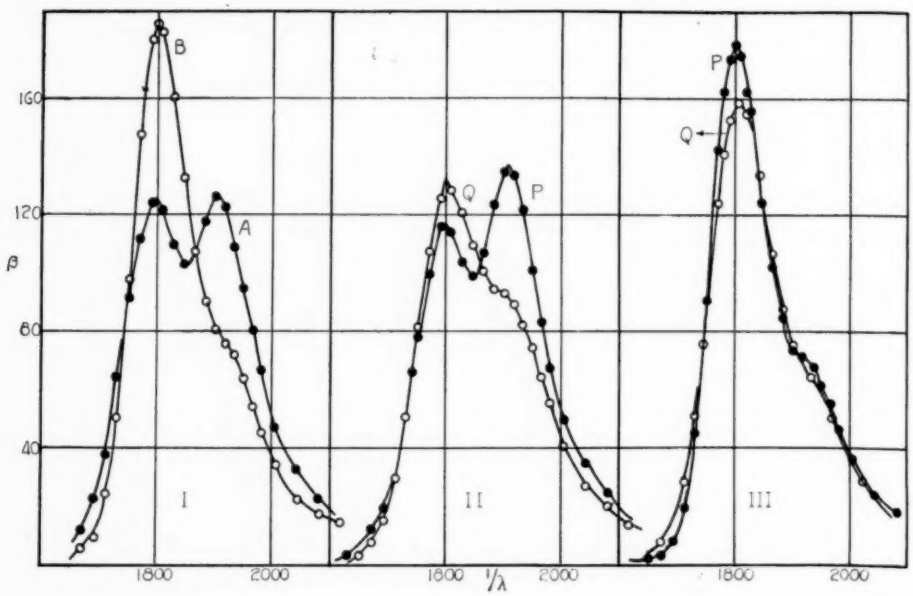

Fig. 2. Rhodamin-B in aqueous solution. I. Concentration effect: *A*, concentration 1000 mg per liter; *B*, concentration 1 mg per liter. Temperature of each 20°C. II. Temperature effect: *P*, temperature 0°C; *Q*, 90°C. Concentration of each 1000 mg per liter. III. Temperature effect: *P*, temperature 0°C; *Q*, 85°C. Concentration of each 1 mg per liter.

towards the red begins to decrease in intensity while the small band towards the violet grows until it is the more intense of the two.

Increase in the temperature of a concentrated solution produces the same sort of change as decrease in the concentration (Fig. 2, II). As the temperature is lowered the more refrangible band becomes more pronounced while the intensity of the other is reduced; when the temperature is raised the shorter wave-length band is greatly reduced while the one towards the red is increased.

Changes with concentration similar to those here described have been found by Holmes[4] not only with rhodamin-B but also with a number of

[4] W. C. Holmes, Ind. and Eng. Chem. **16**, 35 (1924).

other dyes in aqueous solution. Pringsheim[5] observed the same sort of changes in the bands of alkaline aqueous solutions of fluorescein and eosin as the concentrations were varied. The form of the bands for a concentrated aqueous solution of rhodamin-B has also been determined by Uhler and Wood.[6] The effect of temperature changes has not been previously studied.

Holmes concludes that the two bands are probably due to two constitutional forms of the material in dynamic equilibrium, and that equilibrium depends on concentration. The writer is of the opinion that the temperature

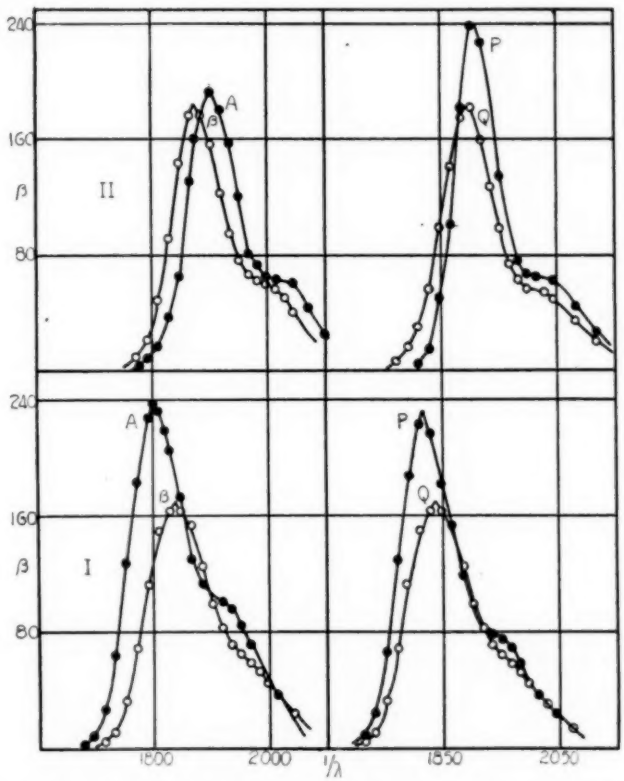

Fig. 3. I. Rhodamin-B in alcoholic solution. Concentration effect (left); *A*, concentration 500 mg per liter; *B*, concentration 1 mg per liter. Temperature of each 20°C. Temperature effect (right): *P*, temperature −70°C; *Q*, 17°C. Concentration of each 1 mg per liter. II. Eosin+12 molecules of KOH in alcoholic solution. Concentration effect (left): *A*, concentration 500 mg per liter; *B*, concentration 1 mg per liter. Temperature of each 20°C. Temperature effect (right): *P*, temperature −75°C; *Q*, 20°C. Concentration of each 2 mg per liter.

effect tends to confirm this view. Equilibrium apparently depends on both concentration and temperature.

It has been found that changes in concentration and temperature affect the form of the bands less with dilute solutions than with concentrated solutions. There is no observable difference in the absorption curves for concen-

[5] P. Pringsheim, Fluorescenz und Phosphorescenz, p.183 (1923).
[6] Uhler and Wood, Atlas of Absorption Spectra.

trations of 1 mg per liter and 2 mg per liter, whereas there is a marked difference in the curves for concentrations of 500 mg per liter and 1000 mg per liter. The effect of change in temperature for a dilute solution is shown in (Fig. 2, III). It seems reasonable that thermal agitation should destroy the equilibrium, spoken of above, more readily when the molecules of the material are close together then when they are further apart.

The observed changes are not due to any permanent alteration of the material, for the same curves were found at a given temperature no matter how often the solution had been heated and cooled.

Rhodamin-B in alcoholic solution. The effect on the absorption bands of changes in concentration is quite different from the effect on the bands of aqueous solutions (Fig. 3, I). The most striking effect is the shift of the bands

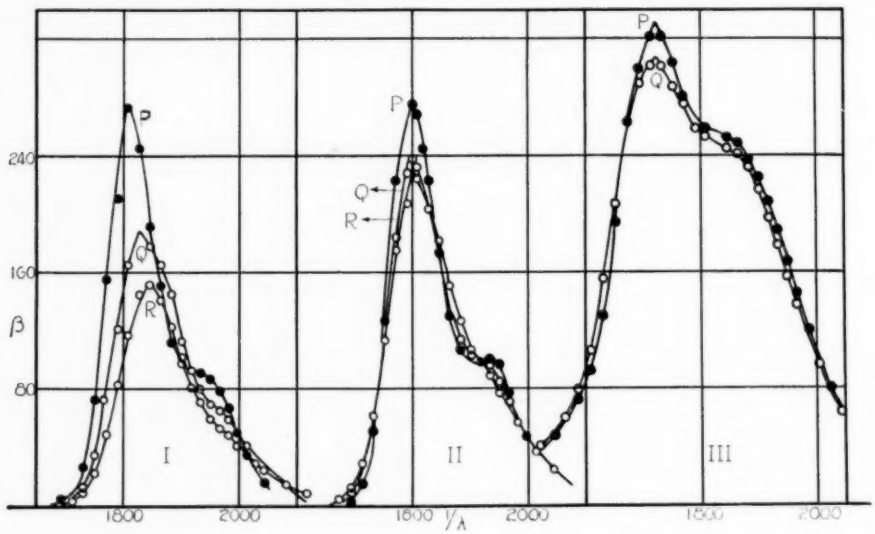

Fig. 4. Rhodamin-B in alcoholic solution. Temperature effect: I. *P*, temperature −90°C; *Q*, 18°C; *R*, 60°C. Concentration of each 4 mg per liter. II. *P*, −70°C; *Q*, 15°C; *R*, 60°C. Concentration of each 500 mg per liter. III. Film on glass plate; *P*, −75°C; *Q*, 20°C.

towards the longer wave-lengths as the concentration is increased. It will be seen that most of the shift occurs on the long wave-length side of the band. The absorbing power increases with increase in concentration, i.e., the same number of molecules absorb more light in a concentrated solution than in a dilute one. Baly[7] found the reverse effect for pyridine, namely, that as dilution increased the coefficient of absorption increased until a certain value of dilution was reached after which there was no further change.

As in the case of aqueous solutions a lowering of the temperature produces the same effect on the bands as an increase in concentration. The similarity of the curves in Fig. 3, I is striking. The changes produced in the absorption bands by temperature variations are much more marked in dilute solutions (Fig. 4, I, II). In fact for a concentration of 500 mg per liter no shift of posi-

[7] E. C. C. Baly, Phil. Mag. **31**, 417 (1916).

tion can be detected in the crests of the bands for a temperature change of 138 degrees. A cell, which contained a solution of concentration 500 mg per liter, was suspended in liquid air in a transparent Dewar cup and the position of maximum absorption was determined with the spectrophotometer. The peak of the band was found to remain in the same position, when the solution was frozen, as at room temperature. For a solution having an intermediate concentration of 160 mg per liter the bands shifted slightly in the same direction as for the more dilute solutions as the temperature was varied. The change in the magnitude of the absorption coefficient is not so great in concentrated solutions as in dilute solutions.

As further evidence of the reduction in temperature effect with increase in concentration, consider the curves of Fig. 4, III which were obtained for a film of alcoholic solution, evaporated to dryness on a glass plate. Here the solvent has been removed, and we have the equivalent of an infinite concen-

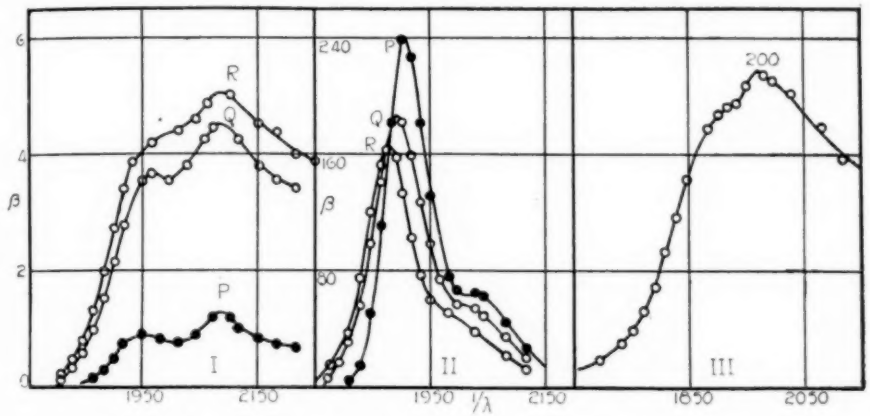

Fig. 5. I. Eosin in neutral alcoholic solution. Temperature effect: *P*, −65°C; *Q*, 20°C; *R*, 60°C. Concentration of each 500 mg per liter. II. Eosin+12 molecules of KOH in alcoholic solution. Temperature effect: *P*, −75°C; *Q*, 20°C; *R*, 60°C. Concentration of each 2 mg per liter. III. Film of eosin+12 molecules of KOH on glass plate. Temperature 20°C.

tration. As will be observed the effect of change in temperature is very small. The position of the crest was determined at liquid air temperature and found to remain in the same position.

Concentrated alcoholic solutions behave like dilute aqueous solutions; both give rise to similar absorption bands in the same position in the spectrum; temperature changes produce similar effects.

The probable explanation which has been given for the behavior of rhodamin in aqueous solution will not hold for alcoholic solutions, for there is not the growing of one band at the expense of the other with alcoholic solutions as the concentration and temperature are varied. Moreover, the temperature shift for dilute aqueous solutions is not so marked as for dilute alcoholic solutions. The solvent plays a decided role.

An explanation which is sometimes given for the shift of the bands resulting from change in concentration is the combination, or tendency towards

combination, of the molecules of the solute with those of the solvent, which results in a loading of the molecules. It is a well established fact that a loading of the molecules of a substance, which absorbs selectively, causes a shift of the bands towards the long wave-lengths and an increase in absorbing power. For example, neutral fluorescein and neutral eosin have similar absorption bands, but the eosin bands are further towards the red and the absorbing power of eosin is greater than that of fluorescein (Figs. 5, I and 6, I). (Eosin is formed from fluorescein when four bromine atoms replace four hydrogen atoms). But the loading of the molecules of the rhodamin by a tendency to combine with the alcohol will hardly account for the facts, because it seems reasonable that the loading per molecule would be greater in a dilute solution than in a concentrated solution, and that the absorption per molecule would increase with dilution, which is the reverse of what has been found. It may be that there is a tendency towards association of the rhodamin molecules in alcohol which would result in what would be equivalent to a loading of the molecules. It seems reasonable also that a lowering of the temperature of a dilute solution would aid association which would account for the shifts towards the red and increase in absorbing power.

Eosin + 12 molecules of KOH in alcohol. The description which has been given of the changes produced in the absorption of alcoholic solutions of rhodamin by alterations of concentration and temperature applies to alkaline alcoholic solutions of eosin except in one particular, namely, the bands shift in the opposite direction from those of rhodamin (Figs. 3, II and 5, II, III). It has been found that shifts of the bands are more marked for a dilute solution than for a concentrated solution, as is true of rhodamin in alcoholic solution. The curve for the film is similar to the curves which Pringsheim[5] found for very concentrated solutions of alkaline eosin.

The behavior of alkaline eosin is more in accord with the behavior of dye solutions in general than that of rhodamin. Investigators have found that in nearly all cases where there is a shift of the bands due to a decrease in concentration the shift is towards the red. Moreover, it is the general rule that an increase in temperature causes the bands to shift towards the red. No satisfactory explanation of these changes has been given.

Eosin and fluorescein in neutral alcoholic solution. (*Figs. 5, I and 6, I*). The absorption bands of the two solutions are similar except for position, the fluorescein bands being further towards the violet. Temperature effects are similar, an increase in temperature causing the absorption to increase. No shift occurs in the crests of the bands as the temperature is varied. Both solutions become nearly colorless at low temperatures.

Ionization might possibly account for the changes. If the absorption bands were due to ions of definite types there would be no shift of the bands as the number of ions varied, but the amount of the absorption would depend on the number of ions. The ionization would probably increase with a rise in temperature which would account for the observed increase in absorption as the temperature is increased.

Resorcinol-benzein in neutral alcoholic solution. The two absorption bands are similar to those of neutral fluorescein, but the absorbing power of the solution is greater. Since the two substances are similar in chemical constitution it might be expected that temperature changes would produce similar effects on the bands. Such is not the case however, for the absorption of the resorcinol-benzein solution increases with a lowering of the temperature while the reverse effect is found for the fluorescein solution (Fig. 6, I and II). The behavior of these two chemically similar substances shows very strikingly that there is as yet no way of predicting how a change in temperature will affect the absorption of a given substance in solution.

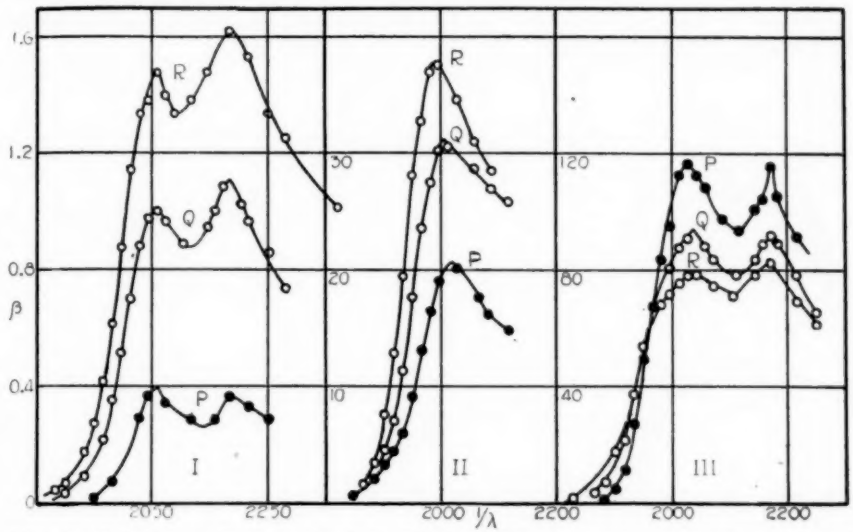

Fig. 6. I. Fluorescein in neutral alcoholic solution. Temperature effect: *P*, −55°C; *Q*, 16°C; *R*, 60°C. Concentration of each 500 mg per liter. II. Uranine in alcoholic solution Temperature effect: *P*, −60°C; *Q*, 20°C; *R*, 60°C. Concentration of each 20 mg per liter. III Resorcinol-benzein in neutral alcoholic solution. Temperature effect: *P*, −60°C; *Q*, 20°C *R*, 60°C. Concentration of each 6 mg per liter.

Uranine in alcoholic solution—(*Fig. 6, II*). Uranine is a sodium salt of fluorescein about 95 per cent pure, sodium carbonate and salt. It might be expected that uranine would behave like alkaline eosin since both are alkaline forms of fluorescein. It does not, as an inspection of the curves reveals, except in one particular, namely, an increase in temperature causes the bands to shift towards the red.

Test of Theory proposed by Merritt. In developing a theory to account for the great width of the absorption bands in solutions as compared with the narrow bands that are observed in gases, Merritt[8] finds that in certain cases it is to be expected that the relation between the absorption coefficient and the frequency on the red side of the band will be given by an expression of the form

$$\beta = Ke^{ah\nu/kT}$$

[8] E. Merritt, Phys. Rev. **28**, 684, (1926).

where h is Planck's constant, k is Boltzman's constant, T the absolute temperature, and s a constant determined by the relative values of the electric moment of the absorbing molecule in the normal and the excited states. This relation has been verified by Merritt in the case of dilute aqueous solutions of rhodamin-B and uranine at room temperature and for these substances s was found to be very nearly unity.

To test the relation the values of $\log \beta$ for the long wave-length side of each band were plotted against wave-numbers. If the above relation holds a straight line should result; and if the number of absorbing molecules is not altered by temperature changes—a condition that is most likely to be met in the case of dilute solutions—the theory shows that the slant of this line should be proportional to $1/T$.

In the case of dilute solutions of rhodamin both in water and in alcohol, straight lines were in fact obtained and the slopes of the lines increased with a lowering of the temperature as demanded by the theory. For dilute aqueous solutions the slopes were also nearly in the inverse ratio of the absolute temperatures; the ratio of the slopes was 5 to 10 per cent greater than the inverse ratio of the absolute temperatures. But in the case of dilute alcoholic solutions the ratio of the slopes was about 20 percent less than the inverse ratio of the absolute temperatures. With the concentrated solutions there was scarcely any approach to agreement with the relation that would be expected if K were constant. Since a considerable temperature change in the number of absorbing molecules is to be expected in concentrated solutions as the result of dissociation or temporary chemical changes, this is not surprising.

In conclusion, the writer wishes to express his indebtedness to Professor Merritt, at whose suggestion and under whose guidance the work was done; and to Professor Gibbs and Mr. C. V. Shapiro for helpful suggestions.

CORNELL UNIVERSITY,
ITHACA, N. Y.
September, 1927.

THE PROBLEM OF THE NORMAL HYDROGEN MOLECULE IN THE NEW QUANTUM MECHANICS*

By S. C. Wang

Abstract

The solution of Schroedinger's equation for the normal hydrogen molecule is approximated by the function $C[e^{-z(r_1+p_2)/a}+e^{-z(r_2+p_1)/a}]$ where $a=h^2/4\pi^2me^2$, r_1 and p_1 are the distances of one of the electrons to the two nuclei, and r_2 and p_2 those for the other electron. The value of Z is so determined as to give a minimum value to the variational integral which generates Schroedinger's wave equation. This minimum value of the integral gives the approximate energy E. For every nuclear separation D, there is a Z which gives the best approximation and a corresponding E.* We thus obtain an approximate energy curve as a function of the separation. The minimum of this curve gives the following data for the configuration corresponding to the normal hydrogen molecule: the heat of dissociation = 3.76 volts, the moment of inertia $J_0=4.59\times10^{-41}$ gr. cm^2, the nuclear vibrational frequency $\nu_0=4900$ cm^{-1}.

CONSIDERABLE work has been done by the various authors[1-8] in finding the energy value of specific atoms or molecules as prescribed by Schroedinger's wave equation. It is well known that the wave equation has not been rigorously solved for any other atoms or molecules beside hydrogen. Consequently some kind of an approximate method has to be introduced to make the energy calculation. While some of the authors use ordinary perturbational methods as given by Schroedinger[9] or the equivalent as given by Born, Heisenberg and Jordan,[10] others devise special schemes to solve particular problems. One such scheme was introduced in a paper by Kellner[8] who calculated the energy values of normal He by trying to solve directly the variational problem corresponding to the wave equation. The present

* A preliminary note appeared in the Bulletin of the American Physical Society, Chicago meeting, November, 1927. When the paper was near completion, a recent issue of the Zeitsshrift für Physik arrived containing a paper by Dr. Y. Sugiura (Zeits. f. Physik **45**, 484, 1927) who continued the work of Heitler and London (Zeits. f. Physik **44**, 455 (1927) by evaluating the integral referred to in the present paper in footnote 18 and calculated in Eq. (13). As is to be expected, Sugiura made calculations of the different atomic constants such as we do here. However, the present paper is still submitted here for the reason that we used a new method of calculation and arrived at some results in a little better agreement with the experimental data than Sugiura's.

[1] Unsöld, Ann. d. Physik **82**, 355 (1927); Zeits. f. Physik **43**, 563 (1927).
[2] Heisenberg, Zeits. f. Physik **39**, 499 (1926).
[3] Sugiura, Zeits. f. Physik **44**, 190 (1927).
[4] Heitler and London, Zeits. f. Physik **44**, 455 (1927).
[5] Burrau, Danske Vidensk, Selskab, Math-fys. Meddel. **7**, 14, Copenhagen, (1927).
[6] Condon, Proc. Nat. Acad. Sci. **13**, 466 (1927).
[7] Slater, Proc. Nat. Acad. Sci. **13**, 423 (1927).
[8] Kellner, Zeits. f. Physik **44**, 91 (1927).
[9] Schroedinger, Ann. d. Physik **80**, 437 (1926).
[10] Born, Heisenberg and Jordan, Zeits. f. Physik **35**, 557 (1926).

paper will be chiefly concerned with the problem of the normal hydrogen molecule investigated along similar lines.

When the two hydrogen atoms are at a great distance apart, the problem has been treated in the quantum mechanics in a recent paper by the author.[11] In that case, the two atoms more or less retain their individuality and, according to a perturbation calculation, the total energy of the two-atom problem is, to a first approximation, the sum of the energies of two single atoms plus a mutual term which can be ascribed to the polarizability of the atoms. When the atoms are close together, such a procedure is no longer valid and we shall have to resort to a different method.

Two previous attempts have been made to treat that phase of the H_2 problem. Condon[6] proposed to regard it as the perturbed problem of the case where we have two non-interacting electrons, each in the configuration of an H_2^+ ion. The "Eigenfunktion" of such an unperturbed problem is not yet available but the "Eigenwerte" for different nuclear separations has been worked out by Burrau[5] by a numerical method. To Burrau's results Condon then incorporated his approximate estimate of the perturbation energy curve as a function of the nuclear separation, which arises out of the interaction of the two electrons, from the experimental energy data in the He problem. (However, in view of the recent work of Slater[7] and of Kellner,[8] we may say the data are also theoretical.) The resulting energy value for normal H_2 is in remarkably good agreement with the experimental value. It will be referred to again in a table near the end of the present paper.

Heitler and London,[4] also using a perturbational method, started their calculations from hydrogen-like "Eigenfunktionen." Of course, they recognized the weakness of assigning each of the electrons to only one of the nuclei, which would amount to saying that in the zero-order approximation each electron is not affected by the other nucleus. To remedy this defect, they construct, out of considerations of the degeneracy of the problem, an "Eigenfunktion," consisting of hydrogen-like terms but symmetrical to the two nuclei so far as each of the two electrons is concerned. They did not carry through the numerical part in the calculation of the first order perturbation energy; that was done in a later paper by Sugiura, already referred to at the beginning of the present article.

In the calculations here presented, we propose to attack the problem from a slightly different angle. Schroedinger[12] has shown that the wave equation for an atomic system of k degrees of freedom with a Hamiltonian $T(q_k,p_k) + V(q_k)$ is nothing more than Euler's differential equation for the minimizing of the following generalized volume integral

$$I = \int \left\{ \frac{h^2}{4\pi^2} T\left(q_k, \frac{\partial \psi}{\partial q_k}\right) + \psi^2 V(q_k) \right\} \Delta_p^{-1/2} dx \qquad (1)$$

[11] Wang, Phys. Zeits. **28**, 663 (1927).
[12] Schroedinger, Ann. d. Physik **79**, 734 (1926).

subject to the condition

$$J=\int \psi^2 \Delta_p^{-1/2} dx = 1 \tag{2}$$

where $\int dx$ is an abbreviation for $\int \cdots \int dq_1 \cdots dq_k$, and $\Delta p^{-1/2}$ is the reciprocal of the square root of the determinant belonging to the quadratic form T. Besides, what is perhaps of more importance here, the minimum values of the volume integral are just the "Eigenwerte" of the wave equation.

To solve the variational problem directly, we can use what is commonly called the Ritz method.[13] It consists of first setting up an infinite sequence of functions of the coordinates (known functions of the independent variables), satisfying certain requirements regarding completeness, and so forth, which we shall not go into here, and then approximating the unknown function ψ by a linear combination of a finite number of the selected coordinate functions with constant coefficients to be determined later. When this approximate ψ is substituted into the integral I and the integration performed, I reduces to a homogeneous quadratic function of the coefficients. The latter are then so determined as to minimize this quadratic function, subject to the restriction that condition (2) is always satisfied. The calculation made in this paper corresponds, though only roughly, to a Ritz approximation of two terms; the approximate ψ function used involves the two constants in a quite complicated way instead of linearly.

We shall first set up the variational integral connected with the problem of the hydrogen molecule. Let r_1 and p_1 be the distances of the first electron to the two nuclei and r_2 and p_2 those for the second electron. Let s be the distance between the two electrons and ϕ_1 be the azimuthal angle of one of the electrons, say the first, referred to the line joining the nuclei as the polar axis. We shall use these six quantities r_1, p_1, r_2, p_2, s and ϕ_1 as independent variables; the separation between the nuclei, which we shall designate by D enters into the problem as a fixed parameter. We may also have occasion to use the ordinary spherical coordinates r_1, ϑ_1, ϕ_1 and r_2, ϑ_2, ϕ_2 for the two electrons referred to one and the same nucleus.

Now let us first remark that if we try on the wave equation of the hydrogen molecule the substitution $\psi = U\Phi$ where Φ is a function of ϕ_1 alone and U of the remaining variables, it is found that the part involving ϕ_1 can be separated from the rest. For the lowest "Eigenwerte," we therefore need only to take $\Phi =$ constant so that the solution ψ is actually a function of five variables.

In spherical coordinates the integral to be minimized is

$$I=\int\left\{\frac{h^2}{8\pi^2 m}\left[\left(\frac{\partial\psi}{\partial r_1}\right)^2+\frac{1}{r_1^2}\left(\frac{\partial\psi}{\partial\vartheta_1}\right)^2+\frac{1}{r_1^2\sin\vartheta_1}\left(\frac{\partial\psi}{\partial\phi_1}\right)^2+\left(\frac{\partial\psi}{\partial r_2}\right)^2 +\frac{1}{r_2^2}\left(\frac{\partial\psi}{\partial\vartheta_2}\right)+\frac{1}{r_2^2\sin\vartheta_2}\left(\frac{\partial\psi}{\partial\phi_2}\right)^2\right]+\psi^2 V\right\} d\Omega_1 d\Omega_2 \tag{3}$$

[13] See Riemann-Webers Differentialgleichungen der Physik, 7th ed., vol. I, p. 678 or Ritz, Ann. d. Physik **28**, 737 (1909).

where

$$d\Omega_1 d\Omega_2 = r_1^2 r_2^2 \sin\vartheta_1 \sin\vartheta_2 dr_1 dr_2 d\vartheta_1 d\vartheta_2 d\phi_1 d\phi_2 \tag{4}$$

and

$$V = -\frac{e^2}{r_1} - \frac{e^2}{p_1} - \frac{e^2}{r_2} - \frac{e^2}{p_2} + \frac{e^2}{s} + \frac{e^2}{D}.$$

We now make the following change of independent variables for the integrand

$$r_1 = r_1, \qquad r_2 = r_2,$$

$$p_1^2 = r_1^2 + D^2 - 2r_1 D\cos\vartheta_1, \qquad p_2^2 = r_2^2 + D^2 - 2r_2 D\cos\vartheta_2$$

$$s^2 = r_1^2 + r_2^2 - 2r_1 r_2 [\cos\vartheta_1\cos\vartheta_2 + \sin\vartheta_1\sin\vartheta_2\cos(\phi_1 - \phi_2)], \qquad \phi_1 = \phi_1.$$

Noting that $\partial\psi/\partial\phi_1 = 0$, we find

$$\begin{aligned} I = \int \Big\{ \frac{h^2}{8\pi^2 m} \Big[&\Big(\frac{\partial\psi}{\partial r_1}\Big)^2 + \Big(\frac{\partial\psi}{\partial p_1}\Big)^2 + \Big(\frac{\partial\psi}{\partial r_2}\Big)^2 + \Big(\frac{\partial\psi}{\partial p_2}\Big)^2 + 2\Big(\frac{\partial\psi}{\partial s}\Big)^2 \\ &+ \frac{r_1^2 + p_1^2 - D^2}{r_1 p_1} \frac{\partial\psi}{\partial r_1}\frac{\partial\psi}{\partial p_1} \quad \frac{r_2^2 + p_2^2 - D^2}{r_2 p_2} \frac{\partial\psi}{\partial r_2}\frac{\partial\psi}{\partial p_2} + \frac{s^2 + r_1^2 - r_2^2}{r_1 s} \frac{\partial\psi}{\partial s}\frac{\partial\psi}{\partial r_1} \\ &+ \frac{s^2 + r_2^2 - r_1^2}{r_2 s} \frac{\partial\psi}{\partial s}\frac{\partial\psi}{\partial r_2} + \frac{s^2 + p_1^2 - p_2^2}{p_1 s} \frac{\partial\psi}{\partial s}\frac{\partial\psi}{\partial p_1} \\ &+ \frac{s^2 + p_2^2 - p_1^2}{p_2 s} \frac{\partial\psi}{\partial s}\frac{\partial\psi}{\partial p_2} \Big] + \psi^2\Delta \Big\} d\Omega_1 d\Omega_2 \end{aligned} \tag{5}$$

while the restricting condition remains formally

$$J = \int \psi^2 d\Omega_1 d\Omega_2 = 1 \tag{6}$$

As for the volume element $d\Omega_1 d\Omega_2$ we can either preserve its meaning in Eq. (4), or we can write it in the new variables. In the latter case, we find that the expression is in general very complicated. But, in case the integrand is independent of s as well as ϕ_1 so that we can integrate with respect to these two variables at the very beginning, then the volume element expressed in the remaining four variables has the very simple form

$$d\Omega_1 d\Omega_2 = \frac{4\pi^2}{D^2} r_1 p_1 r_2 p_2 dr_1 dp_1 dr_2 dp_2 \tag{7}$$

In the subsequent work we shall interpret $d\Omega_1 d\Omega_2$ either by (4) or by (7) as occasion demands.

The next question has to do with the precise form of the two constant approximation for ψ. Let us note in the first place that the lowest "Eigen-

funktion" must be symmetrical[14] with respect to the two electrons and the two nuclei; or more explicitly, it should be invariant to the substitutions

$$\begin{pmatrix} r_1 & r_2 \\ p_1 & p_2 \end{pmatrix} \text{ and } \begin{pmatrix} r_1 & p_1 \\ r_2 & p_2 \end{pmatrix}.$$

Now, if we have two H-atoms so far apart that their mutual influence is negligible and if we assign electron 1 to nucleus 1 and electron 2 to nucleus 2, then the lowest "Eigenfunktion" for the two atom problem would be $Ce^{-(r_1+p_2)/a}$. On the other hand, if we interchange the assignment of the electrons to the nuclei, we would have the "Eigenfunktion" $Ce^{-(r_2+p_1)/a}$. A function which satisfies the properties of symmetry just mentioned and which approaches the one or the other of the above functions as the separation between the atoms becomes greater and greater, is evidently the following: $C[e^{-(r_1+p_2)/a}+e^{-(r_2+p_1)/a}]$.[15] If we had two nuclei of charge Ze each to start with, we would have instead the function

$$C\left[e^{-Z(r_1+p_2)/a}+e^{-Z(r_2+p_1)/a}\right]. \tag{8}$$

It is this latter function that we shall use as the approximate solution for our problem. Perhaps, instead of considering our calculation as a modified form of the Ritz process, we had better regard it as one similar to that of Kramers in the He problem[16] (or more recently, that of Hutchisson[17] for H_2) in the classical quantum theory. Roughly speaking, Kramers uses for the unperturbed motion of the He problem a potential due, in part, to a fictitious nuclear charge Ze, the value of Z being determined by the condition that the ratio of the perturbing force to the actual force shall be a minimum on the average. In our work, following the ideas of the new quantum mechanics, we have replaced the latter criterion by the one that Z shall have the "best" value in making the variational integral a minimum.

Returning to our calculations, we first make use of the symetrical properties of ψ and of $d\Omega_1 d\Omega_2$ and we find that (5) reduces to

$$I=\int\left\{\frac{h^2}{8\pi^2 m}\left[4\left(\frac{\partial\psi}{\partial r_1}\right)^2+2\left(\frac{\partial\psi}{\partial s}\right)^2+\frac{4(s^2+r_1^2-r_2^2)}{r_1 s}\frac{\partial\psi}{\partial s}\frac{\partial\psi}{\partial r_1}\right.\right.$$
$$\left.\left.+\frac{2(r_1^2+p_1^2-D^2)}{r_1 p_1}\frac{\partial\psi}{\partial r_1}\frac{\partial\psi}{\partial p_1}\right]-e^2\psi^2\left[\frac{4}{r_1}-\frac{1}{s}-\frac{1}{D}\right]\right\}d\Omega_1 d\Omega_2 \tag{9}$$

The above equation holds rigorously for the case of the lowest "Eigenwerte" and the exact solution is that symmetric function of $r_1 p_1 r_2 p_2$ and s that

[14] See Hund, Zeits. f. Physik **42**, 93 (1927) and also Heitler and London, loc. cit. In the latter problem the same problem of H_2 was investigated. They were, however, more interested in the general aspect of the formation of the molecule than in the methods of calculating particular energy values.

[15] Heitler and London decided upon this function as the unperturbed Eigenfunktion after considering a modified form of the resonance phenomenon first pointed out by Heisenberg.

[16] Kramers, Zeits. f. Physik **13**, 312 (1923).

[17] Hutchisson, Phys. Rev. **29**, 270 (1927).

minimizes (9) among the entire class of such symmetric functions. We now substitute the approximate form for ψ as given by (8) into Eqs. (9) and (6), we find they become

$$I=C^2\int\left\{\frac{h^2Z^2}{8\pi^2ma^2}\left[4e^{-2Z(r_1+p_2)/a}+\frac{2(r_1^2+p_1^2-D^2)}{r_1p_1}e^{-Z(r_1+p_1+r_2+p_2)/a}\right]\right.$$
$$-e^2\left[\frac{4}{r_1}-\frac{1}{s}-\frac{1}{D}\right]\left[e^{-2Z(r_1+p_2)/a}+e^{-2Z(r_2+p_1)/a}\right.$$
$$\left.\left.+2e^{-Z(r_1+p_1+r_2+p_2)/a}\right]\right\}d\Omega_1d\Omega_2 \tag{10}$$

$$J=C^2\int\left[e^{-Z(r_1+p_2)/a}+e^{-Z(r_2+p_1)/a}\right]^2d\Omega_1d\Omega_2=1 \tag{11}$$

The condition (11) evidently just determines the value of C. We can therefore dispose of it by dividing (10) by (11). The function to be minimized then becomes

$$E=I/J \tag{12}$$

We will have to simplify this expression by actually carrying out the integration. Most terms in the above expression can be readily integrated by a judicious choice of one form or the other of $d\Omega_1d\Omega_2$. In the integration of the terms of the type $(1/s)e^{-Z(r+p_2)/a}$, use was made of the well known theorems concerning the averages of a harmonic function over a sphere.

The only integral that gives rise to some difficulty is due to the term $(1/s)e^{-Z(r_1+p+r+p)/a}$.[18] It is the total Newtonian potential energy of that distribution of mass which consists of homogeneous confocal ellipoidal layers of revolution with the density falling off as $e^{-\kappa\lambda}$ where κ is a constant and λ is the major axis, the fixed foci being in all cases the two nuclei. The result of the integration process gives:

$$\int\frac{1}{s}e^{-Z(r_1+p_1+r_2+p_2)/a}d\Omega_1d\Omega_2=\frac{a^5\pi^2}{60Z^5}\left\{\frac{1}{Q}\left[e^{-Q}(Q^2+6Q+12)^2\left(\log\frac{Q}{2}+\gamma\right)\right.\right.$$
$$+2\mathrm{Ei}(Q)\times(Q^2+6Q+12)(Q^2-6Q+12)-e^{Q}\mathrm{Ei}(2Q)(Q^2-6Q+12)^2] \tag{13}$$
$$\left.\left.-e^{-Q}\left(\frac{Q^3}{2}+9Q^2+\frac{69}{2}Q-\frac{75}{2}\right)\right\}\right.$$

where Q is the abbreviation for $2ZD/a$, γ is the Euler's constant and $\mathrm{Ei}(x)=\int_x^\infty(1/u)e^{-u}du$, the numerical values of which can be found in tables in a paper by Glaisher.[19]

[18] Essentially the same integral came up in the calculation of Heitler and London (loc. cit.) but they did not attempt to evaluate it exactly. See, however, the note after the asterisk on the first page of this paper.

[19] Glaisher, Phil. Trans. **160**, 367 (1870).

Collecting the different integrals in (12), we find it finally reduces to

$$\frac{E}{R}=\left\{64+\frac{4}{9}e^{-Q}(Q^2+6Q+12)^2\right\}^{-1}\left\{128+\frac{8}{9}e^{-Q}(Q^2+6Q+12)(-Q^2+6Q+12)\right\}$$
$$\frac{Q^2a^2}{4D^2}-\left\{64+\frac{4}{9}e^{-Q}(Q^2+6Q+12)^2\right\}^{-1}\times\left\{128(1+Q)-\frac{16}{15}\Big[(Q^2+6Q+12)^2e^{-Q}\right.$$
$$\left(\log\frac{Q}{2}+\gamma\right)+2\mathrm{Ei}(Q)(Q^2+6Q+12)(Q^2-6Q+12) \tag{14}$$
$$\left.-e^{Q}\mathrm{Ei}(2Q)(Q^2+6Q+12)^2\Big]+e^{-Q}(11.2Q^4+97.6Q^3+316.8Q^2+176Q\right.$$
$$\left.-128)\right\}\left(\frac{a}{D}\right)+\frac{a}{D}$$

where R is the Rydberg constant. For every separation D we choose a value of Z which minimizes E; or, equally well, since D is a fixed parameter in each case, we may choose the Q that makes E a minimum. The energy curve of two H-atoms expressed as a function of the nuclear separation D is therefore obtained by eliminating Q between the following two equations:

$$E=E(Q,\ D) \tag{14^1}$$

$$\partial E/\partial Q=0 \tag{15}$$

The minimum of this energy curve gives the data for the equilibrium configuration, which corresponds to the normal hydrogen molecule.

However, there does not seem to be any feasible way of making the general elimination between Eqs. (14) and (15), either analytically or graphically. We can only give the solution of the most interesting case of the equilibrium configuration which can be treated in the following manner. The set of values E_0, Q_0 and D_0 for this case is evidently the solution of the simultaneous equations:

$$E=E(Q,\ D) \tag{14^1}$$

$$\partial E/\partial Q=0 \tag{15}$$

$$(dE/dD=0)\text{ or }\partial E/\partial D=0 \tag{16}$$

where the total differentiation denotes the one on E as a function of D alone obtained by elimination of Q between Eqs. (14) and (15). It turns out to be a very simple matter to eliminate analytically the quantity D between Eqs. (14) and (16). If we then plot the resulting as a function of Q alone, the minimum of this curve evidently just gives the E_0 and Q_0 for the equilibrium case. They are thus found to be $E_0=-2.278R$, and $Q_0=3.28$. The value D_0 can now also be computed from one of the equations. We find $D_0=1.406a$,

which corresponds to a moment of inertia $J_0=4.59\times10^{-41}$ gr. cm^2. From the relation $Q=2ZD/a$ we also find $Z_0=1.166$.

By using this same value of Z_0 found for the equilibrium separation to calculate the approximate energy values for separations in its neighborhood, we obtain an approximate value for the nuclear vibrational frequency $\nu_0=4900$ cm^{-1} from the curvature of the resulting energy curve.

For comparison, we tabulate below the values found in the above calculation and the values obtained by Condon[6] and Sugiura* of the various atomic constants and those values determined experimentally, mostly from band spectra data:

Calculated values	E_0	J_0	ν_0	Z
This paper	$-2.278R$	4.59×10^{-41} gr.cm^2	4900 cm^{-1}	1.166[22]
Condon	$-2.325R$	4.26×10^{-41}	5300	
Sugiura	$-2.24R$	5.2×10^{-41}	4800	
Observed value	$-2.326R$[20]	4.67×10^{-41} [21]	4360[20]	

Finally as a check on the calculations leading to the energy equation (14), the latter equation is examined for very large and very small values of D. In the first case, we have two independent H-atoms and it is found that the optimum value of Z is unity, giving $E=-2R$ as we should expect. In the second case we have the normal helium atom; the value of Z found is 1.6875 and that of E is -77.4 volts. They are in complete agreement with the results obtained by Kellner[23] for the helium atom.

I take this opportunity to thank Professor A. P. Wills for his encouragement and his kindness in going over the manuscript.

Department of Physics,
Columbia University,
December 12, 1927.

[20] Witmer, Proc. Nat. Acad. Sci. **12,** 238 (1926); also Phys. Rev. **28,** 1223 (1926).

[21] Hori, Zeits. f. Physik **44,** 834 (1927); Dennison, Proc. Roy. Soc. **A115,** 483 (1927).

[22] Hutchisson (loc. cit.) obtained the value $Z=0.823$ from the classical quantum theory calculations. It must be mentioned, however, that he introduced another term of the form $\beta e^2/s^2$ in his unperturbed problem. Our value of Z is also to be compared with those given by Van Vleck (Proc. Nat. Acad. Sci. **12,** 662 (1926), who, using the new quantum mechanics obtained for the Z of H_2 the values 1.08, 1.14 and 1.11 from the experimental values of the energy, the dielectric constant and the diamagnetic susceptibility of H_2 respectively.

[23] Kellner, loc. cit.[8], see especially Eq. (9) of that paper.

ON DIELECTRIC CONSTANTS AND MAGNETIC SUSCEPTIBILITIES IN THE NEW QUANTUM MECHANICS PART III—APPLICATION TO DIA- AND PARAMAGNETISM

By J. H. Van Vleck

Abstract

1. General mathematical theory.—Modifications are given in the general derivation of the Langevin-Debye formula by means of quantum mechanics published in part I which are required by the moment now being magnetic rather than electric. The main additions are the appearance of a diamagnetic term, and allowance for the fact that the magnetic moment consists of two parts arising respectively from orbital electronic motions and from the electrons' internal spins. These parts cannot always be treated as rigidly coupled to form a "permanent" resultant moment. The Hamiltonian function used for the internal spin is that of a spherical top.

2. Diamagnetism.—The writer's previous claim that Pauli's formula for the diamagnetic susceptibility can be applied to molecules as well as atoms is shown to be invalid because of the anomalous fact that the square of the angular momentum, unlike the average angular momentum, does not vanish even in S states when there is more than one nucleus. Pauli's formula is instead an upper limit to the diamagnetism in non-monatomic molecules and is a good approximation when the Schrödinger wave function has nearly as much symmetry as in an atomic S state.

3. Paramagnetism of atoms.—Limiting values for the paramagnetic susceptibilities of atoms are $\chi = N[4s(s+1)+k(k+1)]\beta^2/3kT$ and $\chi = [Ng^2j(j+1)\beta^2/3kT]+N\alpha$ where β is the Bohr magneton and α is a constant. These two formulas are rigorously applicable when the multiplet intervals are respectively very small or very large compared to kT, and are valid regardless of whether the magnetic field is strong enough to change the quantization by producing a Paschen-Back effect. The formula for small multiplets yields susceptibilities slightly different from those given by Laporte and Sommerfeld's expression for this case, and is much simpler, as they overlooked the contribution of the portion of the magnetic moment which is perpendicular to the invariable axis.

4. Paramagnetism of molecules.—The susceptibility is calculated on the basis of the Hund theory of molecular quantization. Formulas are given applicable to his couplings of type (a) and type (b) provided in the former the multiplet intervals are either very large or very small compared to kT. The experimental susceptibilities for O_2 and ClO_2 are in accord with the assumption that the normal states are respectively ^3S and ^2S terms. In the particular case of S terms the numerical results are the same in the atomic and molecular formulas, but, unlike previous theories, it is not necessary to suppose the orbits are as freely oriented in molecules as in atoms. Polyatomic molecules may have lower paramagnetic susceptibilities than diatomic ones because the dissymmetry causes large fluctuations in electronic angular momentum.

5. Paramagnetism of nitic oxide.—Spectroscopists have recently found that the normal states of the NO molecule are ^2P terms separated by 120.9 cm^{-1}. This permits an unambigous calculation of the susceptibility of NO which agrees with the experimental value within 1.5 per cent. Deviations from Curie's law are calculated which result from the doublet interval being comparable with kT. These deviations should be detectable experimentally if the susceptibility of NO could be measured over a wide temperature range.

IN PART I[1] a very general derivation was given of the Langevin-Debye formula for the temperature variation of the susceptibility. This proof was based on the new quantum mechanics, and assumed only that the molecule has a "permanent" moment of constant magnitude, and that the energy intervals between the various component levels of the normal state are small compared to kT. The latter requirement implies that the precession frequencies of the moment vector are small compared to kT/h Part II[2] was less mathematical, and described various applications of the theory of part I to phenomena connected with dielectric constants. Part III will similarly discuss applications to magnetism. The theories of electric and magnetic polarizations are sufficiently similar so that the analysis in part I gave simultaneously the main elements of a proof of Langevin's formula for the paramagnetic susceptibility and of Debye's formula for the dielectric constant. However, in the detailed demonstration in part I we assumed for simplicity that the moment of the molecule was electrical rather than magnetic, and so before proceeding to the magnetic applications we must in section 1 give the modifications in the derivation which are required by the fact that magnetic moments result from angular momentum, both of the orbital and spin type, rather than from electrostatic charge distributions. This section may be omitted by readers not interested in the mathematical detail. As mentioned in part I, we believe our analysis is considerably more comprehensive than most of the usual treatments with specialized models, but at the same time it must be emphasized that we do not aim to probe into the electrodynamics of the interior of the electron which is responsible for the anomalous spin moment.

Note added in proof. A remarkable paper by Dirac (Proc. Roy. Soc., Feb. 1928) has just appeared in which he shows that the requirement that the Schroedinger wave equation have the invariance demanded by relativity is adequate to give the terms ordinarily ascribed to internal spins of the electron. Thus our treatment of the electron as a spherical top to derive the Hamiltonian function inclusive of spin terms in a magnetic field suddenly loses much of its interest. However, it must at the same time be emphasized that all the essential results of the present paper are unaltered; the only difference is that our work prior to about p. 594 becomes rather antequated, as Dirac's postulates give a Hamiltonian function such as (5) directly and elegantly. From there on everything goes as before. The internal spin may indeed be a myth, but as Dirac's magnetic terms are the same to the first order as for a top model of the electron, the phrase "internal spin" may well continue to be a convenient label for Dirac's duality effect. The calculation of the susceptibility (unlike the ordinary linear Zeeman effect) necessitates, to be sure, knowledge of the energy through terms of the second order in the magnetic field H. Here there is only an academic difference between the Hamiltonian with the top model and Dirac's Hamiltonian, as in the latter

[1] J. H. Van Vleck, Phys. Rev. **29**, 727 (1927). This and the following reference are referred to as respectively parts I and II throughout the present paper.

[2] J. H. Van Vleck, *Ibid.* **30**, 31 (1927).

the duality or apparent spin anomaly introduces no terms at all in H^2 in an Eq. analogous to our (4) whereas we show that with the spherical top such terms, which represent diamagnetic induction in the internal motion, are negligible because the radius of an electron is small compared to the radius of an orbit.

1. General Mathematical Theory

Hamiltonian function. The first step is to derive expressions for the Hamiltonian function and magnetic moment in a magnetic field. We shall start the calculation with classical mechanics and later give the quantum modifications. If we regard the molecule as composed of a number of charged particles (nuclei and electrons) then it is well known that in a magnetic field derived from a vector potential $\boldsymbol{A}$, the Lagrangian function is[3] $L_0+\sum_i(\epsilon_i/c)\ (\mathbf{v}_i\cdot\boldsymbol{A})$, where L_0 is the Lagrangian function in the absence of the field and where ϵ_i and $\mathbf{v}_i$ are respectively the charge and vector velocity of a particle. The summation, of course, extends over all the particles in the system. For simplicity in printing we shall henceforth omit the subscript i, so that an expression such as $\sum p_\phi$, for instance, means $\sum_i p_{\phi_i}$, etc. In virtue of their large masses, the nuclei have such small velocities that we may disregard[4] their contribution to the sum. Hence the summations will be taken only over the electrons in the system, permitting us to put $\epsilon_i=-e$ with $e=+4.774\times10^{-10}$. It is, however, to be understood that the coordinates and velocities of the nuclei will still enter in the part L_0 of the Lagrangian function. As the Uhlenbeck and Goudsmit[5]

[3] Cf., for instance, Schott, "Electromagnetic Radiation," p. 284.

[4] According to Langevin's formula the paramagnetic susceptibility coming from a particle of charge ϵ and mass m moving in an orbit with an angular momemtum p is proportional to $p^2\epsilon^2/m^2$. This shows that the paramagnetic susceptibility coming from nuclei is small compared to that coming from electrons, for the value of ϵ/m for nuclei is less than 10^{-3} that for electrons, while the average value fo p for nuclear motions (i.e. the average rotational quantum number in band spectra) is well under 10^2 quantum units $h/2\pi$ at ordinary temperatures. As a matter of fact the contributions of the nuclei to the susceptibility are even smaller than suggested by this estimate, for at ordinary temperatuers the rotational quantum numbers specifying the motion of the nuclei about the center of gravity, though $<10^2$, are sufficiently large so that the part of the susceptibility due to nuclear angular momentum is nearly the same as though we used classical theory, where the angular momentum assumes a continuous distribution of values. Now Miss van Leeuwen (Leyden Thesis; also J. de Physique (6), 2, 361, 1921) has shown that when there is a classical distribution of angular momenta the paramagnetic and diamagnetic susceptibilities cancel, leaving zero resultant susceptibility. Consequently the contribution of the nuclei to the susceptibility is very approximately zero and can be disregarded in comparison with the electronic terms even in molecules whose electrons give only diamagnetic effects. The magnetic moments due to nuclear motions can, however, be detected in the Stern-Gerlach effect (Knauer and Stern, Zeits. f. Physik, **39,** 780, 1926). It has been variously suggested that nuclei have internal spins, as do electrons, but the contribution to the susceptibility is, of course, negligible because of the factor $1/m^2$. The molecular rotation may change the susceptibility slightly by distorting the electronic angular momentum, but this is a second order effect which we will not consider.

[5] Uhlenbeck and Goudsmit, die Naturwissenschaften **13,** 953 (1925); Nature, **117,** 264 (1926).

electron which possesses an internal or "spin" degree of freedom is quite generally accepted, we cannot treat the electron as a point charge, but rather a continuous charge distribution. Hence we cannot use a Lagrangian function of quite the form given above, but instead must take it to be

$$L=L_0+\sum\int\int\int(\rho/c)(\mathbf{v}\cdot\mathbf{A})dV, \tag{1}$$

where dV denotes an element of volume of the electron and ρ is the corresponding charge density. Far too little is known at present about the mechanics of the spin electron to determine how $\mathbf{v}$ and $\mathbf{A}$ are distributed in its interior. Nevertheless, following Darwin[6] and others, we will treat the electron as a charged spinning body of spherical symmetry, the justification for this model being that it is adequate to give the facts connected with the Zeeman effect.[7] Then as generalized coordinates specifying each electron we may use three cylindrical coordinates R, z, ϕ fixing its center, and three Eulerian angles[8] θ, ψ, ζ associated with its internal spin. If the magnetic field is of uniform magnitude H and directed along the z-axis, then $A_x=-\frac{1}{2}Hy$, $A_y=\frac{1}{2}Hx$, $A_z=0$, and it is readily seen that (1) becomes

$$L=L_0+(H/2c)\sum[-eR^2\dot{\phi}+D(\dot{\psi}+\dot{\zeta}\cos\theta)]. \tag{2}$$

Here D denotes the electrical moment of inertia $\int\int\int\rho(R-R_0)^2dV$ of an electron, where R_0 is the value of R at its center. The second and third right-hand terms of (2) are respectively the contributions of the orbital and internal motions of the electron to the integral in (1). These two contributions are separated by adapting to electrical rather than gravitational density the familiar mechanical theorem that the angular momentum of a system relative to a fixed point equals the angular momentum relative to the center of gravity plus the angular momentum which would result if all the mass were located there.

The momenta conjugate to the various generalized coordinates q_k are $p_k=\partial L/\partial\dot{q}_k$. Hence p_R, p_z, p_θ have the same kinematical significance[9] as

[6] C. G. Darwin, Proc. Roy. Soc. **115A,** 1 (1927).

[7] There is, however, the much-emphasized difficulty of double-valued Schroedinger characteristic functions; see Darwin, ref. 6, also Proc. Roy. Soc. **116A,** 227 (1927); Pauli, Zeits. f. Physik, **43,** 601 (1927).

[8] Here θ and ψ denote polar and azimuth angles specifying a given axis in the electron, while ζ is the third Eulerian angle required to determine the amount of rotation around this axis. Darwin notes[6] that by a proper transformation it is possible to eliminate one of the three internal coordinates of the electron from the Hamiltonian function because the choice of axis is immaterial in a body with spherical symmetry; this however, need not concern us, in the present work.

[9] The physical basis for the need of modifying the definition of momenta in a magnetic field is perhaps more apparent when it is recalled that the angular momentum of a dynamical system about an axis is not an adiabatic invariant when a magnetic field is applied along this axis. For instance, in the simple case of a system of one particle without internal spin, p_ϕ is instead an adiabatic invariant and the extra term $-HeR^2/2c$ in the definition of p_ϕ is just equal and opposite to the change in angular momentum brought about by application of the

without the magnetic field, whereas p_ϕ, p_ψ, p_ζ are modified by the addition of terms linear in H. For instance, p_ϕ equals $\partial L_0/\partial\dot{\phi}-HeR^2/2c$, where $\partial L_0/\partial\dot{\phi}$ is the ordinary definition $mR^2\dot{\phi}$ (neglecting relativity corrections etc. to be mentioned on p. 593).

In accordance with general dynamical theory, the Hamiltonian function is $\sum_k \dot{q}_k(\partial L/\partial\dot{q}_k)-L$. Since the added terms in the Lagrangian function are linear in the generalized velocities, this is the same as $\sum_k \dot{q}_k(\partial L_0/\partial\dot{q}_k)-L_0$. Thus the Hamiltonian function E is exactly the same as in the absense of the field except that some of its arguments are modified. The physical meaning of this is, of course, that magnetic forces do no work, so that the energy is the same function of the coordinates and velocities as in their absence. Among the arguments of E we must now take

$$p_\phi+HeR^2/2c,\quad p_\psi-DH/2c,\quad p_\zeta-DH\cos\theta/2c \tag{3}$$

instead of p_ϕ, p_ψ, p_ζ, for the expressions (3) are the same functions $\partial L_0/\partial\dot{q}_k$ of the coordinates and velocities as are p_ϕ, p_ψ, p_ζ when $H=0$. Thus the Hamiltonian function is

$$E=\sum(1/2m)\left[p_R{}^2+p_z{}^2+(p_\phi{}^{02}/R^2)\right]+T+V+U$$
$$+\sum(1/2I)\left[p_\theta{}^2+p_\zeta{}^{02}+\operatorname{cosec}^2\theta(p_\psi{}^0-p_\zeta{}^0\cos\theta)^2\right], \tag{4}$$

where $p_\phi{}^0$, $p_\psi{}^0$, $p_\zeta{}^0$ are abbreviations for the expressions given in (3) and hence are functions of H. This result is one which has been often given[10] except for inclusion of the spin terms. The first sum in (4) is the orbital kinetic energy. The second line is the kinetic energy of internal spin, with I denoting the electron's moment of inertia. T is the kinetic energy of the nuclei, whose magnetic effect we have disregarded. V is the mutual electrostatic potential of the charges composing the molecule. U is the mutual intra-atomic magnetic energy, including that resulting from the torques on the electrons' spin axes exerted by the other charges in the atom or molecule. These torques are, of course, responsible for the "spin doublets," "multiplet structures," etc. U, unlike V, is a function of the momenta as well as the coordinates, and hence will involve H, as in a magnetic field the arguments (3) must be used. However, U is already small, and its dependence on H enters as essentially a correction term, so that its contribution

field. Thus in such a system it is the elements of the matrix p_ϕ and not $mR^2\dot{\phi}$ which must be equated to integral multiples of $h/2\pi$ in the new quantum mechanics. In other words we must quantize the constant angular momentum before application of the field rather than the fluctuating value in the field. When we consider spin effects or more than one particle, an individual p_ϕ is not constant even in the absence of the field and cannot be quantized; it is rather the sum $\Sigma(p_\phi+p_\psi)$ which equals the magnetic quantum number times the factor $h/2\pi$.

[10] The orbital part of the Hamiltonian function (4) has often been given in the literature including the magnetic terms resulting from the modification in the definition of the momenta (cf., for instance, Born, Atommechanik, p. 239). The part of (4) resulting from spin kinetic energy is obtained by modifying in accordance with (3) the arguments of the usual expression for the Hamiltonian function of a spinning body, which is given, for example, in Born's Atommechanik, p. 31.

to the part of the Hamiltonian function involving H is very small in comparison with the ordinary paramagnetic terms. This contribution is, in fact, shown in fine print below to be of the same order as the relativity corrections to the Zeeman effect and henceforth will be disregarded. Furthermore we may neglect the terms in H^2 in the spin kinetic energy of the electron in comparison with those in H^2 in the orbital kinetic energy, for D^2/I is very small in comparison to e^2R^2/m since the internal radius of an electron is insignificant compared to the radius of an orbit. This will later be seen to mean that the internal spins make no contribution to diamagnetic susceptibilities. With this discarding of inconsequential terms, the Hamiltonian function (4) may be written with the aid of (3)

$$E=E_0+(He/2mc)\sum(p_\phi+2p_\psi)+(H^2e^2/8mc^2)\sum R^2, \tag{5}$$

where E_0 is a Hamiltonian function of the same form and arguments as in the absence of the field, and the remaining terms may be regarded as perturbative ones. In forming (5) we suppose, following Uhlenbeck and Goudsmit, that $D/2cI=-e/mc$, or that the ratio of spin magnetic moment to spin angular momentum is twice the corresponding orbital ratio.

Magnetic moment. The magnetic moment of the molecule in the direction of the applied field is

$$M_z^{(H)}=-(e/2c)\sum R^2\dot{\phi}+(D/2c)\sum(\dot{\psi}+\dot{\zeta}\cos\theta). \tag{6}$$

The first right-hand term ensues since the equations of electron theory show that the magnetic moment due to the orbital motion of a charge $-e$ is[11] $-(e/2c)\mathbf{r}\times\mathbf{v}$. The second term is the analogous expression for the magnetic moment of a spinning charge distributed with spherical symmetry, for $\dot{\psi}+\dot{\zeta}\cos\theta$ is the z-component of spin, and D is the electrical moment of inertia. Instead of using (6) it is convenient to have a formula expressing $M_z^{(H)}$ in terms of the coordinates and momenta rather than coordinates and generalized velocities. Such a formula is immediately deducible from the Hamiltonian function by a simple differentiation, for

$$M_z^{(H)}=-\partial E/\partial H. \tag{7}$$

To prove (7) we note that E involves H only through the arguments (3) and consequently

$$-\frac{\partial E}{\partial H}=-\sum\left(\frac{\partial E}{\partial p_\phi}\frac{eR^2}{2c}-\frac{\partial E}{\partial p_\psi}\frac{D}{2c}-\frac{\partial E}{\partial p_\zeta}\frac{D\cos\theta}{2c}\right). \tag{8}$$

The identity of (8) and (6) follows immediately since by Hamilton's equations $\partial E/\partial p_\phi=\dot{\phi}$, etc.

Relativity Corrections. We have so far for simplicity used Newtonian mechanics. It is, however, not difficult to determine the relativity corrections for the orbital part of the magnetic moment. In the relativity mechanics, the part of the Hamiltonian function arising from

[11] See, for instance, "Theories of Magnetism," p. 21 (Bulletin no. 18 of the National Research Council).

the orbital kinetic energy is[12] $\sum mc^2[(1+Km^{-2}c^{-2})^{1/2}-1]$ instead of $\sum K/2m$, where $K=p_R^2+p_s^2+p_\phi^2/R^2$. By expanding the radical as a series in H, it is easy to show that the relativity corrections change the part of the orbital energy which is of the first order in H by a factor γ, where $\gamma=(1-v^2/C^2)^{1/2}$. This result has, in fact, already been obtained by Sommerfeld, Debye,[13] and Pauli.[14] The relativity corrections to the paramagnetic and diamagnetic susceptibilities, second order Zeeman effect, etc. can likewise be calculated. Here the correction factors are of the same order of magnitude as $\gamma-1$.

We give only a subordinate place to the relativity corrections because usually they do not appreciably affect the susceptibilities. It is readily found[14] that in a hydrogenic atom the time average of γ, which is the significant part of γ for the first order Zeeman terms is $1-(2\pi^2Z^2e^4/n^2h^2c^2)=1-2.7\times10^{-5}Z^2/n^2$, where n is the principal quantum number and Z is the effective nuclear charge. This expression differs appreciably from unity only for the innermost orbits. Many such orbits (*e.g.* the K orbits), however, have no orbital angular momentum, and furthermore the inner orbits are grouped in "closed configurations" without resultant angular momentum, such as are completed in forming inert gases, so that $\sum p_\phi$ taken over a completed group vanishes even when the individual angular momenta do not vanish. Since similar orbits have the same average value of γ, the sum $\sum\bar{\gamma}p_\phi$ also vanishes, and thus there are no first order terms involving important relativity corrections. Pauli[14] shows, however, that these corrections would be contrary to experiment if we supposed the inner groups had a resultant angular momentum, as in the old Landé model of a magnetic atom core which has been discarded since the advent of the spin electron. It is not immediately obvious, especially in the quantum mechanics, that the phase relations in a completed group are such that $\sum\gamma p_\phi$ vanishes instantaneously as well as on the average, so that conceivably even with zero resultant angular momentum the inner orbits might give rise to appreciable rapidly fluctuating terms proportional to $\bar{\gamma}-\gamma$ in the Hamiltonian function, and thus make a contribution to the paramagnetic part of the second order Zeeman effect. This, however, seems quite improbable. Individual electrons do not compensate each other as regards their contribution to diamagnetism, but the inner electrons have such small values of r^2 that they are responsible for a small fraction of the total diamagnetism, and so here also the relativity corrections are unimportant.

Along with the orbital relativity corrections one must consider the term arising because the intra-atomic magnetic energy U involves H through the arguments (3). Thomas and Frenkel[15] have shown that in a hydrogenic atom the secular part of U is the mean value of $e^2Z(\boldsymbol{p}_1\boldsymbol{p}_2)/2r^3m^2c^2$ where r is the radius of the orbit and $\boldsymbol{p}_1$ and $\boldsymbol{p}_2$ are respectively the orbital and spin angular momentum vectors. To calculate accurately the correction coming from U it would be necessary (unlike the usual calculation of spin doublets to terms in $1/c^2$ for $H=0$) to know the periodic part of U, for the product of this part of U and the factor R^2 involved by (3) will give a significant secular contribution. Unfortunately the periodic part of U is unknown at present, but for calculating only orders of magnitude we may assume U is given rigorously by the preceding expression. In a magnetic field the change in $\boldsymbol{p}_1$, is by (3) of the order HeR^2/c, while we neglect the change in $\boldsymbol{p}_2$ since the spin electrical moment of inertia is small compared to eR^2. Thus to first order terms in H the contribution of U to the additional energy due to the magnetic field is roughly of the order $\pi HZ^2e^5/nhmc^3$, as R^2/r^3 is of the order $4\pi^2Ze^2m/n^2h^2$. This contribution is clearly comparable with the relativity correction to the Zeeman terms, which is the mean value of $eH(\gamma-1)p_\phi/2mc$ and in fact involves the constants e, h, c in the same way. In the foregoing we have discussed primarily the effect on the energy, but the corresponding corrections to the magnetic moment can be deduced from Eq. (12) below.

In studying internal spins of the electrons it is probably quite vital that one use relativity mechanics, as Breit, Thomas,[16] and others show that the spin may be so rapid that peripheral

[12] Cf. for instance, Born, Atommechanik, p. 232.

[13] A. Sommerfeld, Phys. Zeits. **17,** 491 (1916). P. Debye, *Ibid.* **17,** 507 (1916).

[14] W. Pauli, Jr., Zeits. f. Physik, **31,** 373 (1925).

[15] L. H. Thomas, Nature, **117,** 514 (1926). J. Frenkel, Zeits. f. Physik, **37,** 243 (1926).

[16] G. Breit, Proc. Nat. Acad. **12,** 451 (1926). L. H. Thomas, Phil. Mag. **3,** 1 (1927).

velocities are comparable with that of light. However, far too little is known about the internal structure of the electron to permit us to use the relativistic analysis, as in the preceding work we would have to know how the charge distributes itself inside the electron. Nevertheless, the value $-e/mc$ for the ratio of spin magnetic moment to spin angular momentum seems well established from evidence on the Zeeman effect and multiplet separations, and this must be regarded as applying inclusive rather than exclusive of relativity corrections since they are important for the spins. (Then m denotes the rest mass, and spin angular momentum is to be defined in the generalized relativity sense which allows for variation of mass with speed). In using this value of the ratio we have thus perhaps rather illogically incorporated the relativity corrections in our Newtonian model of the electron's spinning motion. We use this model simply to show that internal spins do not contribute appreciably to diamagnetism, and also, as do others, because it is a convenient way of formulating what is known about the electron's spinning motion in the absence of an adequate electrodynamics of its interior. (Note added in proof: Dirac's work alredy quoted clears up this situation greatly.)

Passage to quantum mechanics. In studying actual molecular systems it is, of course, necessary to use quantum mechanics, but fortunately the adaptation of the preceding analysis to this is immediate. The Hamiltonian function is still (5), and Eq. (7) is still applicable. Only, of course, the coordinates and momenta, also E and $M_z^{(H)}$, are now matrices.[17] The justification for these statements is that the Hamiltonian function (5) involves no non-commutative products, except possibly in E_0. In other words there are no terms of interest involving simultaneously a coordinate and its canonically conjugate momentum, so that by the correspondence principle there can be no ambiguity in the quantum adaptation. This is the same argument as that given by Heisenberg and Jordan[18] in their paper on the Zeeman effect, in which they use a matrix Hamiltonian function similar to (5) except for omission of the diamagnetic term. If we use the abbreviation

$$M_z = -(e/2mc) \sum (p_\phi + 2p_\psi), \tag{9}$$

then a typical matrix element of the perturbative part of the Hamiltonian function is by (5)

$$-HM_z(njm;\ n'j'm') + (H^2e^2/8mc^2) \sum R^2(njm\ ;\ n'j'm'). \tag{10}$$

We use in (10) and elsewhere in this paper the same notation as in part I, except we no longer print matrices in bold-face type, and the reader is referred to p. 733 of I for a full explanation of its significance. Briefly, the first index n represents the totality of quantum numbers whose effect on the energy is large compared to kT, while the index j represents those, other than m, whose effect is smaller than, or comparable with kT. The third

[17] As already mentioned on p. 731, part I, we use the matrix rather than wave formulation of the new quantum mechanics. The same results are, of course, obtained with either formulation in virtue of their general mathematical identity, and the popularity of susceptibility calculations by means of the wave equation seems rather surprising inasmuch as the matrix method has usually yielded the susceptibility formulas first and most directly. Except for the spin terms, a wave equation corresponding exactly to the Hamiltonian function (5) is deducible from the generalized Schroedinger equation given by Gordon (Zeits. f. Physik, **40**, 117, 1926) and others, which includes the vector as well as electrostatic potentials.

[18] W. Heisenberg and P. Jordan, Zeits. f. Physik, **37**, 263; (1927).

index m is the magnetic quantum number specifying the spacial orientation, and is not to be confused with the mass of the electron, which appears as a factor in the denominator and is also denoted by m. It is to be clearly understood that $R^2(njm;\ n'j'm')$ denotes an element of R^2, not the square of an element of R. Also it is to be noted that the summation sign immediately preceding R^2 means a sum over all the electrons in the molecule, and is not to be confused with the other sums of the matrix elements over various quantum numbers indicated by subscripts after the summation signs.

Energy and moment of a stationary state. The effect of the magnetic field on the energy may now be calculated by the perturbation theory for the new quantum mechanics which has been developed by Born, Heisenberg, and Jordan,[19] provided the field is weak enough to permit power series development in H. We may suppose the system non-degenerate as this involves no essential loss of generality in calculating susceptibilities (see note 19 and p. 740 of part I). If we retain terms through H^2, the energy of the state njm is

$$W^{(H)}(njm)=W(njm)-HM_z(njm\ ;\ njm)+H^2\sum{}'_{n'j'm'}\frac{|\ M_z(njm\ ;n'j'm')\ |^2}{h\nu(njm\ ;\ n'j'm')}$$
$$+(H^2e^2/8mc^2)\sum R^2(njm\ ;\ njm), \qquad (11)$$

as the first and second terms of (10) correspond to H_1, H_2 in the notation of Born, Heisenberg, and Jordan. The prime after the summation sign means that the one term $n'j'm'=njm$ is to be excluded. The frequencies ν, energy elements $W(njm)$, and other matrix elements appearing on the right-hand side of (11) are to be calculated for $H=0$, as indicated by the absence of the superscript$^{(H)}$.

The time average of the magnetic moment of a state in the direction of the applied field can be obtained directly from (11) by means of the formula[20,21,22]

[19] Born, Heisenberg, and Jordan, Zeits. f. Physik, **35**, 557 (1927); especially Eqs. (29) and (31), p. 567.

[20] Eq. (12) is not to be confused with (7), as (12) gives the average rather than instantaneous value of the magnetic moment defined by (6); also the Hamiltonian function E in (7) is the energy expressed in terms of the generalized coordinates and momenta, whereas in (12) W denotes the energy expressed as a function of the quantum numbers. The distinction between the instantaneous and average values of the magnetic moment is only a nominal one, at least with the definition (6) we use, for (6) is based on the conventional formula $(-e/2mc)\mathbf{r}\times\mathbf{v}$ of the electron theory for the orbital magnetic moment and this formula is valid only on the average, as in its derivation terms are omitted which average out if the motion is recurrent.

[21] It is interesting to note that formulas similar to (7) and (12) also hold in the case of electric rather than magnetic polarization. In the electric case $E=E_0+\sum Fez$ so that $\partial E/\partial F=\sum ez=-M_z^{(F)}$ and from this a formula analogous to (12) can be established by the same method as that given above.

[22] Eq. (12) can also be established by application of the principle of adiabatic invariance. As magnetic forces do no work, the change in energy of a stationary state when subject to a magnetic field is due to the work done by electric forces attendant to creation of a magnetic

$$\overline{M}_z^{(H)} = -\partial W^{(H)}/\partial H \text{ or } M_z^{(H)}(njm\,;\,njm) = -\partial W^{(H)}(njm)/\partial H. \qquad (12)$$

Eq. (12), which is even taken by some writers as the definition of the moment, is easily proved to follow from our definition (6) by the theorem that the change in energy brought about by the addition of a perturbative term to the Hamiltonian function is to the first order the mean value of this term. This is a well known theorem in the old quantum theory, and Born, Heisenberg, and Jordan[19] show that it also holds in the new quantum mechanics, with, of course, the understanding that the requisite mean value is formed by keeping only diagonal elements in the matrix representing the perturbative term. If we change the magnetic field from H to $H+\Delta H$ and if we neglect terms in $(\Delta H)^2$, the term thereby added to the Hamiltonian function is $(\partial E/\partial H)\Delta H$, and by the theorem just quoted the corresponding change $\Delta W^{(H)}$ in energy is very approximately the average value of this term. Eq. (12) now follows on using (7).

The formula for the magnetic moment obtained by combining (11) and (12) is similar to Eq. (3) of part I except that it applies to magnetic rather than electric polarization, and except for addition of the diamagnetic term, which arises from the second line of (11) and finds no analog in the electrical case. It is to deduce this term that we have given most of the preceding analysis, as otherwise we could have started directly with a formula similar to (3) of part I. The diamagnetic effect is essentially a correction for the fact that in a magnetic field the moment is no longer given by (9) because of modifications in the kinematical significance of the canonical momenta. Even without the diamagnetic term, however, the time average $M_z^{(H)}(njm;\ njm)$ of the z-component of magnetic moment of a stationary state in the presence of the field would not equal the time average $M_z(njm;\ njm)$ of this component in its absence, for there is another term in H^2, on the first line of (11), which is similar to that in the electrical case. This other term is associated with the type of second-order Zeeman effect for which the formula is given by E. Hill and the writer in a preliminary abstract (No. 41) on p. 715 of this issue, and would be absent were Larmor's theorem applicable.

Calculation of susceptibility. Because of the similarity of (11–12) to Eq. (3) of part I, the analysis in sections 2 and 3, part I, may now be applied, and should be read conjunctly by those desirous of following the present section in detail. The addition of the diamagnetic term occasions no particular difficulty, for it was shown on p. 744, part I, that the effect of averaging over the various quantum-allowed orientations is to replace R^2 by $2r^2/3$, just as in the classical theory where the orientations are random. We use r^2 to denote $x^2+y^2+z^2$, the square of the radius, while $R^2=x^2+y^2$. We now separate the matrix M_z defined by (9) into "high" and "low" frequency elements, as fully explained on p. 733, part I, which are denoted respectively

field, which can be shown to give (12) if the field is applied adiabatically. We do not use this method because it would require us to enter into the rather involved quantum mechanics of non-conservative systems. However, a paper by Born shows how the concept of adiabatic invariance can be given a meaning in the new mechanics (Zeits. f. Physik, **40**, 167, 1927).

by $M_z(njm; n'j'm')$ $(n' \neq n)$ and $\mu_z(jm; j'm')$. Similar expressions without the subscript z will be used to denote the high and low frequency elements of the scalar magnitude of the magnetic moment vector measured, of course, before application of the field H.

There is, however, one respect in which it is necessary to modify the calculation of the susceptibility given in section 3, part I. The magnetic moment in general consists of two parts, viz., the "orbital" and "spin" moments. In the various component levels constituting the normal state these two parts may be inclined to each other at different angles, so that their vector resultant may have different values. Thus we cannot always suppose the resultant magnetic moment "permanent," so that we cannot always effect the simplification given at the top of p. 738, part I. Instead the contribution of the low frequency elements must be expressed as in the first line of (12), part I. If we make only the fundamental assumption that the "low" and "high" frequencies are respectively small and large compared to kT/h, the analysis in part I shows that the formula for the susceptibility is

$$\chi = N\alpha + N\overline{\overline{\mu^2}}/3kT, \tag{13}$$

where by (6) and (12), part I,

$$\overline{\overline{\mu^2}} = \frac{\sum_{j,m}\left[\left\{\sum_{j'm'} \left|\mu(jm\,;j'm')\right|^2\right\} e^{-W(nj)/kT}\right]}{\sum_{j,m} e^{-W(nj)/kT}}. \tag{14}$$

Eq. (13) differs from (1), part I, only in the insertion of the double bar in the second right-hand term. The expression (14) has the significance of being the time average of the square of the low frequency part of the magnetic moment vector, this average itself being averaged over the various component levels of the normal state weighted in accordance with the Boltzmann factor $e^{-W(nj)/kT}$. This follows since by the rules for matrix multiplication the expression in the inner sum of the numerator of (14) is a diagonal element of the matrix μ^2, i.e. the time average of μ^2 for the state njm, which is no longer assumed to have a numerical value invariant of j. The sum over j, m, of course gives the average over the various component levels of the normal state. We use a double rather than single bar in (13, 14) in order to emphasize the distinction between the statistical mean (14) of the time average, and pure time average for a single state.

The term $N\alpha$ in (13) represents the diamagnetic effect, together with the contribution of the high frequency elements, which may be simplified as on pp. 738–740, part I. Using (17), part I, and adding the diamagnetic term, the value of this term is seen to be

$$N\alpha = \frac{2N}{3h}\sum_{n'(n'\neq n)} \frac{\left|M(n\,;n')\right|^2}{\nu(n'\,;n)} - \frac{Ne^2}{6mc^2}\sum\overline{r^2}, \tag{15}$$

where $M(n; n')$ is defined as on p. 739, part I. In order to make the denominator positive, we use the emission frequencies $\nu(n'; n)$ which have the

opposite sign from the negative or absorption frequencies $\nu(n; n')$ used in (17), part I. We have assumed in (15) that the matrix element $r^2(njm; njm)$ representing the time average of the square of the radius of a given orbit for the state njm has the same magnitude in all the component levels of the normal state; i.e., has a value invariant of j or m, which we denote by $\overline{r^2}$. This condition is usually met in gases, as the magnetic quantum number m merely quantizes the spacial orientation, and in atoms the various j-levels usually represent various relative orientations of the spin and orbital angular momenta. Such differences only in orientation clearly do not affect the size or shape of an orbit. In molecules the index j may in addition be associated with a splitting into components due to different amounts of molecular rotation, but the rotational quantum number does not influence the magnitude of r if we neglect the slight centrifugal expansion studied on p. 54, part II.[2]

2. Diamagnetism—Discussion of Eq. (15)

If the magnetic moment matrix M contains low frequency elements, the second right-hand term of (13) is usually much greater than the first, and the material is paramagnetic. If, however, the moment contains only high frequency elements; i.e., vanishes if we average over the high frequency part, this second term vanishes. The susceptibility is then given by (15), and is paramagnetic or diamagnetic according as the first or second-right-hand member of (15) is the greater. Now the expression (15) is independent of the temperature as long as the number of molecules N per cc. does not vary. This is in accord with the fact that experimentally in gases the diamagnetism is usually independent of the temperature at constant density. On the other hand the diamagnetism of many solids vary with the temperature. A possible explanation of this difference is that in solids conditions are more complicated than assumed above in deriving (15), so that possibly the different levels constituting the normal state do not have the same radii. When this is the case it is necessary to replace $\overline{r^2}$ by the statistical mean of the time average of r^2, i.e., by an expression $\overline{\overline{r^2}}$ defined by an equation identical with (14) except that μ is replaced by r; the term $N\alpha$, of course then varies with temperature due to varying distributions among orbits of different sizes. Also (15) breaks down if the frequencies $\nu(n'; n)$ are not all large compared to kT/h.

Diamagnetism of atoms. If it were not for the spin anomaly, the constancy of angular momentum in atoms would also imply the constancy of magnetic moment, and the matrix M would consist solely of diagonal elements so that the first right member of (15) would be wanting. Actually because of different ratios for the spin and orbital parts, the resultant magnetic moment and angular momentum vectors are not parallel, and M contains periodic elements whose frequencies are classically that of the mutual precession of the spin and orbital angular momenta, and quantically are proportional to the energy intervals in multiplets whose components differ as to inner quantum number. However, the normal level of a diamagnetic

atom is ordinarily a ^1S state, for the existence of either a spin or orbital angular momentum different from zero implies paramagnetism (see also note 34). Consequently the periodic terms in the moment matrix still disappear, and the expression for the susceptibility becomes

$$\chi = -(e^2N/6mc^2)\sum\overline{r^2}. \tag{16}$$

This formula is one which has been derived clasically by Pauli,[23] and as noted by Glaser and Barnett,[24] differs by a factor 2 from the original Langevin-Weber formula, which was derived not with real electronic motions, but with the assumption of hypothetical particles confined to move in one plane. Pauli assumed Larmor's theorem, which is legitimate in singlet states.

The average value of r^2 needed in Eq. (16) is easily deduced for hydrogenic atoms from Waller's formula for mean values in Keplerian motion in the new quantum mechanics, and has been calculated by the writer[25] and by Pauling,[26] both of whom find $\overline{r^2} = \frac{1}{2}a_0^2n^2(5n^2-3k^2-3k+1)$, where $a_0 = h^2/4\pi^2mZe^2 = .53\times10^{-8}Z^{-1}$, the radius of a one-quantum orbit in the old theory, while n is the principal quantum number, and k is one unit lower than the conventional azimuthal quantum number of the old theory. The old quantum theory would have $-3(k+1)^2$ in place of $-3k^2-3k+1$. An experimental value of the diamagnetic part of the susceptibility of atomic hydrogen can only be deduced rather indirectly by applying the method of mixtures to compounds. Even if hydrogen gas could be dissociated into the monatomic form, it would be paramagnetic like the alkali vapors because of spin doublets. However, approximate comparisons of the theory with experiment can be made by assuming the orbits in other atoms to be approximately hydrogenic in character if a proper value be assigned the effective nuclear charge. Such comparisons have been given by the writer for helium,[25] and especially by Pauling[26] for a large number of other atoms. The reader is referred to their papers for details. The diamagnetism calculated for atomic hydrogen and helium is three times as great as in the old quantum theory, and agrees much better with experiment.

Diamagnetism of molecules. In non-monatomic molecules the first right member of (15) does not vanish. The reason is that the total electronic angular momentum contains fluctuating terms due to the continual transfer of angular momentum back and forth between the electrons and nuclei even though the resultant angular momentum of the entire molecule is constant. The low frequency and constant elements of the magnetic moment vanish, to be sure, in a diamagnetic molecule but because of this transfer effect the high frequency elements will not disappear even if the molecule is in a ^1S state. This statement will be proved in detail in the following paragraphs in fine print. Hence in non-monatomic molecules the square of the magnetic moment or of the electronic angular momentum does not vanish even when

[23] W. Pauli, Jr., Zeits. f. Physik, **2,** 201 (1920).
[24] A. Glaser, Dissertation, Munich, 1924; S. J. Barnett, Phys. Rev. **25,** 835 (1925).
[25] J. H. Van Vleck, Proc. Nat. Acad. **12,** 662 (1926).
[26] L. Pauling, Proc. Roy. Soc. **114A,** 181 (1927).

the average amount is zero. This result at first seems contrary to the correspondence principle, for in classical theory most diamagnetic models of the molecule have zero magnetic moment instantaneously as well as on the average. The explanation of this paradox is that the expression in classical mechanics which corresponds to the first right member of (15) involves the derivatives with respect to the action variables of the amplitudes in the Fourier expansion of the magnetic moment,[27] and these derivatives, of course, do not necessarily vanish because the amplitudes themselves do. Also, the frequencies involved in transfers of angular momentum between nuclei and electrons are, in the terminology of band spectroscopists, "electronic frequencies" associated with transitions from normal to excited states. In applying the correspondence principle we must consider both the initial and final states in classical models, and classically the excited states may be paramagnetic and have non-vanishing amplitudes in the Fourier expansion of the moment because of the transfer effect. This effect is, of course, absent in atoms, and the periodic part of their magnetic moment arises only because of the spin anomaly previously discussed.

Proof that periodic part of electronic angular momentum does not vanish in non-monatomic molecules.[28] We shall neglect the spin moment, as this does not enter appreciably in the transfer effect. From the relations between matrix and wave mechanics established by Schroedinger, Eckart, or Dirac, a diagonal matrix element of the square of the orbital electronic angular momentum is

$$P^2(n;\ n) = -(h^2/4\pi^2)\int \cdots \int u_n^*[(\sum P_x)^2+(\sum P_y)^2+(\sum P_z)^2]u_n dx_1 \cdots dx_s dy_1 \cdots dz_s \qquad (17)$$

where u_n is the Schroedinger wave function for the state n, u_n^* is its conjugate, and P_x is the operator $y\partial/\partial z - z\partial/\partial y$, with similar definitions of P_y, P_z. The index n symbolizes the aggregate of all the electronic quantum numbers. To prove (17) different from zero it suffices to prove that $P_z^2(n;n)$ does not vanish. Let us suppose that the axis joining two of the nuclei is located in the xy plane and makes an angle θ with the x-axis. Let us introduce the new coordinates

$$x_i' = x_i \cos\theta + y_i \sin\theta,\ y_i' = -x_i \sin\theta + y_i \cos\theta,\quad z_i' = z_i \quad (i=1, \cdots, s)$$

which are fixed relative to the nuclei, and let us suppose that $u_n(x_1', \cdots, z_s')$ is expressed in terms of the coordinates $x_1, \cdots, z_s$ and θ. Then we find

$$P_z^2(n;\ n) = P_z'^2(n;\ n) = -(h^2/4\pi^2)\int \cdots \int u_n^* \partial^2 u_n/\partial\theta^2 dx_1 \cdots dz_s. \qquad (18)$$

Now (18) has a value $P_z'^2(n;n)$ invariant of θ, and so it is immaterial if we average over θ. This permits a partial integration with respect to θ which throws (18) into the form

$$P_z^2(n;\ n) = (h^2/4\pi^2)\int \cdots \int |\ \partial u_n/\partial\theta\ |^2 dx_1 \cdots dz_s. \qquad (19)$$

The expression (19) can clearly vanish only if u_n is independent of θ. This is, however, incompatible with the fact that the wave equation involves θ through the mutual potential energy of the electrons and the two nuclei under consideration. In other words the wave function in the xyz system will be different depending on how the molecular axis is oriented relative to this system. Thus the square of the electronic angular momentum will vanish only if u is a

[27] This may be verified by noting that Eq. (17), part II, is the classical analog of (3), part I.

[28] This method of proof is suggested by Born and Oppenheimer's paper on molecules, Ann. der Physik. **84,** 457 (1927).

a function only of the relative positions of the electrons and their distances from a single fixed center. This is, of course, possible only if the nuclei exerted no forces or if all the nuclei coincided, *i.e.* an atom.

It may be remarked that the above proof applies to a molecule with any number of nuclei and electrons. In the particular case of a diatomic molecule we may distinguish between the different behaviors of the components of angular momentum parallel and perpendicular to the axis of figure. The parallel component is constant, and an integral multiple of $h/2\pi$ and so may vanish, as it does in S states. The perpendicular component is easily shown to vanish on the average (due, essentially to the continual precession of the electronic angular momentum vector about the axis of the molecule), but its square does not vanish, as we have taken the z-axis in (18) perpendicular to the line joining the nucleus. In the very special case of a molecule with only one electron, the vanishing of (17) or (18) requires that the wave function be a function of r only.[29]

The foregoing shows that I was in error in stating in a former article[25] that Pauli's formula (16) could be applied to molecules as well as atoms. Instead the complete expression (15) must be used.[30] The cause of my mistake was that I naturally supposed the electronic angular momentum vanished instantaneously rather than only on the average. I am indebted to Dr. Kronig for questioning my extension of Pauli's formula to molecules. His letter, which advanced considerations closely related to those given in note 30, led me to discover the need of always including both terms of (15) in non-monatomic molecules. This modification does not affect my calculation[25] of the diamagnetism of H_2, as this was made by treating the hydrogen molecule as a hydrogenic atom with properly adjusted "effective charge," and with this rough approximation the first right member of (15) is zero, as it vanishes for atoms in the S state.

Experimentally most gases are found to be diamagnetic, and this shows that the first right member of (15) is ordinarily less than the second in ^1S molecules. Perhaps the symmetry of the wave function is often sufficiently close to that of a ^1S atom so that (16) is a fair approximation. It is to be noted that in any case Pauli's formula (16) is an upper limit to the diamagnetic susceptibility.

3. Paramagnetism of Atoms

We shall treat only the case where the spin angular momenta can be considered firmly coupled together to form a resultant spin angular momen-

[29] This can also be seen by transforming to polar coordinates in the manner of L. Brillouin, J. de Physique, **8**, 74 (1927), especially footnote, p. 77.

[30] A simple general illustration of the need of considering both members of (15) is furnished by a hypothetical system of two concentric rigid bodies of spherical symmetry, *i.e.*, two spherical magnetons, of electrical and mechanical moments of inertia D_1, I_1 and D_2, I_2 respecitvely. The diamagnetic susceptibility to be expected if we treat the magnetons as separate bodies and keep only terms analogous to the second member of (15) is readily shown to be $-(N/4c^2)$ $(D_1^2/I_1+D_2^2/I_2)$, whereas if we let the two magnetons be rigidly joined together to form a single body, the true susceptibility is $-(N/4c^2)$ $(D_1+D_2)^2/(I_1+I_2)$, as D_1+D_2 and I_1+I_2 are the total moments of inertia. Thus a different result is apparently obtained depending on whether we treat the magnetons as a single rigid body or as two bodies so strongly coupled as to form a virtually rigid whole. The cause for this discrepancy is that when the magnetons are considered as separate bodies the first right member of (15) will not vanish if there is interaction between them.

tum vector $\boldsymbol{P}_s$ of permanent magnitude, and where the orbital angular momenta likewise form a resultant $\boldsymbol{P}_k$ of permanent size. The quantum mechanics shows that the matrix elements of the squares of these vectors are then

$$P_s^2(n\ ;\ n)=s(s+1)h^2/4\pi^2, \qquad P_k^2(n\ ;\ n)=k(k+1)h^2/4\pi^2, \tag{20}$$

where $s=\frac{1}{2}$ in doublets, 1 in triplets, etc., while k is the Russell-Saunders quantum number which quantizes the total orbital angular momentum. Thus $k=0$, 1, 2, 3 in S, P, D, F terms. This k (often denoted by l) is not to be identified with the azimuthal quantum number of an individual electron unless there is only one not in a completed group. The type of coupling which we are considering is characteristic of the simpler forms, of spectra, the so-called "normal multiplets" or "multiplet structures of the first order." The extension of the theory to other types of coupling where the interaction between individual spin and orbital momenta is stronger than the coupling of spin or orbital momenta among themselves, furnishes no particular difficulty.

The spin and orbital magnetic moment vectors are, of course, connected with the corresponding angular momentum vectors by the relations

$$\boldsymbol{M}_s=-e\boldsymbol{P}_s/mc, \qquad \boldsymbol{M}_k=-e\boldsymbol{P}_k/2mc. \tag{21}$$

The various values of the total angular momentum $\boldsymbol{P}$, which is the resultant of $\boldsymbol{P}_s$ and $\boldsymbol{P}_k$, give the various components of a "multiplet" level. Because of the different proportionality factors in the two Eqs. (21), the resultant magnetic moment is not in general parallel to $\boldsymbol{P}$. We may consider two limiting cases, in which the separation of components, or in other words the energy of interaction between $\boldsymbol{P}_s$ and $\boldsymbol{P}_k$, is respectively very large or very small compared to kT.

1. *Multiplet intervals small compared to kT.* As already mentioned on p. 598, the only periodic elements involved in the magnetic moment vector of an atom are those associated with the mutual precession of the spin and orbital angular momentum vectors. Thus when the multiplet intervals are small compared to kT, these elements will be entirely of the "low frequency" category, and the first right member of (15) disappears. If then we neglect the small diamagnetic effect always superposed on the paramagnetic we may set $\alpha=0$ in the expression (13) for the susceptibility. Since $\boldsymbol{\mu}$ is the resultant of the vectors $\boldsymbol{\mu}_s$ and $\boldsymbol{\mu}_k$ we have

$$\boldsymbol{\mu}^2=\boldsymbol{\mu}_s^2+\boldsymbol{\mu}_k^2+\boldsymbol{\mu}_s\cdot\boldsymbol{\mu}_k+\boldsymbol{\mu}_k\cdot\boldsymbol{\mu}_s. \tag{22}$$

By $\boldsymbol{\mu}$, $\boldsymbol{\mu}_s$, $\boldsymbol{\mu}_k$ we mean the "low frequency parts" of the vectors $\boldsymbol{M}$, $\boldsymbol{M}_s$, $\boldsymbol{M}_k$. Now in the absence of high frequency elements the distinction between the $\boldsymbol{\mu}$'s and $\boldsymbol{M}$'s disappears, and we may take $\boldsymbol{\mu}_s\cdot\boldsymbol{\mu}_k=\boldsymbol{\mu}_k\cdot\boldsymbol{\mu}_s$ in (22) since $\boldsymbol{P}_s$ and $\boldsymbol{P}_k$ commute in multiplication (cf. ref.[18]).

Since the temperature factor $e^{-W/kT}$ may be disregarded under the supposition of energy intervals small compared to kT, the statistical average of the product $\boldsymbol{\mu}_s\cdot\boldsymbol{\mu}_k$ may be taken as zero. This is an obvious result in very

strong fields, where $\boldsymbol{P}_s$ and $\boldsymbol{P}_k$ are quantized separately relative to the axis of the field and hence have no correlation between their directions if we average over all orientations. Furthermore the statistical average of this product is invariant of the field strength (neglecting small saturation terms proportional to H^2) and hence vanishes in all fields if it does in very strong ones, for an easy extension[31] of the spectroscopic stability relations given in section 4, part I, shows that it is invariant of the mode of quantization if the system is made degenerate with respect to j, m by neglecting the interaction between $\boldsymbol{P}_k$ and $\boldsymbol{P}_s$ and between H and both $\boldsymbol{P}_k$, $\boldsymbol{P}_s$. We can also verify directly that the statistical average of $\boldsymbol{P}_k \cdot \boldsymbol{P}_s$ vanishes in weak fields by noting that here $P^2(nj;\ nj) = j(j+1)h^2/4\pi^2$, so that using (20) and a relation between the components of P analogous to (22) we have

$$\overline{\overline{\boldsymbol{P}_s \cdot \boldsymbol{P}_k}} = (h^2/4\pi^2 B) \sum_{j=|k-s|}^{j=k+s} (2j+1)\left[j(j+1) - s(s+1) - k(k+1)\right] = 0.$$

The constant factor B in the denominator is the total number $B = (2k+1) \cdot (2s+1)$ of components constituting the normal state and the factor $2j+1$ is the a-priori probability or number of m components belonging to a given value of the inner quantum number j.

The values of the first two terms of (22) are furnished immediately by (20, 21). Since (20) does not involve the indices j, m, the insertion of a double bar over these terms in substituting (22) in (13) is unnecessary. Since the preceding paragraph shows the third and fourth terms of (22) give no effect on the average, we see that the expression (13) for the susceptibility becomes

$$\chi = N\left[4s(s+1) + k(k+1)\right]\beta^2/3kT \tag{23}$$

where β is an abbreviation for the Bohr magneton

$$\beta = he/4\pi mc. \tag{24}$$

It is to be emphasized that the derivation of (23) has not rested upon a quantization peculiar to a particular field strength, as this is not involved in (20). Consequently if we neglect saturation effects, which are disregarded throughout the article, and which are ordinarily small in paramagnetic media, the susceptibility is invariant of the field strength, even though the Paschen-Back effect may materially alter individual Zeeman components. As we have so often mentioned, such results are typical of the new mechanics. If the field is so strong that the separation of Zeeman components is larger than the multiplet intervals, it would be necessary to develop the energy in descending rather than in ascending powers of H as assumed in part I, but (23) then clearly applies if we neglect small terms proportional to $1/H, \cdots$, as there is then separate spacial quantization of the spin and orbital momenta; our main result is that (23) applies also in weak fields.

[31] A proof similar to that given in section 4, part I, establishes the invariance of sums of products of the form fg^* as well as ff^*.

2. *Multiplet intervals large compared to kT.* When the separation of multiplet components is large compared to kT, only the one component which has the lowest energy is the normal state. The matrix elements of $\boldsymbol{M}$ are now all of the "high frequency" type unless $J=J'$. Here J is the inner quantum number, which we denote by a capital letter when it is different than the general index j used throughout parts I, II, III. In the previous case 1, J and j were identical, but now J belongs to the high frequency category n. The low frequency part of $\boldsymbol{M}$ is now only the part which is parallel to the resultant angular momentum $\boldsymbol{P}$ and so does not involve the precession about the "invariable axis" of $\boldsymbol{P}$. Heisenberg and Jordan's analysis[18] shows that the square of this part of $\boldsymbol{M}$ is $g^2J(J+1)\beta^2$ where g is the Landé g-factor $(3/2)+(s^2+s-k^2-k)/2(J^2+J)$. Thus (13) becomes

$$\chi=Ng^2J(J+1)\beta^2/3kT+N\alpha. \tag{25}$$

The first member of (25) can also be deduced from quite elementary considerations, as is usually done, by noting that in the present instance the mean square of the magnetic quantum number m is $J(J+1)/3$ in either the old[32] or new[33] quantum theory. The second member, given by (15), is usually disregarded, as it is often small. A later paper by E. Hill and the writer on the second order Zeeman effect shows that in the present case it becomes

$$N\alpha=\frac{N\beta^2}{6(2j+1)h}\left[\frac{f(j)}{\nu(j-1\,;\,j)}+\frac{f(j+1)}{\nu(j+1\,;\,j)}\right]-\frac{Ne^2}{6mc^2}\sum\overline{r^2} \tag{26}$$

with the abbreviation $f(j)=j^{-1}[(s+k+1)^2-j^2][j^2-(s-k)^2]$. Usually the normal state is a minimum or maximum of J, depending on whether the multiplet is normal or inverted, and then the first or second term of (25) vanishes. The frequencies in the denominator of (26), although assumed large compared to kT/h, are usually small enough to make the sum of the first two terms large compared to the third, except in S states, where only the diamagnetic effect remains.[34]

Comparison with other work. We shall omit comparisons of Eqs. (23, 25) with experiment, as we have nothing new to contribute. In the absence of

[32] Sommerfeld, "Atombau," 4th Ed., pp. 630–648 and references.

[33] J. H. Van Vleck, Nature, **118,** 226 (1926).

[34] A peculiar situation arises when the only level in which there is normally an appreciable concentration of electrons is a multiplet-component which has a zero inner quantum without being an S-term. The first member of (25) will then vanish, so that the susceptibility will be equal to the expression (26), and further the second term of (26) will be different from zero. Thus the material will exhibit a weak paramagnetism which is independent of the temperature, in striking contrast to the usual Curie law. Hund interprets the lowest level in Eu^{+++} as a ^7F term having $j=0$, while Laporte and Sommerfeld consider the lowest level in Cr^{++} to be a ^5D term likewise with $j=0$. These are thus cases in which there might conceivably be this weak paramagnetism invariant of temperature. However, the strong paramagnetism of Eu^{+++} and Cr^{++} seems to show pretty definitely that in these ions there is an appreciable concentration of electrons in states having inner quantum numbers different from zero, so that if the assignment $j=0$ to the lowest level is really correct there must be other components separated from the lowest by an interval small compared to kT/h.

data on paramagnetic monatomic vapors, most of the experimental check is furnished by monatomic ions in solution. The calculations of other writers[32,35] have ordinarily been made on the supposition that only one multiplet component need be considered, so that (25) is applicable. Now neglecting the second right hand term, Eq. (25) is exactly the formula which Sommerfeld and others have derived with the old quantum theory, so that it is unnecessary to revise their comparisons with experiment. This agreement between the old and new theories is rather fortuitous, and results because both give the same z-components of the angular momentum P even though they give different values of P and of the angle between P and z. This agreement, however, applies only with "strong" special quantization in the old theory, and as discussed by the writer on p. 37, part II, and also in an earlier note,[33] the new mechanics has the great advantage that it is immaterial whether there is weak or strong special quantization. The most satisfactory experimental confirmation of (25) consistent with existing spectroscopic data seems to be found in Hund's[35] calculation of the susceptibilities of the rare earths.

The susceptibilities of ions of the iron group, also even the rare earths in some cases, are not adequately explained by Eq. (25) without contradicting spectroscopic theory on normal terms. In a noteworthy article Laporte and Sommerfeld[36] attribute this to the fact that the multiplet intervals may not be large compared to kT. They show that susceptibilities in the iron group are intermediate between those predicted for very wide and very narrow multiplets, provided "inverted" multiplets are assumed in some instances. One correction, however, must be noted to the work of Laporte and Sommerfeld. Their formula for the limiting case of intervals small compared to kT is not (23) but a considerably more complicated expression (their Eq. 6). The reason is that they overlook the fact that the second as well as first order Zeeman effect, in other words both terms on the first line of (11), contribute to the second right member of the susceptibility expression (13) in narrow multiplets. This extra contribution results from the component of magnetic moment perpendicular to the resultant angular momentum, as the Landé g-factor embodies only the parallel component. The effect of this correction is usually not large and so leads to no important change in their results. (It makes the magneton numbers $\mu_w(0)$ in their table 2 become 0, 14.9, 22.2, 25.8, 27.2, 29.4 instead of 0, 14.5, 21.6, 24.7, 26.0, 29.6)

When spectroscopists have accurately determined the width of multiplets contiguous to the normal state it will, of course, be possible to make exact calculations of the susceptibility by means of equations such as (5), part I, instead of relying on the limiting formulas (23) and (25) which are rigorously applicable only to infinitely narrow or wide multiplets.

[35] F. Hund, Zeits. f. Physik, **33**, 855 (1925).
[36] Laporte and Sommerfeld, *Ibid.*, **40**, 333 (1926).

4. Paramagnetism of Molecules

Diatomic molecules will first be treated. Hund[37] has emphasized that in such molecules we must distinguish between two kinds of coupling of the spin axis relative to the rest of the molecule, which he disignates as types (a) and (b). In (a) the energy of interaction between the spin and orbital angular momentum is large compared to that between the spin and the angular momentum due to rotation of the molecule as a whole, and consequently the spin axis is firmly quantized relative to the "axis of figure" which connects the two nuclei. In (b) the reaction between the spin and the molecular rotation is the more important; the spin axis then no longer makes a fixed angle with the axis of figure, and instead the spin angular momentum vector and the remaining (or orbital+rotational) angular momentum of the molecule are quantized relative to each other to form a resultant represented by the quantum number j. In either (a) or (b) the component of the orbital angular momentum $\boldsymbol{P}_k$ which is parallel to the axis of figure equals $\sigma_k h/2\pi$, where σ_k is an integer. The perpendicular component of $\boldsymbol{P}_k$ will generally belong entirely to the high frequency category, for the effect of the value of σ_k (unlike σ_s below) on the energy is very considerable, or, interpreted kinematically, the vector $\boldsymbol{P}_k$ precesses rapidly about the axis of figure. This ineffectiveness of the perpendicular component is perhaps the main distinction from the atomic case, and is exemplified by the fact that terms in band spectra are classified as of the $S, P, D, F, \cdots$, type according as $\sigma_k = 0, 1, 2, 3, \cdots$, rather than on the basis of the value of k. Thus in (22) we must identify μ_k^2, the square of the low frequency part of the orbital moment, with the square $\sigma_k^2\beta^2$ of the component of this moment parallel to the axis of figure. At first thought it may appear as though $\sigma_k(\sigma_k+1)$ should enter in place of σ_k^2, as it so often does in quantum mechanics, but the square under consideration is one of a component rather than of the entire magnitude of a vector, and so can have the same value $\sigma_k^2\beta^2$ as in the old quantum theory. (In the hydrogen atom, for instance, the square of the z-component of angular momentum is $r^2h^2/4\pi^2$, not $r(r+1)h^2/4\pi^2$, where r is the magnetic quantum number.) That our value of the square is correct, can of course, also be verified by writing down the matrix elements[38] representing the x, y, z projections of this component, and then actually calculating the square.

Case (a). In (a) the component of spin angular momentum parallel to the axis of figure is $\sigma_s h/2\pi$, where σ_s is a half or whole integer according as the multiplicity is even or odd. A multiplet is generated by giving σ_s different

[37] F. Hund, Zeits. f. Physik, **36,** 657 (1926); **42,** 93 (1927).

[38] These matrix elements are those of the symmetrical top and have been given by Dennison (Phys. Rev. **28,** 318, 1926); Kronig and Rabi (Ibid. **29,** 262, 1927) and Rademacher and Reiche (Zeits. f. Physik, **41,** 453, 1927). They are, of course, the equivalent of the Hönl-London intensity formulas. In applying these matrices to our problem, it is, of course, necessary to determine the constant factors in accordance with a magnitude $\sigma_k h/2\pi$ parallel to the axis of figure, as in Condon's (Phys. Rev. **30,** 781, 1927) work on the Zeeman effect. This means, for instance, taking $a_j = b_j = 0$, $c_j = \sigma_k\beta$ in Dennison's paper.

values ranging from $-s$ to $+s$. As with atoms, the susceptibility will be different according as the intervals in such a multiplet are small or large relative to kT. In the former event the matrix elements of the spin moment vector will be entirely of the low frequency type, for the only motion of the spin vector relative to the figure axis is a precession about the axis of figure, whose frequency is identified with the multiplet intervals. Therefore there is no distinction between M_s^2 and μ_s^2, permitting us to calculate μ_s^2 from (20) and (21). Furthermore the statistical average of the product $\mathfrak{y}_s \cdot \mathfrak{y}_k$ is zero, for with narrow multiplets we may neglect the temperature factor, so that components in which the sign of σ_s is the same as or opposite to that of σ_k have the same weight. Thus by (13) and (22) the susceptibility now becomes neglecting the small term (15)

$$\chi = N[4s(s+1)+\sigma_k^2]\beta^2/3kT. \tag{27}$$

In the alternative event that the multiplet intervals in case (a) are large compared to kT, the quantum number σ_s assumes in the normal state only the one value which gives the lowest energy. The matrix elements representing the component of the spin moment vector perpendicular to the axis of figure belong to the "high frequency" type, for they represent transitions $\Delta\sigma_s = \pm 1$ to other multiplet components which must now be classed as excited states. Thus only the parallel component of the spin moment is effective, and so μ_s^2 is given by an expression $4\sigma_s^2\beta^2$ analogous to that for μ_k^2. Furthermore $\mathfrak{y}_s \cdot \mathfrak{y}_k = \mathfrak{y}_k \cdot \mathfrak{y}_s$ is now simply $2\sigma_k\sigma_s\beta^2$, and so we have

$$\chi = N(2\sigma_s+\sigma_k)^2\beta^2/3kT, \tag{28}$$

as is also obvious from the fact that now the low frequency part of M is the component $(2\sigma_s+\sigma_k)\beta$ parallel to the figure axis.

Case (b). In Hund's (b) coupling, the matrix elements of the spin moment are clearly all of the low frequency kind, for case (b) arises only when the spin multiplets are narrow compared to the spacing between the different rotational energy levels, and it has already been shown in part II, pp. 34 and 46–49, that the latter intervals can be considered small relative to kT. Further the statistical average of the product $\mathfrak{y}_s \cdot \mathfrak{y}_k$ is zero, as follows by the spectroscopic stability relation indicated in note 31 or as can also be seen by averaging the expression for this product in case (b) to be given by E. Hill and the writer in a later paper. Consequently the susceptibility is given by (27), the same formulas as for case (a) when in (a) the multiplets are small compared to kT. Formula (27) will likewise hold for types of coupling intermediate between (a) and (b), where the rotational and multiplet energy intervals are comparable, as (27) demands only that the spin moment contain no high frequency elements. This is just another example of the invariance of the susceptibility of the mode of quantization, so long as the magnitudes of frequencies relative to kT are unaltered. As a matter of fact, case (b) is most often encountered only when $\sigma_k = 0$, as usually a value of σ_k different from zero will give sufficient interaction between orbital and spin moment to yield the firmer coupling (a).[39]

[39] Cases, however, are known in which there is approximately (b) type coupling even with $\sigma_k = 1$. Cf. Mulliken, Phys. Rev. **30**, 785 (1927).

Paramagnetism of O_2. The two common paramagnetic gases are O_2 and NO. There is at present no definite spectroscopic evidence on the proper term assignment to the normal state of the oxygen molecule, so that all that can be done is to see what assignments will explain the observed magnetism. This is nicely accounted for by supposing the normal state of O_2 to be closely spaced ^3S levels, for substitution of the values $s=1$, $\sigma_k=0$ in (27) yields a volume susceptibility $.142\times10^{-6}$ at 20°C and 76 cm pressure. Bauer and Piccard's[40] experimental value is $.1434\times10^{-6}$, while Wills and Hector find[41] $.1447\times10^{-6}$. We have here applied the formula (27) appropriate to narrow multiplets which is, of course, legitimate on account of the weak interaction between the spin and the rest of the molecule in ^3S states. The odd multiplicity demanded by ^3S states is reasonable since O_2 contains an even number of molecules. Usually, to be sure, the singlets have lower energies than the triplets, and so the expectation for the normal state would be a diamagnetic ^1S term, but an unusual assignment is not surprising inasmuch as the paramagnetism of the oxygen molecule is itself extraordinary. It is, in fact, the only known paramagnetic molecule with an even number of electrons, whereas paramagnetism is the usual rule for molecules with an odd number of electrons.[42]

The suggestion of ^3S terms for the normal state of the oxygen molecule is by no means new, for Sommerfeld,[32] Stoner,[43] and others have called attention to the fact that its susceptibility is the same as that of an atom in a ^3S state. The same susceptibility is obtained whether we set $s=1$, $k=0$ in (23) or $s=1$, $\sigma_k=0$ in (27), for the atomic and molecular formulas (23) and (27) are the same for S states, and these only. However, there does not appear to have previously been any adequate theoretical justification as to why the atomic formula could apply to a non-monatomic molecule unless we supposed the electronic angular momentum so loosely oriented to the rest of the molecule that it is quantized relative to the direction of any applied magnetic field of ordinary magnitude, so that its component in this direction is an integral or half-integral multiple of $h/2\pi$, as in the atomic case. Such a supposition would be entirely incomprehensible if the electronic angular momentum were orbital in character, but after the advent of the spin electron it is known that electronic angular momentum in S states is due to internal spins of the electron, and is there so loosely coupled to the rest of the molecule that it is by no means impossible that a magnetic field might be strong enough to uncouple the spin axis from the rest of the molecule. The wide Zeeman separations found by Watson and Perkins[44] and others in the band spectra of certain metallic hydrides are strongly suggestive of this condition. If the width of the oxygen multiplets were known we could, of

[40] Bauer and Piccard, J. de Physique, **1**, 97 (1920).

[41] Wills and Hector, Phys. Rev. **23**, 209 (1924).

[42] N. W. Taylor, J. Amer. Chem. Soc. **48**, 854 (1926); Taylor and G. N. Lewis, Proc. Nat. Acad. **11**, 456 (1925).

[43] E. C. Stoner, Phil. Mag. **3**, 336 (1927); also "Magnetism and Atomic Structure."

[44] W. W. Watson and B. Perkins, Jr., Phys. Rev. **30**, 592 (1927) and references.

course, immediately determine how large a field would be required to produce a Paschen-Back effect on the quantization. Hund mentions that the multiplet intervals found by Fassbender[45] in the S states of N_2^+ are of the order .01 cm^{-1}. If the O_2 fine structure were of this magnitude a field of about 1,000 Gauss would be necessary, as the normal Lorentz Zeeman separation is $.472\times10^{-4}$ cm^{-1}. Such a field is lower than that used in most susceptibility measurements. The feature of the theory in the present paper, however, is that it shows that the susceptibility is the same whether there is coupling of Hund's type (b) or whether the field is strong enough to break down such coupling, and so the preceding speculations as to what field strength is required to produce a Paschen-Back effect are unnecessary.

Polyatomic molecules. When the molecule contains more than two atoms, there is in general no axis of figure about which any component of electronic angular momentum remains constant. Consequently we cannot at present assign any definite amount of orbital angular momentum to the low frequency category, and it is quite conceivable that there is so little symmetry in the forces on the electron that the orbital contribution is entirely of the ineffective, high frequency type. If this is the case, or if the molecule is in something corresponding to an S state, the energy of interaction of the spin axis with the rest of the molecule will presumably be small compared to kT, and then we will still have at least approximately $\mu_s^2=4s(s+1)\beta^2$. The susceptibility will then be $\chi=4Ns(s+1)\beta^2/3kT+N\alpha$. This accords nicely with the susceptibility $.0557\times10^{-6}$ found experimentally by Taylor[42] for ClO_2 at 20°C and 76 cm, for the value calculated from this formula if we set $s=\frac{1}{2}$ and neglect $N\alpha$ is $.0534\times10^{-6}$. The discrepancy is no greater than Taylor's estimate of the experimental error as about 5 per cent. The assumption $s=\frac{1}{2}$ means a doublet system, and is, of course, reasonable since ClO_2 contains an odd number of electrons. In contrast to ClO_2 the low susceptibility $.009\times10^{-6}$ observed by Soné[46] for the triatomic molecule NO_2 is not explained by assuming a formula like that for an S-term in a diatomic molecule. The low paramagnetism found for NO_2 as compared to most other paramagnetic gases including NO, suggests that sometimes, though not in ClO_2, the asymmetric structure of triatomic molecules causes rapid fluctuations even in the spin angular momentum, which make this considerably less effective than in diatomic molecules.

5. Paramagnetism of Nitric Oxide

Nitric oxide gas provides the most striking confirmation[47] of our entire theory, both because the NO band spectrum furnishes unambiguous term assignments, and because the doublet width is of such magnitude as to test quantitatively the finer points of the theory. Various attempts have been made to explain the susceptibility of NO on a quantum basis. The best

[45] M. Fassbender, Zeits. f. Physik, **30,** 73 (1924).

[46] T. Soné, Tohoku Univ. Sci. Reports, **11** (3), 139 (1922).

[47] A brief account of this part of the paper has been given by the writer in Nature, May 9, 1927; also presented at the Feb. 1927 meeting of the American Physical Society.

known of these is perhaps Pauli's early work,[48] now renounced by Pauli himself.[49] Sommerfeld[32] and Stoner[43] suggest the possibility that the normal states of NO are ^2S terms as this gives a susceptibility within about 15 per cent of the experimental value, a mediocre agreement. All these attempts lack adequate theoretical foundation both as regards the type of quantization and the assignment of term values, but this is only natural since both the Hund theory of molecular quantization and the quantum analysis of the NO spectrum are subsequent developments. The systematization of the NO band spectrum by Birge, Mulliken, Miss Guillery, and Jenkins, Barton, and Mulliken[50] has recently shown that the normal state of the NO molecule is a doublet P level. The doublet is "regular"; i.e., the P_1 component ($\sigma_s = -\frac{1}{2}$) has a lower energy than the $P_2(\sigma_s = +\frac{1}{2})$, but the spectroscopic data on this particular feature were not available when the writer made his susceptibility calculations which led him to conclude independently that the order was regular. Upper and lower limits to the susceptibility, corresponding to doublet widths very narrow and very wide relative to kT, can now immediately be obtained by substituting respectively $s=\frac{1}{2}$, $\sigma_k=1$ in (27) and $\sigma_s=-\frac{1}{2}$, $\sigma_k=1$ in (28). The upper limit would apply were the temperature so high as to give equal concentrations of molecules in the P_1 and P_2 states; it gives a Curie constant corresponding to two Bohr magnetons, and yields a volume susceptibility $.071\times10^{-6}$ at 20°C, 76 cm. The lower limit, on the other hand is zero, for in the lower or P_1 state, where all the molecules are concentrated at $T=0$, the components of spin and orbital moment parallel to the axis of figure are equal and opposite. The actual susceptibility observed by Bauer and Piccard[40] is $.0609\times10^{-6}$ and by Soné[46] is $.0610\times10^{-6}$, and so is much closer to the upper than the lower limit, but nevertheless intermediate between the two. The reason for this is not hard to discover, for the spectroscopists find that the doublet interval between the two P components is 120.9 cm^{-1}[51]. Now expressed in wave numbers, kT equals $.70T$, and so this interval is about $.6kT$ at ordinary temperatures. Consequently it is necessary to carry through a special calculation in which the energy intervals are allowed to be comparable with kT, thus introducing what we might call "medium frequency terms," which we have not admitted previously. The details of this computation are given below, but we will state

[48] W. Pauli, Jr., Phys. Zeits. **21,** 615 (1920).

[49] W. Pauli, Jr., Handbuch der Physik, Band **23,** p. 274.

[50] The interpretation of the normal states of *NO* as doublet P levels appears to have been reached more or less independently by Mulliken and by Birge (Nature, Feb. 27, 1926) in connection with Baldet's analysis of the comet-tail bands (Comptes Rendus, **180,** 820, 1925) which indicated the existence of doublets. The evidence for this view has, however, been greatly strengthened by the extensive recent measurements of Miss Guillery (Zeits. f. Physik, **42,** 121, 1927) and of Jenkins, Barton and Mulliken (Phys. Rev. **30,** 150, 1927) on the γ and β bands respectively of *NO*.

[51] We take the doublet interval as 120.9 cm^{-1} rather than the value 124.4 quoted by Jenkins, Mulliken, and Barton, as for our purposes it is better to use energy differences which are inclusive rather than exclusive of the term $-B\sigma^2$ representing the part of the rotational energy independent of j. It makes little difference which value is used, as (34) shows that the corresponding change in the effective number of Bohr magnetons is only $\frac{1}{2}$ percent.

in advance that it gives a susceptibility $.0600\times10^{-6}$ at 20°C, 76 cm, agreeing with the experimental value to within 1.5 per cent, or less than the experimental error. This removes the apparent contradiction between band spectrum theory and magnetism encountered by Stoner,[43] who to explain the susceptibility even proposed an electron orbit as freely oriented in the NO molecule as in an atom. The calculation shows that there is a very vital contribution to the susceptibility from the component of spin moment perpendicular to the axis of figure, for a doublet interval comparable with kT means that this component is partially effective, as it precesses about this axis with a frequency of the order kT/h. If one overlooked the perpendicular component (as the writer naively did when he first began the work) the computed susceptibility would be too small, even if the doublet were supposed "inverted" so that the state with the higher moment parallel to the axis of figure had the lower energy.

Details of calculation. We must now go back to section 3, part I, and modify the work to admit energy intervals comparable with kT. The absorption frequencies of NO are so high that we may neglect the contribution of the "high frequency" elements of the moment matrix which correspond to transitions in the electronic quantum numbers, and which represent the part of the orbital moment perpendicular to the figure axis. If at the same time we discard the small diamagnetic term, this is equivalent to omitting the part (15) of the susceptibility. We may thus drop the index n used in part I, and the elements in which we are interested may be characterized by a set of indices σjm, where j is the rotational quantum number of the molecule, m is the magnetic quantum number specifying the component of j parallel to the field, and σ is the quantum number $\sigma=\sigma_k+\sigma_s=1\pm\frac{1}{2}$ proportional to to the total angular momentum parallel to the axis of figure. Elements in which $\sigma\neq\sigma'$ will be of the "medium frequency" type, while those in which $\sigma=\sigma'$ but in which j may change will be of the low frequency catagory. The analysis on pp. 733–737 of part I including simplification of the low frequency elements, is now applicable if we substitute the index σ for n, (in other words introduce "medium" for "high frequency" terms), and provided we introduce the two following modifications: 1) the abbreviated notation $\mu(jm;j'm')$ can no longer be used for $M(\sigma jm;\sigma j'm')$ as there are two values of σ, and 2) the summation must include σ in addition to j,m, since there is an appreciable concentration of molecules in both the P_1 and P_2 states.[52] Thus Eq. (12) of

[52] The assumption at the top of p. 737, part I, that $\nu(\sigma jm;\sigma'j'm')$ can be replaced by a value $\nu(\sigma;\sigma')$ independent of j, m, however, calls for some comment, as it is not strictly valid. For one thing the values of j are different in the initial and final states but as j cannot change by more than one unit this does not cause difficulty as then the approximation is good if merely the rotational energy intervals rather than the rotational energies themselves be small compared to the doublet width (cf. note 26, part I). A more important fact is the circumstance that if spectral terms be represented by the customary formula $A+Bj(j+1)$, the constant B, which is inversely proportional to the apparent moment of inertia, has slightly different values in the P_1 and P_2 states. The theoretical reason is the rotational distortion of spin doublets (E. C. Kemble, Phys. Rev. **30**, 387, 1927). The data of Jenkins, Barton, and Mulliken shows that the difference of the B values is .049 cm^{-1}. By the classical equipartitution

part I now becomes

$$\chi=(B/3kT)\sum_{\sigma,j,m,j',m'}\left|M(\sigma jm\,;\,\sigma j'm')\right|^2 e^{-W(\sigma j)/kT} \qquad (29)$$
$$-\frac{2B}{3h}\sum_{\sigma,j,m,\sigma',j',m'(\sigma'\neq\sigma)}\frac{\left|M(\sigma jm\,;\,\sigma'j'm')\right|^2}{\nu(\sigma\,;\sigma')}e^{-W(\sigma j)/kT},$$

with the abbreviation (cf. Eq. 6, part I)

$$B=N\Big/\sum_{\sigma,j,m}e^{-W(\sigma j)/kT}. \qquad (30)$$

The summation over σ, of course, embraces only the two values 1/2 and 3/2.

Now elements of the form involved in the first line of (29) arise from the component of moment which is parallel to the axis of figure, while those in the second line are to be ascribed to represent the component which is perpendicular to this axis. This can be seen by inspection of the familiar matrix formulas for the symmetrical top, and is also obvious from the fact that changes in the value of σ are identified kinematically with precessions about the axis of figure, and so will appear in the perpendicular but not the parallel component. Hence we have

$$\sum_{j'm'}\left|M(\sigma jm\,;\,\sigma j'm')\right|^2=M_{par}{}^2=(\sigma_k+2\sigma_s)^2\beta^2=(1\pm1)^2\beta^2 \qquad (31)$$

since by the foregoing and by the rules for matrix multiplication the sum in (31) is the square of the component of combined orbital and spin moment parallel to the axis of figure. Similarly

$$\sum_{\sigma'j'm'(\sigma'\neq\sigma)}\left|M(\sigma jm\,;\,\sigma'j'm')\right|=M_{perp}{}^2=4(s+s^2-\sigma_s{}^2)\beta^2=2\beta^2, \qquad (32)$$

where $M_{\text{perp}}{}^2$ is the square of the component of purely spin moment perpendicular to the axis of figure, for we have already mentioned that the perpendicular orbital component is of the discarded, high frequency type. The value of $M_{\text{perp}}{}^2$ is that given in (32) since the square $4s(s+1)\beta^2$ of the total spin magnetic moment is equal to the sum of the squares of the perpendicular and parallel components, and since the square of the parallel spin component is $4\sigma_s{}^2\beta^2$. These results would not be true if any part of the spin moment were of the discarded, high frequency type, but actually the

theorem the average value of the rotational energy $Bj(j+1)$ is approximately kT. As B is about 1.7, the effect of the different B values is to make the average value of $\nu(3/2\ jm;\ \frac{1}{2}\ jm)$ exceed $\Delta\nu$ by about 5 percent. Eq. (33) shows that change of x in (34) by 5 percent alters the susceptibility only about 1 percent. This is, of course, only a crude estimate of the order of magnitude of the error. An accurate calculation would have to use the amplitudes inclusive of rotational distortion to be given by E. Hill and the writer in a later paper, rather than the ideal symmetrical top matrices. Such a computation would be laborious and give only a minor correction.

We may mention that at least the P_1 levels show the characteristic "σ-type doubling" or hyperfine structure of the band spectroscopists, but it seems clear that the effect of this on the susceptibility is negligible, as the width of this hyperfine structure is negligible, and as we showed in part I the susceptibility is invariant of the way degeneracy is removed.

motion of the spin axis is very closely that of a secular precession about the axis of figure without appreciable rapid nutations.

Now $\nu(\sigma;\sigma')$ equals $\Delta\nu$ if $\sigma=\frac{3}{2}$, $\sigma'=\frac{1}{2}$, while $\nu(\frac{1}{2};\frac{3}{2})$ equals $-\Delta\nu$ where $\Delta\nu$ is an abbreviation for the frequency difference 120.9 cm^{-1} of the two doublet components. Also we may set $W(\frac{3}{2}, j)=W(\frac{1}{2}, j)+h\Delta\nu$ as $\nu(\frac{3}{2}jm;\frac{1}{2}jm)$ is approximately $\Delta\nu$. Since furthermore the expressions (31) and (32) have values invariant of j, m, the sum $\sum_{j,m}e^{-W(1/2,j)/kT}$ is thus by (30) a common factor which can be cancelled from numerator and denominator of (29). Using these simplifications and substituting (30–32) in (29) we get the final formula

$$\chi=N\theta^2/3kT, \tag{33}$$

with

$$\theta^2=4\beta^2(1-e^{-x}+xe^{-x})/(x+xe^{-x}), \qquad x=h\Delta\nu/kT=173.2/T. \tag{34}$$

Deviations from Curie's law. Eq. (34) shows that θ will not be a constant independent of T as it would according to Curie's law. Because of the formal similarity of (33) with (13) we may term θ/β the apparent number of Bohr magnetons. The variation of this expression with T predicted by (34) is shown in the following table:

Apparent Bohr magneton number θ/β as a function of absolute temperature

T	0	50	100	175	250	293	350	500	1000	∞
θ/β	0	1.098	1.489	1.713	1.806	1.836	1.864	1.908	1.954	2.000

It is seen that at room temperatures the apparent number of Bohr magnetons varies but slightly with T, so that the departures from Curies Law are not great and so may be difficult to measure. The only reliable experimental data are Bauer and Piccard's[40] and Soné's[46] value 1.85 at $T=293$, which we have already quoted as agreeing well with the theory. Curie's law has been verified to be nearly applicable to oxygen even down to liquefaction,[53] which is not surprising since the multiplet structure in S states is exceedingly fine. If the susceptibility of NO had been measured over anything like the large temperature range that it has for 0_2 the departures from Curie's law should certainly come to light. It would be most interesting if experimental data could be obtained on this.

The writer wishes to thank Professor Kronig for correspondence on diamagnetism, and Professors Mulliken and Birge for data on the NO band spectrum.

DEPARTMENT OF PHYSICS,
UNIVERSITY OF MINNESOTA,
February 1, 1928.

[53] Onnes, "Atoms et Electrons" (Paris, 1923), p. 144.

LOW VOLTAGE ARCS IN IODINE

By H. F. Fruth

Abstract

Ionizing and radiating potentials in molecular and atomic iodine vapor.—Low voltage arcs in monatomic and molecular iodine vapor were investigated together with their spectra. From a study of the current-voltage curves it was concluded that 6.5 volts is the minimum radiating potential of the atom, 8.0 the ionizing potential of the atom, and 9.5 the ionizing potential of the molecule. Non-oscillating abnormal low voltage arcs were maintained down to 4.9 volts and oscillations were observed around 12 volts. With arc currents of about 2 amperes the filament current could be cut off and the arc sustained indefinitely at 30 volts or above.

Variation with potential of spectra of molecular and atomic iodine.—At 4.9 volts the spectrum contained only three lines, (λλ2062, 2535, 3135), the continuous band 3460, and several groups of bands. At slightly higher voltages arc lines appear and at 8 volts the strongest spark lines begin. These lines are succeeded by new ones at higher voltages, making it probable that the stripping of the atom is in progress. Peculiar behavior of the lines 2535 and 3135A was observed. Three continuous bands (at 4080, 4300 and 4800A) are present in molecular but disappear in atomic iodine. A band system lying between 2224 and 2050A was observed and two groups of four bands each were found at 2880, 2833, 2776, 2716A and 2480, 2379, 2290 and 2243A.

Introduction

THE connection between the critical potentials of an atom or a molecule and the terms of its spectrum makes the knowledge of the critical potentials of great value in the analysis of the spectrum or as a test of the correctness of such an analysis. One of the difficulties in the identification of the critical potentials of a substance is that of distinguishing between ionizing and radiating potentials. And in case the substance may exist as a vapor in various types of molecules, monatomic, diatomic, etc., it is of great importance to identify the critical potentials with the proper molecule. It is the purpose of this investigation to determine the critical potentials of iodine and to distinguish those of the diatomic molecule from those of the atom. Very little progress has been made in the analysis of the spectrum of the iodine atom and only one of the band systems of the iodine molecule has been extensively investigated. The determination and identification of the critical potentials of iodine will then be invaluable in the problems of the analyses of its line and band spectra.

The critical potentials of iodine that have been reported hitherto are given in Table I.

The agreement between the values reported by different observers is not good, and there is little certainty of the correctness of the interpretations of the critical potentials found. There is no spectroscopic confirmation of any of the critical potentials reported in the table.

TABLE I

Critical potentials of nitrogen. M refers to the molecule, A to the atom. R indicates radiating potential.

Volts	Method	Observers
9.89	Glow Discharge	A. Noyes[1]
10.1 ± .5M	Modified Lenard	Foote and Mohler[2]
2.34 ± .2MR	" "	" " "
8.0 A	" "	Smyth and Compton[3]
9.4 M	" "	" " "
6.8*	" "	" " "
8.5	Total Current	Found[4]
10.5	Photographic	Foote and Mohler[5]
10.25	Low Voltage Arc	Duffendack[6]
10.0 M	Lenard	Mackay[7]

* Ionizing potential of the fluorescing molecule.

A number of observers have attempted to obtain the line absorption spectrum of iodine in order to locate the first several members of the absorption series. E. J. Evans[8] as early as 1910 found that dissociated iodine vapor has no absorption in the visible spectrum. Angerer and Joos[9] observed no absorption lines in the region 6700 to 2400A though they heated the vapor to 1050°C. Zumstein and the writer, using the former's well-known method,[10] failed to obtain a single line in the region 5800 to 2200A. Fuchtbauer, Weibel, and Holm[11] have, however, recently reported several absorption lines, among them 2062A and 1877A which they suggest as possible first members of the absorption series. Compton and Turner[12] are of the opinion that 2062 is not a resonance line but that it has a final state (in emission) approximately 0.55 volt above the normal state. Turner[13] has recently obtained the spectrum of iodine in the Schuman region and reports some 66 lines. He gives reasons for believing that λ1782.9, having a radiating potential of 6.9 volts is the first resonance line. Among the 66 lines he finds 11 that have a wave number difference of approximately 7600 cm^{-1}. This corresponds to an energy difference of 0.94 volt, and he suggests that this is the separation of the two levels of the spectral term the lowest of which is the normal state. This separation is in fair agreement with the value of 0.9

[1] A. Noyes, Am. Chem. Soc. **45,** 337 (1923).
[2] Foote and Mohler, Phys. Rev. **15,** 321 (1920).
[3] Smyth and Compton, Phys. Rev. **16,** 501 (1920).
[4] Found, Phys. Rev. **16,** 41 (1920).
[5] Foote and Mohler, Phys. Rev. **21,** 382 (1923).
[6] Duffendack, Phys. Rev. **20,** 665 (1922).
[7] Mackay, Phys. Rev. **24,** 319 (1924).
[8] Evans, Astrophys. J. **32,** 1 (1910).
[9] Angerer and Joos, Ann. d. Physik **74,** 754 (1924).
[10] Zumstein, Phys. Rev. **25,** 523 (1925).
[11] Fuchtbauer, Weibel and Holm, Zeits. f. Physik **31,** 523 (1925).
[12] Compton and Turner, Phys. Rev. **25,** 791 (1925).
[13] Turner, Phys. Rev. **27,** 397 (1926).

volt calculated by Franck[14] by extrapolation from the frequency separation of the lowest term in neon.

Method

The method employed in the present investigation is a combination of those of the total current and of the low-voltage arc. The total current passing between an incandescent tungsten cathode and an appropriate anode was measured for increasing values of the difference of potential applied to the electrodes. It has been shown[15] that space-charge-limited currents through neutral gases with elastic impacts are proportional to the three-halves power of the applied potential difference. This condition may be expected to obtain in iodine vapor at voltages below the voltage at which ionization begins. Hence the voltage at which a deviation from this relationship between current and voltage was first observed was taken as a critical potential of iodine. The first marked deviation may ordinarily be expected when the applied potential difference reaches the ionizing potential of the gas. In monatomic gases, however, cumulative ionization becomes an important factor, and in such cases the deviation from the three-halves power law may be expected to occur at the minimum radiating potential.

The increase in current that is obtained after ionization occurs depends largely on the thermionic emission from the filament. When the filament is sufficiently hot, the increase in current becomes large enough so that an arc is said to strike. An arc can easily be made to strike and be maintained at the ionizing potential of a gas and under favorable conditions at the minimum radiating potential.[16] By this means the critical potentials determined by the total current method were checked and interpreted. Spectrograms of the low voltage arcs were also taken in order to get additional information of aid in the interpretation.

The critical potentials of the atom were separated from those of the molecule by operating on vapor in a heated chamber so as to effect a high degree of dissociation of the iodine into monatomic vapor in one case and on vapor in which the degree of dissociation was reduced to a minimum in the other case. It was found possible to maintain a sufficiently high degree of dissociation to cause the critical potentials of the diatomic molecule to be completely absent.

Apparatus

The experimental tube employed is shown schematically in the diagram Fig. 1. The tubes were of Pyrex or Corning G702P glass. There were two removable ground stoppers of Corning G702P glass, one containing four and the other three 100-mil tungsten lead-in-wires. The filaments, anodes and grids were fastened upon these leads by means of platinum clamps furnished

[14] Franck, Trans. Farad. Soc. **21,** 438 (1926). Dymond, Zeits. f. Physik **34,** 553 (1925). Langmuir, Phys. Rev. **2,** 450 (1913).

[15] Richardson & Bozzoni, Phil. Mag. **32,** 426 (1916).

[16] Compton and Mohler, Critical Potentials, Bull. Nat. Res. Council.

with platinum-iridium set screws. With these seven large leads available, various combinations could be made. Usually single or double 12-mil tungsten filaments were mounted at F_1. A tungsten or molybdenum box, A, about 1 cm on each edge was used as an anode. The box had a small slit in each side for spectroscopic observation. Immediately in front of the filaments, F_1, and fastened to the box was a sheet tungsten frame holding a platinum gauze, G. Inside the box and about 3 mm from the end were two pairs of 15-mil or 20-mil tungsten filaments, F_2. At times the gauze was omitted and the tube was used as a simple two electrode tube using the end of the box as an anode. On one side of the bulb was mounted a clear fused quartz window. The ground glass stoppers as well as the quartz windows were sealed with hard De Khotinsky cement which was kept cool by means of complete rings made of lead and brass tubing through which water flowed.

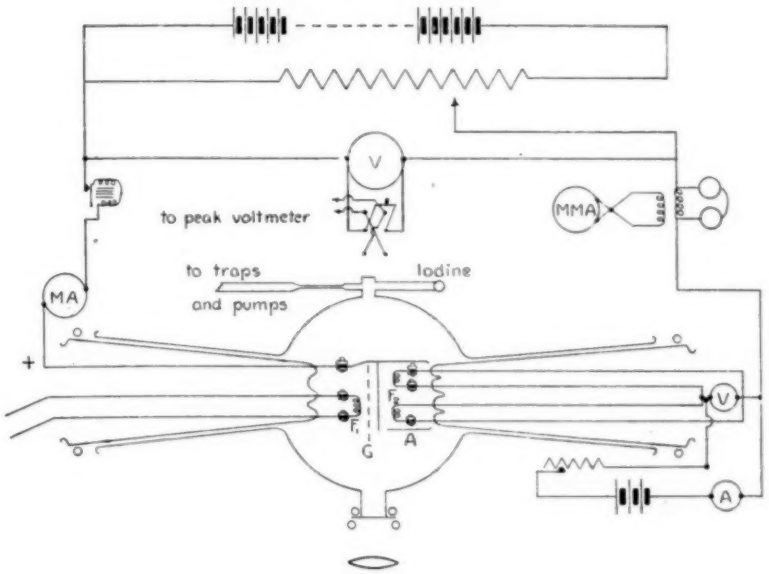

Fig. 1. Diagram of apparatus and electrical connections.

This arrangement allowed rather complete baking and outgassing of the tube and metallic parts. The usual baking was accomplished by means of an electrically heated oven. The filaments were glowed simultaneously, the outside filaments heating the gauze and the inside filaments heating the box to a yellow heat. After a vacuum of 10^{-4} mm or better was obtained, an arc was struck either in nitrogen or iodine or both to the inside and the outside of the box to heat and further outgas the metals.

In the early experiments iodine was introduced into the tube by means of a glass capsule that had previously been evacuated and filled with iodine. After the baking and the outgassing was completed these capsules were cracked open by electrically heating a tungsten wire by means of which the capsules were suspended from the leads. This method, at first suc-

cessful, finally proved a failure. In the flowing process these capsules would sometimes explode and break the entire experimental tube. A side tube containing a large quantity of iodine was later attached. An ice bath was kept on this tube during the baking and glowing process, after which the iodine could be driven into the experimental tube by applying heat. The iodine tube was then heated to drive off absorbed gases. A bath of the desired temperature was then placed on the iodine tube and the iodine was driven back by the baking oven. Two large liquid air traps were placed between the tube and the pumps. A capillary at *C* prevented a too rapid diffusion of iodine into the liquid air traps and gave the desired vapor pressure of iodine in the experimental tube, all parts of which together with connecting tube and windows were kept hotter than the bath on the iodine. Vapor pressures were determined from the curve of Baxter and Grose.[17]

The arrangement was adaptable to both molecular and atomic investigations. When molecular data were desired the outside filaments were used either alone or in connection with a gauze. The gauze as well as the large area of the box anode served to radiate and conduct away much of the heat, thus keeping down the degree of dissociation in the impact region. The gauze also prevented dissociated iodine near the filament from diffusing into the force field between the gauze and the plate.

When investigating atomic iodine the inner filaments were employed. The outer filaments were also glowed to give additional heat and to make up heat losses on that side of the box. With this arrangement no difficulty was experienced in maintaining a high degree of dissociation inside of the box as will be seen later from the results obtained.

The apparatus described above was the final equipment used in obtaining all the results reported in this paper. Preliminary runs were taken with other tubes containing metals other than tungsten, molybdenum and platinum. Very pure and well cleaned iron, copper and nickel were tried and anomalous results were obtained. Iodine attacks these metals forming polarizing, insulating or conducting layers. Some of these layers vaporize readily. At one instance a layer of a dark rubber-like compound covered a nickel anode so completely that only a small plate current could be drawn. After long heating of the filaments, the layer pealed off and touched the filaments. Its resistance was measured and found very high. Some of the discrepancies among the critical potential values obtained by former experimenters can possibly be accounted for by impurities in the tubes caused by the use of metals attacked by iodine. In the final tube only tungsten and platinum, and at times, molybdenum were used. If great care was taken as to cleanliness of the inside of the tube, these metals were left quite unaffected by the action of the arc. In the region near the arc the tungsten came out clean and white, though molybdenum and platinum suffered a slight discoloration. Molybdenum caused a slight brown discoloration of the inside of the tube after continuous runs aggregating up to 90 hours for one "loading" of the tube.

[17] Baxter and Grose, J. Amer. Chem. Soc. **37**, 1061 (1915).

The electrical connections are schematically given in Fig. 1. The potential difference applied to the electrodes was obtained from high capacity storage batteries and was applied to the box and the negative end of the filaments. Its value could be varied by controlling rheostats. This potential difference was corrected to that which obtained between the middle of the filament and the plate by subtracting from the reading of the voltmeter half of the potential drop across the filament. This has been found to be an adequate total correction to reduce voltages read on the voltmeter to the true average accelerating potential of the electrons in low voltage arcs.[18] The plate current was read by means of a Cambridge and Paul unipivotal instrument. A low resistance radio-frequency transformer was also placed in the plate circuit. The secondary was connected to a sensitive thermocross which in turn was connected to a micrometer. This device was a very sensitive detector of oscillations. When oscillations were observed, their peak and minimum voltages were measured by means of a peak voltmeter.

Results

Determination of ionizing potential of molecular iodine. After the tube had been thoroughly baked out and the metallic parts outgassed, iodine was allowed to enter the tube to any desired vapor pressure. The pumps were kept going to sweep out impurities that might accumulate during a discharge. The anode voltage was varied through a series of steps and the corresponding plate currents recorded. A large numbers of such runs were taken using various numbers and sizes of filaments and various distances and arrangements of filaments, gauze and plate. Some resulting current-voltage curves are given in Fig. 2. These curves are typical of a large number taken under conditions of low dissociation. The filament temperature was kept as low as possible and in several instances iodine vapor was made to flow through the discharge region. While these curves show no sharp arcs, they indicate an ionizing potential of the molecule between 9 and 10 volts. The location of the breaks in the curves was fairly independent of pressure over the range from 0.1 to 1.5 mm, though the breaks seem to be sharper at the lower pressures. The average potential of the breaks in the curves, corrected for fall of potential along the filament and initial velocity of emission of the electrons, was 9.25 ± 0.2 volts. The curves with decreasing voltage always repeated the increasing voltage curves within the experimental error except when an arc was made to strike at voltages above the ionizing potential of the molecule, in which case the arc broke at about 8 volts. In such cases the discharge caused an appreciable amount of dissociation so that the arc could be maintained as low as the ionizing potential of the atom. Most of the curves show a slight amount of ionization near 8 volts even when the current is quite small. Long and careful exposure by means of a small Hilger spectrograph either showed no lines at all or only faint traces of lines and a few bands at about 8 volts, but slightly above 9 volts more band spectra were photographed.

[18] Duffendack and Fox, Astrophys. Jour., **65**, 214 (1927).

Arcs in atomic iodine. In studying the critical potentials of the iodine atom, the filaments inside of the box were used as a source of heat to dissociate the iodine as well as a source of electrons. Four 15-mil or 20-mil tungsten filaments carrying total currents from 40 to 75 amperes were used in most of the runs. The box was heated to yellow heat estimated at about 750°C.

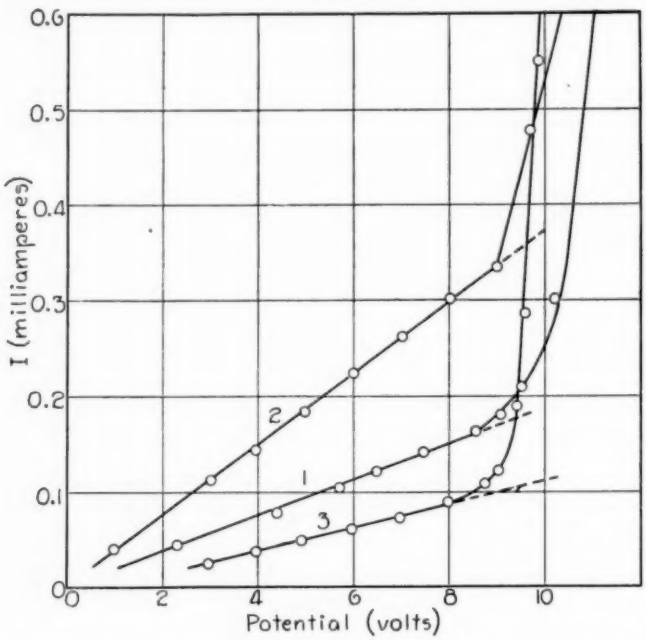

Fig. 2. Current-potential curves in iodine vapor in which there is little dissociation. Curve 1, pressure 0.5mm, I scale×1; curve 2, pressure 0.15 mm, I scale×1; curve 3, pressure 1.5 mm, I scale×2, vapor flowing.

Calculations upon the basis of the work of Stark and Bodenstein[19] on the thermal dissociation of iodine vapor show that iodine is completely dissociated at a temperature of 1200°C at pressures up to 5 mm. The percent of dissociation at 727°C at various pressures covering the range employed in this work are given in Table II.

TABLE II

Dissociation at various pressures of iodine vapor at 727°C.

Pressure	Percent	Pressure	Percent	Pressure	Percent
0.113 mm.	95.	0.699 mm.	81.	2.15 mm.	63.5
.305 mm.	89.5	1.02 mm.	75.5	3.08 mm.	57.
.469 mm.	85.	1.49 mm.	69.		

Thus the dissociation of the iodine vapor near the filaments was always complete and that near the inner surface of the box anode large.

[19] Stark and Bodenstein, Zeits. f. Electrochemie, **16**, 966 (1910).

By setting the applied potential or the filament resistance very critically, an oscillating arc could often be obtained. At one time the arc potentials varied between 17 and 26 volts while the plate current varied from 0.7 to 0.86 ampere respectively. At another time the arc oscillated at a frequency of about 900 cycles, as estimated from the pitch heard in the phones placed across the primary of the radio frequency transformer as shown in the diagram Fig. 1. At the same time the micrometer placed across the thermocross read 60 microamperes. The direct arc current was 0.5 amperes and the voltmeter connected across the arc read 11.8 volts. The peak voltmeter showed a difference of about 4 volts between the peak and the minimum. A third example might be of interest. Using the filaments outside of the box and a vapor pressure of 1.60 mm, the arc oscillated at a frequency of about 200 cycles, 2.5 volts above and below the D.C. voltmeter reading of 12.5 volts. The plate current, as read on a D.C. ammeter, was 0.6 ampere.

The above cases of oscillations are typical of many other instances. In no case were radio-frequency oscillations detected and in no case was there any evidence of oscillations when the arc was maintained below 11.8 volts. In a number of instances when oscillations were detected the attempt was made to lower the voltage so as to obtain the so-called oscillating abnormal low voltage arc. It was thought that by obtaining such an arc at lower and lower voltages and measuring its peak at the lowest voltage obtainable one could get an indication of the minimum radiating potential, for it has hitherto been thought that the upper peak is always at or above this potential. Any attempt to lower the voltage by decreasing the applied voltage or increasing the plate current in such oscillating arcs failed. The arc would either break or stop oscillating.

When the oscillations of the arc stopped in the manner described above, the voltage could be brought down considerably so that a non-oscillatory abnormal low voltage similar to those described by Compton and Eckart[20] was obtained. This could also be obtained from an ordinary arc by lowering the applied voltage by decreasing the resistance in series with the arc or by increasing the current through the arc by raising the filament temperature. Such arcs were maintained at voltages ranging from 6.5 volts to 4.9 volts with currents ranging from 0.5 to 2 amperes. In all cases the plate current was large and the conditions such that the dissociation was of a high degree.

Under certain conditions the current would go up enormously when an attempt was made to raise the voltage beyond a certain value. A circuit breaker that would open and close the plate circuit at a given current was inserted in the plate circuit. An arc was then struck and the voltage raised. To prevent too large currents the filament current was reduced. When the potential reached 60 volts, the filament current was zero. Thus the arc became self-sustained. It was possible to hold this self-sustained arc at a potential as low as 30 volts. The filaments were heated by positive ion bombardment, and they together with the arc current heated the box anode to a

[20] Compton and Eckart, Phys. Rev. **25**, 139 (1925).

bright red. The plate current as read on a D.C. ammeter was steady at times and pulsating at other times and ranged from 2 to 4 amperes. This arc could be maintained for long periods permitting its spectra to be photographed with a spectrograph of large dispersion.

Ionizing and radiating potential of the iodine atom. Of the thirty runs that were made with the box anode at 727°C and the vapor more than 57 percent dissociated, twenty-five showed ionization setting in at 6.5 volts and all showed a large increase of current between 8 and 9 volts. Fig. 3 illustrates the manner in which ionization set in. The first change in slope at 6.5 volts points to a minimum radiating potential and the larger and more persistent change between 8 and 8.5 volts to an ionizing potential. The $I-V$ curves

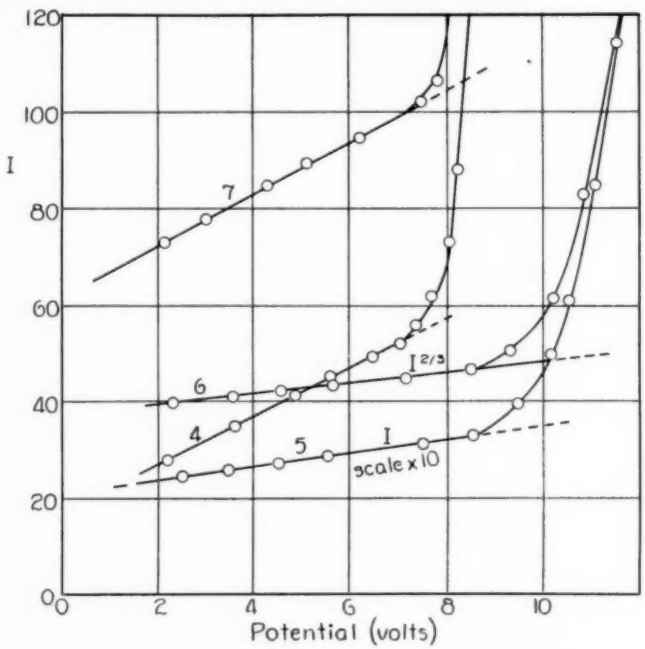

Fig. 3. Current-potential curves for iodine vapor which is more than 57 percent dissociated. Curve 4, pressure 3 mm, I scale×1; curve 5, pressure 2.7 mm, I scale×10; curve 6, pressure 2.7 mm, I scale×1; curve 7 pressure 15 mm, I scale×1.

seem to be linear up to 6.5 volts. This linearity is, however, only apparent, for by plotting them on a more sensitive scale, they have considerable curvatures. In order to test the three-halves power law for space-charge-limited currents through gases when the electrons make elastic impacts, the two-thirds power of the current was plotted against the voltage. Fourteen of these runs covering a wide range of conditions were plotted this way. It was found that a linear relation in these curves existed up to 6.5 volts. The break in the $I^{2/3}-V$ curve occurs between 6.5 and 9.5 volts depending upon condition. Under conditions at which a high degree of dissociation existed, i.e., high temperature or low pressures, the break invariably occurs between 6 and 7 but, not lower, indicating the beginning of inelastic impacts and

ionization by cumulative action. Upon changing conditions so that there is a lesser degree of dissociation, the point where the departure from linearity occurs moves to higher voltages.

A second break occurs at 8.3 volts as seen in Curve 9 Fig. 4. The 8.3 break generally persists in cases where the iodine is largely molecular because dissociation could not be completely prevented. Curve 9 of Figure 4 shows the three effects in one run. The first departure from the straight line occurs

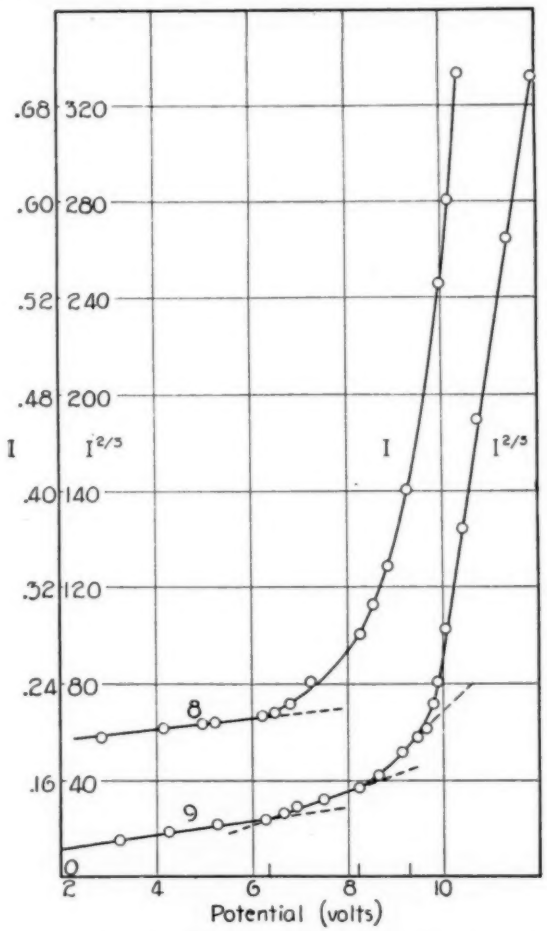

Fig. 4. Current-potential curves for iodine vapor which is largely dissociated, pressure 1.25 mm.

at 6.5 volts, a second break is seen at 8.3 and a third one at 9.5. This, supported by the numerous occurrences of these breaks in many of the other atomic and molecular curves, seems to place the minimum radiating potential of the atom at $6.5 \pm .2$ volts, the ionizing potential of the atom at $8.3 \pm .2$ volts and the ionizing potential of the molecule at $9.4 \pm .2$ volts.

In a recent paper Dymond[21] reports on an investigation of the fluorescence of iodine vapor. He finds that fluorescence can be stimulated by mono-

[21] Dymond, Zeits. f. Physik **34**, 553 (1925).

chromatic light of wave-lengths from λ6438 to λ4995 and that the bands emitted by the fluorescing vapor are of maximum intensity at the wave-length of the stimulating light. The short wave-length limit λ4995 is approximately the long wave-length limit of the continuous absorption band of iodine in this region. Dymond concluded that light of wave-length shorter than λ4995 is absorbed, and, as a consequence, the molecule is dissociated into a neutral and an excited atom: $I_2 \rightarrow I + I_1'$. The heat of dissociation of iodine into neutral atoms, $I_2 \rightarrow I + I$, is 1.4 equivalent volts whereas light of wave-length 4995A corresponds to 2.5 volts. It is suggested that the excited iodine atom absorbs the 1.1. volts excess energy. This would be possible only in case the atom has an energy level 1.1 volt above its normal state, and there is some evidence[13] that this is the case. In view of this, Dymond suggests that the 6.8 volt critical potential reported by Smyth and Compton[3] as the ionizing potential of the fluorescing molecule might be the ionizing potential of an excited atom possessing 1.1 volt potential energy. The sum of these two is 7.9 volts or nearly the ionizing potential reported for the atom.

In the experiments which form the basis of this report, it is certain that a high degree of dissociation of iodine in the region of electron impacts obtained in cases when the box anode was used, and considerable dissociation occurred in all other cases. It would seem more probable that the 6.5 volt potential is a radiating potential of the atom, revealed by ionization by cumulative action and that it depends upon dissociation of a molecule into a neutral and an excited atom and a subsequent ionization of the excited atom. There is at least a strong possibility that the 6.8 volt potential is the same as the 6.5 volt potential determined from these experiments. As yet the analysis of the iodine spectrum has not proceeded far enough to get spectroscopic confirmation of this interpretation, but Turner[13] has expressed the opinion that λ1782.9 is the first resonance line and if so it has a radiating potential of 6.92 volts.

The modern theory of atomic spectra[16] leads one to expect the lowest term in the spectrum of the iodine atom to be a $^2P_{1,2}$ term with the $^2P_2$ as the lowest level and hence the term corresponding to the normal state of the atom. In the light of Turner's[13] investigations the separation of the doublet term is 0.94 equivalent volts. The lines 2062.1 and 1782.9, on this view, originate in a common term, ^2S, and have the excitation potential of 6.92 volts. Since atoms in the $^2P_1$ state may be present in concentration approximating that of atoms in the normal $^2P_2$ state due to the high temperature maintained in the box anode and to the mechanism of ionization, one should expect to find evidences of ionization at 6 volts (6.92 − 0.94) due to cumulative action on the metastable atoms. As has been mentioned previously, the "break" in the curves at about 6.5 volts was not sharp but occurred between 6 and 7 volts. A critical examination of the curves shows that the break never begins below 6 volts. It is probable, therefore, that cumulative ionization of both normal atoms, $^2P_2$, and metastable atoms, $^2P_1$, is setting in between 6 and 7 volts and that the two "breaks" were not separated. The critical potential thus determined, 6.5 volts, is the mean of the 6.0 and 6.9

voltages necessary to ionize the iodine atoms by cumulative action. The process of ionization suggested by Dymond[21] would lead to a value of the ionizing potential of $6.92+0.94=7.86$ volts which is less than any yet reported. Ionization by this process probably occurs in electric discharges through iodine and according to the results of this investigation should require $8.3-0.9=7.4$ volts. This would still further emphasize the rounded character of the "break" at 6.5 volts. The values of the ionizing potentials of the atom and of the molecule, determined by this investigation are in agreement with those of Smyth and Compton.

It was explained in the introduction that very large increases in current might be expected as soon as positive ions are formed. This is in practice seldom realized. The curves instead of having sharp breaks at the critical potentials are rounded. This is due to the distribution of initial velocities of the electrons which has been shown both theoretically and experimentally to be Maxwellian. Another factor entering in here is the distribution of the probabilities of ionization by an electron of sufficient energy. The probability that an electron should ionize an atom or molecule rises from a very small value for an electron with just enough energy to a very large value for an electron of a large excess of energy.[22]

Not even in cases of the striking of an arc are the increases of current as large as might be expected from the theory of space charge neutralization by positive ions. A thousand fold increase at the striking of an arc was hard to obtain even if two to three thousand fold increases are theoretically possible in iodine. This might be explained from a consideration of the conditions in the space between the hot cathode and the anode before the striking of the arc. Immediately surrounding the cathode is a dense electron atmosphere which becomes less dense nearer the anode. Suppose the applied potential difference is above the ionizing potential. Nearly the entire fall of potential is very near the anode. Hence by far the greatest potential gradient is at this place. Only the electrons falling through this potential gradient will have enough energy for ionization. Positive ions are thus formed only near the anode where the electron density is the least. Thus a positive iodine atom will not neutralize its full quota of 1936 electrons and may become neutralized immediately as it passes out of the space of greatest potential gradient and thus pass as a neutral atom into the electron atmosphere where the electron velocity is insufficient for ionization. Since iodine has a very large electron affinity, this atom may even pick up an electron and thus form a negative ion whose size and mobility is the same as that of the positive ion and whose effective space charge is that of 1936 electrons. Moreover, the distance near the anode where the potential gradient is a minimum through which an electron must pass in order to acquire sufficient energy to ionize, might be smaller than the mean free path of the electrons in the iodine vapor at the given pressure, thus making it possible for many electrons to pass through this region without encountering an iodine atom.

[22] K. T. Compton, Phys. Rev. **20**, 283 (1922).

One should thus be able to increase the sharpness of the breaks of the *I-V* curves taken with the same geometric arrangement of filament and plate and the same filament heat by increasing the vapor pressure through a certain range. This was found to be the case for three different sets of filaments and plates and a variety of filament heats. The pressures ranged from 0.15 to 1.5 mm. The maximum sharpness was obtained at about 0.6 mm. The above explanation seems to account for the difficulty of making the arc strike at the minimum radiating potential or even at the ionizing potential. It also accounts for the gradual change of slope of the curves as the applied potential difference is raised through the critical potentials. Gases and vapors in which the electron impacts below the first critical potential are more completely elastic and those which do not have a strong electron affinity yield much sharper breaks in similar *I-V* curves.

Spectroscopic observations. Although it was not the main object of this investigation to obtain and analyze the various spectra of iodine, nevertheless, it seemed advisable to photograph the arcs in iodine under various conditions in order to get additional clues that might help to interpret the critical potentials. A large number of plates were taken and a number of characteristic plates were measured. Since the accuracy of the measurements as taken from dispersion curves was not better than ± 1A, only a few characteristic lines and bands as well as certain general conclusions are reported in this work.

In general a strong line spectrum was obtained whenever conditions were such as to cause a high percentage of dissociation, bands appearing whenever the degree of dissociation was less.

At 4.9 volts, the lowest voltage at which the arc was ever maintained, only three measurable lines and some bands appeared. These lines were 2062A, 2535, 3135 of intensities, 10, 8 and 1 respectively. The arc current in the above low voltage arcs was 1.6 amperes or more and no additional lines appeared when this current or the length of exposure was increased. Upon raising the voltage across the arc, three lines between 3135 and 3200 appeared definitely. The line 2062 remained strong at all voltages but weakened when the voltage was raised above 50 volts. Line 2535 probably 2534.4 discussed by Cario and Oldenberg[23] increased in intensity up to 10 volts and then began to decrease. At 20 volts a companion appeared at 2532. At 23 volts 2532 was by far the stronger of the two lines and at 28 volts, both lines had definitely disappeared.

As the voltage and the current of the arcs were changed, the spectrum of iodine underwent many changes. It was altered from the five line spectrum at 4.9 volts to one of many hundreds of lines at about 40 volts or above. These changes are not only in number of lines, but there are also very marked changes in the relative intensities of the lines. At about 6 volts a few of the "arc" lines and some of the strongest "spark" lines reported and classified by Wood and Kimura[24] were identified. At 7 volts more spark lines showed

[23] Cario and Oldenberg, Zeits. f. Physik **31**, 12, 914 (1925).
[24] Wood and Kimura, Astrophys. **46**, 181 (1917).

up and relatively fewer arc lines. At 8 and 9 volts only some of the strongest spark lines and three of the strongest arc lines were observed. Thus through the successive stages the arc lines disappeared or grew fainter while new spark lines appeared. Some spark lines that showed up at lower voltages either vanished or remained as faint lines at higher voltages. Thus at 40 volts relatively few of the strongest arc lines reported by other observers remained while a large number of new lines not reported in the literature made their appearance. We have thus strong evidence of successive stripping of the atom by electronic bombardment.

A large number of observers have reported line and band spectra of iodine. These spectra contain a large number of lines and differ a great deal amongst each other both in number of lines and in intensity distribution of the lines. The explanation for this variance probably lies in that these spectra were all due to high voltage excitation and probably differed greatly from each other in voltage and other conditions. The spectrograms show qualitatively the development of the iodine spectrum in the region from 5300A to 2050A. They show clearly that the method of low voltage arcs would offer a powerful method in the study of the development of the iodine spectrum.

Unless conditions in the discharge tube were such as to favor a high degree of dissociation, the line spectra were always accompanied by band spectra, both emission and absorption. The bands in the red end of the visible spectrum classified by R. Mecke[25] were observed in absorption and in emission. Bands similar in general appearance were photographed farther into the violet. These will be discussed later.

At voltages somewhat below 20 volts or at higher voltages and currents below 0.5 ampere, four band groups were photographed with a small Hilger spectrograph whose dispersion was not enough to show details of fine structure. Group I consists of three narrow somewhat diffuse bands which cross the faint extension of the so-called electron affinity continuous band whose red end is at about 3460A. Their maxima are at about 3265, 3242, 3215. These bands are equally shaded on both sides. These are probably the same as some of the 44 bands reported by Oldenberg.[26] Group II contains four bands at 2880, 2833, 2776, 2716. These have a fairly sharp red edge at about 25A, 25A, 25A and 50A wide respectively. Group III has four members whose red limits are 2480, 2380, 2290 and 2240 of which 2480 is by far the most distinct and the widest. The other members rapidly become fainter, narrower and more diffuse. Overlapping this region, i.e., from 2567 to 2230 a great deal of fine structure (lines about 3.5A apart) is seen.

The fourth group is by far the largest and most interesting. It consists of twenty narrow equally spaced bands. This group likely extends farther into the ultra-violet as the last band at 2052.5 is very near the violet end of the spectrograph employed. Microphotometer traces show that these bands

[25] Mecke, Zeits. f. Physik **7**, 73 (1921); Ann. d. Physik **71**, 104 (1923).
[26] Oldenberg, Zeitz. f. Physik **25**, 136 (1924).

have a fairly sharp edge towards the red end and that they all have nearly the same structure. They appeared in molecular iodine at low voltages, up to 16 volts, and with plate currents below .5 ampere. Their wave-lengths are as follows: 2052.5, 2062, 2071, 2080.5, 2089.5, 2098, 2107, 2116, 2125, 2133.5, 2142.5, 2151, 2160, 2169.5, 2178, 2188, 2198, 2206, 2215, 2224.

Continuous bands. A number of observers, principally Wood,[27] Steubing,[28] Oldenberg,[26] Gerlach and Gröman[29] have reported continuous bands in the spectrum of iodine. Such bands have been observed at λ5100, 4800 and 3460A. The continuous bands might be formed by an electron attaching itself to a neutral atom. Both the atom and the electron may have kinetic energy. The frequency of the long wave length limit of the continuous spectrum corresponds to the difference of the energy between a neutral atom plus an electron and the negative ion, i.e., the electron affinity of the atom. This entrance of the electron with a definite kinetic energy will be accompanied by the emission of energy equal to the electron affinity plus the kinetic energy of the electron, and, since the latter may have all possible values, the spectrum will be continuous. The band at 5100 was found by Oldenberg[25] only in mixtures of hydrogen and iodine. Gerlach[29] and Groman regard the band at λ3460 as due to the electron affinity of the atom and suggest that λ4800 may be due to the electron affinity of the molecule because the former grows stronger while the latter grows weaker as the molecular band spectrum yields to the atomic line spectrum. Oldenberg, however, regards the 3460 continuous band as a recombination spectrum. Thus $I^- + I^+ \rightarrow I_2 + 5.8$ volts. The energy of 5.8 volts is more than sufficient for the emission of the band at 3460 which needs but 3.6 volts. He suggests that the excess energy is used in emitting the diffused bands into which part of this band breaks up when the pressure of another gas, (e.g. nitrogen) is raised. He also suggests that the continuous band at 4800 might arise from a transformation of the excited molecule.

It seems certain from this investigation that the band at λ3460 is due to the atom. There is nothing in its manner of appearance in the arc which is contradictory to the proposal that it is the electron affinity spectrum of the iodine atom. It also seems certain that the other continuous bands observed are connected with the iodine molecule. Further spectroscopic observations on these continuous bands are highly desirable.

In conclusion the writer expresses his sincere gratitude to Professor O. S. Duffendack at whose suggestion and under whose direction this investigation was conducted at the University of Michigan during the years 1924 and 1925. The writer wishes further to acknowledge his indebtedness to Professor H. M. Randall for interest in the work and for obtaining the necessary means for conducting this research.

DEPARTMENT OF PHYSICS,
UNIVERSITY OF MICHIGAN,
September 23, 1927.

[27] Wood, Researches in Phys. Optics, Part II, p. 51, 1919.
[28] Steubing, Ann. d. Physik **64,** 673 (1921); Zeits. f. Physik **32,** 159 (1925).
[29] Gerlach and Groman, Zeits. f. Physik **18,** 239 (1923).

THE REFLECTION OF POSITIVE RAYS BY A PLATINUM SURFACE

By George E. Read

Abstract

Intensity, energy and directional distribution of Li^+ and K^+ ions reflected from platinum.—In studying the reflections of positive rays by a platinum surface an apparatus similar to a spectrometer was set up in a good vacuum. A beam of lithium ions accelerated through a known *P. D.* impinged upon a platinum reflector. The intensity, energy and direction of the reflected beam were measured by means of a rotating collector. Providing the reflector were "clean," i.e. white hot or cold but a few seconds, a considerable reflection was observed at certain angles. The angle of reflection was approximately specular but varied slightly with the accelerating voltage. The percentage reflected depended markedly upon the accelerating voltage. The maximum occurred approximately at 48 volts where approximately 75 percent were reflected. The reflected beam consisted of ions which had lost the major portion of their energy. Using a beam of potassium positive rays, approximately the same type of results was obtained.

THE reflection of positive rays from a metallic surface has hitherto been studied mainly in connection with the problem of the production of secondary electrons. Of the more recent work Klein[1] deduced from observations that a large number of slowly moving positive rays were reflected. Jackson[2] was unable to repeat these observations and attributed the results of Klein to the geometrical and electrical arrangement of the apparatus and not to the reflection of any considerable portion of the incident positive rays. The experiments described in this paper were undertaken to determine the relative amount reflected under various experimental conditions and especially to investigate the distribution in angle of the reflected rays.

The experimental arrangement is shown in Fig. 1. The apparatus resembles a spectrometer with fixed collimator and reflector and a rotating collector. The source S was a layer of spodumene on a platinum strip which could be heated electrically. According to Hundley[3] the emission from spodumene ($Li_2O \cdot Al_2O_3 4SiO_2$) at a dull red temperature consists almost entirely of the heavier lithium isotope. The ions could be accelerated through a known potential difference applied between the anode and the cathode about one cm above it by means of the potentiometer arrangement shown. The portion of the beam that passed through the slit in the cathode entered the main portion of the tube which was shielded by the gauze G and impinged upon the reflector R. The reflector consisted of a platinum strip $1 \times 2 \times 0.001$ cm. It was supported by current leads which were insulated from the cathode and which served to raise the reflector to a white hot temperature.

[1] Klein, Phys. Rev. **26**, 800 (1925).
[2] Jackson, Phys. Rev. **28**, 524 (1926); **30**, 473 (1927).
[3] Hundley, Phys. Rev. **30**, 864 (1927).

The collector C consisted of two thin nickel strips insulated from each other. The inner one served as a guard allowing only a narrow beam of rays to reach the outer. It was found that the angular dimensions of the initial beam of positive rays were so large that the two strips could be connected together and used as a single collecting electrode with no appreciable loss of resolution. Because of this and the very considerable gain in intensity, the second arrangement was used almost entirely. The collector could be rotated through an angle of 320° by means of the ground joint shown. The current to the collector was measured by means of a string electrometer and compensating ionization chamber similar to that used by Dempster.[4]

At the beginning of a series of observations the collector was turned so as completely to cover the slit in the cathode; this position corresponding to the angle 0°. The current to the rear of the collector was taken as the measure of the number of positive ions impinging on the reflector. A number

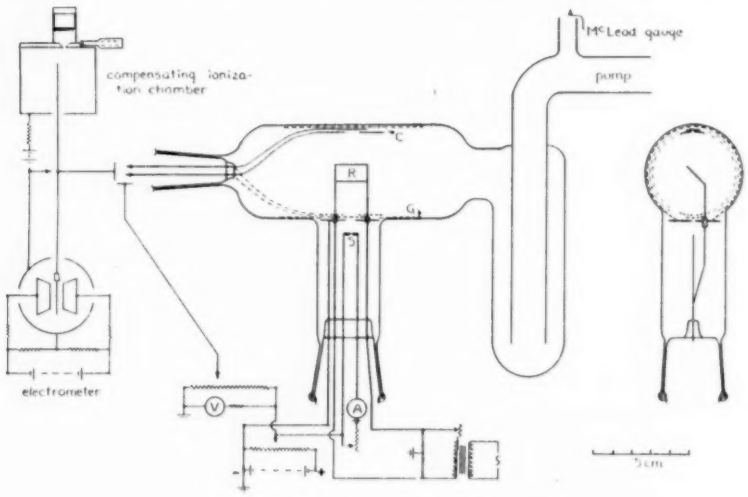

Fig. 1. Experimental arrangement.

of readings was then taken with the collector at known angles. In these cases the current to the front of the collector was taken as a measure of the number of reflected ions. Usually one or more extra readings were taken at zero to check the constancy of the source even though there was little change.

The tube containing the apparatus was directly connected to a liquid air trap as shown. This was done in an attempt to get rid of the vapors from the two ground-glass joints. As is customary, the wax did not extend the full length of either seal. The line to the pump consisted of tubing of at least 20 mm outside diameter. The pumping system was made up of two mercury diffusion pumps with an oil backing pump.

It was found that the fraction of the positive rays reflected depended very markedly on the condition of the reflector. If the reflector were white hot, a considerable reflection was observed at certain angles. This reflection

[4] A. J. Dempster, Phys. Rev. **18**, 415 (1921).

persisted for a short time after the heating current had been cut off, but gradually became less and less until after a few minutes no ions at all were reflected. This behavior suggests that a film of gas or vapor on the platinum surface prevents reflection. In the experiment the observations were therefore taken within a few seconds after the reflecting strip had been cleaned by heating to a high temperature for a short time. As no reflection was found from an old surface, it may be assumed that the current to the collector is a measure of the ions falling upon it.

In general the type of results obtained with a "clean" reflector bombarded with Li_7^+ ions is shown in Figs. 2 and 3. In both these the relative intensity of the current due to the reflected rays with respect to that of the incident rays is plotted against the angle of the collector. The direction of the incident

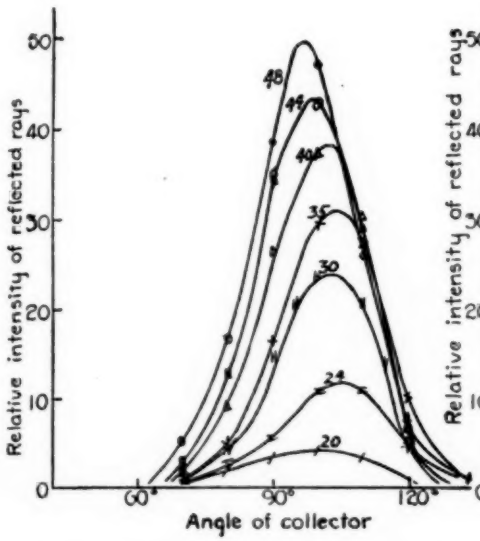

Fig. 2. Variation with angle of reflected positive rays. Accelerating potentials 48 volts and less.

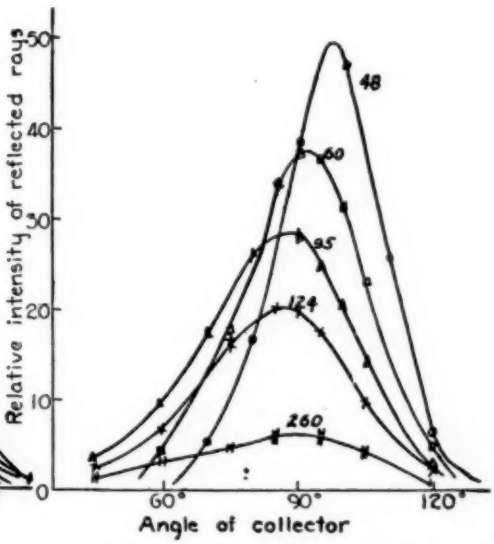

Fig. 3. Variation with angle of reflected positive rays. Accelerating potentials 48 volts and greater.

beam is taken as 0°. As the reflector is placed approximately at 45° to this beam, the reflected beam, for which the angle of reflection equals the angle of incidence, occurs at 90°.

In Fig. 2 the ratios of the collector current at various angles to the total ion current are shown for different accelerating potentials of 48 volts and less. Fig. 3 shows the same type of results for accelerating potentials greater than 48 volts. It is seen that the reflected beam is distributed fairly widely about a maximum which falls near the angle of regular reflection, i.e., 90°. The angular breadth of the reflected beam is large because of the divergence of the incident beam and the width of the collector.

Figs. 2 and 3 show that the number of ions reflected depends upon the accelerating potential. The maximum reflection occurs at 48 volts. The relation of the ratio I (reflected)/I(incident) to the accelerating potentials

is shown in more detail in Fig. (4). At 48 volts approximately 75 percent of all the incident rays are reflected. The number of positive ions reflected decreases sharply as the accelerating potential is decreased from 48 volts and also decreases although more gradually as it is increased.

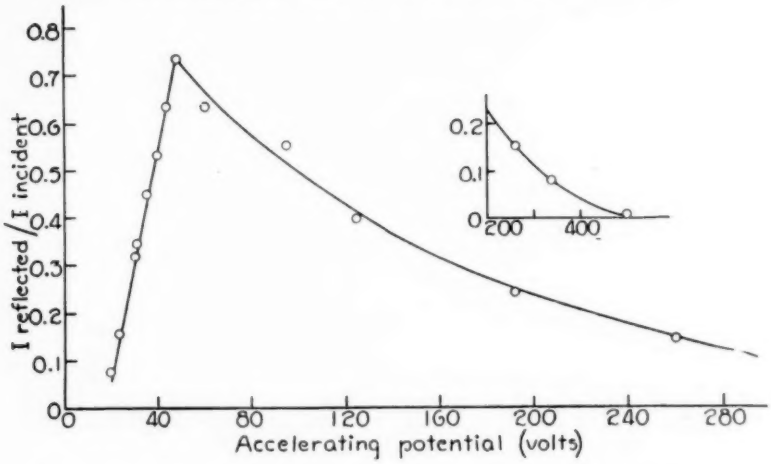

Fig. 4. Variation of I(reflected)/I(incident) with accelerating potential.

Figs. 2 and 3 also show that the angle at which the maximum reflection occurs varies with the accelerating potential. Fig. 5 indicates this variation. The angle of maximum reflection appears to approach 90° as the accelerating voltage is decreased from 30 volts. As the accelerating potential is increased from 30 volts the angle of maximum reflection becomes greater than 90°, and then appears to approach it again at much higher voltages. In this region and in that of small accelerating potentials there was difficulty in taking accurate measurements because of the small relative intensity of the reflected beam.

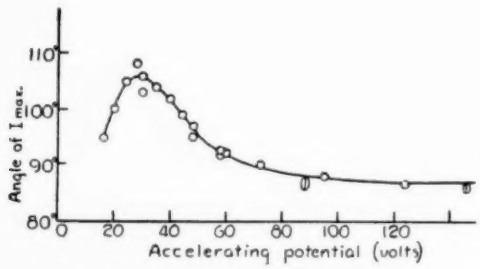

Fig. 5. Variation of angle of maximum reflection with accelerating potential.

Fig. 6 shows the energy distribution of the positive particles in the reflected beam. The data for this curve were taken by applying various retarding potentials between the reflector and collector and measuring the current to the collector. The ratio of the current I with a given retarding potential V to that of the current I_0 with zero potential difference V_0 is plotted against the ratio of the retarding to the accelerating potentials.

The curve in Fig. 6 does not continue on through the axis of abscissas, showing that the production of secondary electrons was not an important factor. This point was checked by applying a magnetic field to the tube. No effect was noticed so that we may conclude that within the range of this experiment the production of secondary electrons was not a disturbing factor.

In all the above work the Li_7^+ positive rays impinged upon a "clean" platinum plate, the angle of incidence being 45°. In this work the "clean" plate may be hot or cold with approximately the same results. After a few minutes, however, the cold plate becomes ineffective as a reflector. In general the same type of effects are found when the angle of incidence is 30° or 60°.

With leucite as a source of K^+ ions similar results were obtained. In general, however, the percentage of ions reflected did not vary as markedly

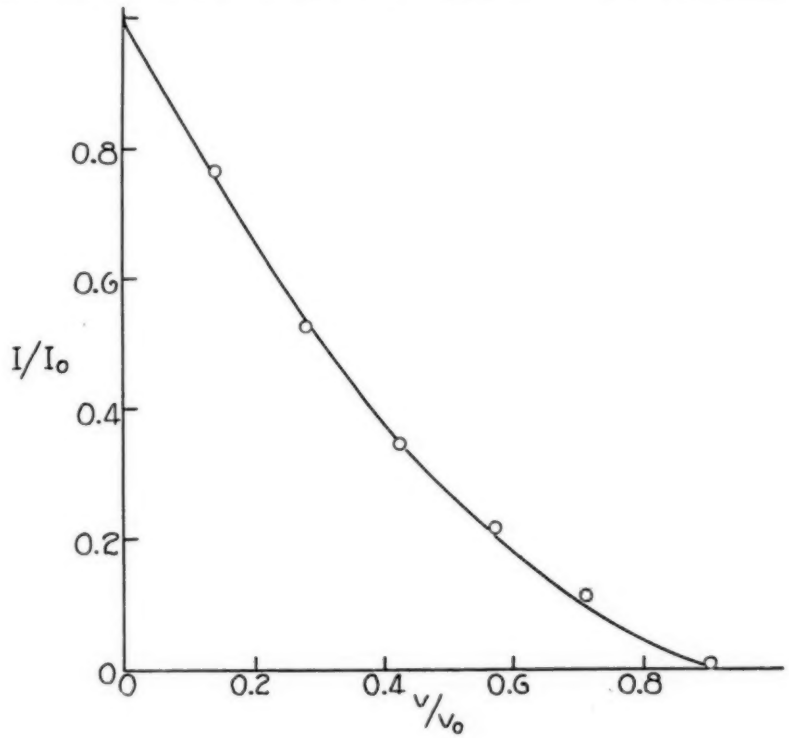

Fig. 6. Energy distribution of reflected positive ions.

with the accelerating potential. The relative energy of the reflected ions is less than in the case of Li_7^+.

The results of this investigation seem to show that alkaline positive rays are partially reflected from a "clean" platinum surface. The percentage reflected depends markedly upon the accelerating potential. While the reflection is approximately specular the angle of reflection varies slightly with the accelerating voltage, also the energy of the reflected beam is appreciably smaller than that of the incident beam.

The above work was done at Ryerson Laboratory, University of Chicago. The writer wishes to express his thanks to Professor Dempster, who suggested the problem and gave valuable criticism during the course of this investigation.

UNIVERSITY OF BUFFALO,
December, 1927.

SOME EXPERIMENTS IN POSITIVE ION KINETICS

By Gaylord P. Harnwell[1]

Abstract

Mean free path and mean energy loss per collision of positive ions of potassium and caesium in helium, neon, argon, hydrogen and nitrogen.—The motion of certain positive ions through gases was investigated in an experimental tube of simple design. The ions were obtained from the potassium and caesium catalyst sources developed at the Fixed Nitrogen Laboratory, and their behavior was studied in helium, neon, argon, hydrogen, and nitrogen. It was found that the results were best explained on the basis of a free path approximately equal to the kinetic theory value, and on an average fraction of energy lost per collision considerably less than would be expected on ordinary considerations. It is suggested that the explanation of this is to be found in a more accurate consideration of the fields of force involved at these encounters.

CERTAIN anomalous effects have been observed by all experimenters who have worked with positive ions in an analysing apparatus. One class of these effects appears to be due to an abnormality in the length of the free path of a positive ion or to the behavior of these ions at a collision with a gas molecule. A. J. Dempster[2,3] has found that protons with a velocity corresponding to a potential drop of 900 volts pass through a large number of helium atoms without neutralization, with very little change in direction, and with a loss of energy of less than half a volt per collision. The singly charged hydrogen molecule was also found to pass through a number of helium atoms without dissociating and with very little loss of energy. Singly charged helium atoms were found on the average to be neutralized after two or three collisions. The writer in working with a similar apparatus under slightly different conditions found evidence of the same type of phenomenon in neon, argon, and nitrogen. The average energy lost at a collision was found to be less than one hundredth the energy possessed by the ion before the impact. In a positive ion analyser when the magnetic field is held constant and the accelerating voltage for the ions varied, the peak corresponding to a certain ion is registered at a particular voltage, say V_1. Let this value, V_1, be obtained when the pressure is so low that very few collisions are made by the ion before reaching the collector. If the pressure is increased, after a certain point the area under the peak begins to decrease showing that certain of the ions are being deflected and are not being recorded. Also the accelerating voltage corresponding to the particular peak has shifted to a slightly different value, V_2. The difference between V_1 and V_2 is the average energy loss of an ion in passing over the necessary path through the gas at that pressure. It is easy to explain these effects qualitatively, but some

[1] National Research Fellow.

[2] A. J. Dempster, Phys. Rev. **27**, 108, 514 (1926).

[3] A. J. Dempster, Phil. Mag. **3**, 115 (1927).

very surprising results are obtained when the deduced free paths are compared with the calculations from kinetic theory. For the free path for a deflection is found to be from ten to a hundred times the length of the kinetic theory mean free path at that pressure, or if the free path is considered normal there is practically no deflection at a collision and the energy lost is only a small fraction of what would be predicted from ordinary mechanics. It is well known that investigators working with electrons have found abnormally long free paths when the velocity is approximately that of the positive ions we have been considering. It is not difficult to conceive that any explanation of this phenomenon will be applicable also to the case of the proton which is a simple positive charge, but it seems very much more difficult of explanation when the same anomalous free path phenomenon is observed for more complicated ions which are positive charges with a definite electronic structure around them. It was with the idea of investigating these effects under different conditions than had heretofore been used that the present experiments were undertaken.

The apparatus was essentially the same in form as that used for the investigation of inelastic impacts of electrons. A source of positive ions was surrounded by two coaxial cylindrical grids, closed at one end, and beyond the second grid was a cylindrical plate. The tube containing this system could be evacuated and then disconnected from the pumps by a mercury cut-off. Different gases could then be admitted in known quantities and the resulting pressure measured by a McLeod gauge connected with the apparatus. There were liquid air traps separating the tube from the McLeod gauge and mercury cut-off. The positive ion sources were those which have been described by C. H. Kunsman.[4] Both the potassium and the caesium sources were used during the course of the experiments. The potassium source was known to emit only singly charged potassium ions, but probably there were slight traces of rubidium in the caesium source.[5] No doubly charged ions were present. After some experiments a slightly different form of filament was evolved which was found to be more stable and less likely to burn out than those which have been used previously for these sources. It consisted of a thin walled hollow semi-cylinder of very pure graphite, supported at each end by the filament leads. A platinum wire to carry the heating current ran down the center of the trough and the powdered source was packed in on top of it. It was found more convenient to mount it in a horizontal position, but after the necessary reduction process the powdered source forms a hard cake and it could be mounted vertically if desired. The apparatus and connections are represented diagrammatically in Fig. 1. D_1 and D_2 were about 1.5 cm each and D_3 was between 0.2 and 0.3 cm. A variable field could be applied across D_1. This potential was obtained from a two thousand volt generator and potentiometer, the current flowing in this circuit was measured by the multimeter, M. The filament was capable of supplying a milliampere but during these experiments currents of less than twenty-five microamperes

[4] C. H. Kunsman, Jour. of Phys. Chem. **30,** 525–534 (1926).

[5] Barton, Harnwell, and Kunsman. Phys. Rev. **27,** 739–746 (1926).

were used as the thermionic emission was found to be more stable below that value. A small constant field of about three volts per centimeter was applied between G_1 and G_2. The potential between F and P was constant during any run but several values of this potential were used in the course of the experiments. The current in this circuit was measured by the galvanometer, G. This system of connections allowed great flexibility and all the necessary experimental conditions could be obtained with it. The filament leads entered the tube through a ground glass joint so that it could be easily removed, but it was found most convenient to perform the necessary reduction of the positive ion source with the filament in place. For this purpose a hydrogen generator was connected with the apparatus. The hydrogen was purified by passing it over heated platinized asbestos and then through P_2O_5 and a liquid air trap. The same generator was used for supplying hydrogen later

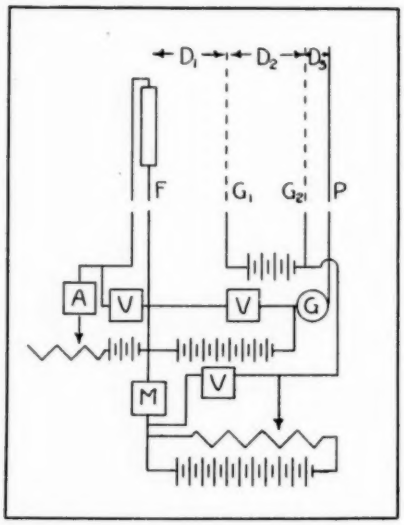

Fig. 1. Diagram of apparatus and connections.

during the experiment. The other gases used were only purified to about the same extent. The nitrogen was left for several weeks in contact with phosphorous. This had been found previously to give a fairly pure sample. Nitrogen and the rare gases used were dried by passing through P_2O_5 and the liquid air traps.

It can be seen from Fig. 1 that the ions pass through no field free region and the field around the filament is in general quite intense so that the possibility of the positive ions being neutralized by electrons emitted from the elements of the tube can be neglected. Also the ionization potentials of potassium and caesium atoms are so low that there will probably be no collision of the second kind with the atoms or molecules of the gas contained in the tube. However, there is the difficulty that photo-electrons will be produced by the grids and the plate under the influence of light from the filament, and an arc will form after the potential across D_1, which will be

referred to subsequently as V, reaches a certain value. This value will vary with the nature of the gas in the tube, and with the pressure. A large resistance was put in the circuit to protect the instruments, but because of the entire change in conditions readings were always stopped as soon as the arc struck.

Before proceeding to the main experiments in view it was necessary to determine exactly what ionization was to be expected from these positive ions under the experimental conditions in the tube. It is very doubtful if the ions produce any ionization in the gas through which they pass, but it has been demonstrated by a number of observers that metals emit electrons under the influence of positive ion bombardment. Hence the potentials in the tube were so arranged that the positive ions were drawn from the filament to the first gauze, then slightly retarded in D_2, and retarded in D_3 to such an extent that they could not reach the plate. Under these circumstances any liberated electrons would reach the plate and be recorded by the galvanometer. Also any negative ions produced in D_2 or D_3 would also be registered by the galvanometer. If the potential in D_2 were reversed negative ions produced in D_2 would not emerge in the direction of the plate (neglecting any possible interchange of momentum between the positive ions and the atom or molecule they might ionize). In this way the effect of emission of electrons from the second gauze could be differentiated from the effect of electrons from the first gauze or ionization in the gas, for the region D_3 was so short that collisions in it could be neglected. With these arrangements a small current was observed in the galvanometer and it varied almost linearly with the voltage V until an arc struck. The difference in the galvanometer current when the potential in D_2 was reversed was of such an order of magnitude that the additional current was probably due to electrons emitted from G_1 under the influence of light from the filament or under the positive ion bombardment. Voltages as high as fifteen hundred were used under such pressure conditions that the arc did not strike but no evidence of any negative ionization of the gas by the positive ions was obtained. The gases which were used were: hydrogen, nitrogen, helium, neon, and argon. No polar molecules were worked with in the apparatus.

During the main body of experiments the ptential between the plate and filament was such that positive ions starting from the filament were able to reach the plate. Under these conditions the ions were accelerated to G_1, then moved under a very small accelerating field to G_2, from which place they were retarded till they had a very small velocity by the time they reached the plate. All the ions leaving the filament which were not interfered with by the grids reached the plate, and were recorded by the galvanometer, when there was no gas in the apparatus. Curves obtained by plotting the plate current against the accelerating voltage, V, were very much like the ordinary thermionic saturation curves. Some difficulty was experienced under these conditions, however, by an apparent instability of the tube just as the current reached its maximum value. If readings were taken rapidly over this region a slightly higher curve was obtained than if five minutes

were allowed between readings. This effect was attributed to oscillations similar to those in an ordinary three electrode tube. They might theoretically occur and slightly alter the plate current. However, the energy in the oscil-

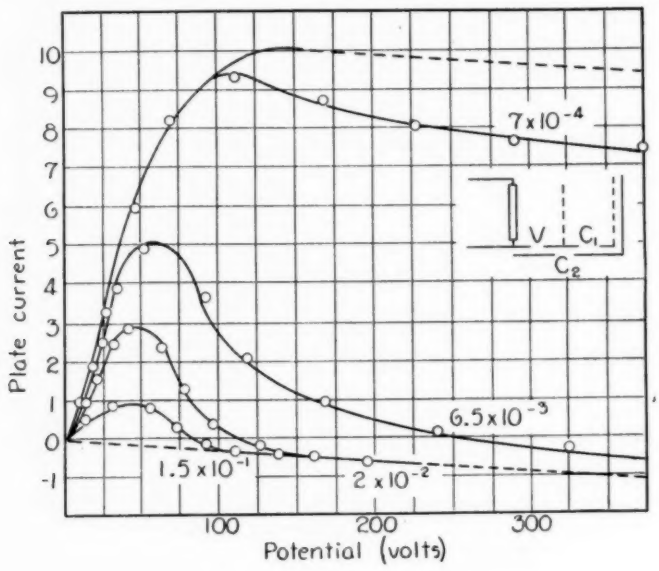

Fig. 2.

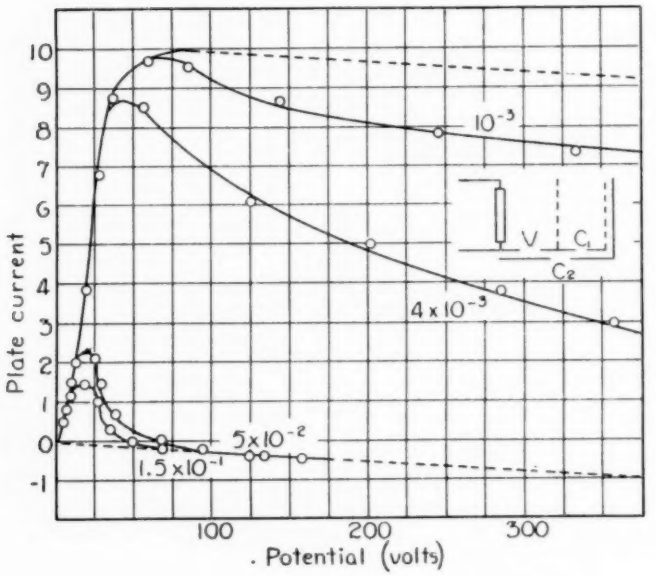

Fig. 3.

lations was so small that they could not be detected by ordinary methods. No similar unstable condition was observed when there was any gas present in the apparatus. As the gas pressure increased, however, the curves altered

considerably in shape. The positive ions in moving through D_1 and D_2 collided with the gas molecules in those regions and as a consequence lost some of their energy at these impacts. Hence some of the ions which would have continued on through D_3 to the plate against the reverse field were unable to do so. At still higher values of the pressure this effect increased until as can be seen from Figs. 2 and 3 none of the positive ions were able to reach the plate. At these pressures after a certain voltage is reached the curves lie approximately along the dotted line extending from the origin. This dotted line is the curve obtained by the arrangement of the potentials described in the preceding paragraph. The upper dotted line represents the curve which is obtained when there is no gas in the apparatus.

The experimental results may be conveniently interpreted in the following way. If e is the charge on an ion, V is the potential across D_1, and l_1 is the average free path parallel to V then the energy possessed just before the first collision is: eVl_1/D_1. If an average fraction f of the energy of an ion is lost at a collision, and if this fraction is independent of the total energy of the ion, the energy it will possess after the first collision will be: $(eVl_1/D_1)(1-f)$. The energy it will have at the end of two free paths will be: $(eVl_1/D_1)\{(1-f)+1\}[1-f]$, and if $(1-f)$ is replaced by x the energy after n free paths will be: $(eVl_1/D_1)x\{x^{n-1}+x^{n-2}+\cdots,\}$ which can be written: $(eVl_1/D_1)x(1-x^n)/(1-x)=E_1$. The region D_2 can be considered in a similar way, the potential in that case being c_1 and the free path l_2. The energy at the end of m free paths will be:

$$E_1x^m+(ec_1l_2/D_2)x(1-x^m)/(1-x)=E_2$$

Neglecting collisions in D_3 the current will just cease flowing to the plate when: $E_2=e[V-c_2]$ where c_2 is the difference in potential between the filament and the plate. Since in the experimental tube D_1 was approximately equal to D_2 they can both be put equal to d. Likewise l_1 and l_2 may both be put equal to l. This is not strictly true, for l_1 is the average distance of advance per collision in the field V, while l_2 is the average distance of advance when the ion has an initial velocity but is moving only under a very small field. However, it is not probable that any great error will be introduced by assuming them approximately equal, for what amounts to an average value of the two will be obtained. It also follows that n will be equal to m. On this assumption the following value of V is obtained for which the positive ion current just ceases to flow: $x^{d/l}V+c_1=(V-c_2)d(1-x)/[lx(1-x^{d/l})]$. To a first approximation changes in the direction of the momentum of the ions need not be considered for, neglecting collisions in D_3 with sufficient energy. The value of l obtained from the above equation will not be exactly the mean free path of kinetic theory. For l is the length of the path parallel to the field hence it will be the actual free path times the cosine of the angle between its direction and the radius of the cylindrical electrode through the point. This will give too small a value for the free path, but the ion is also subject to a constant acceleration in the direction of the field which tends to counteract the first effect. The value of l obtained is the

result of these two tendencies acting on the ordinary mean free path. They will have greater or less effect depending on the pressure and the strength of the field, but under the experimental conditions used it is unlikely that the order of magnitude of the quantity will be changed.

In the equation given in the last paragraph V, c_1 and c_2 are experimentally determined quantities, hence it can be seen that the equation determines a rather complicated relation between x and l. Taking the expression given by J. J. Thomson[6] for the exchange of energy at an encounter between two bodies of mass m_1 and m_2: $[4m_1m_2/(m_1+m_2)^2]T \sin^2\theta$, where θ is half the angle through which their relative velocity is turned and $2T$ is the momentum of the system multiplied by the relative velocity and the angle between these vectors, the loss of energy of the ions at a collision can be calculated. For the simplest case where the ions and molecules are considered as elastic spheres one of which is at rest the average fraction of energy which should be lost at a collision is: $2m_1m_2/(m_1+m_2)^2$. Using this value for f and the experimental values of V, c_1 and c_2 values of l can be calculated. The approximate results of this calculation are given in the table below where the figure at the intersection of a column and row represents the factor by which the kinetic theory mean free path must be multiplied to obtain the calculated value of l.

	H_2	N_2	He	Ne	A
K^+	15	150	5	75	150
Cs^+	5	100	10	100	25

These values are calculated from curves obtained at the highest pressures used. They are most surprising and tend to lead one to look for another explanation.

It was mentioned in the preceding paragraph that the equation used determined a relationship between x and l for a constant value of V. If the reasonable supposition is made in addition that l is an inverse function of the pressure two experimental values of V at different pressures will serve to determine x and l separately. The second alternative of varying c_2 has also been used but this changes the value of the plate current many fold and makes the determination of V more difficult. The values of l given in the preceding paragraph do not satisfy the equation except for the value of the pressure at which they were obtained. When this assumption of the dependence of l on the pressure is made the values of l all come out to be only slightly different from the kinetic theory value of the free path. The method does not serve to determine l accurately but in no case does it differ by a factor of more than three or four from the kinetic theory value. However, the average fraction of energy lost at a collision comes out very much smaller than would be expected from the ordinary kinetic theory concepts. The values obtained are given in the table below.

	H_2	N_2	He	Ne	A
K^+	0.008	0.003	0.025	0.005	0.002
Cs^+	0.005	0.002	0.005	0.003	0.002

[6] J. J. Thomson, Phil. Mag. 47, 337 (1924).

These values of f are consistent within limits of error with all the data that has been obtained. The value of l coming out very nearly that of the kinetic theory mean free path has additional support from the fact that A. J. Dempster[3] found that positively charged helium atoms were neutralized after going a distance approximately equal to the kinetic theory free path. But the average fraction of energy lost differs very greatly from that calculated on the basis of collisions between smooth, non-attracting, elastic spheres. Of course, this conception is probably very far from the facts but it might be expected to give results of the correct order of magnitude. On referring to the more general expression for the loss of energy at an encounter it is seen to depend on a number of factors. Neglecting T, which is a function of the masses and velocities alone, θ can be considered as a function of these quantities, of the apsidal distance and of the nature of the interacting fields. The calculations for the case of a point charge passing near a molecule in which an electric doublet is induced are given by J. J. Thomson.[7] For more complicated distributions of potential about the interacting bodies the calcalculations are very involved. However, it can be seen qualitatively that if the force of attraction between the two bodies is of the form: $1/r^n$ the factor $\sin^2\theta$ and hence the fraction of energy lost at an encounter will decrease as n increases. The fields of the ions and molecules used in these experiments are doubtless of a rather complicated nature and the fraction of energy lost would be expected to be smaller than for the cases of colliding spheres or inverse square fields. The results obtained then depart from the simple theory in the correct direction, but in the absence of an accurate knowledge of the molecular fields it is not possible to state whether the energy lost is quantitatively what would be expected. Similarly it can be seen from the foregoing table that the values of f in the cases of the rare gases vary in accordance with these considerations. The value of f for K^+ in helium seems out of proportion to the rest of the table. It may be that the conditions are such in this case that the potassium ion may supply energy of excitation at a certain fraction of the collisions which would, of course, entirely change the nature of the phenomenon. No further information was obtained on this point. These explanations are merely qualitative, but are the only ones which can be offered for the low values of f observed. But it should be mentioned that this very small loss of energy at an encounter is exactly what would be predicted from the phenomena observed in a positive ion analyser mentioned at the beginning of this paper.

Figs. 2 and 3 are the experimental curves for the cases of Cs^+ in argon and K^+ in helium respectively. The curves are seen to rise more abruptly in the latter case than in the former which is due largely to the different characteristics of the sources of the positive ions. The curves in the latter case are also seen to descend more abruptly. As was mentioned previously this is the effect that would be expected if f were greater for potassium ions in helium than for caesium ions in argon. This, however, is not as conclusive as the table which has been given, for these slopes will depend considerably on the total plate current and it was not always possible to reproduce this

exactly. These figures also illustrate the difficulty of accurately measuring the intersection of the curves with the lower dotted line which represents the negative current to the plate. The values of V obtained from these intersections are the ones substituted in the equation which was developed for the determination of x and l, and the uncertainty in the measurement of V is probably the largest experimental error.

In conclusion it is a pleasure for the writer to express his indebtedness to the National Research Council for its support and to California Institute of Technology for the facilities placed at his disposal.

CALIFORNIA INSTITUTE OF TECHNOLOGY,
November 15, 1927.

REFLECTION OF ATOMS BY A CRYSTAL*

By A. Ellett and H. F. Olson

Abstract

Directional distribution of cadmium, mercury, sodium, and hydrogen atoms reflected from rock-salt.—Beams of cadmium and mercury atoms striking a clean rock-salt surface are reflected so that incident and reflected beams make equal angles with the normal to the crystal surface. The divergence of the reflected beam is only a little greater than that of the incident beam. Sodium is not reflected from a rock-salt surface. Hydrogen atoms striking a rock-salt surface leave as atomic hydrogen. The distribution of the directions in which they leave the surface has never been the same for any two crystals. This may be due to failure to remove all adsorbed gas.

THE wave mechanics of de Broglie[1] and Schroedinger[2] and the recent experiments of Davisson and Germer[3] who have secured definite evidence of diffraction maxima in the distribution of electrons scattered by crystals raise the question whether the reflection of atoms at a crystal surface may give rise to similar phenomena. Whether several diffraction maxima are to be expected depends upon the form of the function representing the potential energy of an atom in the vicinity of the reflecting crystal. If this function possesses distinct maxima and minima having a space periodicity corresponding to the lattice space of the crystal then we may expect the crystal to behave with respect to the phase waves of the approaching atom either as a space-grating or as a cross-ruled plane-grating. The fact that the atoms in the crystal surface are spaced in a regular manner does not necessarily imply that there will be a marked periodicity in the potential energy function in all cases, as it may be that the potential energy of the approaching atom will become equal to its initial kinetic energy while its distance from the crystal surface is several times the lattice space of the crystal. In this case the effect upon the phase waves of the increase of the potential energy function in the vicinity of crystal may be analogous to that of a plane, or nearly plane, mirror in optics. In this connection it may be well to remember that a mirror with a rippled surface will produce no appreciable diffraction maxima other than that of zero order unless the amplitude of the ripples, as well as their "wave-length," is comparable with the wave-length of the incident light.

Former attempts to reflect atomic beams do not appear to have shown definitely that such reflection occurs. R. W. Wood[4] obtained results which appeared to indicate more or less specular reflection, while Langmuir[5]

* Read at the Nashville meeting of the American Physical Society December 30, 1927.

[1] de Broglie, Ann. d. Physique **3,** 22 (1925).

[2] Schroedinger Ann. d. Physik **79,** 361 (1926).

[3] Davisson and Germer, Nature, **119,** 558 (1927); Phys. Rev. **30,** 705 (1927).

[4] R. W. Wood, Phil. Mag. **30,** 300 (1913).

[5] Langmuir, Phys. Rev. **8,** 149 (1916).

on the other hand has interpreted his own experiments as indicating adsorbtion and subsequent re-evaporation. The present paper presents the results of a study of the reflection of mercury, sodium, cadmium, and hydrogen at a cleavage surface of rock salt. The initial experimental arrangement is shown in Fig. 1A. The diaphragms *a* and *b*, each 0.5 mm in diameter limited the divergence of the incident beam of atoms. A well defined spot whose diameter was that to be expected from the dimensions of the diaphragm system was produced on a liquid-air-cooled surface ten centimeters above the upper diaphragm. When a reflector was placed in the path of the atomic beam the development of the coating of reflected atoms on the inner surface of the liquid-air-cooled bulb could be followed without interrupting the course of the experiment. While this design of apparatus is not

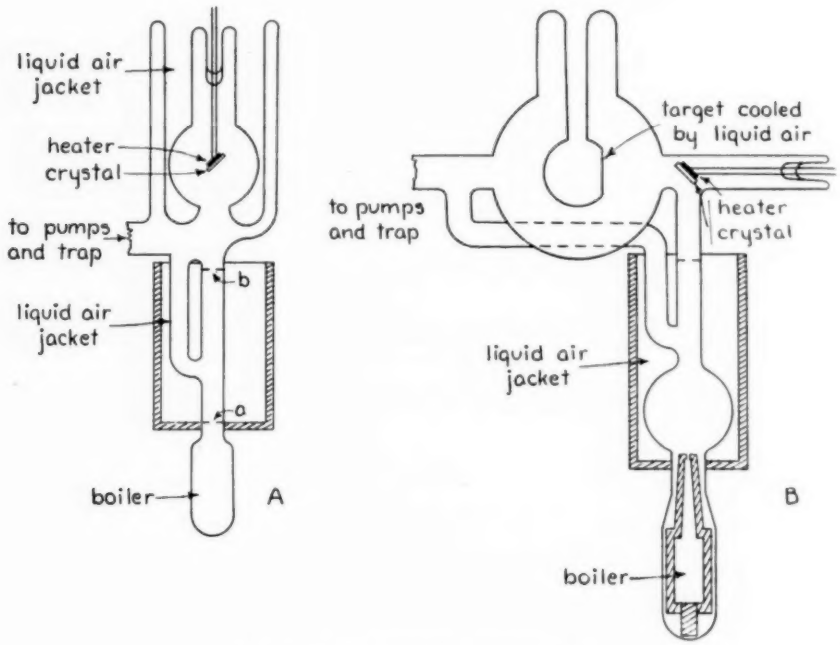

Fig. 1. Experimental arrangements.

well adapted to the measurement of the angles between the reflecting surface and the incident and emergent beams, it has the advantage that no matter in what direction an atom leaves the surface of the reflector it strikes a liquid-air-cooled surface.

With this form of apparatus it was found that mercury and cadmium are almost *specularly* reflected from a *clean* rock-salt surface. The reflected atoms produced a single sharply defined spot about 0.8 mm in diameter, while the rest of the receiving surface remained perfectly clear even when the apparatus was operated for several times the length of time required to make the one spot produced perfectly opaque. If the reflecting rock-salt surface is not freed from adsorbed gases by heating it in vacuum before the

run no such spot is obtained but a coating is produced over an entire hemisphere of the collecting surface. This coat is heaviest in the direction of the normal to the crystal surface, as we would expect for a process of adsorbtion and re-evaporation. If a fire polished glass surface is used instead of rock salt the same character of reflected coating is obtained as with unheated rock-salt crystals. Heating the glass does not appear to improve the situation. The type of coating obtained with a glass reflector and with rock salt not degassed is shown in Figure 2. Sometimes the maximum density appeared slightly displaced from the direction of the normal toward the point where a specularly reflected spot would have appeared. This probably means that specular reflection of a few atoms occurred, though most of them were adsorbed and re-evaporated.

All attempts to secure reflection of sodium from rock salt failed. The crystal was kept at various temperatures up to 400°C, where evaporation

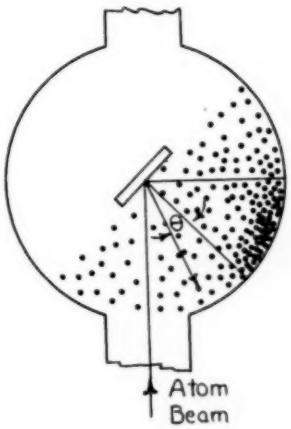

Fig. 2. Distribution over spherical receiving surface of atoms leaving a glass or unheated rock-salt surface.

of the rock salt itself begins to be trouble-some, and runs were continued as long as four hours, but no evidence of reflection was obtained. The intensity of the incident beam of sodium atoms was such that it produced an opaque spot on a liquid-air-cooled surface in five minutes.

Experiments with the form of apparatus shown in Figure 1A demonstrated that mercury and cadmium atoms are reflected from a clean rock-salt surface in a beam whose divergence does not greatly exceed that of the incident beam, but as we remarked above this form of apparatus does not permit easy measurement of the angles of incidence and emergence of the atomic beams. In order to measure these angles more exactly an arrangement such as is shown in Fig. 1B was used. Cadmium was used for these experiments rather than mercury since if any diffraction pattern were formed it would be on a larger scale, and also because the spots remained after removal of the liquid air from the collector. Examination of the deposits secured in this way failed to show any periodic variation in

density. In fact the spots did not exceed by more than four times the diameter of the circle formed by projection of the diaphragms limiting the incident beam. Fig. 3 is a reproduction of a photograph of a cadmium deposit produced by a two-hour run, with the incident beam striking the crystal at an angle of 45°. It may be seen that the density drops off rapidly near the edge of the deposit giving it a rather clearly defined boundary. Similar spots were obtained with angles of incidence varying from 20° to 80°, and in every case the angle of reflection was equal to the angle of incidence with exactness limited only by the accuracy with which the center of the reflected spot could be determined. The increase of the divergence of the atomic beam upon reflection at the crystal surface may obviously be due to any of several causes, such as slight residual contamination or local irregularities of the crystal surface. Indeed it might conceivably be due to the crystal behaving like a plane grating and producing spectra of

Fig. 3. Spot produced by condensation of cadmium atoms reflected from rock-salt surface in apparatus shown in Fig. 1B

the zero and first orders, since the region of maximum density of the first order spectrum would fall within the confines of the spot produced. If the crystal possessed sufficiently high "resolving power" we would then expect to find a significant variation of the density of the deposit, in spite of the Maxwell distribution of the velocities of the incident atoms. In this connection it may be noted that the spots obtained with high angles of incidence are elliptical rather than circular, with the long axis of the ellipse in the plane of the incident and emergent beams, and it may be remembered that the dispersion of the crossed gratings of the crystal face is greatest in this plane. However if this mechanism is to be considered seriously it is obviously necessary to explain the vanishingly small intensity of all spectra of order higher than the first. Certainly there is nothing at present to suggest that the potential energy function of an atom in the vicinity of a crystal is of the highly arbitrary form necessary to account for any such phenomenon as this.

To obtain a beam of atomic hydrogen apparatus similar to that devised by Phipps and Taylor[6] was used. It was found necessary to dry the hydrogen used before admitting it to the discharge tube, as water vapor carried along with the beam of atoms rapidly attacked the salt crystal, producing a small pit at the point struck by the beam. By operating the tube with a very heavy discharge it was however possible to obtain a considerable concentration of atomic hydrogen, as shown by the fact that the emergent beam rapidly produced the typical color change in a molybdic oxide film.[6]

We have obtained no evidence of specular reflection of hydrogen by rock-salt surfaces. If the rock-salt surface is not freed of occluded gases by heating the atomic hydrogen striking it is evidently catalized to molecular hydrogen, as it loses its ability to reduce molybdic oxide. If the rock salt is heated at least part of the incident hydrogen atoms leave the surface in the atomic state but the direction in which a majority of them leave has not been found to bear any relation to the direction of either the incident beam or the normal to the reflecting surface. In fact runs made under apparently identical circumstances have never twice produced the same result. This might be due to the fact that local irregularities of the crystal surface produce a greater effect with hydrogen, or it may be the effect of contamination of the crystal surface. Every effort has been made to eliminate the latter, short of baking out the entire apparatus before a run, but unless this is done there will surely be enough residual gas to build up a film on the crystal surface in a short time.

PHYSICS LABORATORY,
UNIVERSITY OF IOWA,
January 5, 1928.

[6] Phipps and Taylor, Phys. Rev. **29**, 309 (1927).

THE LONGITUDINAL THERMOMAGNETIC POTENTIAL DIFFERENCE IN A BISMUTH CRYSTAL

By C. W. Heaps

Abstract

The longitudinal thermomagnetic potential difference in a bismuth crystal has been measured at room temperature for various orientations of heat current, magnetic field, and crystal axis. The results are plotted to show the change of thermoelectromotive force as a function of magnetic field strength. When the heat current is parallel to the crystal axis the field produces an apparent increase of thermoelectromotive force, the maximum being about 7 percent in a field of 7000 gauss. When the heat current is perpendicular to the crystal axis the field produces a decrease of thermoelectromotive force, the maximum being 23 percent in a field of 7000. Some of the data are in poor agreement with previous work by Lownds and Defregger. The results may be explained qualitatively by assuming that a magnetic field produces a structural change of some sort in the atomic system of bismuth. This change, in the direction normal to the field, is essentially different from the change parallel to the field.

IF A copper-bismuth thermocouple is arranged so that the bismuth is in a magnetic field it is found that the thermoelectromotive force of the couple is changed by the field. At room temperatures most observers have found an increase of electromotive force. When the bismuth is placed so that the heat current in it is transverse to a uniform magnetic field the phenomenon is frequently called the longitudinal thermomagnetic potential difference, and may be represented[1] by the equation $e=LIH(T_2-T_1)$. Here e is the difference of potential of the junctions produced by the field H, the junctions being at temperature T_1 and T_2 respectively. The coefficient L is positive when e is in the same direction as the heat flow in the specimen.

The profound influence of crystal structure on galvano- and thermomagnetic phenomena suggests that an accurate knowledge of these effects can only be obtained by making measurements with single crystal specimens. Defregger[2] and Lownds[3] have used single crystals but they were limited by the form of their specimen to certain restricted orientations of the crystalline axis with respect to field and heat flow. The writer has made a series of measurements on specimens cut from a single crystal,—the same crystal for which the Hall effect has been investigated[4]—and quite different results have been obtained for different orientations of the crystal axis.

[1] Hall and Campbell, Proc. Am. Acad. **46**, 625 (1911); A. W. Smith, Phys. Rev. **2**, 383 (1913). Nernst, Ann. d. Physik **31**, 760 (1887), proposed the equation $e=LH^2(T_2-T_1)$, and Lownds, Ann. d. Physik **4**, 776 (1901), uses the expression $e=n(T_2-T_1)$, where n depends on H. Campbell, Galvanomagnetic and Thermomagnetic Effects, defines L by Nernst's method but gives numerical values not calculated by Nernst's formula.

[2] Defregger, Ann. d. Physik **63**, 97 (1897).

[3] Lownds, Ann. d. Physik **6**, 146 (1901).

Apparatus and Method

The specimen, in the form of a plate or bar, had its ends soldered with Wood's metal to copper tubes. Cold water was passed through one tube, hot through the other, constancy of flow being maintained by large storage vessels in each line. The elevation of these storage vessels determined the water pressure. Since the water was cooled (by a refrigerating plant) or heated (by an electrical heater) before entering the tanks these vessels also served to smooth out irregularities of temperature of the inflowing water streams.

Two separate copper-manganin thermojunctions of fine wire were fixed to the bismuth crystal with a tiny particle of Wood's metal. They were a short distance apart and on a line parallel to the length of the specimen. The specimen was wrapped in cotton and supported between the poles of a Weiss electromagnet. The pole-pieces were 10 cm in diameter and 3.15 cm apart.

When heat was flowing through the bismuth the temperatures of two points on the line of flow could be determined by means of the thermocouples. When the thermomagnetic potential difference was to be measured, a galvanometer, in series with a potentiometer, was connected to the two copper wires of the thermojunctions soldered to the bismuth. The manganin wires from these junctions were left with their ends electrically insulated. The potentiometer was then adjusted to balance the thermoelectromotive force of the copper-bismuth couple formed by this arrangement. When the magnet was excited the change of setting of the potentiometer for balance gave the value of e.

In practice certain precautions were necessary. If the copper wires soldered to the specimen are not exactly on a thermal line of flow a component of the transverse thermomagnetic electromotive force will act. This effect was eliminated by measuring e for opposing directions of H and taking the mean. The potentiometer setting for zero field was always observed immediately before and after each observation with the field.

A magnetic field changes the thermal conductivity of bismuth, hence the temperatures of the two copper junctions may be changed by the field. This temperature change, however, will not be instantaneous,—an appreciable time will be required for the attainment of thermal equilibrium after the field is applied, so if observations are made rapidly enough the error due to this effect will be negligible. In the present experiments it is believed that changes of thermal conductivity have produced no appreciable error. It was possible to secure a new balance of the potentiometer about four seconds after the magnetic field was removed, and this potentiometer setting did not change gradually as would be expected in case the junctions were coming to new temperature differences in the absence of the field. In other words, there was no observable time lag between e and H.

The sensitivity of the apparatus was such that a value of e of about 1 microvolt could be measured.

Results

In Fig. 1 the results are exhibited graphically. Here e is the change produced by the magnetic field H in the original electromotive force E. The relative directions of heat current h, magnetic field H, and crystal axis a, are indicated for each curve by the sets of arrows on the diagram. The curves marked A were obtained with a bar of dimensions $1.0\times0.216\times0.414$ cm,

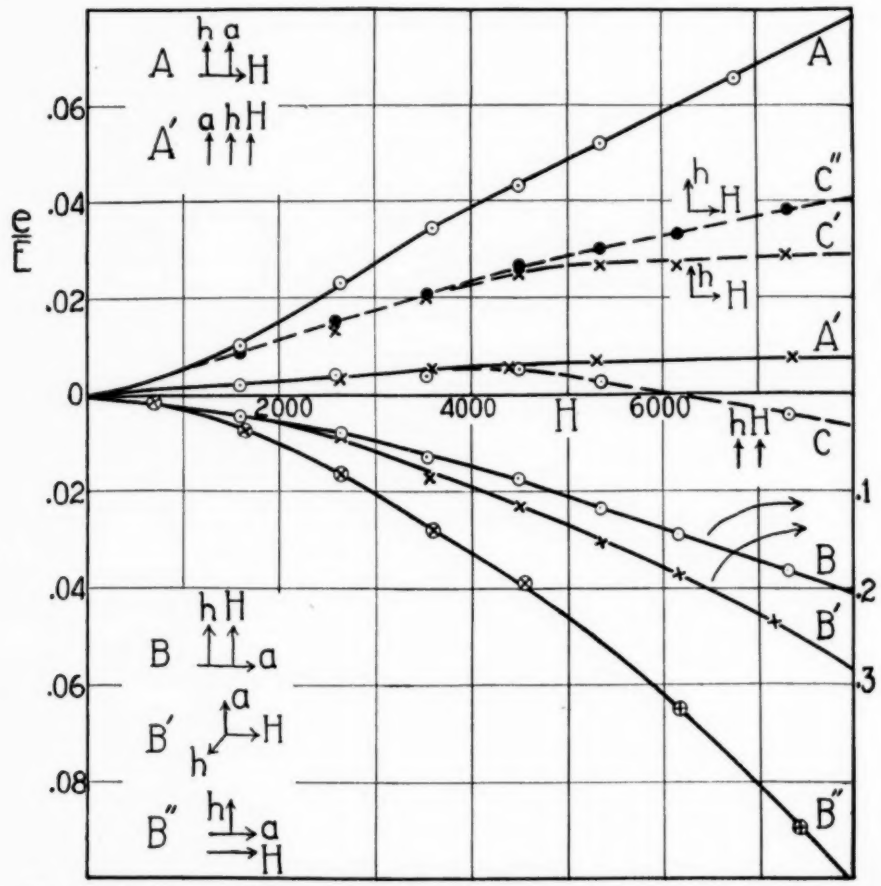

Fig. 1. Variation with magnetic field of the fractional change of thermoelectromotive force for different crystal orientations. The symbols for each curve give relative directions of heat current h, magnetic field H, and crystal axis a. The right hand scale of ordinates is used for curves B and B'.

the heat flow being in all cases along the long dimension which was cut from the large crystal so as to be parallel to the crystal axis.

The curves marked B were obtained with a plate of dimensions $1.3\times0.47\times0.115$ cm. This plate was the one designated as B in the writer's work[4] on the Hall effect, its dimensions being slightly altered by removal of side arms.

[4] Heaps, Phys. Rev. 30, 61 (1927).

The dotted curves C are for a plate of compressed bismuth powder, (also one used in the experiments on the Hall effect) the powder having been made by grinding a piece of the crystal in a mortar. For C' the field H was perpendicular to h and to the plane of the plate; for C'' the field was perpendicular to h but parallel to the plane of the plate. For C both h and H were in the plane of the plate.

It appears from the curves that when the heat current is perpendicular to the crystal axis the magnetic field produces an apparent decrease of thermoelectromotive force for the different orientations of the field. When the heat current is parallel to the crystal axis the field produces an apparent increase of thermoelectromotive force.

At first sight it appears surprising that the crystal conglomerate should give a positive effect. Two of the B curves give a negative value of e/E several times larger than any positive effect observed. For a random distribution of the component crystals of a conglomerate there are as many crystals with their axes perpendicular to h as parallel; it might be supposed, therefore, that since the decrease of thermoelectric power for the first type of orientation is so large, the resultant would be a decrease. The fact that it is not may be due to a very rapid change in the magnitude of the effect as the crystal orientation passes through the perpendicular position. Such a change would have to be considerably more rapid than in the case whcre the orientation passes through the parallel position in order to account for the observed curves.

In the present experiments we find that the direction of the heat current is of considerable importance. If the magnetic field is kept perpendicular to the crystal axis and to the heat current we note that the value of e/E is changed from its maximum negative value, when h is perpendicular to a, to a maximum positive value when h is parallel with a. We may interpret this observation as follows. The magnetic field, maintaining a fixed direction with respect to the crystal axis, produces some sort of temporary atomic structural change such that thermoelectric power is increased along the axis but decreased at right angles to the axis. It is improbable that the magnetic field produces its effect by direct action on the electrons concerned in the thermoelectric process, since in each of the above cases the field was normal to the flow of these electrons and yet produced quite different effects.

For the plate of compressed powder the plane of the plate (which was perpendicular to the direction of compression) is a plane of symmetry as regards crystalline structure. For both C and C'' the magnetic field was in the plane of the plate, consequently the marked difference between these two curves must be attributed to the difference of orientation of H with respect to h in the two cases. It appears probable that the magnetic field affects atomic relationships in such fashion that the thermoelectric process parallel to H is essentially different from that parpendicular to H, no matter how the crystal axis may be orientated.

There is at present no theory of electrons in metals which adequately accounts for the observed facts of thermoelectricity in crystals. The results

reported above are of a type which it is especially difficult to fit into any simple theory.

For purposes of comparison with other experiments some of the data of this experiment are given in the following table. In calculating L electromagnetic units are used.

TABLE I

Values of e/E. Comparison with the results of others.

	T_1 °C	T_2 °C	E microv.	H gauss	L	e/E Lownds	e/E Defregger	e/E Heaps
A	23.0	40.5	1540	6100	−.086	+.085	+.069	+.060
A'	23.0	40.5	1540					
B	17.3	29.5	552					
B'	16.5	30.0	587	6100	+.132	−.035	−.0006 +.0069	−.185
B''	7.0	27.8	886	4400	+.037	+.0097	+.0085 +.0060	−.038
C	18.0	31.3	1120					
C'	18.2	32.0	1160					
C''	18.2	32.0	1160	7300	−.044			

For each of the cases B' and B'' the two results of Defregger (quoted by Lownds) are for different specimens. The values of e/E of Lownds and Defregger are for average temperatures of about 50°C, and while this is considerably higher than the mean temperatures of the present experiment the difference does not seem to be sufficiently great to account for the poor agreement of results.

For a cast bismuth plate A. W. Smith finds L to be -0.13 at 20° and with a field of 9600. This value is considerably larger than the result of the present experiment on a pressed plate at 25.1° in a field of 7300.

THE RICE INSTITUTE,
HOUSTON, TEXAS,
January 12, 1928.

DIELECTRIC CONSTANTS OF DILUTE SOLUTIONS OF POLAR LIQUIDS IN NONPOLAR SOLVENTS

By J. D. Stranathan

Abstract

Dielectric constants of solutions of methyl, ethyl, propyl and amyl alcohols in benzene and carbon tetrachloride.—Failure of the Debye theory to represent the behavior of such polar liquids as the alcohols is usually attributed to association. With hope of eliminating the effects of association, the dielectric behavior of dilute solutions of several alcohols in benzene have been studied. Dielectric constants were determined by a heterodyne beat method. Both dielectric and density data were obtained at each 10° temperature interval from freezing to boiling. The molecular polarization found for the dissolved alcohol was plotted against concentration; one such curve was plotted at each 10° interval. With hope of obtaining the polarization of the alcohol in the unassociated state, these curves were extended to cut the zero concentration axis. The resulting intercepts for the various temperatures were checked against theory.

Electric moments of methyl, ethyl, propyl and amyl alcohol molecules.—By taking the contribution due to electron displacement from optical data, it was found that the zero concentration intercepts for methyl, ethyl, propyl, and amyl alcohol (using benzene as solvent) lead to values of the electric moment of the molecule which are essentially independent of temperature. This is in agreement with the Debye theory; it is in contrast to the behavior of the pure liquid alcohols. The moments found are 1.64, 1.74, 1.75, and 1.62×10^{-18} for methyl, ethyl, propyl, and amyl alcohol, respectively. If use of the molecular refraction is avoided by plotting values of P_0T against T, where P_0 is the zero concentration intercept, it is apparent that the data can in no way lead to imaginary electric moments, as do data on the pure liquids. If straight lines with the extreme slopes justified by the data are drawn through the group of points for any alcohol, the zero temperature intercepts so found limit the electric moment to a range whose extremes differ by not more than 20 percent. In every case the moment obtained through use of the molecular refraction falls within this range.

Introduction

THE Debye theory[1] of dielectrics leads to the expression

$$\frac{K-1}{K+2}\frac{M}{d}=A+\frac{B}{T}$$

where K is the dielectric constant, M the molecular weight, d the density, and where A and B are constants for a given dielectric. Theoretically, the constant A is equal to the molecular refraction $(M/d)(n^2-1)/(n^2+2)$ extrapolated to infinite wave-length; it includes only the effect of electron displacement, and not that of doublet orientation. The constant B measures the contribution due to the permanent electric moment of the molecule. The moment u is given by

$$u=(9kdB/4\pi NM)^{1/2}=1.27\times10^{-20}B^{1/2}$$

[1] See, for example, Marx, Handbuch der Radiologie, 6, 614–619 (1925).

where k is the Boltzmann gas constant per molecule and N the number of molecules per cubic centimeter. The quantity $(M/d)(K-1)/(K+2)$ is known as the molecular polarization P; hence, the first equation may be written

$$PT=AT+B$$

The theory can be tested for agreement with experimental data by plotting values of PT against T; theory demands a straight line with slope A and intercept B. Numerous data on gases by Zahn,[2] Smyth and Zahn,[3] and others, have shown that in general the theoretical expression represents well the experimental findings. The electric moment of the molecule is calculated from the experimental intercept B. In most cases the experimental slope A agrees moderately well with the molecular refraction calculated from optical data.

In general the data on liquids do not agree well with the Debye expression. As an example of a typical failure of the expression, attention is called to the data on liquid ethyl alcohol as quoted by Debye.[4] In this case the data do conform to the linear relationship between PT and T required by theory, but the intercept B is clearly negative. Since the electric moment of the molecule is proportional to the square root of the intercept B, the theory here leads to an imaginary moment. Or, if the value of A be taken over from optical data and B calculated at various temperatures, the resulting electric moment is found to increase with rising temperature. Thus the simple theory is quite inadequate. Similar statements can be made regarding data on liquid methyl alcohol.

The failure of the simple theory in the case of polar liquids is usually attributed to association and changes of the degree and manner of association with temperature. Such changes would clearly result in an electric moment which varies with temperature; the moment measured would be an effective value, averaged over the various types of associated groups present.

Dielectric data on solutions of polar liquids in a nonpolar solvent furnish illuminating data as to the effects of association. The dielectric constant of a solution of known concentration, say alcohol in benzene, may be measured, and thence the molecular polarization P of the mixture calculated; for this calculation the weighted molecular weight $(M_1c_1+M_2c_2)$ is used,[5] where M_1 and M_2 are the molecular weights, and c_1 and c_2 the mole fraction concentrations of the solvent (benzene) and the solute (alcohol), respectively. On the basis of the additive law the polarization P of the mixture is made up of two parts, one due to the solvent, the other due to the solute; that is,

$$P=P_1c_1+P_2c_2$$

[2] C. T. Zahn, Phys. Rev. **24**, 400 (1924); **27**, 455 (1926).
[3] C. P. Smyth and C. T. Zahn, Jour. Am. Chem. Soc. **47**, 2501 (1925).
[4] Marx, Handbuch der Radiologie, **6**, 625 (1925).
[5] See Marx, Handbuch der Radiologie, **6**, 628 (1925).

where P_1 and P_2 are the molecular polarizations of the solvent and the solute, respectively. P_1c_1 can be calculated from dielectric data on the pure solvent; hence, P_2, the polarization of the alcohol at concentration c_2, can be obtained. Debye[6] and his students have shown that the molecular polarization P_2 depends markedly on concentration; at some concentrations it increases, at others it decreases, as c_2 decreases. This is presumably due to association changes.

Debye has suggested that if the experimental curve of P_2 versus c_2 (for small concentrations) be extrapolated to zero concentration, the molecular polarization of the solute in the unassociated state would be obtained. This is based upon the assumption that association disappears as the concentration approaches zero, an assumption which is in agreement with data[7] on the lowering of the freezing point of benzene due to the addition of alcohol. It would be interesting to know whether these extrapolated values obey the Debye theory. While there is considerable data in the literature on solutions, practically all of it is for much too large concentrations to be useful here. The author is aware of only two works dealing with the subject. Debye[8] has used data of J. C. Philip on several alcohols in benzene and toluene at mole fraction concentrations ranging from somewhat under 0.01 to 0.11. He extrapolates to zero concentration and calculates the electric moment u, taking the constant A as equal to the molecular refraction obtained from optical data. Unfortunately, the data are all at one temperature, and therefore furnish no test of the Debye theory. The second work is that of L. Lange.[9] She has studied solutions of several alcohols in nonpolar solvents, but a great majority of her data pertain to relatively high concentrations. She has never more than three points under a mass concentration 0.10, and never any under 0.031. Data were taken at most at three temperatures, and usually for only one or two. Judging from the data, it would seem quite unreliable to extrapolate using so few points at low concentrations, and to test the Debye theory with data at so few temperatures.

In the present work the author has therefore made an effort to secure accurate data for somewhat more dilute solutions, and at numerous temperatures, for the purpose of checking the zero concentration intercepts against the Debye theory.

Experimental Procedure

Capacity measurements. Because of the fact that a relatively small error in the initial measurements of either the dielectric constant or the density, becomes greatly magnified during the process of calculation, and all the more so as the concentration is lowered, it is essential that the original errors of measurement be small. In view of this, the method used for the measurement of dielectric constant was a heterodyne beat arrangement commonly used for

[6] Marx, Handbuch der Radiologie, **6**, 627–633 (1925). L. Lange, Zeits. f. Physik **33**, 169–182 (1925).

[7] Cited by Debye, Marx, Handbuch der Radiologie, **6**, 640 (1925).

[8] Marx, Handbuch der Radiologie, **6**, 630 (1925).

[9] L. Lange, Zeits. f. Physik **33**, 169–182 (1925).

measurements on gases.[10] It is true that the sensitivity of this method is far greater than is here necessary, but this is no disadvantage.

The apparatus consisted of two high frequency oscillators, as shown in Fig. 1. The frequency of one oscillator was maintained constant at 476 kilocycles by a quartz crystal, while that of the second could be adjusted at

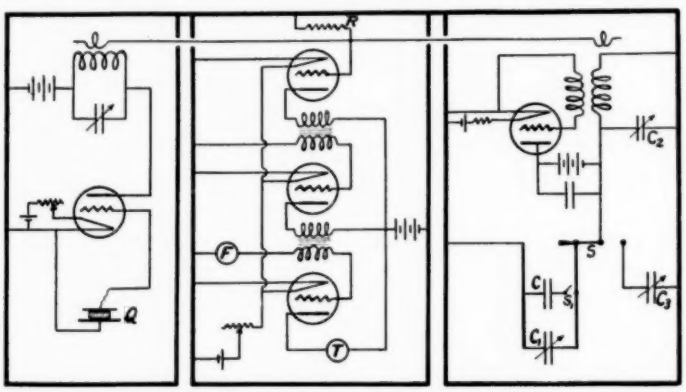

Fig. 1. Diagram of apparatus.

will by variable condensers. The amplified beat note between the two oscillators could be heard from the telephone T. The frequency of the second oscillator could be made accurately 1000 cycles less than that of the crystal controlled oscillator, through use of the electrically driven tuning fork F coupled electrically to the grid circuit of the last stage amplifier; the note due to this tuning fork also issued from the telephone T. The secondary beat-note formed between the tuning fork note and the beat-tone between the two high frequency oscillators, was adjusted to zero by varying the capacity of the second oscillatory circuit. In this way the frequency of the second oscillator could always be brought to a fixed value. The oscillators were shielded, and run from independent batteries to avoid synchronizing effects.

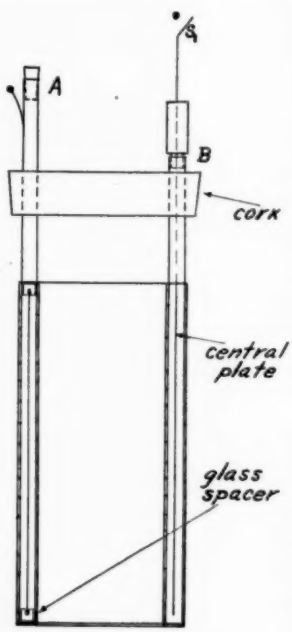

Fig. 2. Test condenser.

The liquid whose dielectric constant was desired was placed in a three plate, cylindrical, brass condenser C whose construction is made clear by Fig. 2. The central plate was held in place by three small Pyrex glass spacers at both top and bottom. This condenser was of such dimensions as to fit into a wide mouth quart thermos bottle containing a water (or alcohol) bath. The temperature, which was read from a mercury thermometer projecting through the cork of the thermos bottle, could be

[10] See, for example, C. T. Zahn, Phys. Rev. **24**, 400 (1924).

adjusted at will by means of an electric heater placed in the bath. Uniformity of temperature was insured by a stirrer projecting through the cork.

The capacity of the test condenser C under any particular conditions was determined by observing the change in capacity of C_1 necessary to compensate for placing the test condenser in parallel with it; the General Radio precision condenser C_1 was readable consistently to 0.1 micro-microfarad. The function of condensers C_3 and C_2 of Fig. 1 was to eliminate any effect of drift in frequency. The circuit including C_3 served as a standard circuit by means of which it could be ascertained whether the tube had drifted in frequency during the process of measurement; C_2, a very small capacity which was always in the oscillatory circuit regardless of the position of switch S, served to compensate for any drift observed.

The capacity of C thus determined must be corrected for both lead capacity and capacity occasioned by the solid dielectric spacers; the glass projecting into the condenser tube at B, Fig. 2, also necessitates a correction. The lead capacity, including that due to the glass at B was determined by direct measurements on a set of dummy leads placed just as were the actual leads during the measurements proper. Several independent sets of measurements gave very consistent results. In order to obtain the capacity correction due to the solid dielectric spacers, use was made of a second cylindrical condenser exactly similar to the one used except that it contained twice as many spacers. The spacers were identical in the two condensers, and they were placed in exactly similar positions. It was therefore assumed that the capacity due to solid dielectric in the second condenser was just twice that in the first. Hence, by expressing the dielectric constant of the same liquid at the same temperature, measured first with one condenser and then the other, in terms of the unknown solid dielectric capacity, and equating the two values of dielectric constant, it is possible to solve algebraically for the solid dielectric capacity. Several measurements gave consistent results. The total correction necessitated by the leads and the spacers was 5.1 micro-microfarads.

The capacity of the empty test condenser, approximately 300 micro-microfarads, was determined for various temperatures ranging from $-30°$ to 80°C. The capacity, corrected for solid dielectric and lead capacity, and also for the air present in the condenser during measurement, was found to be a linear function of the temperature. The temperature coefficient of capacity was 0.0000144 per °C. This is of the same order as the temperature coefficient of linear expansion of brass, as should be expected. An indication of the consistency with which measurements could be duplicated is given by the fact that not one of the 19 experimental points deviates from the straight line by more than one part in 6000.

Mixing of solutions. Solutions of known concentrations were mixed by weighing the components. Great care was exercised in making up the solutions to avoid evaporation of components during the process of weighing and mixing. The best chemically pure materials that could be purchased were used. No further effort was made to remove traces of water except in the

case of propyl alcohol, since its presence should cause but insignificant errors.

Density measurements. The densities of solutions were measured by the loss of weight method, using a Pyrex sinker and an analytical balance for weighing. The calibration was obtained by measurements on distilled water at temperatures ranging from 0° to 80°C, the densities of water being taken from tables. The material being tested was maintained at any temperature desired by immersion in a bath contained in a thermos bottle. The temperature could be changed at will by an electric heater immersed in the bath. By comparison with numerous tabular values wherever possible, it appears that the densities thus determined are quite reliable. For example, the present density determinations on benzene as read from a smooth curve at each 10° temperature interval from freezing to boiling, show an average deviation from Young's values[11] of only 3 parts in 10,000. Also, the author's densities of carbon tetrachloride show about the same percent deviation from Young's values.[12]

Data and Results

Methyl alcohol in benzene. Nine solutions of methyl alcohol in benzene were mixed, the mole fraction concentration of alcohol ranging from 0.00890 to 0.07135. The dielectric constants of each of these solutions, and of the

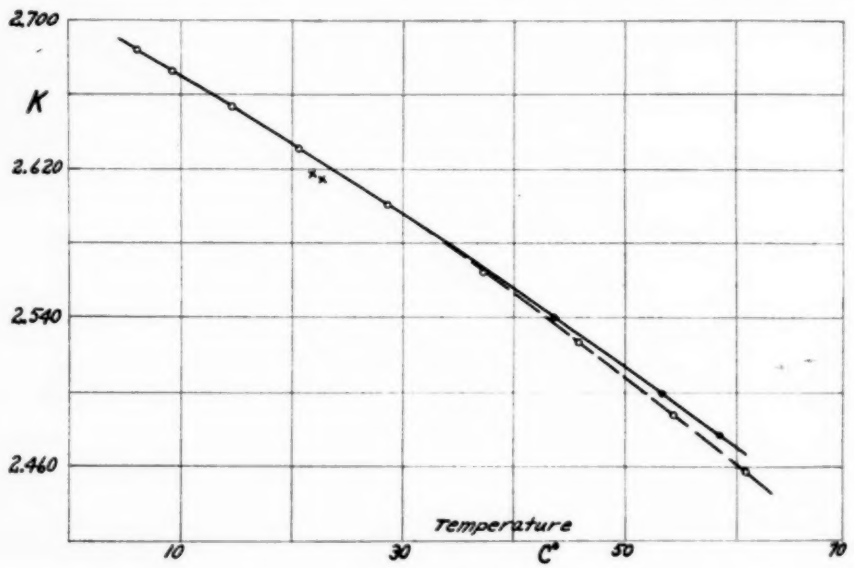

Fig. 3. Correction for evaporation.

pure solvent benzene, were determined at temperatures ranging from freezing to boiling. The test condenser was filled, immersed in a bath at about 6°C, and the dielectric constant of the solution measured. The temperature was

[11] Quoted in Landolt and Börnstein, p. 152, 1912.
[12] Quoted in Landolt and Börnstein, p. 160, 1912.

increased, time allowed for temperature equilibrium, and the measurements repeated. As long as the temperature was never allowed to fall, and as long as no vapor bubbles formed in the liquid, the expansion of the liquid with rising temperature served to keep the test condenser full. Excess liquid forced itself out around the capillary fitting at *B* of Fig. 2. When necessary, additional liquid was put into the condenser through the grounded lead *A*.

Considerable difficulty was experienced, especially with methyl alcohol, due to evaporation of alcohol during the run and the consequent changing of concentration. This was the case in spite of the fact that the lead from the inner plate of the condenser was surrounded by a tight fitting capillary ground to fit tightly into the brass tube of the condenser at *B*, Fig. 2, and the fact that a cork was kept in the tube *A* at all times except when replenishing the solution. The effect of evaporation is shown by Fig. 3, on which points represented by circles are those obtained during a run. The solution was then cooled to room temperature, and the dielectric constant measured; the fact that the two resulting points represented by crosses fall below the original curve indicates that the concentration has decreased. An approximate correction for evaporation would be to raise the curve at the highest temperature point by the same amount that the points represented by crosses deviate from the original curve. As a second, and somewhat better method of correction, the following procedure was adopted. After the first run, the test condenser was refilled with a fresh sample of the solution under test. A point was taken at room temperature (not shown on the curve) to insure that later measurements could be relied upon. The temperature was increased rapidly and a point taken at a temperature somewhat above that at which evaporation began to introduce errors in the original curve. A subsequent measurement at room temperature showed that evaporation had been inappreciable; the time for which the solution had remained at a high temperature was much shorter than for the original measurements. The condenser was again refilled with a fresh sample and the procedure repeated. Points obtained in this way are represented on the curve by black dots. The final curve representing dielectric constant as a function of temperature was drawn through these points rather than the original ones at high temperatures. Dielectric constants were read from this curve at each 10° temperature interval, and tabulated. The procedure was repeated for each of the nine different solutions. The resulting dielectric constants for various concentrations and temperatures are collected in Table 1.

The density of each solution was measured at temperatures ranging from freezing to boiling. The experimental densities for each solution were plotted against temperature, and the density read from the curve at each 10° interval. The densities for the various solutions at any one temperature were then plotted against concentration of alcohol in the solution, and a smooth curve drawn through the points. The density corresponding to any particular concentration and to any particular temperature was then read from these curves. The resulting densities are shown in Table I.

TABLE I

Methyl alcohol in benzene

Summary of dielectric constant and density values. The upper figure in each group of two is the dielectric constant; the lower figure is the density. The same is true for all subsequent tables of this nature.

T	$c_2=0$	.00890	.01507	.01929	.02248	.02929	.03904	.05278	.06266	.07135
10°	2.300	2.335	2.362	2.381	2.394	2.426	2.475	2.550	2.610	2.669
	.8897	.8895	.8893	.8892	.8891	.8889	.8887	.8884	.8881	.8879
20°	2.279	2.313	2.338	2.355	2.369	2.398	2.445	2.517	2.575	2.633
	.8794	.8792	.8790	.8789	.8788	.8786	.8784	.8781	.8778	.8776
30°	2.258	2.290	2.313	2.329	2.434	2.371	2.415	2.483	2.539	2.595
	.8687	.8685	.8683	.8682	.8681	.8679	.8677	.8674	.8671	.8669
40°	2.236	2.266	2.288	2.303	2.316	2.342	2.383	2.448	2.501	2.554
	.8579	.8577	.8575	.8574	.8573	.8571	.8569	.8566	.8563	.8561
50°	2.214	2.243	2.262	2.277	2.289	2.313	2.352	2.414	2.463	2.512
	.8470	.8468	.8466	.8465	.8464	.8462	.8460	.8457	.8454	8452
60°	2.192	2.218	2.237	2.251	2.262	2.284	2.321	2.380	2.425	2.470
	8361	.8359	.8357	.8356	.8355	.8353	.8351	.8348	.8345	.8343

The procedure followed in calculating the contribution of the dissolved alcohol to the polarization of the mixture, is made clear by Table II. The second and third columns represent experimental data. The fourth is calculated from the second and third. The fifth contains values of molecular

TABLE II

Sample calculations.

Methyl alcohol in benzene $c_2=0.07135$

T	K	d	$\frac{K-1}{K+2}\frac{1}{d}$	P	P_1c_1	P_2c_2	P_2
10°C	2.669	0.8879	0.4026	30.11	24.64	5.47	76.7
20	2.633	.8776	.4016	30.04	24.65	5.39	75.5
30	2.595	.8669	.4004	29.95	24.66	5.29	74.1
40	2.554	.8561	.3986	29.82	24.67	5.15	72.2
50	2.512	.8452	.3965	29.66	24.67	4.99	69.9
60	2.470	.8343	.3942	29.49	24.67	4.82	67.6

$M_1c_1+M_2c_2=78.08\times0.92865+32.04\times0.07135=72.51+2.29=74.80$

polarization of the mixture; these values are obtained by multiplying those of the fourth column by the weighted molecular weight of the solution; the method of weighting is indicated below the table. These values of P include two contributions, one P_1c_1 due to the solvent, the second P_2c_2 due to the dissolved alcohol. Polarizations of the pure solvent at various temperatures are shown in Table III. Values of P_1c_1 are calculated and tabulated in the sixth column of Table II; these are subtracted from the P values to give the contribution P_2c_2. This contribution divided by the concentration of alcohol gives the molecular polarization P_2 of the solute. It will be noticed that the

P_2 values decrease with rising temperature, as should be expected from theory.

Before proceeding further, a word should be said regarding data on the pure solvent, benzene. Theoretically, the molecular polarization of benzene should be independent of temperature. Experimentally, however, it has been shown by Graffunder,[13] Grützmacher,[14] and others, that for carefully dried benzene the molecular polarization increases very slightly with rising temperature. This fact has been verified by the author, who finds a steady increase slightly less than that observed by Graffunder. For benzene not entirely dry the deviation from constancy is less, and seems to reverse sign at high temperatures. (See Table III; the initial increase in P_1 and the subsequent decrease are even more apparent for the benzene used as solvent for ethyl alcohol.) In order to avoid quite appreciable errors which would be introduced if the polarization of the solvent were assumed independent of temperature, the author has determined this polarization at various temperatures, always for the particular sample of benzene used in mixing the solutions. The particular value found for any temperature was then used in calculations at that temperature. This procedure avoids also any effect of slight impurities in the solvent, except the minor effect of these upon the manner of association of the solute.

TABLE III

Polarizations of the benzene used as solvent for methyl alcohol.

T	$\frac{K-1}{K+2}\frac{M}{d}=P_1$
10°C	26.53
20	26.54
30	26.55
40	26.56
50	26.56
60	26.56
70	26.55

The procedure of calculation outlined above was carried out for each of the nine solutions. This all done, there is available a value of P_2 at each 10° interval and for each concentration used. These final values for the polarization of the alcohol for a particular temperature are plotted against concentration in Fig. 4. Smooth curves are drawn through points of equal temperature. The dependence of the polarization of the alcohol on concentration is supposedly due to association. If it be assumed that the effects of association vanish as the concentration approaches zero, the polarization of the alcohol molecules in the unassociated state is represented by the intercepts of these curves on the zero concentration axis. The curves are produced to obtain these intercepts.

Before proceeding further, a word should be said concerning the extrapolation. It is inherent in the method of calculating P_2 that any small error in the original values of K or d for the mixture becomes greatly magnified in the final values of P_2. This magnification of error enters in obtaining the small quantity P_2c_2 by subtracting two large quantities, P and P_1c_1, from one another. The magnification of error becomes greater as the concentration

[13] W. Graffunder, Ann. d. Physik, **70**, 232 (1923).
[14] M. Grützmacher, Zeits. f. Physik **28**, 349 (1924).

of the alcohol becomes smaller. For this reason the accuracy of points for concentrations under 0.02 is not very good. For the lowest concentration used, 0.00890, the final values of polarization of the alcohol can be expressed to only two significant figures even though the original measurements were to four; and the second place in this final value is none too good. Hence, in extending the curves to the zero concentration axis, much less weight is given the points at low concentrations. In fact, the lower concentration points should be considered more as showing that the data are not inconsistent with the curves drawn than as showing where to draw these curves. Everything considered, the intercepts are rather well defined.

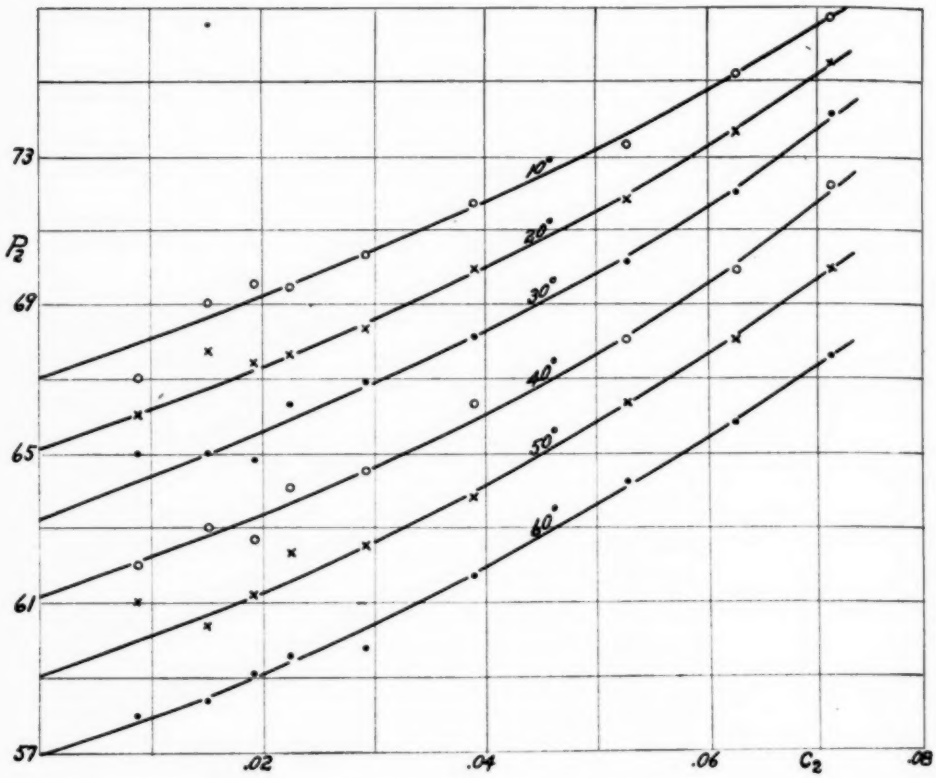

Fig. 4. Polarization curves for methyl alcohol.

The intercepts on the zero concentration axis are read from the curves and tabulated under the heading P_0 in Table IV. In order to check these values against the simple Debye theory, one might proceed in either of two ways. On theory the products P_0T when plotted against T should lead to a straight line whose slope is the molecular refraction extrapolated to long wave-lengths, and whose intercept furnishes a value from which the electric moment u can be calculated. Unfortunately, the data extend over a small temperature range, and the nature of the work is such that precise values of P_0 can not be obtained; such a test is therefore not applicable with any

degree of precision. It is true that L. Lange[15] has used the equivalent of this method to calculate the electric moment of the molecule. Critical inspection of her data will show, however, that the intercepts are so poorly defined, due both to extreme scarcity of points under a concentration 0.10 and to

TABLE IV

Methyl alcohol. Calculation of the electric moment u. (Benzene used as solvent).

T	P_0	$(P_0-A)T=B$	u
10°C	67.1	16670	1.64×10^{-18}
20	65.2	16700	1.64
30	63.3	16700	1.64
40	61.2	16590	1.64
50	59.2	16470	1.63
60	57.0	16250	1.62
		Mean value of u	$=1.64\times10^{-18}$

inconsistencies in density and dielectric data, that the calculated moments mean little. Even with the present data, which certainly define the zero concentration intercepts better than any data in print, this procedure of calculation leads to values of the electric moment u whose extreme limits may differ by as much as 20 percent in some cases.

The second method of checking the experimental values of P_0 against theory makes use of the molecular refraction taken from optical data. This procedure is open to the objection that this value may be in error due to infrared absorption; on the other hand, the electric moment u is not seriously affected by small errors in this constant. Following this procedure, the molecular refraction for methyl alcohol, 8.2, is subtracted from the P_0 values. These differences multiplied by the absolute temperature should give a constant B, column three of Table IV. The electric moment is calculated at each temperature, and the results shown in the last column of the table. The constancy is apparent. The slight falling off at the two higher temperatures may possibly be due to inadequate correction for the effects of evaporation.

TABLE V

Electric moments of methyl alcohol calculated from data on the pure liquid.

T	u
−100°C	$.839\times10^{-18}$
−70	.926
−40	1.007
−10	1.086
0	1.113
20	1.162

The present constancy of electric moment is in contrast with the variable value obtained by similar calculations from data for the pure liquid methyl alcohol. As far as the author knows, data on the pure liquid are not available for the temperature range here used. Data cited by Smyth,[16] however, extend from −100° to 20°C. The author has calculated the electric moment at various temperatures from these data, again taking the constant A as 8.2. The results are shown in Table V. These values

[15] L. Lange, Zeits. f. Physik **33**, 169–182 (1925).
[16] C. P. Smyth, Phil. Mag. **45**, 860 (1923).

are much lower than those found by the author; furthermore, the moment increases steadily with rising temperature. The average increase for a 10° temperature interval is approximately 0.03×10^{-18}. The last column of Table IV shows that no variation comparable with this exists in the present data. The present average value of 1.64×10^{-18} agrees exactly with the value found by Debye,[17] using the same procedure as here followed, at a single temperature 16°C. It also agrees rather closely with the value 1.61×10^{-18} found by Jona[18] from data on vapor alcohol. The data on vapor are not subject to the effects of association; hence, the agreement may be taken as an indication that these effects have been pretty well eliminated by the low concentration work.

TABLE VI

Methyl alcohol in carbon tetrachloride. Summary of dielectric constant and density values.

T	$c_2=0$	.02219	.02566	.02819	.03867	.04358	.05390	.06162	.07089
−18°	2.297	2.351	2.358	2.365	2.396	2.409	2.447	2.476	2.514
	1.6643	1.6564	1.6551	1.6542	1.6505	1.6487	1.6450	1.6421	1.6385
−10°	2.281	2.338	2.345	2.353	2.383	2.397	2.434	2.463	2.499
	1.6505	1.6428	1.6416	1.6407	1.6371	1.6354	1.6317	1.6289	1.6254
0°	2.262	2.322	2.329	2.336	2.367	2.380	2.417	2.446	2.480
	1.6322	1.6248	1.6236	1.6228	1.6193	1.6176	1.6141	1.6114	1.6081
10°	2.242	2.304	2.312	2.318	2.350	2.362	2.399	2.428	2.461
	1.6130	1.6060	1.6048	1.6041	1.6006	1.5991	1.5957	1.5930	1.5898
20°	2.221	2.286	2.294	2.300	2.332	2.344	2.381	2.409	2.441
	1.5938	1.5871	1.5860	1.5852	1.5820	1.5804	1.5772	1.5747	1.5716
30°	2.200	2.266	2.275	2.282	2.313	2.326	2.363	2.389	2.421
	1.5746	1.5681	1.5671	1.5663	1.5632	1.5618	1.5587	1.5563	1.5533
40°	2.180	2.245	2.255	2.262	2.293	2.307	2.343	2.368	2.400
	1.5554	1.5492	1.5482	1.5475	1.5446	1.5432	1.5402	1.5379	1.5351
50°	2.159	2.222	2.234	2.242	2.272	2.287	2.321	2.346	2.378
	1.5360	1.5301	1.5292	1.5285	1.5257	1.5243	1.5216	1.5194	1.5165
60°	2.138	2.199	2.211	2.221	2.252	2.265	2.299	2.323	2.354
	1.5166	1.5111	1.5102	1.5095	1.5068	1.5055	1.5029	1.5008	1.4981

The author has also tested the present data by plotting P_0T against T. This procedure avoids taking the constant A from refractive data. As has already been mentioned, the intercepts are not sufficiently precise and do not extend over a sufficiently large temperature range to test the linearity of the resulting curve. However, if a straight line be drawn through any pair of points, or an average straight line through the whole group, it is apparent that the data can in no way lead to an imaginary electric moment, as do data on pure liquid methyl alcohol. The extreme values of electric

[17] Marx, Handbuch der Radiologie, **6**, 627 (1925).

[18] M. Jona, Phys. Zeits. **20**, 19 (1919).

moment which can be obtained by drawing any just straight line through the group of points are 1.60×10^{-18} and 1.75×10^{-18}. The value found above falls within this range.

Methyl alcohol in carbon tetrachloride. A similar procedure was followed, again using methyl alcohol, this time in carbon tetrachloride as solvent. Dielectric constant and density data are summarized in Table VI. The molecular polarization of the particular sample of carbon tetrachloride used here as solvent showed no consistent variation with temperature; the average value 27.91 was therefore used in the calculations. The molecular polarizations calculated for the dissolved alcohol for various concentrations and temperatures are plotted in Fig. 5. The curves are produced to the zero

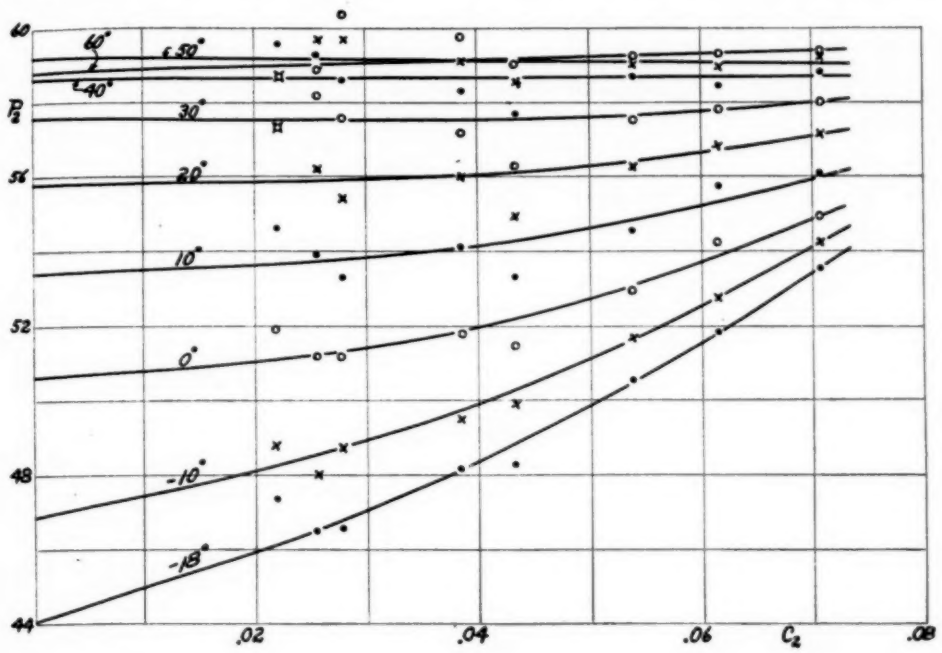

Fig. 5. Polarization curves for methyl alcohol. (Carbon tetrachloride used as solvent).

concentration axis as before, though the intercepts are by no means as well defined.

It is apparent that these data are not even qualitatively in agreement with the simple Debye theory; on theory the molecular polarization should decrease with rising temperature, while actually it increases. The author does not believe this can be construed as evidence against the Debye theory; rather, there are probably large association effects existing at the lowest concentrations used, and the intercepts obtained by extrapolating therefore do not give the polarization in the unassociated state. There are two features of the curves which are noticeable. First and most important, the curves become closer together at high temperatures and even tend to reverse their upward shift with rising temperature, as they would have to do to be quali-

tatively in accord with theory. Secondly, the curves at the higher temperatures are more nearly horizontal. Each of these facts may be taken as an indication that the effects of association decrease with rising temperature. If the quite reasonable assumption that the effects of association approach zero at sufficiently high temperatures be made, the values of $(P_0-A)T$ plotted against T would be expected to approach a constant value at high temperatures. The experimental values of $(P_0-A)T$ are plotted against T

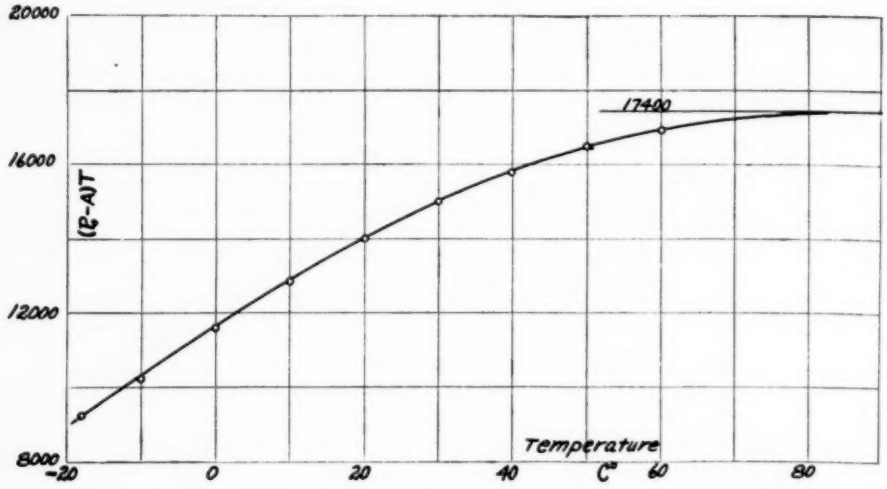

Fig. 6. For methyl alcohol. (Carbon tetrachloride used as solvent).

in Fig. 6. The tendency of the curve to become horizontal at high temperatures is quite noticeable. If it be assumed that the value 17,400 approached asymptotically represents the value of $(P_0-A)T$ when the alcohol is unassociated, the electric moment can be calculated. This leads to a value 1.67×10^{-18} which agrees rather well with the value 1.64×10^{-18} found for methyl alcohol when used in benzene.

TABLE VII

Ethyl alcohol in benzene. Summary of dielectric constant and density values.

T	$c_2=0$	.00551	.01000	.01682	.02157	.02709	.03333	.04144	.05133	.05919	.07080
10°	2.300	2.324	2.345	2.375	2.396	2.422	2.451	2.489	2.540	2.581	2.643
	.8897	.8895	.8893	.8890	.8888	.8886	.8884	.8881	.8877	.8874	.8870
20°	2.280	2.302	2.322	2.351	2.371	2.397	2.425	2.462	2.511	2.551	2.611
	.8794	.8792	.8790	.8787	.8785	.8783	.8781	.8778	.8774	.8771	.8767
30°	2.259	2.280	2.299	2.327	2.347	2.371	2.399	2.434	2.481	2.519	2.577
	.8687	.8685	.8683	.8680	.8678	.8676	.8674	.8671	.8667	.8664	.8660
40°	2.238	2.258	2.276	2.303	2.321	2.344	2.370	2.404	2.449	2.485	2.540
	.8579	.8577	.8575	.8572	.8570	.8568	.8566	.8563	.8559	.8556	.8552
50°	2.217	2.236	2.253	2.278	2.295	2.317	2.342	2.374	2.416	2.450	2.503
	.8470	.8468	.8466	.8463	.8461	.8459	.8457	.8454	.8450	.8447	.8443
60°	2.195	2.213	2.229	2.253	2.269	2.289	2.311	2.342	2.381	2.416	2.464
	.8361	.8359	.8357	.8354	.8352	.8350	.8348	.8345	.8341	.8338	.8334
70°	2.172	2.189	2.203	2.226	2.241	2.259	2.281	2.309	2.346	2.377	2.424
	.8251	.8249	.8247	.8244	.8242	.8240	.8238	.8235	.8231	.8228	.8224

Ethyl alcohol in benzene. Solutions of ten different concentrations were studied. Dielectric constant and density data for various concentrations and temperatures are collected in Table VII. The molecular polarizations calculated for the dissolved alcohol are plotted in Fig. 7. The curves are again extended to the zero concentration axis to obtain the values P_0, small weight being given to the points at concentrations under 0.02 for the reason already mentioned. The value of A is taken equal to 12.7 from refractive data, and the electric moment calculated for various temperatures. The

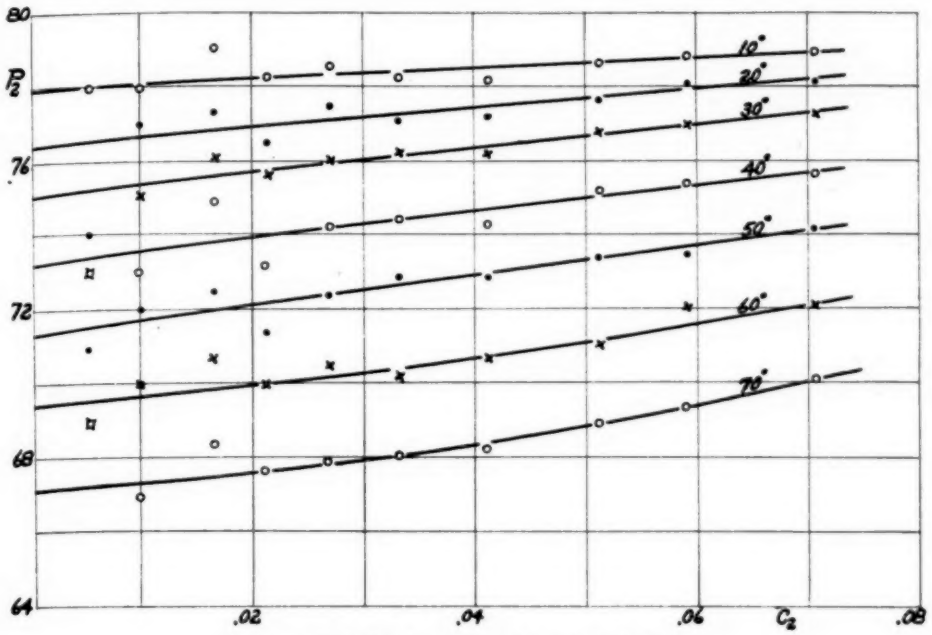

Fig. 7. Polarization curves for ethyl alcohol.

resulting values are shown in the third column of Table X near the end of the paper. The value is essentially independent of temperature, as it should be on the Debye theory.

The constancy of the moment found from the present data is in contrast with the variable, and lower value found from data on pure liquid ethyl alcohol. The values[19] for the pure liquid are shown in the fourth column of Table X. The average moment found by the author, 1.74×10^{-18}, agrees fairly well with the value 1.79×10^{-18} as calculated from data by Bädeker[20] on the vapor, using A equal to 12.7. It is somewhat larger than the value 1.66×10^{-18} found by Debye,[21] following the same procedure as here followed, at a single temperature. These values are all markedly higher than the value 1.11×10^{-18} recently reported by Sänger[22] from data on vapor at sufficiently high temperatures.

[19] Calculated from data cited in Marx, Handbuch der Radiologie, **6**, 625 (1925).
[20] K. Bädeker, Zeits. f. Phys. Chem. **36**, 315 (1901).
[21] Marx, Handbuch der Radiologie **6**, 632 (1925).
[22] R. Sänger, Phys. Zeits. **28**, 455 (1927).

As in the case of methyl alcohol, in order to avoid taking the constant A from refractive data, values of P_0T were plotted against T. A straight line drawn through any pair of points, or an average straight line drawn through the group, can in no way lead to an imaginary moment, as do the data on pure liquid ethyl alcohol. The extreme values of electric moment that can be obtained by drawing any just straight line through the group of points are 1.50×10^{-18} and 1.78×10^{-18}. The value found above falls within these limits.

TABLE VIII

Propyl alcohol in benzene. Summary of dielectric constant and density values.

T	$c_2=0$	.01002	.01667	.02205	.02714	.03360	.04402	.05501
10°	2.300	2.343	2.374	2.397	2.422	2.449	2.501	2.556
	.8897	.8889	.8884	.8880	.8876	.8871	.8864	.8856
20°	2.280	2.321	2.351	2.373	2.397	2.424	2.475	2.529
	.8794	.8786	.8781	.8777	.8773	.8768	.8761	.8753
30°	2.259	2.298	2.327	2.349	2.372	2.397	2.448	2.501
	.8687	.8679	.8674	.8670	.8666	.8661	.8654	.8646
40°	2.238	2.275	2.303	2.324	2.345	2.370	2.419	2.470
	.8579	.8571	.8566	.8562	.8558	.8553	.8546	.8537
50°	2.217	2.251	2.277	2.297	2.317	2.342	2.388	2.437
	.8470	.8462	.8457	.8453	.8449	.8445	.8438	.8429
60°	2.194	2.227	2.251	2.269	2.289	2.312	2.357	2.404
	.8361	.8353	.8348	.8344	.8341	.8336	.8328	.8319
70°	2.172	2.202	2.225	2.243	2.261	2.281	2.325	2.370
	.8251	.8243	.8238	.8235	.8231	.8226	.8218	.8209

Propyl alcohol in benzene. Solutions of seven different concentrations of iso-propyl alcohol in benzene were studied. Dielectric and density data are collected in Table VIII. The molecular polarizations of the alcohol at various concentrations and temperatures are plotted in Fig. 8.

It should be mentioned here that the author does not consider the dielectric data on propyl alcohol solutions as reliable as that on the other alcohols. Even though an effort was made to remove traces of water from the propyl alcohol, sufficient water remained to cause temporary clouding of the solutions for the higher concentrations. No such clouding occurred in solutions of other alcohols.

Taking A equal to 17.4 from refractive data, values of electric moment u were calculated from the P_0 intercepts at various temperatures; they are shown in column five of Table X. The constancy of u is in agreement with theory. The average moment 1.75×10^{-18} is somewhat higher than the value 1.66×10^{-18} found by Debye,[23] following a similar procedure at a single temperature.

[23] Marx, Handbuch der Radiologie, **6**, 627 (1925).

In order to avoid taking the constant A from refractive data, values of P_0T were again plotted against T. Straight lines drawn justly through the group of points limit the electric moment to some value between 1.60×10^{-18} and 1.85×10^{-18}. The value found above falls within these limits.

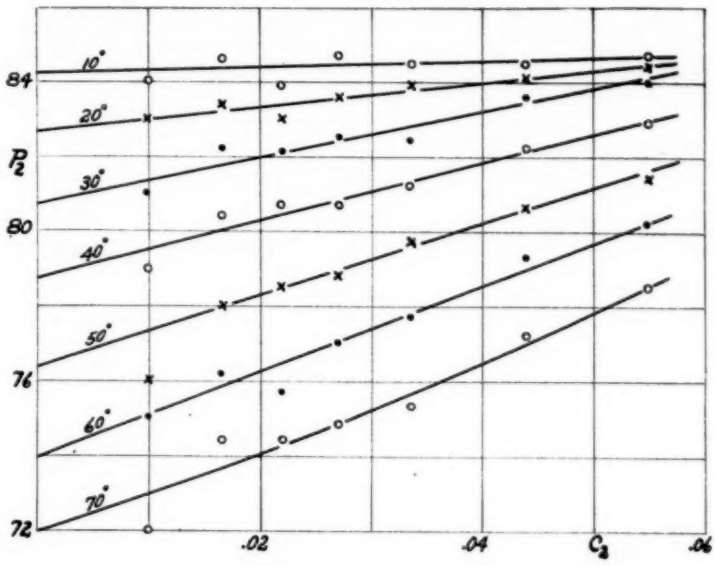

Fig. 8. Polarization curves for propyl alcohol.

Amyl alcohol in benzene. Solutions of eleven different concentrations of iso-amyl alcohol in benzene were studied. Dielectric and density data are summarized in Table IX. The molecular polarizations of the alcohol are plotted in Fig. 9.

TABLE IX

Amyl alcohol in benzene. Summary of dielectric constant and density values.

T	$c_2=0$	.01028	.01578	.01677	.02261	.02661	.03190	.03662	.04102	.05001	.05906	.06900
10°	2.300	2.337	2.357	2.361	2.383	2.398	2.420	2.439	2.457	2.494	2.531	2.573
	.8897	.8885	.8879	.8877	.8871	.8867	.8861	.8857	.8853	.8846	.8840	.8833
20°	2.279	2.315	2.334	2.338	2.359	2.374	2.396	2.414	2.432	2.470	2.508	2.550
	.8794	.8782	.8776	.8774	.8768	.8764	.8758	.8754	.8750	.8743	.8737	.8730
30°	2.258	2.291	2.310	2.313	2.334	2.349	2.370	2.388	2.406	2.444	2.482	2.525
	.8687	.8675	.8669	.8667	.8661	.8657	.8651	.8647	.8643	.8636	.8631	.8624
40°	2.236	2.268	2.286	2.289	2.309	2.323	2.344	2.361	2.379	2.415	2.453	2.497
	.8579	.8567	.8561	.8559	.8554	.8550	.8544	.8540	.8536	.8529	.8523	.8516
50°	2.214	2.244	2.262	2.265	2.284	2.298	2.317	2.334	2.351	2.386	2.424	2.466
	.8470	.8458	.8453	.8451	.8445	.8441	.8435	.8431	.8427	.8420	.8414	.8407
60°	2.192	2.221	2.237	2.240	2.259	2.272	2.290	2.307	2.323	2.356	2.392	2.433
	.8361	.8349	.8344	.8342	.8336	.8332	.8326	.8322	.8318	.8311	.8306	.8299
70°	2.170	2.197	2.213	2.216	2.233	2.246	2.263	2.279	2.294	2.325	2.358	2.396
	.8251	.8239	.8234	.8232	.8226	.8222	.8217	.8213	.8209	.8202	.8196	.8189

Taking A equal to 26.6 from refractive data, values of electric moment were calculated from the P_0 intercepts at various temperatures; they are

shown in the last column of Table X. The constancy of the value is in agreement with the demands of the Debye theory. The average moment found is 1.62×10^{-18}.

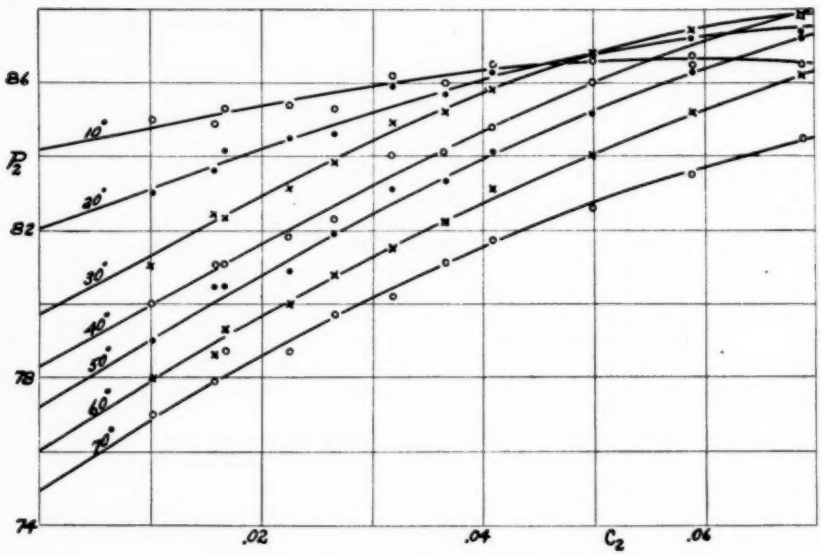

Fig. 9. Polarization curves for amyl alcohol.

In order to avoid taking A from refractive data, values of P_0T were again plotted against T. Straight lines drawn justly through the group of points furnish extreme limits for the moment equal to 1.41×10^{-18} and 1.67×10^{-18}. The value found above falls within these limits.

Summary and Discussion of Results

The electric moments of methyl, ethyl, propyl, and amyl alcohol have been determined through a study of dilute solutions of these in benzene, at various

Table X

Summary of moments found. The figures given are electric moments times 10^{18}.

T	Methyl alcohol	Ethyl alcohol		Propyl alcohol	Amyl alcohol
10°C	1.64	1.73	1.34*	1.75	1.62
20	1.64	1.73	1.37	1.76	1.62
30	1.64	1.74	1.40	1.76	1.61
40	1.64	1.75	1.42	1.76	1.62
50	1.63	1.75	1.45	1.75	1.62
60	1.62	1.74	1.47	1.74	1.63
70		1.73	1.50	1.74	1.64
Mean	1.64	1.74		1.75	1.62

* Calculated from data on the pure liquid, taking A from refractive data.

temperatures. The moments in each case come out essentially independent of temperature, as is apparent from Table X summarizing results. The

independence of moment upon temperature is in agreement with the Debye theory; it is in marked contrast with the variable moments found from data on the pure liquid alcohols; the data therefore lend weight to the supposition that the failure of the simple theory for pure polar liquids is due to association phenomena.

If use of the molecular refraction for the constant A is avoided by plotting P_0T against T, it is apparent that no straight line drawn through any pair of points can lead to an imaginary moment for any of the alcohols studied; data on the pure liquids are known to lead to imaginary moments. If straight lines with the extreme slopes justified by the data be drawn through the group of points for any alcohol, the moment so found is limited to a range whose extremes differ by not more than 20 percent. In every case the moments found through use of the molecular refraction fall within these ranges.

It would be highly desirable to have still more accurate dielectric data over a greater temperature range; this available, the linearity of the P_0T versus T curve could be tested, and the moment could be determined more accurately without making use of the molecular refraction. The greater temperature range might be procured by using a solvent other than benzene. Judging from data here presented, carbon tetrachloride would not be suitable; carbon disulphide or toluene might serve. To define the intercept at any particular temperature more accurately, it is necessary to have dielectric data to more than four significant figures. Two difficulties seem to prohibit this; the first is evaporation of the solute; the second is the formation of vapor bubbles within the liquid in the test condenser at the higher temperatures. Errors due to the first of these could probably be eliminated by suitable precautions. The author found the second difficulty very troublesome. Fortunately, the experimental method was such as to allow rapid adjustment following disappearance of a vapor bubble; the reading corresponding to maximum capacity of the test condenser was taken as that free from the presence of bubbles. Boiling the components of the solution before using eliminated part of the difficulty, possibly by driving off absorbed gases. At best the uncertainty was sufficient to preclude the possibility of obtaining reliable data to more than four significant figures.

RYERSON PHYSICAL LABORATORY,
UNIVERSITY OF CHICAGO,
January 1, 1928.

THE ELECTRIC MOMENT OF ALKALI ATOMS

By J. J. Weigle

Abstract

The electric moments of atoms can be calculated if we know the constant a of van der Waals. This constant can be obtained from the vapor pressure equation. Thus for all the substances for which the vapor pressure curve has been determined it is possible to calculate the electric moment or the electric moment of inertia. These computations have been made for the alkali atoms giving 0.18×10^{-18}, $0.24+10^{-18}$, 0.24×10^{-18}, gr$^{1/2}$ cm$^{3/2}$ sec$^{-1}\epsilon$ as the electric moments of Na, K, Rb respectively. These values although not very accurate are interesting, for Bohr's picture of the alkali atom, with the penetrating orbit of the valence electron precessing around the nucleus, gives no electric moment. The values above are so small as to be negligible and thus in accord with the theory.

IT IS well known that if we consider the molecules or atoms as made up of movable electric charges, such molecules placed in an electric field will be polarized. Debye[1] has assumed that this polarization is directly responsible for the forces of cohesion of van der Waals, and has thus calculated the equation of state of the gases composed of such molecules. He obtained an expression for the coefficient a of van der Waals as a function of the polarizability of the molecule, and of the distribution of the charges in it. This polarizability is measured by the electric moment induced when the molecule is placed in an electric field and can be obtained experimentally by measuring the index of refraction of the substance or the variation of its dielectric constant with the applied field; for the polarizability is the property of the molecules which is responsible for the index of refraction being different from unity. However the dielectric constant may be different from unity for two reasons the first and most important being the orientation, in the field, of molecules having a permanent electric moment, the second being this polarizability. Following Debye the molecules can be classified in two groups according to their electrical symmetry. If r be the distance of a point from a molecule at the origin composed of z charges $e_k(k=1, 2, 3, \cdots, z)$ coordinates $x_k y_k z_k$ the potential at this distance $r=(x^2+y^2+z^2)^{1/2}$ is (as given by Debye)

$$\phi=\frac{\Sigma e_k}{r}+\frac{1}{r^2}\left\{\frac{x}{r}\Sigma e_k x_k+\frac{y}{r}\Sigma e_k y_k+\frac{z}{r}\Sigma e_k z_k\right\}$$
$$-\frac{1}{r^3}\left\{\left(\frac{1}{r}-\frac{3}{2}\,\frac{x}{r^2}\right)\Sigma e_k x_k^2+\cdots+\cdots\right\}-\cdots$$

As $\sum e_k=0$ for a neutral molecule, ϕ depends on the electric moment of components $\sum e_k x_k$, etc., and on the electric moment of inertia of components

[1] Debye, Phys. Zeits. **21**, 179 (1920).

(tensor) $\sum e_k x_k^2$, etc. If $\sum e_k r_k \neq 0$ the molecule is called a dipole, as the centers of charge of the positive and negative charges do not coincide. If however the electric moment is zero (rare gases for instance) the potential is due to the electric moment of inertia, the molecule is called a quadrupole.

The van der Waals cohesive forces are not directly due to the attraction or repulsion of these electric moments, for on the average such actions would cancel each other; however when the polarizability of the molecule is taken into account the following processes take place: If two molecules are ordered in such a way that their permanent moments repel each other, each receives an additional moment (opposite to the first) because it is polarized by the field of the other molecule. As they move away this superimposed moment decreases (since the field decreases) and the force of repulsion becomes less or we may say that an attraction is superposed. If the two molecules had been disposed in such a way as to attract each other, the moment arising from the polarization would be in the same direction as the permanent moment and, when the two molecules move toward each other, this additional moment would become greater and so would the force of attraction. In both cases the effect of polarization is thus to produce attraction and, on averaging, this force cannot become zero. Falkenhagen[2] has calculated the second virial coefficient B of the equation of state of a gas formed of molecules having a permanent electric moment μ and a polarizability α. He obtained

$$B=\frac{2\pi}{3}Nd^3\left(1-b_1\frac{\theta}{T}-b_2\left(\frac{\theta}{T}\right)^2-\cdots\right) \tag{1}$$

N is Avogadro's number, d the diameter of the molecules, $\theta=\mu^2/kd^3$ where k is Boltzman's constant, $b_1=4z$, $b_2=3.33\ 10^{-1}+3.27z^2\cdots$ where $z=\alpha/d^3$. The value of α can be computed from the molecular refraction P_0 by using the equation

$$P_0=4\pi\alpha/3 \tag{2}$$

Falkenhagen compared the value of B obtained experimentally from the isothermals of a gas with that calculated from (1), knowing μ from the variation of the dielectric constant with the temperature. He found a very satisfactory agreement. If we want to express B as a function of van der Waals constants a and b we have to transform slightly the equation of state. Instead of

$$(p+a/v^2)(v-b)=RT$$

we can write for small densities

$$\frac{pv}{RT}=1+\frac{b-a/RT}{v}+\frac{b^2}{v^2}+\cdots.$$

[2] Falkenhagen, Phys. Zeits. **23**, 87 (1922).

and comparing with the virial equation of Kammerlingh Onnes

$$\frac{pv}{RT}=A+\frac{B}{v}+\frac{C}{v^2}+\cdots.$$

we find

$$B=b-(a/RT) \tag{3}$$

and we know that $b=(2\pi/3)Nd^3$, that is 4 times the volume of the molecules. Thus the experimental values of a and b, or B may be used to calculate the electric moment μ of the molecules.

For the metals we do not possess any experimental data concerning their equation of state, but we do have their vapor pressure curves. Now Planck[3] has given an equation for the vapor pressure as a function of van der Waals constants. This expression is easily obtained by integrating the relation

$$p=\frac{1}{v_1-v_2}\int_1^2 pdv$$

where the indexes 1 and 2 refer to the liquid and gaseous states. By using van der Waals expression for p, van Laar[4] obtains

$$\log p=-a/v_0RT-B\log T-CT+D$$

where v_0 is the volume of the gas at $T=0$, B, C and D are constants.

Thus by means of (3), (2) and (1), if we assume

$$(2\pi/3)Nd^3=4v_0$$

we can calculate the electric moment of the atoms from their vapor pressure curves. Van Laar[5] has already calculated v_0 and a for the alkali atoms from the experimental values of the vapor pressure p and we shall use his result to carry the calculations further. Table I shows the values of v_0 of a and of P_0.

TABLE I

van der Waals constants for alkali metals

v_0(cm³/mole)	a(dynes cm⁴/mole²)		P_0(cm³/mole)
	Na	K	Rb
v_0	22.25	43.25	52.35
$a\times10^{-10}$	3.365	5.250	5.825
P_0	62.7	107	110

The values of the molecular refraction P_0 are taken from Herzfeld.[6] With these values we obtain for $10^{18}\mu$ in $gr^{1/2}\,cm^{3/2}\,sec^{-1}\,\epsilon$ the following values .18, .24, and .27 for Na, K and Rb respectively. It is true that this is a

[3] Planck, Thermodynamik p. 282 (6th edition).

[4] van Laar, Zustandgleichung p. 267.

[5] van Laar, Zeit. fur Anorg. Chemie 146, 263, and 148, 235 (1925).

[6] Herzfeld, Phys. Rev. **29**, 701 (1927).

very inaccurate way of determining the electric moment of atoms, for it is well known that the sodium vapor for instance, is composed of molecules Na_2 and of atoms. However, an investigation of the dielectric constant of metallic vapors is being carried out at the present time in our department and it is hoped that it will yield much more accurate values of the electric moment.

It is interesting to compare the values obtained above with those calculated from Bohr's theory of the atom. The valence electron of the alkalis is on a very elliptical orbit (for sodium a 3_1 orbit) which goes far outside of the other electronic shells. This orbit, being of the penetrating type, precesses very rapidly around the rest of the atom as Hoyt[7] has shown and thus the electrical dissymmetry of the atom is destroyed on the average by this precession and we would expect no electric moment. The values we have obtained above are so small, as will be shown below, as to be negligible and are thus more or less a verification of the theory of precessing penetrating orbits. If the orbit had not been precessing we would have expected an electric moment approximately equal to $e\bar{r}$ where e is the charge of the electron, and $\bar{r}$ its average distance from the nucleus. The value of $\bar{r}$ is[8]

$$\bar{r}=a(1+\tfrac{1}{2}\epsilon^2)$$

where ϵ is the eccentricity of the ellipse and a the major axis. If we take for a the value 10^{-8} cm and for ϵ, $(8/3)^{1/2}$ for a 3_1 orbit, we find $\bar{r}=1.44\ 10^{-8}$ cm and

$$\mu=e\bar{r}=6.910^{-18}gr^{1/2}cm^{3/2}\ \sec^{-1}\epsilon.$$

which is obviously incompatible with the electric moment of sodium derived above.

If we had assumed that the electric moments of the alkali atoms were zero, we could have calculated instead the electric moments of inertia by the method of Debye.[1]

PHYSICS DEPARTMENT
UNIVERSITY OF PITTSBURGH
December 1927.

[7] Hoyt, Phys. Rev. 25, 174 (1925).
[8] Born, Vorlesungen uber Atommechanik p. 164.

A NOTE ON THE MAGNETIC SUSCEPTIBILITY OF SOLUTIONS

By J. J. Weigle

Abstract

It is shown that, when a solution of ions of different magnetic susceptibilities is placed in a magnetic field, there is a difference between the concentrations of the solute in the field and outside of the field. This difference, however, is so small that it can hardly be measured experimentally; therefore, it cannot vitiate the measurements of the magnetic susceptibility of solutions by the classical methods.

WHEN a particle of magnetic moment μ is placed in a non-homogeneous magnetic field of intensity $H(x)$, this particle experiences a force given by $\mu\, dH/dx$. All atoms or ions possess a magnetic moment in a magnetic field. This moment is either permanent (paramagnetism) or induced by the field following the Larmor rotation (diamagnetism). Thus, when a non-homogeneous field is applied to a solution, the ions will be subjected to a force of attraction or repulsion, depending on their para- or diamagnetism and which varies with their susceptibilities. The motion of the ions, would, in general, produce a different concentration of positive and negative charges, but the electric field intensity dv/dx where V is given by $\triangle \mathbf{v} = -4\pi\rho$, ρ being the density of electricity, would be so great compared to the magnetic force or the diffusion, that we will assume the solution to be electrically neutral at every point. When a gradient of concentration is established, the ions will tend to diffuse back and an equilibrium will be reached. It is the conditions of this equilibrium we wish to investigate.

2. Let us suppose that we have a cylindrical container of cross section q, the x axis of our coordinates corresponding to the axis of the container. A magnetic field of intensity $H(x)$ is placed along the x axis, $H(x)$ increasing with x and such that $H(0)=0$.

We have dissolved $N_1\ N_2 \cdots N_i \cdots N_s$ ions of charge $z_1\epsilon,\ z_2\epsilon \cdots z_i\epsilon \cdots z_s$. in the volume V; as the solution is electrically neutral

$$\sum_{i=1}^{s} N_i z_i = 0.$$

The ionic concentrations or the number of ions per unit volume will be denoted by $n_1, n_2, \cdots, n_i, \cdots, n_s$. An ion i has an average magnetic moment in the direction of the field given by

$$\mu_i = \sigma_i H$$

where $\sigma_i = \mathrm{X}_m/N$ if X_m is the molecular susceptibility of the ion and N Avogadro's number, for the diamagnetic moment is proportional to the field inducing it, and the paramagnetic average moment is due to the orientation by the field of the permanent moment.

Let us now calculate the forces acting on an ion. The magnetic force is $\mu_i(dH/dx)=\sigma_i H(dH/dx)$. The electric force is $z_i\epsilon(dV/dx)$ where dV/dx is the field intensity producted by the distribution of the ions of different signs.

The force due to the diffusion is easily obtained if we consider that the osmotic pressure is responsible for this force.[1]

If we take a slice of thickness dx of the solution, on one side there is a concentration $n_i(x)$ of the ions of type i, on the other side $n_i(x+dx)$. The osmotic pressure due to the i ions will then be $p_i(x)$ and $p_i(x+dx)$ so that the total resultant force acting on the volume qdx is

$$-(dp_i/dx)qdx$$

and the force per ion will be

$$-dp_i/ndx$$

as there are n_iqdx ions in the volume qdx.

We shall now assume that the solution follows van t'Hoff Law of osmotic pressure. It will be shown further that for strong electrolytes, for which van t'Hoff Law does not hold, we have to introduce a correction factor which does not greatly modify our conclusions. Then $p_i=n_ikT$ (T absolute temperature, k Boltzmann's constant), and

$$-dp_i/n_idx=-kTdn_i/n_idx$$

When the equilibrium is reached the sum of the forces acting upon the ion must equal zero.

$$-kTdn_i/n_idx+z_iedV/dx+\sigma_iHdH/dx=0 \quad (i=1,2,\cdots,i\cdots s) \tag{1}$$

Between any two equations (1) we can eliminate dV/dx which gives us

$$-kT\left(\frac{z_i}{n_j}\frac{dn_j}{dx}-\frac{z_j}{n_i}\frac{dn_i}{dx}\right)+H\frac{dH}{dx}(\sigma_jz_i-\sigma_iz_j)=0$$
$$(j=1,2,\cdots,i-1,i+1,\cdots,s)$$

or integrating

$$kT\log\left(\frac{n_j}{n_j^0}\right)^{z_i}\left(\frac{n_i^0}{n_i}\right)^{z_j}=\frac{H^2}{2}(\sigma_jz_i-\sigma_iz_j)$$

where the n^0's are the concentrations at $H=0$ or $x=0$. Solving for n_j we have

$$n_j=n_j^0(n_i/n_i^0)^{z_j/z_i}e^{H^2(\sigma_jz_i-\sigma_iz_j)/2kTz_i} \quad (j=1,2,\cdots,i-1,i+1,\cdots,s) \tag{2}$$

Now to adjust n_i so as to satisfy the condition of electrical neutrality at every point

$$\sum_{j=1}^{s}n_jz_j=0 \tag{3}$$

[1] Nernst, Zeits. f. Phys. Chemie **2**, 613 (1888).

Replacing (2) in (3)

$$n_i z_i + \sum_j{}' z_j n_j^0 (n_i/n_j^0)^{z_j/z_i} e^{H^2(\sigma_j z_i - \sigma_i z_j)/2kTz_i} = 0 \tag{4}$$

The accent on the summation meaning that we must omit the term $j=i$ in the addition. As n_i/n_i^0 is very nearly unity we can write

$$(n_i/n_j^0)^{z_j/z_i} = 1 + (z_j/z_i)(n_i/n_i^0 - 1) + \cdots$$

and (4) becomes

$$n_i z_i + \sum_j{}' z_j n_j^0 e^{H^2(\sigma_j z_i - \sigma_i z_j)/2kTz_i}\left(1 - \frac{z_j}{z_i}\right) + \frac{n_i}{n_i^0}\sum_j{}' \frac{z_j^2}{z_i} n_j^0 e^{H^2(\sigma_j z_i - \sigma_i z_j)/2kTz_i} = 0$$

or

$$\frac{n_i}{n_i^0} = \frac{\sum_j z_j n_j^0 e^{H^2(\sigma_j z_i - \sigma_i z_j)/2kTz_i}(z_j - z_i)}{\sum_j z_j^2 n_i^0 e^{H^2(\sigma_j z_i - \sigma_i z_j)/2kTz_i}} \tag{6}$$

For the other ions we would have

$$\frac{n_j}{n_j^0} = \left[\frac{\sum_j z_j n_j^0 e^{H^2(\sigma_j z_i - \sigma_i z_j)/2kTz_i}(z_j - z_i)}{\sum_j z_j^2 n_j^0 e^{H^2(\sigma_j z_i - \sigma_i z_j)/2kTz_i}}\right]^{z_j/z_i} e^{H^2(\sigma_j z_i - \sigma_i z_j)/2kTz_i}$$

The n^0's would have to be determined from the equations $\int n_i dx = N_i$. The solution of our problem is then given by (6) and (7).

3. *Application to N_iSO_4.* This salt is dissociated into two ions Ni^{++} and SO_4^{--}. Thus $s=2$ and $z_1 = -z_2$. The molecular susceptibilities are for *Ni*, $\chi_m = 1.5\ 10^{-3}$ cm/mole and for SO_4, $\chi_m = -3.8\ 10^{-5}$ cm/mole. This gives $\sigma_1 = 2.5\ 10^{-27}$ cm and $\sigma_2 = -6.3\ 10^{-29}$ cm. We will assume $T = 300°K$ and $H = 10{,}000$ gausses.

Equation (3) becomes

$$2n_1 - 2n_2 = 0 \qquad n_1 = n_2 = n$$

and

$$2n_1^0 - 2n_2^0 = 0 \qquad n_1^0 = n_2^0 = n^0$$

Equation (6) finally gives

$$n/n^0 = 1.0000015$$

This small value of the difference in concentrations in the field and outside, is almost impossible to detect, at least it cannot change anything in the results of the measurements of the magnetic susceptibility of solutions. The equations (6) and (7) can also be applied to a mixture of solutions but in this case again it is easy to see that n_i/n_i^0 is going to be of the same order

of magnitude as above. The theory could also be easily extended to a mixture of liquids. In this case the result is simply

$$n/n^0 = e^{\sigma H^2/2kT}$$

That is to say n/n^0 is again of the same order of magnitude.

4. If instead of van t'Hoff formula for the osmotic pressure we use the value given by the Debye and Huckel's theory,[2] we shall have to modify our equations somewhat.

$$p_k = \sum_i [n_i kT - (e^2\kappa/6D) n_i z_i^2 \eta_i]$$

where D is the dielectric constant of the solvent, $\kappa^2 = (4\pi\epsilon^2/DkT) \sum_j n_j z_j^2$ and η_i is a function of $u_i = \kappa a_i$ where a_i is the diameter of the ion.

$$\eta_i = (3/u_i^3)[(1+u_i) - 2\log(1+u_i) - 1/(1+u_i)]$$

If we follow the same procedure as before we get a very complicated expression which for a solution containing two types of ions only reduces to (supposing n_1/n_1^0 almost equal to one)

$$n_1 - n_1^0 = [(z_2\sigma_1 - z_1\sigma_2)H^2/2]/(kT/n_1^0)(z_1 - z_2) + (\epsilon^2\xi z_1 z_2/6D)\{\xi[a_1(1+2z_1) - a_2(1+2z_2)] + (1/2(n_1^0)^{1/2})(z_2 - z_1)(1+z_1 z_2)\}$$

where

$$\xi = [(4\pi\epsilon^2/DkT)(z_1^2 - z_1 z)_2]^{1/2}$$

This is again a value of the same order of magnitude as that derived from van t'Hoff equation.

PHYSICS DEPARTMENT
UNIVERSITY OF PITTSBURGH
November, 1927.

[2] Debye and Huckel, Phys. Zeit. **24**, 185 (1923).

THE ENTROPY AND THERMODYNAMIC POTENTIALS OF REAL GASES AND MIXTURES OF REAL GASES, AND A MASS ACTION LAW FOR CHEMICAL REACTION BETWEEN REAL GASES

I. GENERAL THERMODYNAMIC RELATIONS.*

By James A. Beattie

Abstract

Thermodynamic quantities for mixtures of real gases.—Using the two assumptions, that at infinitely low pressures the energies of real gases are additive and the equilibrium pressure is given by the product of the total pressure into the mol fraction, there are deduced general thermodynamic equations for the energy, heat content, entropy, thermodynamic potentials of gas mixtures and the chemical potential of a gas in a mixture in terms of the independent variables p and T, and V and T.

Mass action law for real gases.—Two forms of the mass action law are deduced depending upon the choice of p and T, or V and T as the independent variables.

1. Introduction

In this paper there is developed by the use of two assumptions a general method, which leads to equations for the energy, entropy, and heat content of mixtures of compressed real gases. By use of these results, expressions are derived for the thermodynamic potentials $F_{V,T}$ and $F_{p,T}$ of mixtures, and for the Gibb's chemical potential μ of the individual gases composing a mixture. From the latter there is then developed a general mass-action law for a chemical reaction between real gases. In the succeeding paper there will be obtained, by means of a new equation of state, integrated expressions for all of the above quantities.

It is well known that the mass action equation derived with the aid of the perfect-gas law and Dalton's partial-pressure law, is not valid for gas equilibria at higher pressures. Recently Gillespie[1] by a consideration of the Gibb's chemical potential has derived a general relation for the effect of pressure on gaseous chemical equilibria at constant temperature. This mass action equation which is based on the assumption that Dalton's law of partial pressure can be applied to real gases at infinitely low pressures is

$$lnK_f = lnK_p + (1/RT)\sum\left\{\nu_1\int_0^p [(\partial V/\partial n_1)_{T,p,n_2,n_3,\ldots} - RT/p]dp\right\} \quad (1)$$

where K_f is the equilibrium constant of the reaction at an infinitely low pressure, K_p the value at the pressure p, ν_1 the number of mols of Substance 1 in

* Contribution from the Research Laboratory of Physical Chemistry, Massachusetts Institute of Technology, No. 209.

[1] Gillespie, Jour. Amer. Chem. Soc. **47**, 305 (1925); **48**, 28 (1926).

the stoichiometric equation for the chemical reaction, and $(\partial V/\partial n_1)_{T,p,n_2,n_3,\cdots}$ the partial molal volume of Gas 1 in the equilibrium mixture. This latter quantity is obtained by differentiation of the equation of state for mixtures of the gases taking part in the chemical reaction [i.e. $f(p, V, T, n_1, n_2, \cdots) = 0$]. In general the integral of Equation (1) must be evaluated graphically. Later Gillespie[2] has transformed this expression into one which is more readily integrable.

In a series of papers,[3] van Laar and Lorenz have obtained expressions for the energy, entropy, and the thermodynamic quantities derivable from them, including a mass-action law which they applied to chemical equilibria in condensed systems.

Keyes[4] has given an equation for the entropy and energy of a mixture of gases obeying his equation of state, and has deduced from it a mass action equation for non-ideal gases.

2. The Energy and Entropy of Mixtures of Real Gases.

Let us suppose that a given mixture of gases undergoes a change in state at constant composition from one pressure and temperature (p_1, T_1) to another (p_2, T_2). The change in energy and entropy can be calculated along any reversible path. For the present calculation the path considered is: (1) change the pressure from p_1 to an infinitely low pressure at constant temperature T_1, (2) heat or cool the mixture at constant volume (or pressure) from T_1 to T_2, and (3) increase the pressure at the temperature T_2 from the low value to p_2; each of the steps being carried out reversibly. Thus all pressure variations are brought about isothermally, and all temperature variations are carried out at infinitely low pressures.[5] The assumptions used in the following derivations are summarized in Section 3.

The variations of the energy and entropy with pressure can be obtained by integrating the appropriate differential equations. The application of this method for the energy presents no unusual difficulty, but in the integration of the Maxwell Relations for the effect of pressure or of change in volume on the entropy, the integral becomes infinite at the lower limit because of the presence of a term containing $\ln p$ or $\ln V$. In the present method the lower limit of the entropy is replaced by the expression for the entropy of a mixture of perfect gases, and this contains a term which combines with the infinite term of the integral to give a finite value.

We can use either V and T, or p and T as the independent variables and this leads to two formulations.

[2] Lurie and Gillespie, Jour. Amer. Chem. Soc. **49**, 1146 (1927).

[3] van Laar and Lorenz, the fundamental equations are developed in Zeits. anorg. u. allg. Chem. **145**, 239 (1925).

[4] Keyes, Jour. Amer. Chem. Soc. **49**, 1393 (1927).

[5] van Laar and Lorenz, loc. cit., have used a similar method in the case of the energy. For the entropy of mixtures, however, they corrected the equation for the entropy of a mixture of perfect gases by a consideration of the space occupied by the molecules of the real gas.

(a) *When V and T are the independent variables.* For these independent variables we make use of the general relations for the variation of the energy and entropy of any fluid with the volume

$$(\partial U/\partial V)_T = T(\partial p/\partial T)_V - p \tag{2}$$

$$(\partial S/\partial V)_T = (\partial p/\partial T)_V \tag{3}$$

Integration of (2) and (3) along an isothermal gives

$$U - U^* = \int_{V^*}^{V} [T(\partial p/\partial T)_V - p]dV \tag{4}$$

$$S - S^* = \int_{V^*}^{V} (\partial p/\partial T)_V dV \tag{5}$$

where U and S are the energy and entropy of the system at the volume V, and U^* and S^* the values at V^*, all being taken at the same temperature. The asterisk affixed to a symbol is used to denote its value at an infinitely low pressure.

If the system under consideration is a mixture of real gases, U^* and S^* can be replaced by the equations for the energy and entropy of mixtures of perfect gases.[6] Hence

$$U^* = \sum \left\{ n_1 \left[\int_{T_0}^{T} C_{V_1}^* dT + U_{01} \right] \right\} \tag{6}$$

$$S^* = \sum \left\{ n_1 \left[\int_{T_0}^{T} C_{V_1}^* dT/T + S_{01} \right] \right\} + \sum (n_1 R \ln V^*/n_1) \tag{7}$$

In the above equations n_1 is the number of mols of Gas 1 in the mixture, V is the total volume of the mixture, C_{V1}^* the molal constant volume heat capacity of pure Gas 1 at infinitely low pressures (which in general cannot be replaced by the corresponding constant, perfect-gas value), and U_{01} and S_{01} the molal energy and entropy constants of this gas at the temperature T_0, which may be any arbitrarily chosen "standard temperature."

Substituting (6) and (7) in (4) and (5), we obtain

$$U = \int_{V^*}^{V} [T(\partial p/\partial T)_V - p]dV + \sum (n_1 u_1) \tag{8}$$

$$S = \int_{V^*}^{V} (\partial p/\partial T)_V dV + \sum (n_1 R \ln V^*/n_1) + \sum (n_1 s_1) \tag{9}$$

[6] Gibbs, Scientific Papers, Longmans, Green and Co., New York (1906), Vol. I, pp. 150 et seq.

where the quantities u_1 and s_1 are defined by the relations

$$u_1 = \int_{T_0}^{T} C_{V_1}^{*} dT + U_{01} \tag{10}$$

$$s_1 = \int_{T_0}^{T} C_{V_1}^{*} dT/T + S_{01} \tag{11}$$

They may be considered as the molal energy and entropy constants of Substance 1 at the temperature T.

Equation (9) can be written in the form

$$S = \int_{\infty}^{V} [(\partial p/\partial T)_V - \sum n_1 R/V] dV + \sum (n_1 R \ln V/n_1) + \sum (n_1 s_1) \tag{12}$$

by adding and subtracting the term $\sum (n_1 R \ln V)$, where V is the volume of $\sum n_1$ mols of mixture, and replacing the lower limit V^* by ∞. This is made possible by the fact that at low densities the pressure of real gases can be expanded in a converging power series of the inverse volume and hence the difference between p and $\sum n_1 RT/V$ is a series beginning with a term K/V^2 and containing higher powers of $1/V$. Thus the integrand of Equation (12) approaches zero with sufficient rapidity so that as V^* increases

$$\text{Limit} \int_{V^*}^{\infty} [(\partial p/\partial T)_V - \sum n_1 R/V] dV = 0$$

and hence lower limit V^* can be replaced by ∞ as is done in (12). Also for the same reason the lower limit V^* of the integral in Equation (8) can be replaced by ∞. Equations (8) and (9) then become after reversing the upper and lower limits

$$U = \int_{V}^{\infty} [p - T(\partial p/\partial T)_V] dV + \sum (n_1 u_1) \tag{13}$$

$$S = \int_{V}^{\infty} [\sum n_1 R/V - (\partial p/\partial T)_V] dV + \sum (n_1 R \ln V/n_1) + \sum (n_1 s_1) \tag{14}$$

For the study of the variations of U and S at constant temperature, the quantities u_1, u_2 $\cdots$, and s_1, s_2, $\cdots$, are constant, and if also the composition of the mixture does not change, the terms $\sum (n_1 u_1)$ and $\sum (n_1 s_1)$ are both constant.

(b) *When p and T are the independent variables.* For these independent variables we make use of the heat content H, and the other Maxwell relation

$$(\partial H/\partial p)_T = -T(\partial V/\partial T)_p + V \tag{15}$$

$$(\partial S/\partial p)_T = -(\partial V/\partial T)_p \tag{16}$$

Integration of (15) and (16) gives

$$H-H^*=\int_{p^*}^{p}[-T(\partial V/\partial T)_p+V]dp \tag{17}$$

$$S-S^*=\int_{p^*}^{p}-(\partial V/\partial T)_p dp \tag{18}$$

Applying these equations to mixtures of real gases, we can use equations corresponding to (6) and (7) for H^* and S^*, the independent variables now being p and T

$$H^*=\sum\left\{n_1\left[\int_{T_0}^{T}C_{p_1}^{*}dT+H_{01}\right]\right\} \tag{19}$$

$$S^*=\sum\left\{n_1\left[\int_{T_0}^{T}C_{p_1}^{*}dT/T+S_{01}\right]\right\}-\sum(n_1R\ln p^*x_1/RT_0) \tag{20}$$

where H_{01} and S_{01} are the molal heat content and entropy constants for Substance 1 at the temperature T_0, and x_1 is its mol fraction in the mixture.

Substitution of (19) and (20) in (17) and (18) gives

$$H=\int_{p^*}^{p}[-T(\partial V/\partial T)_p+V]dp+\sum(n_1h_1) \tag{21}$$

$$S=\int_{p^*}^{p}-(\partial V/\partial T)_p dp-\sum(n_1R\ln p^*x_1)+\sum(n_1s_1') \tag{22}$$

in which h_1 and s_1' are defined by relations corresponding to (10) and (11),

$$h_1=\int_{T_0}^{T}C_{p_1}^{*}dT+H_{01} \tag{23}$$

$$s_1'=\int_{T_0}^{T}C_{p_1}^{*}dT/T+R\ln RT_0+S_{01} \tag{24}$$

By use of an argument somewhat similar to that which led to (12) we can write (22) in the form

$$S=\int_{0}^{p}[\sum n_1R/p-(\partial V/\partial T)_p]dp-\sum(n_1R\ln px_1)+\sum(n_1s_1') \tag{25}$$

where p is the total pressure of the mixture, and we can also replace the lower limit, p^*, of the integral in (21) by 0, giving

$$H=\int_{0}^{p}[V-T(\partial V/\partial T)_p]dp+\sum(n_1h_1) \tag{26}$$

For a consideration of the isothermal variations of H and S with pressure the quantities $h_1, h_2, \cdots$, and $s_1', s_2', \cdots$, are evidently constant, and for constant temperature and composition, the terms $\sum(n_1h_1)$ and $\sum(n_1s_1')$ are constant.

There have now been derived four equations which may be classified as follows: general expressions for the variation of U and S with V and T, Equations (13) and (14); general expressions for the variation of H and S with p and T, Equations (26) and (25).

When it is desired to study the *isothermal* variations of these quantities with V, or with p, the same equations are applicable, with certain quantities, namely $n_1, n_2, \cdots, s_1, s_2, \cdots, s_1', s_2', \cdots$, and $h_1, h_2, \cdots$, constant. If further the composition also does not change, the terms $\sum(n_1u_1)$, $\sum(n_1s_1)$, $\sum(n_1s_1')$ and $\sum(n_1h_1)$ are constant.

It may be mentioned that the partial molal entropy of a gas in a mixture can be readily obtained by differentiation of Equation (14) or (25) with respect to n_1; similarly the partial molal energy and heat content result from the differentiation of (13) and (26) with respect to n_1. The method of carrying out such differentiations is indicated in Section 5 of this paper.

3. Assumptions Used in the Derivations of Section 2.

The derivations of the *general equations* of the preceding section rest on only two assumptions:

(a) At infinitely low total pressure, the equilibrium pressure of a gas in a gaseous mixture is equal to the product of its mol fraction into the total pressure.

(b) At infinitely low total pressure, the energy of a mixture of gases is the sum of the energies of the component gases when each is at the temperature and occupies the total volume of the mixture.

For the derivation of the *isothermal equations*, only the assumption (a) is necessary.[7] Eqs. (6) and (19) are a direct consequence of assumption (b), and it is easy to show[8] that (7) and (20) follow from (a) and (b). In order to carry out the solution of the *general equations* to a numerical result it is necessary to have:

(c) An equation of state for mixtures of real gases of the form

$$f(p, V, T, n_1, n_2, \cdots,) = 0$$

for which the integral of pdV can be evaluated either directly or by graphical means. It is to be noted that when evaluating the derivatives $(\partial V/\partial T)_p$ and $(\partial p/\partial T)_V$ from this equation of state, the variables $n_1, n_2, \cdots$, are to be held constant.

(d) The constant volume molal heat capacity at infinitely low pressures C_V^* for all the pure gases as functions of the temperature. (From C_V^* and the equation of state of the pure gases C_p^* can be calculated.)

[7] It was particularly emphasized by Gillespie, loc. cit., that this assumption alone is sufficient for the mass-action law at constant temperature.

[8] Cf. for instance Gibbs, loc. cit

(e) Data necessary to determine the entropy and energy (or heat content) constants for the pure gases, at the standard temperature T_0, which might be for instance 0°C.

For the numerical solution of the *isothermal* equations, it is necessary to have (c) an equation of state for mixtures and (e) the entropy and energy (or heat content) constants for the pure gases at the temperature under consideration.

For a mixture of constant composition it is necessary to have only one value of the entropy, energy, or heat content for some state of the system in order to calculate the value at any other temperature and pressure by means of the equations given.

4. The Thermodynamic Potentials

(a) *When V and T are the independent variables.* The thermodynamic potential $F_{V,T}$ is defined by the relation

$$F_{V,T} = U - TS \tag{27}$$

and using the values for U and S given by Eqs. (13) and (14) we obtain after simplification

$$F_{V,T} = \int_V^\infty (p - \sum n_1 RT/V)dV - \sum [n_1 RT \ln(V/n_1)] + \sum (n_1 F_1) \tag{28}$$

for the general variation of the thermodynamic potential of a gas mixture with pressure and temperature. The quantity F_1 is defined by the relation

$$F_1 = u_1 - Ts_1. \tag{29}$$

For all isothermal variations of $F_{V,T}$, the functions F_1, F_2, $\cdots$, are constant, and if in addition the composition is not varied then the term $\sum(n_1 F_1)$ is constant.

(b) *When p and T are the independent variables.* The thermodynamic potential

$$F_{p,T} = H - TS \tag{30}$$

can be expressed as a function of p and T by the use of Eqs. (25) and (26) giving

$$F_{p,T} = \int_0^p (V - \sum n_1 RT/p)dp + \sum (n_1 RT \ln p x_1) + \sum (n_1 F_1') \tag{31}$$

for the general variation of this thermodynamic potential of a gas mixture, where F_1' is defined by the relation

$$F_1' = h_1 - Ts_1' \tag{32}$$

As before F_1', F_2', $\cdots$, are constant for isothermal variations, and $\sum(n_1 F_1')$ is constant for processes at constant temperature and composition.

5. The Chemical Potential

The chemical potential (the so-called partial molal thermodynamic potential) of a gas in a mixture can be obtained from either of the two thermodynamic potentials by differentiation, thus

$$\mu_1=(\partial F_{V,T}/\partial n_1)_{V,T,n_2,n_3,\cdots}\ ;\quad \mu_1=(\partial F_{p,T}/\partial n_1)_{p,T,n_2,n_3,\cdots} \tag{33}$$

Using for $F_{V,T}$ and $F_{p,T}$ the values given in (28) and (31) we obtain the relations

$$\mu_1=\frac{\partial}{\partial n_1}\left[\int_V^\infty\left(p-\frac{\sum n_1RT}{V}\right)dV\right]_{V,T,n_2,n_3}-RT\ln\frac{V}{n_1}+RT+F_1 \tag{34}$$

$$\mu_1=\frac{\partial}{\partial n_1}\left[\int_0^p\left(V-\frac{\sum n_1RT}{p}\right)dp\right]_{p,T,n_2,n_3,\cdots}+RT\ln px_1+F_1' \tag{35}$$

Carrying out the indicated differentiation of the integral gives

$$\mu_1=\int_V^\infty\left(\frac{\partial p}{\partial n_1}-\frac{RT}{V}\right)dV-RT\ln\frac{V}{n_1}+RT+F_1 \tag{36}$$

$$\mu_1=\int_0^p\left(\frac{\partial V}{\partial n_1}-\frac{RT}{p}\right)dp+RT\ln px_1+F_1' \tag{37}$$

for the chemical potential[9] of Substance 1 in a mixture of gases. The first expression is used when the independent variables are V and T, and the second when they are p and T.

6. The Mass Action Law for Real Gases

From either of the functions $F_{V,T}$ or $F_{p,T}$ the mass-action law can be derived. When a chemical reaction is at equilibrium, the variation of $F_{V,T}$ at constant volume and temperature is zero with respect to a displacement of the equilibrium caused by a small variation in composition. The same is true for $F_{p,T}$ at constant pressure and temperature. From a consideration of the relations (33) it is evident that both of these methods lead to the same expression for the mass action law, namely

$$\sum(\nu_1\mu_1)=0 \tag{38}$$

in which the summation is taken over all of the gases in the reacting mixture, ν_1 is the number of mols of Gas 1 appearing in the chemical equation expressing the reaction, and μ_1 is the chemical potential of the Substance 1 given by either of the two equations (36) or (37) depending upon the choice of independent variables.

[9] The fugacity f_1 of a gas (c.f. Lewis and Randall, Thermodynamics, McGraw-Hill Book Co., New York (1923), p. 191) is related to th chemical potential through the equation $\mu_1=RT\ln f_1+F_1'$.

We thus obtain

$$\sum\left\{\nu_1\int_V^\infty\left(\frac{\partial p}{\partial n_1}-\frac{RT}{V}\right)dV\right\}-\sum\left(\nu_1 RT\ln\frac{V}{n_1}\right)+\sum[\nu_1(F_1+RT)]=0 \tag{39}$$

$$\sum\left\{\nu_1\int_0^p\left(\frac{\partial V}{\partial n_1}-\frac{RT}{p}\right)dp\right\}+\sum(\nu_1 RT\ln px_1)+\sum(\nu_1 F_1')=0 \tag{40}$$

for the mass-action expression in terms of the variables V and T, or p and T. The mass-action equation is usually written for the variation of the equilibrium constant K_p defined by the relation

$$\ln K_p=\sum(\nu_1\ln px_1)$$

which when introduced into (39) and (40) gives

$$\ln K_p=\sum\left(\nu_1\ln\frac{pV}{\sum n_1}\right)-\frac{1}{RT}\sum\left\{\nu_1\int_V^\infty\left(\frac{\partial p}{\partial n_1}-\frac{RT}{V}\right)dV\right\}$$
$$-\frac{1}{RT}\sum[\nu_1(F_1+RT)] \tag{41}$$

$$\ln K_p=-\frac{1}{RT}\sum\left\{\nu_1\int_0^p\left(\frac{\partial V}{\partial n_1}-\frac{RT}{p}\right)dp\right\}-\frac{1}{RT}\sum(\nu_1 F_1') \tag{42}$$

for the general variation of K_p with temperature and pressure. The temperature functions F_1 and F_1' are given in Eqs. (29) and (32).

Usually only the isothermal variation of K_p with pressure is desired. As the pressure approaches zero we obtain from (41) and (42)

$$\ln K_{p_0}=\sum(\nu_1\ln RT)-\frac{1}{RT}\sum[\nu_1(F_1+RT)] \tag{43}$$

$$\ln K_{p_0}=-\frac{1}{RT}\sum(\nu_1 F_1') \tag{44}$$

and substitution of these values into (41) and (42) gives

$$\ln\frac{K_p}{K_{p_0}}=\sum\left(\nu_1\ln\frac{pV}{\sum n_1 RT}\right)-\frac{1}{RT}\sum\left\{\nu_1\int_V^\infty\left(\frac{\partial p}{\partial n_1}-\frac{RT}{V}\right)dV\right\} \tag{45}$$

$$\ln\frac{K_p}{K_{p_0}}=-\frac{1}{RT}\sum\left\{\nu_1\int_0^p\left(\frac{\partial V}{\partial n_1}-\frac{RT}{p}\right)dp\right\} \tag{46}$$

These expressions give the variation of K_p with pressure at constant temperature. It is to be noted that (46) is the same as (1), the mass action law deduced by Gillespie by means of a consideration of the equilibrium of a gas through a semi-permeable membrane. At constant temperature, (45) and (46) can be used to calculate K_p for any pressure from one value at a given pressure.

7. Summary of the Equations Deduced

Symbols: p, total pressure; V, total volume of the mixture; T, Kelvin temperature; n_1 and x_1, number of mols and the mol fraction of Substance 1 in the mixture; ν_1, number of mols of Substance 1 in the stoichiometric equation for a chemical reaction, being negative if the substance disappears in the reaction. $C_{V_1}^*$ and $C_{p_1}^*$, molal heat capacities at constant volume and pressure of pure Substance 1 when the pressure is very small, (i.e. approaches zero). U, energy; S, entropy; H, heat content. $F_{V,T}$, thermodynamic potential at constant V and T; $F_{p,T}$, thermodynamic potential at constant p and T; μ_1, chemical potential of Substance 1 in the mixture. K_p, the equilibrium constant of a chemical reaction in terms of partial pressures of the reacting gases; K_{p_0}, the equilibrium constant at zero pressure. U_{01}, S_{01}, and H_{01} are the energy, entropy, and heat content constants for Substance 1 at some arbitrarily chosen "Standard temperature." u_1, s_1, s_1', h_1, F_1, and F_1' are the energy, entropy, heat content and thermodynamic potential "constants" for Substance 1 at the temperature T. They are given by the relations

$$u_1 = \int_{T_0}^{T} C_{V_1}^* dT + U_{01} \qquad (10) \qquad s_1' = \int_{T_0}^{T} C_{p_1}^* dT/T + R\ln RT_0 + S_{01} \qquad (24)$$

$$s_1 = \int_{T_0}^{T} C_{V_1}^* dT/T + S_{01} \qquad (11) \qquad F_1 = u_1 - Ts_1 \qquad (29)$$

$$h_1 = \int_{T_0}^{T} C_{p_1}^* dT + H_{01} \qquad (23) \qquad F_1' = h_1 - Ts_1' \qquad (32)$$

(a) *When V and T are the independent variables.*

$$U = \int_V^\infty [p - T(\partial p/\partial T)_V]dV + \sum(n_1 u_1) \qquad (13)$$

$$S = \int_V^\infty \left[\frac{\sum n_1 R}{V} - \left(\frac{\partial p}{\partial T}\right)_V\right]dV + \sum\left(n_1 R\ln\frac{V}{n_1}\right) + \sum(n_1 s_1) \qquad (14)$$

$$F_{V,T} = \int_V^\infty \left(p - \frac{\sum n_1 RT}{V}\right)dV - \sum\left(n_1 RT\ln\frac{V}{n_1}\right) + \sum(n_1 F_1) \qquad (28)$$

$$\mu_1 = \int_V^\infty \left(\frac{\partial p}{\partial n_1} - \frac{RT}{V}\right)dV - RT\ln\frac{V}{n_1} + RT + F_1 \qquad (36)$$

$$\ln K_p = \sum\left(\nu_1\ln\frac{pV}{\sum n_1}\right) - \frac{1}{RT}\sum\left\{\nu_1\int_V^\infty\left(\frac{\partial p}{\partial n_1} - \frac{RT}{V}\right)dV\right\}$$

$$- \frac{1}{RT}\sum[\nu_1(F_1 + RT)] \qquad (41)$$

$$\ln K_{p_0} = \sum(\nu_1\ln RT) - \frac{1}{RT}\sum[\nu_1(F_1 + RT)] \qquad (43)$$

$$\ln\frac{K_p}{K_{p_0}}=\sum\left(\nu_1\ln\frac{pV}{\sum n_1RT}\right)-\frac{1}{RT}\sum\left\{\nu_1\int_V^\infty\left(\frac{\partial p}{\partial n_1}-\frac{RT}{V}\right)dV\right\} \tag{45}$$

(b) *When p and T are the independent variables.*

$$H=\int_0^p\left[V-T\left(\frac{\partial V}{\partial T}\right)_p\right]dp+\sum(n_1h_1) \tag{26}$$

$$S=\int_0^p\left[\frac{\sum n_1R}{p}-\left(\frac{\partial V}{\partial T}\right)_p\right]dp-\sum(n_1R\ln px_1)+\sum(n_1s_1') \tag{25}$$

$$F_{p,T}=\int_0^p\left(V-\frac{\sum n_1RT}{p}\right)dp+\sum(n_1RT\ln px_1)+\sum(n_1F_1') \tag{31}$$

$$\mu_1=\int_0^p\left(\frac{\partial V}{\partial n_1}-\frac{RT}{p}\right)dp+RT\ln px_1+F_1' \tag{37}$$

$$\ln K_p=-\frac{1}{RT}\sum\left\{\nu_1\int_0^p\left(\frac{\partial V}{\partial n_1}-\frac{RT}{p}\right)dp\right\}-\frac{1}{RT}\sum(\nu_1F_1') \tag{42}$$

$$\ln K_{p_0}=-\frac{1}{RT}\sum(\nu_1F_1') \tag{44}$$

$$\ln\frac{K_p}{K_{p_0}}=-\frac{1}{RT}\sum\left\{\nu_1\int_0^p\left(\frac{\partial V}{\partial n_1}-\frac{RT}{p}\right)dp\right\} \tag{46}$$

Note: The partial differentials $(\partial p/\partial T)_V$ and $(\partial V/\partial T)_p$ are taken at constant $n_1, n_2, \cdots$; $\partial p/\partial n_1$ is taken at constant temperature and volume; and $\partial V/\partial n_1$ is taken at constant pressure and temperature. All of the derivatives can be evaluated from the equation of state for mixture of gases.

CAMBRIDGE, MASS.
November 23, 1927.

DISPERSION AND ABSORPTION OF HIGH FREQUENCY SOUND WAVES

By K. F. Herzfeld and F. O. Rice

Abstract

The absorption of sound waves in gases had been explained heretofore by friction and heat condution. A third factor is here introduced, namely, the slow rate of exchange of energy between the translational movement and the internal degrees of freedom of the molecules. The formulas determining the absorption and dispersion of sound waves, due to these three effects, are developed. Comparison with the experimental data available shows that the new effect is either of considerable influence or even predominant. The rate of exchange can be calculated.

I. Introduction

THE propagation of high frequency sound waves in gases has recently received great attention because of the improvement of experimental methods. The first absorption measurements by Neklepajew[1] are unfortunately perhaps affected by a carbon dioxide content of the air, and the same may be true for newer experiments by D. L. Rich and W. H. Pielemeier.[2] Abello[3] has measured the absorptions in mixtures of hydrogen and carbon dioxide with air. While the theory of absorption has been developed at least partially long ago by Stokes[4] and Kirchhoff[5,6] no discussion of the change of velocity with frequency exists. This latter effect has been detected by Pierce[7] for air and carbon dioxide in contradiction to earlier workers who, on account of less accurate methods, had looked in vain for it.

There are three things which can affect the phenomena considered here, namely internal friction, heat conduction, and slowness of energy exchange between the translational and the internal degrees of freedom of a gas molecule. While the first two are taken into account by Stokes and Kirchhoff, the third is considered here for the first time. It had occurred to one of us, (F.O.R.) in connection with some considerations on the velocity of chemical reactions in gases that this velocity may be influenced by the rate at which the energy stored up in the translation of gas molecules could be transferred to the internal degrees of freedom where it is available for activation. In the attempt to find other physical phenomena in which this supposed process would have influence and which could, therefore, be used for the calculation

[1] N. Neklepajew, Ann. d. Physik **35,** 175 (1911).
[2] D. L. Rich and W. H. Pielemeier, Phys. Rev. **25,** 117 (1925).
[3] T. P. Abello, Proc. Nat. Acad. **13,** 699 (1927).
[4] C. G. Stokes, Trans. Cambridge Phil. Soc. **8,** 287 (1845).
[5] G. Kirchhoff, Pogg. Ann. **134,** 177 (1868).
[6] See also Lord Rayleigh, Theory of Sound 2nd Ed. Lon. 1896, 2nd Vol. par. 345 and P. Lebedew, Ann. d. Physik **35,** 171 (1911).
[7] G. W. Pierce, Am. Acad. Sci. **60,** 271 (1925).

of the rate of exchange, two such cases appeared: heat conduction[8] and propagation of sound waves.

All three processes mentioned above will increase the absorption, but their effect on the velocity of propagation V is not quite so clear, and will therefore, be discussed first qualitatively.

a. *Internal friction.* For a given geometrical wave-form the effect of internal friction is to retard the movement. Therefore, for a given frequency the wave-lengths will be larger with friction than without. Internal friction, therefore, increases the velocity of propagation.

b. *Heat conduction.*[9] As is well known, Newton's assumption of constant temperature in the gas leads to a velocity, the square of which is given by RT/M where M is the molecular weight, but the experimental results are represented by Laplace's expression, the square of which is $\gamma RT/M$ where γ is the ratio of the specific heats at constant pressure and constant volume, and where an adiabatic state has been assumed. An erroneous opinion on the influence of the frequency upon the completeness of the adiabatic state seems to be often held. It is believed that while ordinary sound frequencies are sufficiently high to guarantee the adiabatic condition, we should expect Newton's velocity for very low frequencies. But a close scrutiny shows that the adiabatic state is best guaranteed for low frequencies, while for higher frequencies the influence of heat conduction is larger; therefore, the velocity should decrease with increasing frequency. This result comes about in the following way:

While it is true that with decreasing frequency the time allowed for heat conduction increases, the amount of heat conducted at a given moment decreases much more rapidly. This latter is proportional to $\partial^2 T/\partial x^2$ and for a given amplitude this expression is inversely proportional to the square of the wave-lengths. Therefore, the heat conducted during one period increases proportionally with the frequency because of the increasing steepness of the temperature gradient. The numerical values, however, are such that for (a) and (b) together the velocity increases with the frequency.

c. A slow rate of exchange between external and internal degrees of freedom keeps the internal degrees from taking up the whole amount of heat, and therefore acts as if the effective specific heat were decreased, and the velocity of sound increased with increasing frequency.

II. Calculation of Dispersion and Absorption

a. *Symbols.* We shall use the following notation: u, velocity of gas; ρ, density of gas, $=pM/RT=\rho_0(1+s)$ where s is the relative compression; T, temperature of the translational kinetic energy of the gas molecules $=T_0(1+\theta)$; αR, specific heat of translational kinetic energy $(\alpha=3/2)$; T', temperature of the internal degrees of freedom $=T_0(1+\theta')$ (for slow movements $T=T'$); βR, specific heat of internal degrees of freedom; $cR=(\alpha+\beta)R$, total specific heat at constant volume; μ, coefficient of internal

[8] A. Eucken, Phys. Zeits. **14,** 324 (1913).

[9] See also C. G. Stokes, Phil. Mag. (4) **1,** 305 (1851). Lord Rayleigh, l.c. p. 25.

friction; L, coefficient of heat conduction; $\epsilon = LM/cR\mu$, a dimensionless constant (according to the kinetic theory of gases it is 2.5 for monoatomic molecules and smaller for others.)[8]

It may be that the heat conduction under nonstationary conditions is different for the heat belonging to the external and to the internal degrees of freedom.[8] We therefore put $L = L' + L''$ and $\sigma = L''/L'$ or $\sigma/(1+\sigma) = L''/L$.

We shall denote by n the frequency of the sound wave, and set $\xi = 8\pi\mu/3V_0^2 = 8\pi c\mu/3(c+1)p_0$, $p_0 = 1.014.10^6$ dynes/cm.^{2} The product ξn is dimensionless and will be considered as small.* τ is a time measuring the rate of exchange between external and internal degrees of freedom. We represent the amount of energy which passes in one mol from the external to the internal degrees of freedom during unit time by $\alpha R dT/dt = \alpha R(T-T')/\tau$. We assume s, u, θ, θ' to be proportional to $e^{i2\pi(nt-kx)}$ We set $k = k_1 - ik_2$ where $k_1 = n/V$ measures the velocity of the propagation of sound. $2\pi k_2$ is the absorption coefficient for the amplitude; therefore $4\pi k_2$ the absorption coefficient for the intensity.

b. *The equations of motion and their integration.* Assuming the amplitude to be small, we have the following equations for a plane wave propagated along the x axis: the equation of motion;

$$\frac{\partial u}{\partial t} - \frac{4}{3}\frac{\mu}{\rho}\frac{\partial^2 u}{\partial x^2} = -\frac{1}{\rho}\frac{\partial p}{\partial x} = -\frac{RT_0}{M}\left(\frac{\partial \ln T}{\partial x} + \frac{\partial \ln \rho}{\partial x}\right)$$

the equation of continuity; $\partial\rho/\partial t = -\rho\,\partial u/\partial x$.

The equation of energy for the degrees of freedom of translation expresses the fact that this energy can be changed by external work, heat conduction and exchange with the internal degrees of freedom.

$$\alpha R\frac{\partial T}{\partial t} = p\frac{M}{\rho^2}\frac{\partial \rho}{\partial t} + \frac{L'M}{\rho}\frac{\partial^2 T}{\partial x^2} - \frac{\alpha}{\tau}R(T-T')$$

The equation of energy for the internal degrees of freedom determines the corresponding change in energy by heat conduction and exchange with the external degrees of freedom.

$$\beta R\frac{\partial T'}{\partial t} = \frac{\alpha R}{\tau}(T-T') + \frac{L''M}{\rho}\frac{\partial^2 T'}{\partial x^2}$$

If we now consider the way in which u, s, θ, θ' depend on t and x we get the following equations:

$$u\left(in + \frac{8\pi\mu}{3\rho_0}k^2\right) = ik\frac{RT}{M}(\theta+s) \qquad ns = ku$$

$$in\alpha\theta = ins - \frac{L'M}{\rho R}2\pi k^2\theta - \frac{\alpha}{2\pi\tau}(\theta-\theta') \qquad in\beta\theta' = -\frac{L''M}{\rho R}2\pi k^2\theta' + \frac{\alpha}{2\pi\tau}(\theta-\theta')$$

* Probably ξ and τ will depend in the same way on temperature and pressure, both being proportional to the time between two collisions, or to (mean free path)/(Velocity).

Eliminating u, s, θ, θ' we get the following "equation of dispersion" for k:

$$-c(c+1)\frac{k^2V_0^2/n^2-1+ik^2V_0^2/n^2}{1-c(k^2V_0^2/n^2-1)-i(c+1)k^2V_0^2/n^2}=\frac{3ic\epsilon\xi nk^2V_0^2}{4(1+\sigma)n^2}$$
$$+\frac{i\beta^2 2\pi\tau n+3\sigma c\epsilon\xi nk^2V_0^2(\alpha i+\beta 2\pi\tau n)/4(1+\sigma)n^2}{\alpha+i\beta 2\pi\tau n+3\sigma c\epsilon\xi n2\pi\tau nk^2V_0^2/4(1+\sigma)n^2}$$

To solve this equation we treat ξn and $2\pi\tau n$ as small quantities. Then it is seen that the solution of zero order will be $k_1=n/V_0$; $k_2=0$.
We write then for the next order which will be sufficient

$$k_1-ik_2=(n/V_0)[1+(K\xi^2+P\xi\tau+Q\tau^2)n^2]-in(D\tau+E\xi)$$

Comparison of equal powers of ξ and τ leads to the final solution.

$$4\pi k_2=\frac{n^2}{V_0}\left[2\pi\left(1+\frac{3}{4}\ \frac{\epsilon}{c+1}\right)\xi+4\pi^2\frac{\beta^2}{\alpha c(c+1)}\tau\right]$$

$$V=V_0\Big\{1+n^2\Big[\frac{3}{8}\left(1+\frac{5}{2}\ \frac{\epsilon}{c+1}-\frac{3}{4}\epsilon^2\frac{c-3/4}{(c+1)^2}\right)\xi^2$$
$$+\frac{3\pi}{2}\ \frac{\beta^2}{\alpha c(c+1)}\left(1-\epsilon\frac{c-1/4}{c+1}+\epsilon\frac{c}{\beta}\ \frac{\sigma}{1+\sigma}\right)\xi\tau$$
$$+2\pi^2\frac{\beta^3}{\alpha^2c^2(c+1)}\left(\alpha+\frac{3}{4}\ \frac{\beta}{c+1}\right)\tau^2\Big]\Big\}$$

III. Numerical Results and Comparison with Experiments

For the following gases we use numerical data given in the following table.

	μ	ϵ	γ	β	c
Air	19×10^{-5}	1.91	1.405	0.96	2.46
Hydrogen	88.5×10^{-5}	1.97	1.408	0.93	2.43
Carbon Dioxide	16×10^{-5}	1.628	1.305	1.78	3.28

The values of μ and ϵ have been taken from Eucken,[8] γ from Landolt-Bornstein tables. β and c have been calculated from these values using $\alpha=3/2$. We find then

Air:

$$4\pi k_2=n^2(2.99\times10^{-13}+0.428\times10^{-4}\tau)$$
$$V=V_0\{1+n^2[9.32\times10^{-19}-(0.084-1.86\sigma/(1+\sigma))10^{-9}\tau+0.635\tau^2]\}$$

Hydrogen:

$$4\pi k_2=n^2(3.65\times10^{-13}+0.106\times10^{-4}\tau)$$
$$V=V_0\{1+n^2[2.05\times10^{-19}-(0.42-8.84\sigma/(1+\sigma))10^{-9}\tau+0.595\tau^2]\}$$

Carbon dioxide:

$$4\pi k_2=n^2(3.16\times10^{-13}+1.16\times10^{-4}\tau)$$
$$V=V_0\{1+n^2[6.48\times10^{-19}-(0.108-2.17\sigma/(1+\sigma))10^{-9}\tau+1.96\tau^2]\}$$

For air we have the absorption measurements of Neklepajew.[1] As mentioned in the introduction, Rich and Pielemeier suspect that these are affected by a content of carbon dioxide as the values are higher than the theoretical ones if only friction and heat conduction are taken into account; but, according to Abello's[3] new measurements one would not expect an influence larger than 5 percent as it seems improbable that more than 1 percent of carbon dioxide would be present. We will, therefore, provisionally use Neklepajew's value which gives for the absorption coefficient $6.6\times10^{-13}\,n^2$. Comparing this with our formula we see, as pointed out by Lebedew,[6] that about half this value is due to heat conduction and friction. The other half, therefore, must be due to slow energy exchange between different degrees of freedom. We get from this a value of τ approximately 0.8×10^{-8} sec. For $n=10^6$ this would modify the velocity of sound by 3 cm per second, a value far below Pierce's[7] results. Neither the shape nor the values of Pierce's curve for the variation of velocity of sound with frequency can, therefore, be explained.

For carbon dioxide, Pierce's curve for the velocity of sound is of the form we should expect according to our formula. Using the value at $n=2\times10^5$ cycles per second, we find that the change of V is primarily due to the exchange rate, and gives a value for $\tau=2.6\times10^{-8}$ seconds. With this we get an absorption coefficient $3\times10^{-12}\,n^2$. This agrees reasonably with his statement that carbon dioxide is opaque for $n=10^6$, as it gives at this frequency an absorption coefficient 3.3. It agrees, furthermore, with his result that at $n=10^5$ a column of CO_2 of 17 mm length is equivalent to one of air of 68 mm, as for the former $4\pi k_2 x$ would be 0.056 while for the latter it would be 0.045, using Neklepajew's data. It would not agree with his other statement that for $n=2\times10^5$ a column of 4 mm CO_2 is equivalent to 204 mm of air, as this would give values of 0.056, 0.55 respectively; but the two results of Pierce do not agree with each other if we assume that the absorption coefficient of carbon dioxide and air depend in the same way on the frequency, because then the ratio of equivalent columns of these two gases should be independent of the frequency. Finally, we may try to exterpolate the absorption coefficient of pure carbon dioxide from Abello's results with the help of his statement that the connection between transmission and percentage of carbon dioxide is a logarithmic one (which statement means that the absorption coefficient is a linear function of the composition.) We then get for the absorption coefficient $-5{,}6\times10^{-12}\,n^2$ which is in sufficient agreement with our value. If we extrapolate, in the same way, Abello's hydrogen measurements we find $3.8\times10^{-12}\,n^2$ giving $\tau\sim3\times10^{-7}$ seconds.

A real test of the theory can be made only if for the same gas absorption and dispersion are measured carefully.

THE JOHNS HOPKINS UNIVERSITY,
PHYSICAL LABORATORY AND DEPARTMENT OF CHEMISTRY,
January 9, 1928.

THE THEORY OF THE HERSCHEL-QUINCKE TUBE

By G. W. Stewart

Abstract

The well known simple explanation of the Herschel-Quincke interference tube is inadequate. It is herein shown that the ratio of the transmitted to incident acoustic energy is

$$[4(\sin(\alpha_3+\alpha_2)/2)(\cos(\alpha_3-\alpha_2)/2)]\{[1-2\cos(\alpha_3+\alpha_2)+\cos(\alpha_3-\alpha_2)]^2+4\sin^2(\alpha_3+\alpha_2)\}^{-1/2}$$

wherein α_2 and α_3 are the phase changes over the two branches of the tube. This ratio is zero not only when $\alpha_3-\alpha_2=(2n+1)\pi$, as formerly explained, but also when $\alpha_3+\alpha_2=2n\pi$, provided $\alpha_3-\alpha_2\neq 2n_1\pi$, where n and n_1 are independent integers.

Comparison of the new theory with experiment.—The transmission in an interference tube having branches 10.0 and 14.3 cm in length was studied and showed satisfactory agreement with the new theory. Practically zero transmission was found at frequencies of 1100 and 3300 d.v. and this is in accord with the simple theory of difference in path, as well as the revision here presented. But there was also serious interference at 1000, 2000, 3000 and 4000 d.v. and this fact is in accord only with the revised complete theory.

THE Herschel-Quincke tube[1] consists of a branched conduit as shown in Fig. 1 constructed with constant total cross-sectional area. Assume a wave travelling to the right. If the difference in path is $(2n+1)\lambda/2$, n an integer and λ the wave-length, then the excess pressure at the distant junction point is zero and the wave therefore is not transmitted to the right but is reflected back. This is the accepted simple explanation. That it is not sufficient was found by the writer in an experimental test shown by the indicated points in Fig. 1. The frequencies A and B are those given by $(2n+1)\lambda/2$. Clearly the actual frequencies at which there is interference are much more numerous. The purpose of this article is to outline the theory, and to make a comparison of theory with experiment.

Theory. Assume a plane wave incident in conduit 1 at junction 123. There are seven possible waves to be considered; two each in conduits 1, 2, and 3, and one in conduit 4. The waves to the right in Fig. 1 will each have the displacement amplitude indicated by A and a subscript designating the conduit. Waves to the left will be similarly designated by B. Excess pressure, p, and displacement, ξ, may be represented as follows:

$$p=\rho a\omega A e^{i\omega t}, \quad \xi=A e^{i\omega t}, \tag{1}$$

wherein ρ and a are respectively the density of and velocity in the medium, ω is 2π times the frequency and $e^{i\omega t}$ represents the simple harmonic nature of the oscillations. In the waves B, it will be necessary to use the positive sign for pressures and negative signs for displacements, for a displacement

[1] Herschel, Phil. Mag. **3,** 401 (1833); Pogg. Annal. **31,** 245 (1834); Quincke, Pogg. Annal. **128,** 177 (1866).

to the right is positive. At the junction 123, the continuity of pressures and displacement may be written:

$$\left.\begin{aligned} &\text{Pressures:} && (A_1+B_1)=(A_2+B_2)=(A_3+B_3) \\ &\text{Displacements:} && S_1(A_1-B_1)=S_2(A_2+A_3-B_2-B_3) \end{aligned}\right\} \quad (2)$$

wherein S indicates the area and the subscript the conduit.

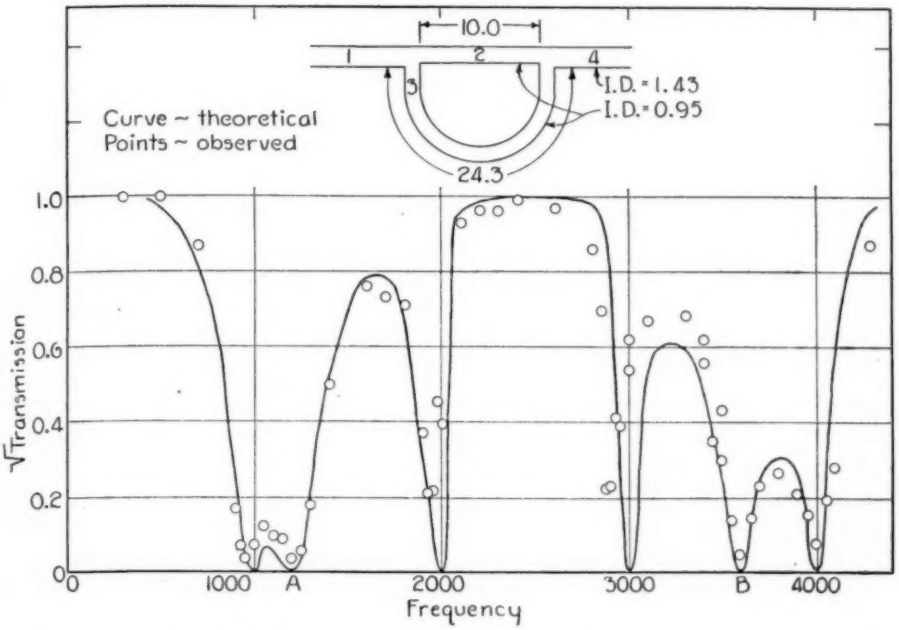

Fig. 1. Diagram of Herschel-Quincke tube and the relation between percentage transmission and the square root of the frequency.

If α_2 is the change of phase in conduit 2 and α_3 in conduit 3, then corresponding equations for junction 234 are:

$$\left.\begin{aligned} &A_2e^{-i\alpha_2}+B_2e^{i\alpha_2}=A_4=A_3e^{-i\alpha_3}+B_3e^{i\alpha_3} \\ &S_2(A_2e^{-i\alpha_2}-B_2e^{i\alpha_2}+A_3e^{-i\alpha_3}-B_3e^{i\alpha_3})=S_1A_4 \end{aligned}\right\} \quad (3)$$

There are in Eqs. (2) and (3) seven unknowns and six independent linear equations. By solving, the ratio between A_4 and A_1 can be found as follows:

$$|A_4/A_1| = \{[4\sin(\alpha_3+\alpha_2)/2][\cos(\alpha_3-\alpha_2)/2]\}$$
$$\{[1-2\cos(\alpha_3+\alpha_2)+\cos(\alpha_3-\alpha_2)]^2+4\sin^2(\alpha_3+\alpha_2)\}^{-1/2} \quad (4)$$

This is the square root of the transmission or of the ratio of the transmitted to the incident intensity.

Inspection of Eq. (4) shows that: transmission $=0$, if $\alpha_2-\alpha_3=(2n+1)\pi$, $n=0, 1, 2, 3$, etc. or if $\alpha_2+\alpha_3=2n\pi$, $n=0, 1, 2, 3$, etc., provided in each case that $\alpha_2-\alpha_3\neq 2n_1\pi$, $n_1=0, 1, 2, 3$, etc. The former condition is well known, but the latter is new.

Measurement of transmission. The apparatus was the same as that described[2] in the measurement of acoustic impedance. The Herschel-Quincke tube was inserted and removed from the conduit and the ratio of the two intensities taken as the transmission of the interference tube.

Comparison of theory and experiment. Fig. 1 is self-explanatory. The frequencies A and B have the well known conditions $\alpha_3-\alpha_2=(2n+1)\pi$. The other minima, at 1000, 2000, 3000 and 4000 d.v., are more numerous and comply with the condition $\alpha_3+\alpha_2=2n\pi$, $\alpha_3-\alpha_2\neq 2n_1\pi$. In fact the curve is drawn by computation from Eq. (4) assuming $a=34300$ cm/sec. The observed values of the minima are not in exact agreement with the theoretical curve and for several reasons. In the first place the junction points are not made with sufficient care to conform to the ideal condition of constancy of total area. The junction should be a Y-tube. Moreover, no consideration is given to viscosity in the theory. In view of these considerations experiments and theory agree very satisfactorily.

The question arises as to why the incorrectness of the theory of the tube, known for almost a century, was not noticed. Apparently the explanation in terms of the difference between α_3 and α_2 was so simple that no one observed that the waves in 2 and 3 travelling to the left do not experience constancy of area on arrival at junction 123 and consequently suffer a reflection. In fact, in general, the waves travel about the circuit in a very complex manner, impossible to follow without resorting to the use of equations.

The conclusion is that the theory of the Herschel-Quincke tube as herein derived is in satisfactory agreement with experiment.

PHYSICS LABORATORY,
UNIVERSITY OF IOWA,
January 15, 1928.

[2] G. W. Stewart, Phys. Rev. **28**, 1038 (1926)

BOOK REVIEWS

Handbuch der Physikalischen Optik. Edited by E. GEHRCKE. Vol. II, Second Half. Second Part. Pp. x+295, 88 figs. Verlag von Johann Ambrosius Barth, Leipzig, 1927. Price 27.60 M. This part of the second volume completes the Handbuch. The subjects treated include thermal radiation, optics of moving media, and the nature of light. The material on thermal radiation is presented in four sections dealing with different aspects of the subject, such as the general theory, black body radiation, selective thermal radiation, and technical light sources. A welcome feature is a well-written section on the important subject of selective thermal radiation. The other sections on thermal radiation are more conventional. The writer of the section on optics of moving media unfortunately does not appreciate the value of the theory of relativity, neither the general nor the special. The many supporting experiments are severely criticized, and more or less plausible alternative explanations of the results are offered. A good deal of space is devoted to various "objections" to the theory of relativity. Occasionally the author cites rather questionable authorities. It would require a volume to criticize the various points brought up and to restore order in the chaos of ideas presented. However, in regard to the experimental side of the subject, this section is fairly satisfactory. Theories as to the nature of light are taken up historically in the closing section. As might be expected, no solution of the modern dilemma is indicated. This part also contains an index to the entire Handbuch.

J. VALASEK

New Methods in Geometrical Optics. CHARLES S. HASTINGS. Pp. 103, 23 figs. The Macmillan Company, New York, 1927. Price $2.00. In this text, the subject matter of geometrical optics is developed in terms of wave surfaces, surface curvatures, and wave velocities. This has an advantage over the usual light ray methods, in that the equations obtained have a less complicated form. Consequently, the derivatives giving the various aberrations are more easily found, and the computations in the design of optical systems are simplified. A number of practical suggestions are given in regard to the design of telescope objectives. However, only a few other practical applications are discussed, and their treatment is very incomplete.

J. VALASEK

Field Astronomy for Engineers and Surveyors. DAVID CLARK. Pp. 164, 50 figs. Constable and Company, London and D. Van Nostrand Company, New York, $3.50. In his preface, the author expresses the hope "that the manual will prove of service as a reference book for engineers who have not regularly to undertake astronomical work, and that it will meet the needs of university and private students of Surveying and Geodesy." As a practical manual, the book possesses the advantages of compactness and conciseness of expression. As a text for students undertaking the study of practical astronomy for the first time, the compactness which involves the use of small type may not be entirely an advantage. With the exception of this tendency to crowd the material into small space, the typography of the book is excellent and the prominence given to the topical headings contributes greatly to the convenience of the reader.

The book is very logically divided into three parts, namely, Principles, Instruments, and Observations. In the first part, the author considers the fundamental formulas of spherical trigonometry as applied to astronomy, a brief introduction, definitions and co-ordinate systems relating to the celestial sphere, fundamental corrections of refraction, parallax, and semi-diameter, and, at some length, the very important subject of time. In the chapter on instruments, considerable attention is given to the micrometer theodolite. The astronomical transit, the zenith telescope, the sextant, the prismatic astrolabe, and the solar attachment are de-

scribed more briefly, as also, the chronograph, watch, and chronometer. In the third chapter, various methods of determining time, azimuth, latitude, and longitude are explained, and a number of numerical examples are solved. The methods in common use are described, together with some which, as the author states, are not ordinarily used, for example, the absolute determination of longitude by observed lunar distances. The modern determination of longitude by wireless telegraph or radio signals is given special consideration.

The absence of any special consideration of the American surveyor's transit and methods and examples especially adapted to its use is explained by the European origin of the work and the consequent emphasis placed upon the micrometer theodolite. To an American engineer, this would probably be a serious omission. Moreover, the absence of actual computations of several determinations would render the work less useful as a field manual, as the engineer in practice can utilize a numerical solution much more easily than he can a theoretical presentation without the solved example.

In common with many works on practical astronomy, this book includes little information concerning the fundamental principles of general or descriptive astronomy. It seems to be taken for granted that the reader is already conversant with the structure of the universe, including the solar system. The study of astronomy is not so common in our schools as it used to be, so that the addition of a very brief statement concerning the heavenly bodies and their motions would be very useful to the average student.

On the whole, the book is commendable. As a British work, it could not be expected to conform to American practice. However, it does approach closer to the American style of presenting this subject than most foreign books. The notation used is a common one. The book is a useful contribution to a subject which is not easy for the average engineer.

O. M. LELAND

Propagation of Electric Currents in Telephone and Telegraph Conductors. J. A. FLEMING. Pp. 422, 25 figs. D. Van Nostrand Company, New York, 1927. $8.00. The fourth edition of Propagation of Electric Currents in Telephone and Telegraph Conductors, which was originally published in 1911, has just been received with the addition of a new chapter on "Recent Advances in the Construction of Telephone and Telegraph Conductors." The book is recognized as one of the standard works on propagation, particularly for communication frequencies. It discusses the propagation of simple periodic currents in lines and cables and also treats of the transmission of irregular currents such as speech forms and telegraphic currents which are far from sinusoidal. A great deal of the mathematical development is done on the basis of hyperbolic functions by means of which the solutions are most readily obtained. Although the author still retains the M.S.C. (mile of standard cable) as a unit of measurement while we Americans have been quite generally converted to the transmission unit (T.U.), the book is well adapted for teaching purposes, either as a text or as an excellent reference book. The added chapter in the new edition treats of artificial loading of lines and the development of the different types of loading coils down to the most recent, that of permalloy cored coils and spirally wound permalloy submarine cables. This chapter further describes in general the thermionic repeater for one-way and two-way operation. A brief description of carrier frequency telephony and wave filters concludes the book.

There is nothing mentioned, however, on the more recent developments and applications of current propagation over wires for accomplishing telephotography (transmission of pictures by wire), nor for realizing television (seeing a moving object over a telephone line). Both of these applications of current propagation have brought out some very interesting and, at first, baffling problems for solution.

G. W. SWENSON

The Human Habitat. ELLSWORTH HUNTINGTON. Pp. 293, 8 figs., 26 plates. D. Van Nostrand Company, New York, 1927. $3.00. "The Human Habitat," as described in the preface, is "an attempt to give the layman a true idea of human geography as interpreted by the American school of geographers." As indicated by typical chapter titles such as "The Desert Borderlands," "Lands that are Too Cool," "Too Warm and Moist," and "The Interplay of

Climatic and Human Changes," the book deals principally with human adjustments to climatic conditions, and to only a minor extent with other factors of the environment as they affect human activities. In this respect, it does not accomplish the objective as stated in the preface, though this descrepancy between accomplishment and stated purpose is of minor importance This overemphasis of climate doubtless results from the author's belief that, "aside from the direct physiological stimulus of climate, geographic conditions are passive." (p. 280).

In the chapter entitled "Tropical Plantations and Future Food Supplies," it is pointed out that the development of the plantation system in the Tropics has not, and probably will not, increase the food supply of the world, but instead, create additional demands upon the products of Intermediate Latitude agriculture, despite the frequently expressed views to the contrary. The chapters, "The Civilization of the Rice Lands" and "The Contrast between Japan and China," together with several others, afford excellent examples of an interesting presentation of geographic facts and constitute valuable object lessons in what can be done with geographic material. This is a contribution of major importance.

In the preface (vii), Dr. Huntington disclaims any intention "to present the proof for the many conclusions" and throughout he appears to have adhered to this decision. This is unfortunate as it is often impossible for the reader to formulate any satisfactory basis for the conclusion. For example, it is difficult to accept without proof such a statement as "Europe would hold nearly its present position in industry even if there were no coal." (In Europe. p. 220). In addition, such pronouncements as "The general opinion seems to be that the most reliable record of the climate of the historic past is found in the rate of growth of the great Sequoia trees of California," (p. 150) are open to question.

Considering the object of the author, that of writing for the layman, the book is excellently conceived. The presentation is clear, the subject matter is interesting, and many of the conclusions are at least provocative of thought. The book should have a wide sale, many favorable reviews, and it will be read with interest. It would be unfortunate, however, if the readers should consider the volume as presenting adequately the viewpoint of the majority of American geographers as to the field of human geography.

D. H. DAVIS

Over statistische Methoden in de Theorie der Quanta. Dissertation Leiden. G. E. UHLENBECK. Pp. 97. Martinus Nijhoff, Hague, Holland, 1927. Price 2 guilden. This book is devoted to the fundamental questions in statistical mechanics. A review of the situation with the classical statistics is given. The work of Boltzmann, the Loschmidt and the Zermelo difficulties are discussed. The present status of the ergodic and the quasi-ergodic hypotheses is summarized. The methods of Gibbs and of Fowler and Darwin are presented next as *mathematical* ways of calculating averages. This point of view is particularly convenient in the understanding of Pauli's recent work on paramagnetism of metals. Applications to Bohr's quantum theory are then taken up with Ehrenfest's adiabatic hypothesis as a foundation. In the last section the newer statistics of Bose-Einstein and of Fermi-Dirac are developed. This is done in a general way using the Fowler-Darwin method so that these two as well as the Boltzmann can be looked at as special cases of general statistical formulae. The connection with Pauli's equivalence principle, Heisenberg's considerations on the helium atom, Wigner's investigations, and Ehrenfest's suggestion of the rôle of the impenetrability of matter are discussed. Several valuable criticisms are brought out in this last section. The discontent with the exclusive attention paid to the μ-ether is perhaps the most important.

The book is written very clearly and comprehensively. It would be very valuable to have a translation of it in English or some other generally known language.

G. BREIT

Elements of Mechanics. HENRY A. ERIKSON. Pp. xvi+150, 78 figs. McGraw-Hill Book Company, New York, 1927. Price $1.75. For two reasons it is rather difficult to appraise this book fairly. In the first place, it covers only the first portion of the course in general physics as given at the University of Minnesota; one may assume that the scant treatment accorded to some topics, especially gases, is made up in succeeding parts of the course. Second, it is appar-

ent from the preface that considerable supplementary material is expected to be furnished in the three demonstration lectures each week. Taken at its face value, the book is in large measure hardly more than a skeleton of definitions and equations, more suitable for use in solving problems and for examination-cramming than as a text for the broad understanding of the subject. There is but little discussion, and hardly any historical treatment or application of principles to pure science or engineering. Still, as a brief summary of essential principles it is very well constructed. Its chief defects seem to be lack of precision and elegance in style, and of the care in preparation which avoids incomplete explanations on the one hand and an occasional overloading with irrelevant detail on the other. There are a number of misspellings and misprints; the misplacing of the angle θ in Fig. 51 should be corrected in the next edition. The emphasis on the dimensions of physical quantities is an excellent feature, as is also the collection of tables at the end. Another outstanding feature is the wealth of good problems, especially such as have to do with relative motion. The index, unfortunately, seems far from complete.

W. G. CADY

Spherical Harmonics. T. M. MACROBERT. Pp. 302+xii, 20 figs. E. P. Dutton and Co., New York, 1927 (printed in England). Price $4.50. The content of this book is considerably more comprehensive than indicated by the title. In the first place, it is replete with applications to mathematical physics, for pure mathematics would seldom necessitate the "twenty diagrams" advertized on the cover. Further, besides spherical harmonics, there is an opening chapter on Fourier series, followed by two more on their applications to conduction of heat and the transverse vibrations of stretched strings. The hypergeometric function is even briefly discussed. There are chapters on the potential of ellipsoids and of eccentric spheres. The three final chapters are on Bessel's functions, their asymptotic expansions and applications.

The degree of difficulty and style of presentation is one which should appeal to the student of physics. The book aims to be thorough, and contains a wealth of information, but at the same time, as stated in the preface, use of contour integration and other mathematical technicalities has been avoided. The exercises given at the end of the chapters are of a more humane variety than the bewildering tripos problems in which many other English texts revel. Incidentally these exercises simultaneously serve as a compendium of many useful formulas. In example 15, p. 106, for instance, $\cos m\theta$ is expanded as a sum of Legendre polynomials for all values of m from 1 to 10.

It is perhaps unfortunate that a chapter could not be included on the use of spherical harmonics in the Schroedinger wave equation of quantum mechanics, but the chapter on associated Legendre functions may nevertheless be helpful in this connection. Why these functions should be defined in this chapter first for the argument $x>1$ rather than $x<1$ seems a little strange since in so many physical problems $x=\cos\theta$. The recursion formula given in example 3, p. 142 is often employed in quantum theory, and is fortunately given somewhat more dignity than a mere exercise by the inclusion of a pretty thorough hint on the method of proof.

Professor MacRobert's book should be welcomed by both physicists and mathematicians. Although intended primarily as a text, it is valuable also as a reference book. The presence of an index and arrangement of material make it probably easier to refer to than Byerly's treatise.

J. H. VAN VLECK

PROCEEDINGS

OF THE

AMERICAN PHYSICAL SOCIETY

MINUTES OF THE NEW YORK MEETING, FEBRUARY 24-25, 1928.

JOINT MEETING WITH THE OPTICAL SOCIETY OF AMERICA.

The 149th regular meeting of the American Physical Society was held in New York City on Friday and Saturday, February 24 and 25, 1928, as a joint meeting with the Optical Society of America. All sessions were held at Columbia University except the joint session on Saturday morning which was held at the Bell Telephone Laboratories, 55 Bethune Street.

The Optical Society held regular sessions for the reading of papers on Friday morning and afternoon. At the special session held on Friday evening Dr. W. F. G. Swann of the Bartol Research Foundation delivered an address on "Recent Theories of the Atom." This was followed by a demonstration of the Baron Sheba fast moving pictures, given through the courtesy of Professor Alexander Klemin of New York University.

On Saturday morning the two societies were the guests of the Bell Telephone Laboratories, Inc. The principal feature of this joint meeting, which was attended by five hundred members and guests, was a demonstration of television by Dr. H. E. Ives. Before the beginning of the formal session the visitors were given a demonstration of talking motion pictures showing the Vitaphone and Movietone. Five papers from the program of the Physical Society were read. Professor K. T. Compton presided.

Regular sessions of the Physical Society were held on Friday afternoon and Saturday afternoon, the latter session being split into two sections. The presiding officers were Professor K. T. Compton and Professor H. G. Gale.

Special Business Meeting. At the Saturday afternoon session of the Physical Society the following resolution was passed:

"Resolved that the By-laws be amended by striking out the whole of Section 4 of Article I—Dues, reading as follows—'Newly elected fellows or members transferred from membership to fellowship shall pay a fee of three dollars. There shall be no entrance fee for newly elected members,' and that this amendment become effective for all those paying fellowship dues for the first time to cover the year 1928."

There was adopted by rising vote the following minute in memory of Professor H. A. Lorentz:

"Hendrik Antoon Lorentz, since 1906 an Honorary Member of the American Physical Society, died at the age of seventy-five on February fourth, 1928.

"All of us well know of his brilliant and long continued contribution toward the advancement of the subject of Physics which he so well loved and served. Many of us found in him as lecturer and teacher on the occasions of his various visits to America a powerful stimulus and source of inspiration. Some of us were privileged to know him well and were continually impressed by the charm of his personality and by his friendliness of manner.

We, members of the American Physical Society, recognize that the death of our distinguished colleague marks the passing of one of the great figures of modern science and it is our wish that there be placed among the minutes of our society this expression of our tribute to his memory."

At the regular meeting of the Council of the Physical Society held on Friday, February 24, 1928, forty-two were transferred from membership to fellowship, and twenty-six were elected to membership. *Transferred from Membership to Fellowship*: Henry A. Barton, Joseph A. Becher, John A. Carroll, Edward Condon, James M. Cork, Harry Clark, John A. Eldridge, Alexander Ellett, Marion Eppley, Alexander Forbes, Hugo Fricke, Lester H. Germer, George R. Harrison, T. R. Hogness, Frank C. Hoyt, J. C. Jensen, Charles F. Kettering, S. M. Kintner, Charles H. Kunsman, Ernest O. Lawrence, George A. Lindsay, Adolph Lomb, F. W. Loomis, J. P. Maxfield, W. H. McCurdy, George S. Monk, Jared K. Morse, Robert A. Patterson, David C. Prince, Chester W. Rice, P. A. Ross, Arthur E. Ruark, A. G. Shenstone, Erwin Schroedinger, John C. Slater, Joseph Slepian, Keith K. Smith, Louis A. Turner, Hugo B. Wahlin, Alan T. Waterman, William V. Watson, Charles T. Zahn. *Elected to Membership*: James T. Adams, Peter P. Alexander, L. W. Blau, Craig M. Bouton, Brooks A. Brice, Gertrude Buggeln, Leslie V. Case, W. C. Ellis, Carl L. Frederick, W. R. Frederickson, G. E. Gates, W. Delmar Hershberger, Frederick R. Hirsh Jr., F. T. Holmes, Joseph Kaplan, C. P. Keim, R. M. Langer, John M. Ort, R. Ronald Palmer, Eugene A. Paulin, William F. Radle, Harold K. Schilling, J. C. Stearns, S. Bradford Stone, William A. Thomas, Glen W. Warner.

The titles and abstracts of papers presented before the Optical Society of America will be found in the Proceedings of that Society, published in the Journal of the Optical Society of America and Review of Scientific Instruments.

The Abstracts of the forty-three papers presented before the American Physical Society are given in the following pages. Numbers 7, 8, 11, 14, 35, 38, 39, 40, 41, 42, and 43 were read by title. An Author Index will be found at the end.

HAROLD W. WEBB, *Secretary*

ABSTRACTS

1. Line structure. D. G. BOURGIN, University of Illinois.—The author's previously published data for the HCl fundamental band lines has been approximated by line patterns of (a) a Doppler broadening type or (b) a Stark effect broadened line (admitting a molecular force field) or (c) a Lorentz interrupted absorption type. The modifications attendant on recognition of the isotopic structure are predictable from the calculations for an infinitely

separated doublet structure. The component line breadth is about 10^{10} frequency units for a class (c) line. Certain considerations make it improbable that the Stark or Doppler effects are determining influences here. The criterion $dp(r_0)/dr \sim q_0$ is suggested.

Badger's data on the rotational spectrum of HCl has been studied on the assumption of a "coupling," pressure line broadening. The value $\int_0^\infty \mu(\lambda)d\lambda = 1.3\,10^{-4}$ is in better agreement with theory than Badger's estimate of $1.1\ 10^{-4}$ but the discrepancy is still excessive and indicates the necessity for further experiment.

2. Quantum analysis of the beryllium oxide bands. JENNY E. ROSENTHAL and F. A. JENKINS. New York University.—The three prominent sequences of BeO bands in the blue-green, blue, and violet have been photographed in the first and second orders of the 21-foot grating at Harvard University. The source was a carbon arc cored with potassium beryllium fluoride. Resolution of the bands is complete except for about five lines at the head. Each band has a P and an R branch, the lines of which remain strictly single as far as they are observed (to about $j=70$). A perturbation occurs in the state $n'=1$, $j'=50$, the result being merely a displacement of the corresponding line by 0.45 cm^{-1} toward lower frequencies, with no sign of doubling. Combination relations between R and P lines are found to hold, and the resulting values of $\Delta_2 F$ may be represented by $4BT$, where T is half-integral. There is probably but one missing line at the origin and no evidence is found of weak Q branches. According to these results, the bands may be interpreted as due to a $^1S \rightarrow {}^1S$ electron transition. The combination relations show that the band at $\lambda 4708.64$ is the (0, 0) band. Preliminary values for the constants in the equation $B = h/8\pi^2 I_0 - \alpha n$ are: $I_0' = 17.65 \times 10^{-40}$ gm. cm.^{2}, $I_0'' = 16.85 \times 10^{-40}$, $\alpha' = 0.0165$, $\alpha'' = 0.0187$. The internuclear distance of BeO in the final state (probably the normal state) is therefore 1.33×10^{-8} cm.

3. The heat of dissociation of Na_2. F. W. LOOMIS. New York University.—From the writer's formula (Phys. Rev. **27,** 607, (1927)) for the vibrational terms in the blue-green band system of Na_2, the heat of dissociation of the normal molecule is calculated, by the method of Birge and Sponer, to be 1.0 ± 0.1 volts. It is also shown that the dissociation energy of the molecule in the upper level of this band system is 0.6 volt and that this upper level molecule dissociates into one normal atom and one atom in a 3^2P state, whereas the lower level molecule dissociates into two normal atoms. By combining the above results with those calculated from the formula of Fredrickson and Watson (Phys. Rev. **30,** 429, (1927)) for the red band system, it is shown that this system has the same lower state as the green system and that its upper state also dissociates into one 3^2P and one normal atom, but with an energy of dissociation of 1.25 volt.

4. Optically excited iodine bands with alternate missing lines. By R. W. WOOD, Johns Hopkins University, and F. W. LOOMIS, New York University.—The iodine fluorescent bands which develop around the fundamental doublets when iodine is in the presence of helium have been studied with higher resolution than heretofore. They are found to contain only alternate lines of the corresponding absorption bands, namely, those for which m' is even. Now the fluorescent bands are known to be developed by collisions of the second kind between excited iodine molecules and helium atoms, wherein m' is changed from 34, the value originally excited, to various neighboring values. The new data, then, show that the rotational quantum number of an iodine molecule can only change by an even number during a collision of the second kind in which the electronic quantum number does not change. This result is entirely in accord with the new mechanics, which, according to Hund, attributes to the successive rotational states of a symmetrical molecule, such as I_2, eigen-functions which are alternately symmetric and anti-symmetric in the two nuclei; and which requires that transitions between symmetric and anti-symmetric states shall be very rare; so rare that, on Dennison's successful theory of the specific heat of hydrogen, they do not occur, even during the time it takes to measure the specific heat.

5. Electron states in diatomic molecules. ROBERT S. MULLIKEN, New York University, Washington Square College.—Applying Hund's recent theories, and developing suggestions of

Hund and the writer, the ordinary physical and chemical properties of diatomic molecules can be accounted for by assigning a quantum state for each electron, and energies of removal (ionization) for each state. The assignments below are probably in the main correct; the order in which the symbols is given is always that of increasing ease of removal. The two $1s$ and two $2s$ electrons represent K electrons of the separated atoms, essentially unchanged except in formal quantum number. Outer electrons are mostly much more firmly bound than the same quantum numbers would indicate for an atom; *e.g.* the $4s$ shell of N_2 (ionization potential 17 volts) is comparable energetically with the $1s$ shell of He. Assignments: Normal LiF, BeO, $(1s)^2(2s)^2(3s)^2(2p)^6$; normal BeF, BO, CO^+, CN, N_2^+. $(1s)^2(2s)^2(3s)^2(2p)^6(4s)$; excited BO, etc., $(1s)^2(2s)^2(3s)^2(2p)^5(4s)^2$; normal CO, N_2, CN^-, $(1s)^2(2s)^2(3s)^2(2p)^6(4s)^2$; excited CO, N_2, $(1s)^2(2s)^2(3s)^2(2p)^6(4s)(x)$ and (or?) $(1s)^2(2s)^2(3s)^2(2p)^5(4s)^2(y)$, x and y variable; NO and O_2^+, $(1s)^2(2s)^2(3s)^2(4s)^2(2p)^6(x)$, with $(x)=(3p)$ for normal state; normal O_2 and F_2, $(1s)^2(2s)^2(3s)^2(4s)^2(2p)^x(3p)^y$ with perhaps $x=y=4$ for O_2 and 5 for F_2. Similarly for analogous higher molecules. The assignments are based mainly on spectroscopic and ionization potential data.

6. A new determination by a photographic method of the water absorption band at 9727 angstroms. J. E. LAMBLY, Cornell University.—A precise determination of the water absorption band in the near infra-red has been made and found to be located at 9727 Angstroms, for a temperature of 22°C. This result, which is the average of three independent determinations, checks with that of Collins (Phys. Rev. **26,** 771, (1925)) at 9740A. Photographic records of spectral intensity from an incandescent lamp, with and without absorption, were made on red sensitive neocyanine plates, hypersensitized with ammonia. Density measurements were made with a photo-electric densitometer, and ratios computed to determine absorption peaks. Care was taken to measure these accurately. Long exposures through heavy filters and a slit of only 40 Angstroms were made. Results were consistent. The average should be accurate to 10 or 12 Angstroms, every precaution having been taken to give the utmost accuracy, both in making the exposures and measuring the plates. Consequently, the result should be considerably more accurate than previous results.

7. The molecular structures of methane. JARED KIRTLAND MORSE, University of Chicago. —The same concepts which were so useful in determining the molecular and lattice structures for ethane (Proc. Nat. Acad. Sci. Jan., 1928) are here used to construct molecular models for methane and the moments of inertia computed from these structures are compared with those obtained by Cooley (Atrophys. J. **62,** 73 (1925)) from the analysis of the infra-red absorption bands. These moments of inertia are found to agree with experiment within the limit of experimental error. Two types of molecules are differentiated, one having a "single electron bond" between the carbon and hydrogen nuclei, the other having two electrons forming this bond. In each of these types, eight "hydrogen positions" are possible, since there are only four hydrogen nuclei available in the molecule, a certain finite number of "dynamic isomers" can be formed determined by the number of ways four nuclei are distributed among the eight positions. The band observed at 7.7μ is due to a symmetrical tetrahedral methane molecule having a "single electron" bond between the hydrogen and carbon nuclei. The band at 3.31μ is due to a symmetrical molecule having a "two electron" bond between them. The weak band at 3.5μ is due to an unsymmetrical "dynamic isomer" of methane with "two electron" bonds.

8. The absorption bands of some hydrocarbons between 1.0μ and $.7\mu$. JAMES BARNES, Bryn Mawr College.—This paper is a continuation of abstract (Phys. Rev. **29,** 922 (1927)). In this region of the spectrum liquid pentane, decane, and tetradecane have each two strong absorption bands which are doublets and their wave-lengths have been measured to an accuracy of $.002\mu$. Their frequencies have lower values than the corresponding bands of the aromatic series and also decrease as the mass of the molecule becomes larger. Their frequency differences are 7 and 8×10^{12} sec^{-1} for the longer and shorter wave-length bands respectively. The shorter wave-length component of all these doublets has the stronger intensity. The densitometer graphs give their relative intensities as 4 to 3 approximately. In addition to the above these substances have weak single bands at $.81\mu$ and $.97\mu$. The strong absorption at $.874\mu$ of benzene and at $.877\mu$ of toluene have also been resolved into doublets. Their frequency differences are the same, 3×10^{1} sec^{-1}, within the limit of error.

9. Certain multiplets in the spectra of cadmium III and indium IV. R. C. GIBBS and H. E. WHITE, Cornell University.—Guided by the transitions from $^3PD'F$, $^1PD'F$, $(4d^95p)$ to ^3D, ^1D $(4d^95s)$, already determined for Pd I and Ag II, (data furnished to the authors by A. G. Shenstone in advance of publication), the corresponding lines have been identified in the spectra of Cd III and In IV. The transitions from $^3D'_1$, $^3P_1$ and $^1P_1(4d^95p)$ to $^1S_0(4d^{10})$, the latter being the lowest level in each of these spectra, have also been identified for Ag II, Cd III, and In IV. These combinations account for nearly all of the strong lines in each spectrum. The term values for the four iso-electronic systems Pd I, Ag II, Cd III, and In IV, together with those for the corresponding elements in the first long period, have been plotted on a Mosely diagram which brings out certain similarities and variations between these two sets of spectra. The validity of the irregular doublet law is again confirmed by the almost constant shift in the corresponding radiated frequencies $(4d^95s-4d^95p)$ on passing in succession from Pd I to Ag II, to Cd III, and to In IV.

10. The spark spectrum of silver (Ag II). A. G. SHENSTONE, Princeton University.—The spark spectrum of silver can be based on a set of terms as follows:- $^1S_0$ from the structure $4d^{10}$; ^3D, ^1D from $4d^95s$; ^3P and ^1P, D', F from $4d^95p$; ^3D, ^1D from $4d^96s$; ^{3} and ^1S, P', D, F', G from $4d^95d$. The lowest term $^1S_0$ is from the measurements of H. E White at Cornell in the region λ1100. There is evidence also for the structure $4d^95f$. The intervals and g-values are very irregular. The ionization potential calculated from the two-member series of $^2D_3$ levels is about 21.9 volts from $^1S_0(d^{10})$ to $^2D_3(d^9)$. The limits calculated from the component series of ^3D, ^1D indicates a divergence from theory as in the analogous cases of Ni I, Cu II, Pd I The intervals of the pentad d^9d also indicate a divergence. The $^1S_0$ term is at 39164 wavenumbers below $^3D_3$. This indicates that the hypothetical $^2D(d^95^2)$ of Ag I should have almost the same value as 2^2P of that spectrum, which in part explains the low intensity of the lines in the spectrum which must be due to it.

11. The arc spectrum of antimony. J. B. GREEN, Ohio State University, and R. A. LORING, Northwestern University.—McLennan and McLay (Trans. R. S. Can. **21**, 63 (1927)) have made a start at the analysis of the spectrum of Sb on the basis of the Hund theory. According to this the lowest levels should be due to the configuration s^2p^3 (hereafter called the a configuration) and are $^4S_{\frac{3}{2}}'$, $^2D_{2\frac{3}{2}}'$, $^2P_{1\frac{1}{2}}$. These levels have also been identified in all the other elements of this group. The b levels, due to $s^2p^2\cdot s$ should be $^4P'_{1\frac{1}{2}3}$, $^2P_{1\frac{1}{2}}'$, $^2D_{2\frac{1}{2}}$, $^2S_{\frac{1}{2}}$. Of these, only the first two terms have previously been identified. The c configuration, $s^2p^2\cdot d$, should yield $^4(F'DP')$, $^3(F'DP')$, $^2(GF'DP'S)$, ^2D. The d configuration gives $^4(D'PS')^2$, $(D'PS')$, $^2(FD'P)$, ^2P. These authors have been successful in assigning all the low levels of each of configurations, and also that due to Sp^4. In addition, a series of terms yields the value 67579 for a $^4S_{\frac{3}{2}}'$ corresponding to an ionization potential of 8.35 volts. Ruark gives 8.5 ± 1.0 volts. The Zeeman effect has been studied for all of the stronger lines in the region 2500–4033 and the g values of the terms computed. The g values do not agree with the theoretical values and not enough lines can be measured with sufficient accuracy to determine whether Pauli's g sum rule is satisfied. A complete report of the work is now in press.

12. Recombination of atom ions and electrons. F. L. MOHLER, Bureau of Standards. A thermionic discharge is maintained in caesium vapor with about 5 volts applied between a fine wire cathode and a cylindrical anode which completely incloses it. Relatively high ion and electron concentrations can thus be obtained and with currents greater than .1 amp. and vapor pressures above .1 mm the spectra show continuous bands extending from each series limit. A paper in press gives photographs and intensity measurements of these continuous spectra. Probe wire measurements have been made in a similar discharge and semilogarithmic plots of the electron current show that the electrons have a strictly random distribution of energy, with unusually low average energies, between .2 and .3 volts. Assuming that the continuous spectra are recombination spectra one can, on the basis of the intensity measurements and the known velocity distribution of electrons, compute relative values of the recombination probability as a function of the electron speed, and of the absorption probability as a function of the frequency. The results of course apply to recombination into a definite energy state or to absorption resulting in ionization of atoms initially in that state.

13. Reflection of electrons by a crystal of nickel. C. J. DAVISSON and L. H. GERMER, Bell Telephone Laboratories, Inc.—A homogeneous beam of electrons is directed against a face of a crystal of nickel cut parallel to a set of its {111} atom planes. The angle at which the beam meets the crystal surface can be varied. The angle of incidence is adjusted to a chosen value, and observations are made in the plane of incidence of the intensity of scattering as a function of direction and of bombarding potential. At certain critical speeds of bombardment a sharply defined beam of electrons issues from the crystal in the direction of regular reflection. When the angle of incidence is 10 degrees the regularly reflected beam appears for speeds corresponding to 38, 70, 133, 210 and 320 volts. The values of the critical speeds increase as the angle of incidence is increased. The phenomenon is the analogue of the Bragg type of x-ray reflection with the incident beam exhibiting the properties of a beam of waves of wave-length inversely proportional to the speed of the electrons. The data cannot be used to calculate wave-lengths on account of the effect of the "spacing factor" of the crystal [Phys. Rev. **30**, 704 (1927)] and because the elementary plane grating beam is of zero order.

14. X-radiation from the impacts of electrons against gas atoms. WILLIAM DUANE, Harvard University.—In a paper presented to this Society last year I described experiments on the x-radiation produced by the impacts of electrons against atoms of mercury vapor. All the electrons had substantially the same velocity, and the radiation at right angles to the direction of motion of the impinging electrons (after it came through the window in the apparatus) appeared to have an average, or effective wave-length somewhat longer than the short wave-length limit given by the quantum equation. This paper describes further experiments on the radiation at right angles to the electron stream, in which thinner windows were used, and also experiments on the radiation projected from the impacts forward in the direction of motion of the electrons. The paper contains also a brief discussion of the degree of approximation with which the results of the experiments can be explained by certain theories of the radiation coming from an electron as it approaches an atomic nucleus.

15. The application of the phonodeik in determining the performance of electro-acoustic devices. DAYTON C. MILLER and JOHN R. MARTIN, Case School of Applied Science.—The phonodeik gives a direct photographic record of a sound wave, as received by the ear. A sound reproduced by an electro-acoustic device may thus be compared directly with the original sound. A loud speaker is connected to the output of a transmitting system which may consist of a microphone and amplifier, and any sound energizing the microphone will be reproduced by the loud-speaker and is recorded by the phonodeik. The distortion introduced by the device, together with its associated electrical system, may thus be determined. This method has been used to study the frequency response of radio loud-speakers, microphones, electrical phonographic pick-ups, and amplifying systems. By replacing the loud-speaker with a vacuum-tube voltmeter, the distortion introduced by the electrical system may be determined. A vacuum-tube oscillator with a frequency range of 40 to 6000 may be used as an electrical source, the energy of the output being maintained constant, and the wave form being checked with an oscillograph. This output is used to actuate a loud speaker and the resulting sound is recorded on the phonodeik at the desired frequencies. The method is also applicable to the study of mechanical-acoustic devices.

16. Extreme ultra-violet spectra excited by controlled electron impacts. K. T. COMPTON and J. C. BOYCE, Princeton University.—A vacuum spectrograph having some new features in design has been used in the study of the spectra of helium, neon, and argon in the wave-length region shorter than 1200A. Electrons from a Wehnelt cathode are accelerated by known voltages through a wire grid anode, beyond which they excite the gas. Fast pumps keep the pressure in the spectrograph at about 0.005 of that in the discharge tube, returning the gas to the discharge through a purifying tube. Spectra are photographed with the pressure in the discharge low enough that electrons in their path make on the average only one collision with a gas molecule, and that arcing is impossible. Exposures made at increasing voltages show successive stages of excitation and ionization brought about by single electron impacts, making the interpretation easier than that of those taken at higher pressures where cumulative ioniza-

tion occurs. In helium ten members of the arc series have been observed from 584 to 507A and five members of the spark series from 303 to 234A. In neon and argon the results of Dorgelo and Abbink have been generally confirmed and many additional lines have been observed.

17. The spark spectra of neon and argon. H. N. RUSSELL, K. T. COMPTON and J. C. BOYCE, Princeton University.—With the vacuum spectrograph described in the previous communication, Neon II shows 15 new lines between 462 and 353A—all of which have been identified as combinations between a low ^2P term of separation 782 frequency units, and higher doublet and quartet terms. Many still higher terms conbine with the latter, giving multiplets in the visible and ultra-violet, some of which have been announced by de Bruin and Kichlu. The corresponding electron configurations have been identified, and the ionization potential fixed at 40.9 ± 0.05 volts. Argon II shows numerous lines between 932 and 487A. The low ^2P term has in this case a separation of 1430—as suggested by Dorgelo and Abbink. The higher terms can be connected with the frequency differences observed in the blue spectrum by Paulson. The ionization potential appears to be not far from 27 volts, supporting the value obtained by Barton by the method of positive ray analysis.

18. On the time required for the photo-electric ejection of an electron by visible light. ERNEST O. LAWRENCE and J. W. BEAMS, Yale University.—We have already reported experiments (Phys. Rev. **29,** 903, (1927)) which indicated that electrons are ejected from a potassium metal surface within $3(10^{-9})$ sec. Although the experimental observations were definite and reproducible, there existed several possible sources of systematic error. We have now completed a more detailed study of the ejection of electrons from a potassium hydride surface which has confirmed the conclusion that the photo-electric effect is instantaneous within $3(10^{-9})$ sec.—and which has eliminated the uncertainties of the earlier research.

19. Photo-electric thresholds and fatigue for iron, cobalt, and nickel. GEORGE B. WELCH, Cornell University.—Preliminary measurements on samples of pure iron, cobalt, and nickel, with surfaces prepared in vacuum, show the photo-electric thresholds for these elements to be 3150, 3150, and 3045A., respectively. With time, the thresholds remain constant within the limits of experimental error. All three elements show photo-electric fatigue. During the course of the experiments, the relation between the photo-electric current and the time is found to be $i=Ct^{-\alpha}$, where α is a quantity which depends upon the substance used and, for a given substance, increases numerically as the threshold is approached.

20. Heisenberg's uncertainty relation and the motion of free particles. ARTHUR E. RUARK, Mellon Institute, University of Pittsburgh and Gulf Production Companies.—In the Nashville program, the author has described (Proc. Am. Phys. Soc., Nashville meeting), an arrangement of apparatus which seemed to make possible simultaneous determinations of the coordinate q and the momentum p of a free particle, so accurately that Heisenberg's relation $\Delta q\cdot\Delta p\sim h$ is violated. It was stated that the violation is only apparent because the precision of measurement of both p and q is limited by statistical fluctuations in the measuring devices. Contrary to this view, the true reason for the validity of the principle is that slight velocity changes occur when the particle passes through a variable slit. The situation is analogous to the frequency changes of light due to modulation. (Breit, Ruark and Brickwedde, Phil. Mag., **3,** 1306 (1927)). Of course, errors due to fluctuations of the measuring devices are also present. Even in the most favorable cases, they are such that $\Delta q\cdot\Delta p\gg h$. Further, the reaction of the measured object on the measuring device introduces an uncertainty similar to that discussed by Heisenberg.

21. A novel optical instrument: spectroscope used as color-filter for telescope. JOHN Q. STEWART, Princeton University.—The slit of any spectroscope is removed from normal position, backed by a mirror, and substituted for the eyepiece of the view-telescope. A condensing lens, as usual, images an object in the focal plane of the collimator. A succession of overlapping images in light of neighboring wave-lengths is thus formed on the slit, after dispersion by

prism or grating. The segment of mirror exposed behind the slit reflects back a different part of each image, in light of corresponding color; and thus a complete image of the original object is again formed in the focal plane of the collimator, but in light of a narrow range of wave-lengths, adjustable over the spectrum. A half-silvered mirror, or other means, forms this image off to one side; where it may be magnified by an eyepiece. Thus the original extended object is viewed in light of a narrow band of wave-lengths. This apparatus was set up and tested in various forms, Mr. S. A. Korff assisting. With the help of Mr. J. Bucher the same principle was found to give practicable means of color-photography without the use of colored screens—the camera being used, reversed, to view the plate.

22. An afterglow spectrum of argon. CARL KENTY and LOUIS A. TURNER, Princeton University.—Using a rapidly rotating sectored disc and commutator the arc spectrum of argon is found to persist approximately 0.001 sec. after an arc of 0.5 amp. in pure argon at 0.5 mm pressure is cut off. This spectrum is not caused by direct excitation by electrons since the D lines which are strong in the arc itself are absent in the afterglow. Sodium vapor from a properly impregnated oxide cathode is always present. Dropping the voltage to 4–11 volts instead of to zero in the off period brings out the D lines in the afterglow and shortens its duration. Reverse potentials up to 45 volts have no effect. Comparison of photographs of the spectra of the afterglow and of the arc shows that, in the afterglow, lines involving jumps from high s and d states to the $2p$ states are much stronger with respect to $1s-3p$ lines than in the arc. The absence of the D lines, the relative enhancement of lines involving high energy levels and the shortening of the duration of the afterglow by electrons suggest the hypothesis that the afterglow spectrum results from recombination. A search is being made for continuous spectra which would probably accompany recombination.

23. The optical dissociation of iodine vapor. LOUIS A. TURNER, Princeton University.—A cell containing iodine vapor at 18°C absorbs the light of the iodine emission line of wave-length 1830.4A more strongly when illuminated by concentrated light from a carbon arc than when not so illuminated. The line at 1844.5 does not show this effect. The increased absorption is attributed to iodine atoms resulting from the optical dissociation of molecules by the light of the arc. Franck suggested that such a dissociation was connected with the continuous absorption of iodine on the short wave-length side of the convergence limit of the absorption bands. The idea was supported by Dymond's experiments on fluorescence, and by the correctness of the value of the heat of dissociation calculated on the basis of this theory. The present experiment gives a direct indication of the presence of the atoms. The 1830.4 line is very probably the $a^2P_2-k^4P_3$ line, the one of longest wave-length which is emitted as a result of a transition to the ground state (a^2P_2).

24. The absorption and fluorescence of a mixture of mercury and zinc vapors. J. G. WINANS, National Research Fellow, Princeton University.—It was observed that light from the aluminum spark of wave-length below 2000 excited vapor distilling from slightly amalgamated zinc, causing the emission of the first triplet of the sharp series of zinc; but excited neither the non-distilling vapor nor that distilling from pure zinc. Vapor distilling from the same kind of mercury zinc mixture showed a continuous absorption, especially strong for wave-lengths below 1860 and extending to 2050. The non-distilling vapor (zinc vapor pressure 37.0 mm) absorbed Hg 1849, width 5A; Zn 2138, width 91A; Hg 2536 and Cd 2288, both narrow; and two unaccounted for bands at 2068, width 7A; and 2001, width 7A. These observations are explained by assuming that HgZn distills from the zinc amalgum and is dissociated into an excited zinc atom in the 2^3S state and a normal mercury atom upon absorption of light of wave-length below 1860. Assuming a very small heat of dissociation, the minimum energy for this process is 6.62 volts, corresponding to a wave length of 1861. The absorption of mercury alone under like conditions was different and appeared the same for distilling and non-distilling vapor.

25. Theory of the excitation of spectra by atomic hydrogen. JOSEPH KAPLAN, National Research Fellow, Princeton University. (Introduced by H. D. Smyth).—An explanation is proposed for the results of Bonhoeffer and of Mohler on the excitation of spectra by atomic

hydrogen. The theories advanced by these authors do not completely explain the experimental results. The theory presented here is based on the hypothesis that in a three-body collision two hydrogen atoms can be bound to form a molecule in any one of the vibration states of its normal electronic level. We make use of the principle, used in collisions of the second k nd, that the probability of excitation increases as the energy of the exciting body and the energy necessary for excitation approach each other. This is done by postulating that the probabliity of the excitation of the third body is greater, the nearer the energy required is to the difference between the energy of recombination and the energy retained by the hydrogen molecule in one of its vibration states. The theory has been applied successfully to the excitation of Na, K, Cd, Zn, Cs and Mg by atomic hydrogen. The excitation of the 2537 line of mercury, which requires more energy than that available from recombination, is explained on the basis of Bonhoeffer's observations.

26. Certain characteristics of the spectra of mercury at the higher radiating potentials. L. R. MAXWELL, National Research Fellow, Bartol Research Foundation.—Electrons in mercury vapor with velocities greater than 150 volts were confined in a beam by a magnetic field. Perpendicular to the beam an electric field withdrew positive ions before they recombined. The arc lines emitted showed no increase in density on removing the electric field. This indicates that recombination contributes very little to the production of these lines which is contrary to the explanation given for the complete arc spectrum appearing above the ionization potential. Consequently the arc spectrum is explained in the following two ways: (1) as being due to inward transitions of one or both of the valence electrons after being removed to outer orbits, (2) due to the return to the 1^1S state by an electron which has been displaced from a soft x-ray level to a virtual orbit, while simultaneously a valence electron falls in to fill the vacancy of the inner level. Resonance radiation exists for lines produced by transitions ending in the 1^1S, 2^3P_0, 2^3P_1 and 2^3P_2 states, but much less for those terminating in the 2^1P state. Several spark lines due to Hg^{++} appear unique in that they show a distinct shift in the direction of motion of the positive ions. This presents a new method for distinguishing this type of spectrum.

27. Photographic determination of the temperature of the tungsten cathode in the electric arc. ERNST K. G. STUECKELBERG, Princeton University.—By means of the blackening of a photographic plate, the value and distribution of the cathode temperature of a tungsten arc in nitrogen were measured. As a fixed point for the scale the black temperature of the carbon arc anode was taken. Its value was found by Henning and Heuse to be 3700°K. The emission power for tungsten was taken from Zwikker. The arc burned in carefully purified nitrogen between small spheres of tungsten (diameter 0.18 to 0.29 cm) on wires. The true temperature was found to have a uniform value over the sphere, independent of pressure and varied between 2600 to 3300°K. The current-density was therefore also supposed to have a uniform value over the sphere. (The current was varied from 0.25 to 6.0 amp.). Plotting the log of the current against the reciprocal temperature, straight lines were found parallel to the curve of thermionic emission for tungsten. For a given current, as the cathode surface was increas d, the temperature dropped according to the emission law. As the temperature gradient along the wire was photographically measured, the loss of energy of the cathode by conduction, radiation and electron emission could be calculated. (This work was done at the University of Basle and will be published in full in the Helvetica Physica Acta, February or March, 1928.

28. The relation between arc stream dimensions and light intensity. W. B. NOTTINGHAM, Bartol Research Foundation.—The three regions of electric arc discharge are (1) the positively charged cathode space, (2) the negatively charged anode space, (3) the arc stream with zero space charge. If the average electrical field along the direction of the arc axis is assumed to be uniform, as indicated by experiment, the average number of electrons per unit volume would be proportional to the average current density crossing a surface perpendicular to the arc's axis. Light given off the arc stream due to single impacts of electrons on neutral atoms should be $l_1 = ai$, and due to double impacts $l_2 = bi^2$. (l = measured light per unit volume; i = measured

average current density; a and b constants). If the slope of the curve "log l" versus "log i" is 1.0 or 2.0, light production by single or double impacts respectively would be indicated.

RESULTS OBTAINED

Metal	Atmosphere	Impacts	Remarks
Cadmium	Argon	Double	Current 1.0 and 2.0 amp.
Cadmium	Argon	Combination	Current 4 amp.
Copper	Air	Combination	Green lines, 8 amp.
			3000 amp./cm.^{2} = Current density at cathode
Copper	Air	Single	Blue lines, 8 amp.
Tungsten	Air	Single	Blue lines
Carbon	Air	Indeterminate	4216 cyanogen bands

29. Effect of an interfering tone upon the hearing of a normal and a deafened ear. JOHN GUTTMAN, New York Post Graduate Medical School and L. B. HAM, Washington Square College, New York University.—Two audible frequency oscilators were connected to a common telephone receiver so that one or two tones could be introduced into the ear. Energy of a given frequency from the first oscillator was increased to threshold intensity. Then an interfering tone of 50 transmission units (T. U.) above threshold for the person examined was introduced by the second oscillator which suppressed the first tone so that its intensity had to be increased for new threshold. Magnitude of the suppression was measured in T. U. also, and plotted against frequencies of the first oscillator. Preliminary experiments show that a given relative increase of energy produces in a deafened ear a greater hearing sensation than in a normal ear in the presence of an interfering tone whose multiple energy value above threshold is the same for every person. Artificial deafening with oils produced similar results. Indications are that, for the same degree of deafness, the effect noted depends upon the type of deafness. Resultant curves are shown.

30. Experiments on audition by bone conduction. C. E. DEAN, Johns Hopkins University.—Bone conduction is a term used by otologists to designate audition due to vibration of the skull. Special telephone receivers to produce this vibration and other equipment from the Bell Telephone Laboratories were used. By a second person listening with a stethoscope for minimum sensation, a standard amplitude of skull vibration may be established. In this way the bone conduction produced by ordinary telephone receivers was found to be negligible except for cases of considerable dea ness. Beats between two bone conduction stimuli are heard, and between ordinary and bone conduction stimuli if both reach one ear. The difference in effect at the near and far sides of the head, of a bone conduction stimulus applied on one side was measured from 362 to 2048 cycles for two cases in which the auditory nerve had been cut on one side, and was found to be small, averaging 4 T. U., or an amplitude ratio of $10^{-0.2}=0.6$. For this reason noise in the opposite ear should be used in all examinations of bone conduction sensitivity. It is also important that calibrations and tests be made in a silent place. An explanation was found of the frequent cases in which all bone conduction sensations seem in one ear.

31. The vibrations of tuning-forks. ELMER A. HARRINGTON, Bureau of Standards.—A study of the energy dissipated by frictional and viscous forces in tuning-forks. Two electrically-driven tuning-forks were used: (1) an ordinary fork, (2) a fork made by clamping two steel bars, with a rectangular block between them, in a vise so that practically no energy was expended in moving the stand. The following properties were investigated: (1) the logarithmic decrement, and the effect on the logarithmic decrement of damping due to vanes at the ends of the prongs; (2) the relation between the current driving a fork and the deflections of the prongs produced, both for steady and resonant deflections; (3) the equivalent length of a rigid straight bar turning through the same angle as the tangent at the end of the prongs; (4) the energy due to emission of sound, and the energy dissipated by internal friction. It was found that: (1) the change in the logarithmic decrement was roughly proportional to the area; (2) the deflections of the prongs were proportional to the square of the current; (3) a straight bar 73 % of the length of the prong is approximately the equivalent length; (4) about 3.5 % of the total energy is converted into sound, while nearly all of the remainder is expended in overcoming internal friction.

32. Internal friction in metals. R. H. CANFIELD, Johns Hopkins University.—A tubular specimen of metal is used as the elastic control of a heavy metal pendulum which is set into forced vibrations by electro-magnetic forces. The mode of vibration is either torsional or transverse, so that the internal friction is determined for two types of stress; the principle being analogous to Searles' method of determining elastic constants. Observations are made on the maximum amplitude (peak of the resonance curve) from which the friction constants are easily deduced. Logarithmic decrement observations can be made, and agree with the results of the other method. The phase of the vibration relative to the impressed forces can be determined and leads to Kimball's conclusion that the dissipative stresses are non-viscous. Preliminary results show two definite discontinuities in the relation between dissipated energy and stress amplitude, of which one depends on the mechanical history of the specimen, and the other is independent of it.

33. Friction and frictional torque in gyroscopic motion. R. C. COLWELL, West Virginia University.—When a rotating top is hung upon two inclined rods the friction at the points of suspension will start and stop the precession in such a way that the top will walk down the rods. The equations are developed for this motion. In a suitably mounted top the frictional torque will cause the top to rotate rapidly about its point of support. The precession of the top may then be made to act with or against the motion due to friction, so that this top will automatically reverse its direction of spin.

34. Motion of the ball on a bowling alley. L. W. TAYLOR, Oberlin College.—This is an experimental study of the motion of the ball on a bowling alley. A recording device registers to hundredths of a second the times of passage of the ball through successive half-meter intervals. Initial velocity is rendered reproducible by launching the ball with a catapult, in place of doing it by hand. Systematic deviations from the behavior prescribed by the simple theory are found, which indicate that the coefficient of friction is a function of the velocity. The results of the experiment suggest a general form for this function.

35. The effect of heat treatment of bismuth in the Hall effect. PALMER H. CRAIG, Premier Laboratory Company.—Investigation of the initial heat treatment of bismuth plates used in the Hall Effect shows that cast plates prepared by very rapid cooling exhibit abnormalities which do not occur in plates prepared by annealing. The high values of the Hall coefficient previously reported in bismuth at low magnetic field strengths were confirmed in plates very rapidly cooled, but the shape of the Hall coefficient-field strength curve was found to be much more regular for slowly cooled, cast bismuth plates, as reported by C. W. Heaps. Similar results were obtained using alternating current, and graphs obtained from experiments on rectification of alternating current by the Hall Effect indicate a possible empirical formula for such cases.

36. **Thermoluminescence excited by high voltage cathode rays.** FRANCES G. WICK and EDNA CARTER, Vassar College. —Specimens of powdered calcite, fluorite and magnesium sulphate containing a small amount of manganese, exposed to the powerful stream of cathode rays outside of the metallic window of the Coolidge cathode ray tube showed brilliant thermoluminescence when heated to a relatively low temperature. The exposures were made in the General Electric laboratory at Schenectady with the generous co-operation of Dr. W. D. Coolidge and the assistance of Dr. Moore. The specimens were immediately put into liquid air and kept at this low temperature until the observations could be made at Vassar College. Photometric observations of maximum brightness and rate of decay of thermoluminescence were made with variation in (1) time of exposure, (2) temperature of exposure, (3) voltage on the cathode ray tube during exposure, (4) temperature of observation. The effect of cathode rays is similar to that of exposure to x-rays but there are some differences. Cathode rays produce a more intense thermoluminescence which appears at a lower temperature and the effect is more permanent than that due to x-rays. Saturation is produced in 10 seconds by cathode rays in specimens which it takes one hour to saturate by exposure to x-rays under the conditions previously described by Wick and Slattery.

37. Evidence obtained by x-ray analysis of films of iron in magnetic fields as to the ultimate nature of magnetism. T. D. YENSEN, Westinghouse El. and Mfg. Co., East Pittsburgh.—The results of K. T. Compton and Trousdale, (1915) and of A. H. Compton and Rognley (1918–1920) showed that there is no change in the crystal structure of single crystals of magnetite and hemetite when subjected to strong magnetic fields. In the present investigation films of electrolytic iron were analyzed by x-rays to determine whether there is any change in the random orientation of the minute crystals (of the order of 150A) found in these films when subjected to strong magnetic fields (up to 2600 gauss). If so, the uniform circular diffraction patterns resulting from the randomly oriented crystals should be changed to show greater density along one diameter than along the other, perpendicular to it, due to the preferred orientation. The circles were analyzed microphotometrically and the results indicate no change in the orientation. The average of all the measurements is a ratio of the intensities along the two diameters of $1.00 \pm .08$, the variation being attributed to incidental sources arising from the developing and handling of the film. The conclusion, therefore, is that the most minute crystal aggregates in iron are not oriented in a magnetic field and lends strength to the previous conclusion in regard to the ultimate nature of magnetism, namely, that the magneton is an atomic property.

38. An apparatus for the measurement of radiation intensity over a wide range of wavelengths (0.02–3A.). OTTO GLASSER and V. B. SEITZ, Cleveland Clinic Foundation.—The instrument consists of, (1) a condenser attached to an ionization chamber, and (2) an improved type of string electrometer with static charger. The procedure is as follows: The condenser unit is electrically connected with the electrometer unit and the whole system charged to a known potential. The condenser unit is then removed and placed together with the ionization chamber in the field of radiation to be measured. After exposure for a specified time it is again returned to the electrometer and the loss of charge read. In order to prevent any radiation from affecting the charge in the condenser unit other than that at the ionization chamber, a solid dielectric completely surrounds the charged part of the system thus dispensing with lead. In order to obtain protection at the point where electrical connection is made between the two units, a mechanically operated cover of dielectric is incorporated in the form of a switch. Ionization chambers of a material with an effective atomic number equivalent to that of atmospheric air are used and range in size from 1/50 c.c. up. Radiation intensities are measured in R units for the range of wave-length from 0.02 to 3A. This complete range is covered with but one change in the ionization chamber.

39. Intensity of reflected x-rays and the distribution of electrons in crystals. G. E. M. JAUNCEY, and W. D. CLAUS, Washington University.—Williams (Phil. Mag., 2, 657 (1926)) and Jauncey (Phys. Rev., **29, 757** (1927)) have suggested that the intensity of x-rays reflected by a crystal is less than that on the classical theory, due to the modified scattering taking place at the expense of regular reflection. Havighurst (Phys. Rev., **31,** 16 (1928)) takes issue with Williams and Jauncey. The present paper is a reply to Havighurst. By trial a reasonable Bohr model of the chlorine ion has been found which gives F values, calculated in accordance with Jauncey's theory, at all angles in good agreement with the experimental values. When a Fourier analysis is applied to the theoretical F values an electron distribution (or U) curve is obtained which is similar to that obtained from experimental F values. The areas under the theoretical and experimental U curves are 16.64 and 16.74 electrons respectively for a grating space of 3.1A. Yet our theoretical U curve gives no particular information about the model from which it is derived. This is because the Fourier analysis is invalid since the number of diffracting centers does not remain constant as the angle of reflection is varied.

40. Quantum mechanics of the rotational distortion of multiplets in molecular spectra. J. H. VAN VLECK and E. L. HILL, University of Minnesota.—A formula is derived with the new quantum mechanics for the rotational distortion of the multiplets in molecular spectra which are due to different orientations of the axis of the electrons' internal spin. This problem was formulated and treated by Kemble with the old quantum theory (Phys. Rev. **30,** 387, (1927)). Our solution is obtained as a determinant which yields an algebraic equation for the

energy W of the same order as the multiplicity. For the doublet case this gives the simple formula

$$W=[(j+\tfrac{1}{2})^2-\sigma_k^2-\tfrac{1}{2}\pm((j+\tfrac{1}{2})^2+[A^2I^2\sigma_k^2-2AI\sigma_k^2])^{1/2}]h^2/8\pi^2I$$

where j, σ_k, I, have their usual significance and $A\sigma_k h^2/4\pi^2$ is the doublet interval in the absence of rotation. Hund's cases (a) and (b) correspond respectively to $I/A=0$ and $A=0$. The adiabatic correlation of energy levels between (a) and (b) in the above formula is precisely that predicted by Hund and Kemble, including the anomalous behaviour of the component $j=\sigma_k-\frac{1}{2}$ in "regular" multiplets ($A>0$). Work is in progress on the derivation of intensity and Zeeman effect formulae applicable, like the above energy equation, throughout the range from case (a) to case (b).

41. The second order Zeeman effect in the new quantum mechanics. E. L. HILL and J. H. VAN VLECK, University of Minnesota.—The formula for the Zeeman effect in atomic spectra has usually been calculated in the new mechanics only to linear terms in the magnetic field, except for the doublet case where Heisenberg and Jordan have shown that Voigt's formula is valid. Landé (Zeits. f. Phys. **30**, p. 329, 1924) has calculated in the old theory the term in H^2 for any multiplicity and we have done likewise in the new mechanics. The resulting equation is:

$$W=W_0+\Omega hgm+(\Omega^2h^2/16)[F(j)/(W_j-W_{j-1})+F(j+1)/(W_j-W_{j+1})]+\cdots\cdot$$

where $F(j)=[(s+k+1)^2-j^2][j^2-(s-k)^2][j^2-m^2]/j^2(j-\frac{1}{2})(j+\frac{1}{2})$ and where $\Omega=He/4\pi\mu c$; and W_j is the energy for a state of inner quantum number j for $H=0$. Besides the above term in H^2 due to the interaction of the anomalous spin magnetic moment with the field, there is another term in H^2 which is related to the diamagnetic effect (proportional to R^2). The formula for this term has also been obtained.

42. Theory of the magnetic nature of gravity and Newton's laws. CORNELIO L. SAGUI, Castelnuovo dei Sabbioni, Arezzo, Italy.—As in a gravitational field the magnetic quanta of two electromagnetic fields spacially superposed, with one lagging behind the other, react elastically upon each other in such a way that those advancing meet those returning. The latter would be pushed farther away and the former would recede, and different magnetic densities would result. An electron would result as an assembly of a large number of elementary electromagnetic fields (energy-wave) with a gravitational atmosphere (gravity-wave). The repelling forces are explained and radiation connected with the oscillation of electrons between attractive and repelling forces. Again high-frequency spectra would be due to oscillating helium atoms and hydrogen molecules within the atom. A magnetic wave would be an atomic asymmetry. A star may possess a movement, due to an asymmetry of its gravitational field, towards its less gravitational density. The equilibrium would be reached after a sufficient crowding up of magnetic quanta by velocity on the side of less density. The Newtonian laws are investigated from this viewpoint by considering the magnetic depression which I have supposed to be formed between two bodies in order to explain attraction.

43. Doublet separation of Balmer lines and the molecule of hydrogen in relation to the electromagnetic quantum theory. CORNELIO L. SAGUI, Castelnuova dei Sabbioni, Arrezzo, Italy.—Doublet separation of Balmer lines of hydrogen is calculated from the point of view of the electromagnetic quantum theory and good agreement found. From the view point of the same theory the continous spectrum was considered as formed by oscillations of electromagnetic quanta within an electron and reasons give as to its intensity variation as a function of the atomic number of the anticathode material and of the second power of the voltage applied. The formation of hydrogen molecules was also investigated. Two atoms of hydrogen would unite by penetrating one another to a certain extent in agreement with the general equilibrium of the new system formed. It is shown how combination lines may be thus formed and how the Lyman ultra-violet spectrum may be formed. The infra-red spectrum was also studied, and it is supposed that many of its lines are due to a general shrinkage of the energy levels of the atom since the attractive forces of the molecule are larger than those of a single atom.

AUTHOR INDEX

Barnes, James.—No. 8
Beams, J. W.—See Lawrence
Bourgin, D. G.—No. 1
Boyce, J. C.—See Compton
———See Russell

Canfield, R. H.—No. 32
Carter, Edna—See Wick
Claus, W. D.—See Jauncey
Colwell, R. C.—No. 33
Compton, K. T.—See Russell
Compton, K. T. and J. C. Boyce—No. 16
Craig, Palmer H.—No. 35

Davisson, C. J. and L. H. Germer—No. 13
Dean, C. E.—No. 30
Duane, William—No. 14

Germer, L. H.—See Davisson
Gibbs, R. C. and H. E. White—No. 9
Glasser, Otto and V. B. Seitz—No. 38
Green, J. B. and R. A. Loring—No. 11
Guttman, John and L. B. Ham—No. 29

Ham, L. B.—See Guttman
Harrington, Elmer A.—No. 31
Hill, E. L.—See Van Vleck
Hill, E. L. and J. H. Van Vleck—No. 41

Jauncey, G. E. M. and W. D. Claus—No. 39
Jenkins, F. A.—See Rosenthal

Kaplan, Joseph—No. 25
Kenty, Carl and Louis A. Turner—No. 22

Lambly, J. E.—No. 6
Lawrence, Ernest O. and J. W. Beams—No. 18
Loomis, F. W.—No. 3
Loring, R. A.—See Green

Martin, John R—See Miller
Maxwell, L. R.—No. 26
Miller, D. C. and John R. Martin—No. 15
Mohler, F. L.—No. 12
Morse, Jared K.—No. 7
Mulliken, Robert S.—No. 5

Nottingham, W. B.—No. 28

Rosenthal, Jenny E, and F. A. Jenkins—No. 2
Ruark, Arthur E.—No. 20
Russell, H. N., K. T. Compton and J. C. Boyce—No. 17

Sagui, Cornelio L.—Nos. 42 and 43
Seitz, V. B.—See Glasser
Shenstone, A. G.—No. 10
Stewart, John Q.—No. 21
Stueckelberg, Ernst K. G.—No. 27

Taylor, L. W.—No. 34
Turner, Louis A.—No. 23
———See Kenty

Van Vleck, J. H.—See Hill
Van Vleck, J. H. and E. L. Hill—No. 40

Welch, George B.—No. 19
White, H. E.—See Gibbs
Wick, Francis G. and Edna Carter—No. 36
Winans, J. G.—No. 24
Wood, R. W.—No. 4

Yensen, T. D.—No. 37